Evaluation of Biogeochemical Models at
Local and Regional Scale

.

J. KROS

EVALUATION OF BIOGEOCHEMICAL MODELS AT LOCAL AND REGIONAL SCALE

Proefschrift

ter verkrijging van de graad van doctor
op gezag van de rector magnificus
van Wageningen Universiteit,
prof. dr. ir. L. Speelman,
in het openbaar te verdedigen
op woensdag 13 februari 2002
des namiddags te vier uur in de Aula

Abstract

Kros, J., 2002. Evaluation of biogeochemical models at local and regional scale, Thesis, Wageningen University, the Netherlands. 286 pp.

In this thesis different nutrient cycling and soil acidification models, developed for use at different scales, are presented and evaluated. The models considered are NUCSAM (NUtrient Cycling and Soil Acidification Model), RESAM (REgional Soil Acidification Model) and SMART2 (an extended version of Simulation Model for Acidification's Regional Trends). These are mechanistic dynamic models, which simulate biogeochemical processes in semi-natural terrestrial ecosystems at a variety of scales. The research tool NUCSAM, which is specifically developed for application on a local scale, includes simulation of the biogeochemical processes in various soil layers and on a daily time-scale. RESAM and SMART2, tools to support policy makers, were specifically developed to evaluate long-term soil responses to deposition scenarios on a regional scale (national to continental, respectively). For that reason, the models RESAM and SMART2 are relative simple models and operate on a yearly time-scale. These models were developed in view of the following research hypotheses:
1. Adequate simulation of temporal responses in soil solution chemistry on a daily basis at various depth requires a detailed multi-layer biogeochemical model (NUCSAM);
2. Annual average responses in soil solution chemistry at the bottom of the root zone can be adequately simulated with a simple, one-layer biogeochemical model (SMART2);
3. Simulation of soil solution chemistry on a regional scale requires a simplified model;
4. Adequate simulation of soil solution chemistry on a regional scale requires parameterisation, calibration, validation and uncertainty analysis on that scale.
Therefore, this thesis primarily aims at testing these hypotheses by (i) validation and calibration, (ii) uncertainty analysis, and (iii) model comparison. More specifically, the models NUCSAM (site scale), RESAM (site scale/regional scale) and SMART2 (regional scale) will be evaluated with respect to the optimal balance between model complexity, data availability and model aim.

The detailed model NUCSAM reproduced the magnitude and trends of measured quantities, such as soil water contents and soil solution chemistry, fairly well. However, the application on a site scale hampers from the lack of sufficiently good quality data. A model, such as NUCSAM, can not be applied at a large spatial scale because of the lack of data availability. The simplified model SMART2 is capable to simulate the observed flux-weighted annual averaged concentrations. Ignoring seasonal variations of weather conditions, ignoring of different soil layers and simplifying process description simplification does not need to greatly affect the modelled long-term annual average responses to acid deposition. A simplified model, such as SMART2, is an acceptable tool for making long-term evaluation of environmental abatement strategies. Model performance is seriously improved and the

Abstract

prediction uncertainties strongly decreased by model calibration at the scale required for the ultimate output. Further improvement through calibration is hampered from the lack of good quality data on a national scale.

Additional index words: nutrient cycling, soil modelling, uncertainty analysis, calibration, scenario analysis, model error

Voorwoord

Lang verwacht, of misschien zelfs niet meer verwacht, maar toch nog gekomen. De grondslag voor dit proefschrift werd alweer zo'n 10 jaar geleden gelegd. Dit betrof min of meer het moment waarop ik een vaste aanstelling kreeg bij het toenmalige Staring Centrum. Al vrij snel daarna kwam de overgang van input-financiering naar output-financiering. Waardoor het produceren van wetenschappelijke output alleen maar mogelijk was indien gekoppeld aan reguliere projecten. Dit betekende dat de vraag van de opdrachtgever op de eerste plaats kwam te staan en wetenschappelijke output op een lagere. Kortom een weinig gunstig gesternte om het plan voor het schrijven van een proefschrift tot een goed einde te brengen. Dat er nu toch een proefschrift ligt is voor groot gedeelte te danken aan externe nationale projecten, o.a. het laatste staartje van het verzuringsonderzoek en diverse EU-projecten, tezamen met morele en soms ook een symbolische financiële steun van enkele sympathiserende programmaleiders.

Zoals gezegd, werd de basis reeds 10 jaar geleden gelegd. In die tijd, de eerste nationale milieuverkenning *Zorgen voor Morgen* was net verschenen, begon vanuit het beleid de belangstelling te ontstaan om niet alleen modellen te ontwikkelen voor toepassing op nationale schaal, maar ook voor het evalueren van de betrouwbaarheid van dergelijke modellen. De hoofdstukken 2.1, 2.2 en 2.4 zijn een direct resultaat van deze belangstelling. In de loop van de daarop volgende jaren is langzaam maar zeker verder gewerkt aan een verdere validatie, calibratie en onzekerheidsanalyse van modellen ten aanzien van bodem- en vegetatieprocessen op landelijke schaal. Belangrijke aanjagers hiervan waren RIVM-opdrachten die uiteindelijk tot het model SMART2 (hoofdstukken 2.3 en 3.1) hebben geleid en een 2-tal EU-projecten DYNAMO en UNCERSDSS waarin met name aandacht werd besteed aan validatie en calibratie (hoofdstukken 2.3, 3.3 en 3.4) en onzekerheidsanalyse (hoofdstuk 3.2).

Dat het schrijven van dit proefschrift 'wat langer' heeft geduurd lag uiteraard ook aan mij zelf. Ik vond namelijk dat ik niet kon volstaan met het aan elkaar nieten van een bundel artikelen. Dit betekende toch veel extra werk, zoals het introduceren van een rode draad en het vervolgens vasthouden daarvan. Dit werk moest dan wel 'tussen de bedrijven door' gerealiseerd worden. Het uit 'de mottenballen halen' van tekst, data en modelbestanden en er vervolgens nog nieuwe berekeningen mee uitvoeren, vraagt meer tijd dan je in eerste instantie zou denken. Maar de voldoening dat alles, zonder ISO-9002 certificering, feilloos reproduceerbaar bleek te zijn was des te groter. Met name door de onaflatende inbreng en stimulans van Wim de Vries, een van mijn co-promotoren, en Janet Mol, een van mijn paranimfen, heeft dit uiteindelijk tot het voorliggende resultaat geleid. Desondanks zie ik dit proefschrift niet als wetenschappelijk hoogtepunt, maar meer als een soort obligate daad voor iemand die al meer dan 13 jaar op grensvlak van wetenschap en praktijk werkt. Daarentegen heb ik er altijd met plezier aan gewerkt en hoop dat het door de lezer als de moeite waard wordt beschouwd.

Een proefschrift schrijf je niet alleen. Dit proefschrift is gebaseerd op 9 artikelen en rapporten, waarvan het eerste uit 1990 dateert. Alle artikelen betreffen multidisciplinaire projecten, waaraan een groot aantal collega's een bijdrage heeft geleverd.

Allereerst wil ik mijn promotor prof dr. ir. N. van Breemen bedanken voor de prettige en flexibele wijze waarop hij richting heeft gegeven aan de totstandkoming van dit proefschrift. Beste Nico, hoewel je me wel eens de indruk gaf dat het hier om een promotie op afstand ging en dat je wat verder van bepaalde aspecten afstond, is jouw bijdrage van onschatbare waarde geweest. Ik denk hierbij met name aan de secure wijze waarop je mijn manuscripten van commentaar voorzag, de zorg die je uitte voor het dreigen te verzanden in details en het waken voor te veel relativerende opmerkingen. Mijn beide co-promotoren dr. ir. Marcel Hoosbeek en dr. ir. Wim de Vries wil ik bedanken voor hun kritische kanttekeningen en waardevolle adviezen. Beste Marcel, je werd pas in vrij laat stadium aan 'dit project' toegevoegd, maar zeker niet te laat. Zo heb je een zinvolle bijdrage kunnen leveren aan het kop- en staartwerk van dit proefschrift. Daarnaast is met jouw betrokkenheid de basis gelegd voor een hechte samenwerking binnen de in de startblokken staande kenniseenheid Groene Ruimte. Beste Wim, jij was de eerste die met het idee van een proefschrift aankwam. Regelmatig hadden we overleg, maar door samenloop van omstandigheden was dat met een lage frequentie en kwam het maar niet tot een eindresultaat. Jij bent altijd degene geweest die met een of ander mooi verhaal wist te voorkomen dat ik de handdoek in ring wierp. Wim, bedankt voor je onuitputtelijke bron van inspiratie en stimulans.

Mijn paranimfen Janet Mol-Dijkstra en Gert Jan Reinds zijn niet zomaar gekozen. Zij hebben, beide als collega, een belangrijke bijdrage geleverd bij de inhoudelijke totstandbrenging van dit proefschrift. Beste Janet, jouw tomeloze inzet en kennis van zaken aangaande de vele SMART-toepassingen, welke een cruciale schakel vormen in dit proefschrift, is ongekend. Beste Gert Jan, jouw bijdrage op het gebied van regionale modeltoepassingen en database-werk vormden eveneens een onmisbare schakel bij de totstandkoming van dit proefschrift. Naast mijn beide paranimfen hebben Caroline van der Salm en Bert Jan Groenenberg, beide collega's vanaf het eerste uur, een belangrijke bijdrage geleverd op het gebied van de ontwikkeling en toepassing van het model NUCSAM. Caroline, bedankt voor je gedetailleerde commentaar en continue belangstelling. Bert Jan, dank voor je continue bereidheid om weer eens assistentie te verlenen bij het achterhalen van hoe we in het verleden bepaalde aspecten gemodelleerd en geparameteriseerd hadden. Jan-Cees Voogd, bedankt voor alle ondersteuning op het gebied dataverwerking, modellen draaien, kaartjes en figuren maken en tekstverwerking.

Daarnaast is er aantal mensen uit 'die goede oude tijd', de laatste dagen van het verzuringsonderzoek, de periode 1988-1994, die op de een of andere mannier betrokken is geweest bij delen van dit proefschrift. Allen wil ik hiervoor hartelijk bedanken. Aan de prettige sfeer waarin we destijds samenwerkten denk ik met weemoed terug. Allereerst zijn de RIVM-collega's Hans van Grinsven en Aldrik Tiktak, zowel de Speuld-toepassing uit het APVIII en de Solling-toepassing uit de Leusden-workshop, waarin jullie beide een grote rol hebben gespeeld zijn in dit

Voor mijn vader

Contents

Contents

I   Introduction

1.1   Background and aim

Background on biogeochemical models

Evaluation of anthropogenic effects on the environment at local, regional and global scales has become a key activity in environmental research. It forms the basis for emission reduction measures needed to achieve policy leading to a sustainable society. Computer models play an increasing role in the evaluation of those environmental effects. In the Netherlands, at the Environmental Policy Assessment Office (MilieuPlanBureau: MPB) and Nature Policy Assessment Office (NatuurPlanBureau: NPB) a large set of integrated predictive models are used to evaluate the effects of policy scenarios on a wide range of environmental problems. These include eutrophication, acidification, climate change and biodiversity decrease. Within these themes, mechanistic dynamical models, which simulate biogeochemical processes in ecosystems, play a crucial role. Biogeochemical models describe the behaviour and cycling of water and a variety of elements within ecosystems. A common aspect of the models used within the MBP and NPB is that they are used for a nation-wide application over a relatively long period of time (10-100 years). Besides their role within environmental policy assessment, modelling of biogeochemical processes serves a research goal viz (i) data integration, (ii) process integration, (iii) testing hypothesis, and (iv) derivation of guidelines for further experimental and field research. To describe biogeochemical processes in semi-natural terrestrial ecosystems several models have been developed. These models can be divided into two major groups, those based on an empirical approach and those based on mechanistic descriptions of processes (cf. Hoosbeek and Bryant, 1992). A disadvantage of empirical models is that they are generally not able to extrapolated, and therefore less suitable for establishing long-term predictions.

During the last decades several dynamic process-oriented models for such purpose have been developed. Examples from the beginning period of this development, including surface water models, are: (i) 1980: simulating of soil nutrient losses based on the mobile anion concept (Reuss, 1980), (ii) 1982: the 'Birkenes model' for soil water and freshwater acidification on the catchment scale (Christophersen *et al.*, 1982), (iii) 1983: a simple model on soil leachate chemistry (Arp, 1983), (iv) 1983: ILWAS, the integrated lake watershed acidification study (Chen *et al.*, 1983), (v) 1985: MAGIC, a model for the acidification of groundwater in catchments (Cosby *et al.*, 1985), (vi) 1985: a simple semi-empirical model on soil pH and base saturation (Bloom and Grigal, 1985), (vii) 1986: the Trickle Down Model on lake acidification (Schnoor *et al.*, 1986). Later on, a large number of new models were developed, which in majority are based on the same concepts as the older models (cf. Tiktak and Van Grinsven, 1995). Several comparisons and performance studies have

been made on these models (cf. Eary *et al.*, 1989, Rose *et al.*, 1991 and Tiktak and Van Grinsven, 1995). From those studies it was concluded that numerical models are useful tools for understanding and integrating processes and disciplines, but the predictive reliability of such models still needs to be tested against long-term monitoring data.

Basically, most of the available biogeochemical models are originally developed as a site scale model. Ideally, the complexity of a model should be in harmony with its intended aim. Important constraints to (realistic) modelling are limited scientific knowledge of underlying processes and lack of data. When going from a small or detailed towards a large or course temporal and spatial scale, the degree of model complexity usually, but not always, decreases (cf. Bierkens *et al.*, 2000).

Aim

In this thesis different nutrient cycling and soil acidification models, developed for use at different scales, are presented and evaluated. I will focus on mechanistic dynamic models, which simulate biogeochemical processes in semi-natural terrestrial ecosystems at a variety of scales. The models considered are NUCSAM (NUtrient Cycling and Soil Acidification Model; Groenenberg *et al.*, 1995; Chapter 2.1), RESAM (REgional Soil Acidification Model; De Vries *et al.*, 1995a; Chapter 2.2) and SMART2 (an extended version of Simulation Model for Acidification's Regional Trends; Kros *et al.*, 1995a,b; Chapter 3.1). The research tool NUCSAM, which is specifically developed for application on a local scale, includes simulation of the daily variability biogeochemical processes. RESAM and SMART2, tools to support policy makers, were specifically developed to evaluate long-term soil responses to deposition scenarios on a regional scale (national to continental, respectively). Consequently, RESAM and SMART2 do not include seasonal dynamics. The temporal resolution of these models is one year, and the hydrologic description in these models is relatively simple.

RESAM and SMART (a precursor of SMART2; De Vries *et al.*, 1989) were part of integrated acidification simulation models that give a quantitative description of the linkages between emissions, deposition and environmental impacts such as soil acidification and effects on terrestrial and aquatic ecosystems. These integrated models are: (i) DAS (Dutch Acidification Simulation model) for application in the Netherlands (Olsthoorn *et al.*, 1990) and (ii) RAINS (Regional Acidification Information and Simulation model) for application in Europe (Alcamo *et al.*, 1990). The model SMART2 is used as the biogeochemical module within the Environmental Policy Assessment Office (MPB) and Nature Policy Assessment Office (NPB).

To evaluate model performance in relation to model simplification and transition to a coarser temporal and spatial scale the models NUCSAM, RESAM and SMART have been applied simultaneously to the same data set (De Vries *et al.*, 1998). This can be seen as a first step in order to check whether model simplification is an acceptable pathway to model on a large temporal and spatial scale. A comprehensive testing, however, of this approach is lacking. Therefore, this thesis primarily aims at testing the underlying approach by (i) validation and calibration, (ii) uncertainty analysis, and (iii) model comparison. More specifically, the models NUCSAM (site

scale), RESAM (site scale/regional scale) and SMART2 (regional scale) will be evaluated with respect to the optimal balance between model complexity, data availability and model aim.

1.2   Scaling Issues

Earth sciences can be divided along boundaries of spatio-temporal scales. For many purposes it is adequate, if not desirable to inquire processes knowledge at one particular narrow range of spatial and temporal scales. On the one hand, processes are studied on a micro-scale such as decompostion and (de)nitrification (cf. Leffelaar, 1987), on the other hand research is performed at the level of landscape ecology, such as catchments (cf. Likens *et al.*, 1977). Crossing these boundaries is not very common and may be considered as a mutual threat of disciplines.

One of the common characteristics of environmental problems such as climate change and air pollution is that they play a role on a local, regional, national, continental and even global scale. The long-term response of soils due to elevated atmospheric deposition, investigated in this thesis, is a typical example. It is imperative that the spatial and temporal aspects considered in a model must fit its objectives. In practice, however, an ideal fit is difficult to achieve, because model input data (e.g. initial conditions and parameters) are often limited or even unknown at the relevant scale. Especially at large spatial scales, many model parameters cannot be measured directly at all. Within the framework of the modelling process we can distinguish three specific scale categories (cf. Van der Zee, 1999; Bierkens *et al.*, 2000):

- the *observation scale*, the scale for which an observation provides an average value, e.g. a soil sample represents only a few dm^3
- the *model scale*, the scale on which the model provides its output
- the *policy scale*, the scale on which research results are required to answer the decision makers questions

Regarding the model scale, Bouma *et al.* (1998) stated that many biogeochemical models developed on a plot scale may be considered for use at larger spatial scales. However, this may cause problems (cf. Heuvelink, 1998a):

- The relative importance of a process or subprocess may vary with scale. A particular process may be negligible at larger spatial and temporal scales, e.g. unsaturated preferential flow (Blöschl and Sivaplan, 1995).
- At small scales, e.g. at those of intensively monitored plots, the data availability can often support the demand of complex models, the data availability is usually sparse at larger spatial scales and model input data have to be derived from generic data sources like maps and pedo-transferfunctions (cf. De Vries, 1994).
- Moving from a smaller scale towards a larger, is generally accompanied by an increase in level of aggregation. Usually, the model input data become some kind of average of point values within a large spatial unit or 'block'. This may require an adaptation of the model (cf. Heuvelink, 1998a).

Consequently, there is a trade-off between scale and model complexity. A general problem that arises from applying a plot scale model on a larger scale is the

parameterisation. The more parameters a model contains, the less likely it is that they can be derived either directly from available data or indirectly by using pedo-transfer functions. In addition, when particular parameters can only be obtained by calibration, identification problems may thwart the calibration.

For a number of specific environmental problems, data availability on a plot scale is relatively large. Often this scale is chosen because it is the most appropriate scale to study biogeochemical processes in situ. The local scale, therefore, is the most logical level to start with model development. Because of sparser data at larger scale, the scale of the model must be adapted to the scale of data availability.

One possibility is to simplify the model description in such a way that the temporal and spatial resolution is comparable to the resolution of the data. During such a simplification of processes, model results must remain reliable. The reliability can usually be determined by comparing results from the simplified model (i.e. SMART) and the local scale model (i.e. NUCSAM). Another possibility is to apply a complex, plot scale model directly to a large temporal and spatial scale. A notable example of this approach is the STONE model (cf. Boers *et al.*, 1995), a model on a national scale describing the fate of nitrate and phosphorous in agricultural soils. Both pathways are propagated in the Netherlands for national applications of biogeochemical models within the Dutch Nature and Environmental Planning Agency (NPB and MPB). Presumably there is an optimal level of model complexity, i.e. a point where the degree of model complexity, e.g. in terms of state variables, match the data resolution and quality, leading to maximal knowledge gain about the modelled system (Jørgensen, 1992; Janssen, 1998). Since, environmental systems are regarded as complex, 'increased complexity in models is interpreted as evidence of closer approximation to reality' (Oreskes, 2000). Whereas Hauhs *et al.* (1996) classified the tendency of putting together as many processes as possible as 'naive modelling' or in words of Janssen (1998) 'a model should be made no more complex than can be supported by the available brains, computers and data'.

In this thesis I will advocate the use of simpler or simplified models with relatively small data requirements, with a relatively high degree of certainty, above complex models with large data requirements, that are difficult to fulfil. Because, even if the model structure is correct (or at least adequately representing current knowledge), the uncertainty in the output of complex models may still be large due to the uncertainty in the input data. A theoretically justification for the use of model simplification in order to obtain more reliable results can be performed by uncertainty analyses (cf. Hornberger *et al.*, 1986; Hettelingh, 1989; Janssen, 1994; Heuvelink, 1998b).

1.3 Overview of the biogeochemical models used in this thesis

General overview

NUCSAM, RESAM and SMART2 are all process-oriented deterministic models. The trade-off between detail and reliability of information obtained and regional applicability is reflected by the desired degree of spatial resolution in model output. This is a factor of crucial importance when selecting the level of detail in both the model formulation and its input data. Application on a coarser scale justifies the use of a simpler model, see Table 1.

Table 1 Characteristics of the used dynamic biogeochemical models

Name	Complexity	Soil layering	Temporal resolution	Spatial resolution	Application scale
NUCSAM	complex	multi-layer	one day	1×1 m²	site
RESAM	intermediate	multi-layer	one year	100×100 m²	Netherlands
SMART2	simple	one-layer	one year	500×500 m²	Netherlands/Europe

The regional-scale models SMART2 and RESAM can be seen as simplified versions of the 'site-scale' model NUCSAM, to reduce input requirements. NUCSAM is a quantitative mechanistic site-scale model with a complex process description, spatial (vertical) and temporal resolution. This model represents the basic model that has the same spatial and temporal resolutions as the data gathered at intensively monitored research plots. The simplifications made in RESAM and SMART2 consist of: (i) reduction of temporal resolution, i.e. using an annual time resolution, thus neglecting interannual variability of both model inputs and processes, (ii) reduction in spatial resolution, by using a smaller number of soil compartments and (iii) the use of less detailed process formulations. To apply a model on a regional scale, the various processes occurring in the soils have either been limited to a few key soil processes, or represented by simple conceptualisations (process aggregation). The degree of process aggregation in the models increases (complexity decreases) when the availability of data decreases, which occurs with an increase in the geographic area of application.

NUCSAM was developed to describe the biogeochemistry of intensively (mostly biweekly) monitored sites during a relatively short-time period. Validation of dynamic models with a one-year temporal resolution such as RESAM and SMART2, is problematic due to a lack of long-term observation records on soil chemistry data. However, long-term simulations with SMART2 and RESAM can be compared to those made with the validated NUCSAM model, that serves as a reference. In this way an indirect model output validation can be accomplished for the regional models RESAM and SMART2.

The multi-layer model RESAM gives insight into the spatial (vertical) variation in soil (solution) chemistry within the root zone. The hydrology of the one-layer model SMART2 eventually only yields the annual precipitation excess draining from the root

zone. Therefore, SMART2 only predicts soil solution chemistry at the bottom of the root zone. Important acidification indicators such as the Al concentration and Al/Ca ratio, however, increase with depth due to Al mobilisation, transpiration and Ca uptake. Since most fine roots, responsible for nutrient uptake, occur in the upper soil layer (0-30 cm soil depth), it is important to obtain reliable estimates for this layer by including water uptake with depth and nutrient cycling (foliar uptake, foliar exudation, litterfall, mineralisation and nutrient uptake) within the root zone.

History of model development

The models that are addressed in this thesis each have their own specific background. The model development started in the mid eighties with the development of RESAM as part of the Dutch Acidification System (DAS, Olsthoorn *et al.*, 1990). RESAM has been applied at various *generic* sites (De Vries and Kros, 1989; De Vries *et al.*, 1995a). to the Netherlands as a whole (De Vries *et al.*, 1994a). Furthermore, this model was subjected to a sensitivity and uncertainty analysis (Kros, *et al.*, 1993). At that same time the European scale model SMART was developed to act as a successor of the existing soil module (Kauppi *et al.*, 1986) in the RAINS-model (Alcamo *et al.*, 1990). SMART has been applied at particular *generic* sites (De Vries *et al.*, 1989) and Europe as a whole (De Vries *et al.*, 1994b). In the beginning of the nineties the Dutch National Institute of Health and Environment (RIVM) requested for a soil module for an integrated model for the evaluation of nature conservation policy (Alkemade *et al.*, 1998). Because RESAM was considered too complex for this purpose and SMART too simple, it was decided to develop the model SMART2. During the development period op the models RESAM, SMART and SMART2, little attention was paid to serious model evaluation. Eventually, during the third and final phase (1991-1995) of the Dutch Priority Programme on Acidification emphasis was put on model validation. In that period the model NUCSAM (Groenenberg *et al.*, 1995) was developed in order to make use of data records from intensively monitored sites for the validation of the models SMART, SMART2 and RESAM. Thereafter, successively more and more attention has been paid to model evaluation.

Process descriptions

NUCSAM, RESAM and SMART2 are all based on the principle of ionic charge balance and on a simplified solute transport description. All models assume that: (i) a soil layer is a homogeneous compartment of constant density and (ii) the element input mixes completely in a soil layer. Furthermore, N-fixation, SO_4 reduction and SO_4 precipitation are not included, and the various process descriptions for biological and geochemical interactions are simplified to minimise input data requirements. Going from NUCSAM to SMART2 process aggregation is achieved by (i) confining to one soil layer, (ii) a simpler hydrological description, (iii) simpler descriptions of processes (e.g. equilibrium equations instead of rate-limited reactions), (iv) ignoring (phosphorous) or lumping elements (e.g. sum of divalent base cations, BC, instead of Ca and Mg

separately), and (v) ignoring several processes (e.g. NH$_4$ adsorption), In RESAM and SMART2 the annual water flux percolating through a soil layer is constant and equals the infiltration minus the transpiration, whereas NUCSAM contains a separate hydrological model. These differences are summarised in Table 2.

Biological processes are all described by rate-limited reactions, usually first-order reactions. An exception is the canopy interactions which are described by linear relationships with atmospheric deposition (cf. Table 2). In SMART2, geochemical reactions are described by equilibrium equations (dissociation of CO$_2$, cation exchange and SO$_4$ adsorption), except silicate weathering, which is described by a zero-order reaction (Table 2). So, unlike SMART2, NUCSAM and RESAM account for the effect of mineral depletion on the weathering rate. In NUCSAM and RESAM the geochemical reactions are either described by equilibrium equations or first-order reactions (protonation of organic anions and weathering of carbonates, silicates and secondary Al compounds).

1.4   Evaluation of the biogeochemical models used

As mentioned before, the aspects of model evaluation that will be addressed in this thesis are (i) calibration and validation by comparing of model results with measurements, (ii) assessment of the uncertainty in model results due to uncertainties in model structure and model inputs and (iii) intercomparison of results of different models.

Table 2 Processes and process formulations included in NUCSAM, RESAM and SMART2

Processes	NUCSAM	RESAM	SMART2
Hydrological processes:			
Water flow	Hydrological submodel	Water balance for multiple layer	Water balance for the root zone
Biological processes:			
Foliar uptake	Proportional to total deposition	Proportional to total deposition	Proportional to total deposition
Foliar exudation	Proportional to H and NH$_4$ deposition	Proportional to H and NH$_4$ deposition	Proportional to H and NH$_4$ deposition
Litterfall	First-order reaction	First-order reaction	Model input
Root decay	First-order reaction	First-order reaction	Model input
Mineralisation/ immobilisation	First-order reaction[1]	First-order reaction	Proportional to N deposition
Growth uptake	Constant growth Logistic growth	Constant growth Logistic growth	Constant growth Logistic growth
Maintenance uptake	Forcing function[2]	Forcing function[2]	Forcing function[2]
Nitrification	First-order reaction[1]	First-order reaction	Proportional to net NH$_4$ input
Denitrification	First-order reaction[1]	First-order reaction	Proportional to net NO$_3$ input

Table 2 (Continued)

Processes	NUCSAM	RESAM	SMART2
Geochemical processes:			
CO_2 dissociation	Equilibrium equation	Equilibrium equation	Equilibrium equation
RCOO protonation	First-order reaction	First-order reaction	First-order reaction
Carbonate weathering	First-order reaction	First-order reaction	Equilibrium equation
Silicate weathering	First-order reaction[3]	First-order reaction[3]	Zero-order reaction
Al hydroxide weathering	First-order reaction	First-order reaction	Equilibrium equation
	Elovich equation	Elovich equation	
Cation exchange[4]	Gaines-Thomas equations for:	Gaines-Thomas equations for:	Gaines-Thomas equations for:
	H, Al, NH_4, Ca, Mg, K and Na	H, Al, NH_4, Ca, Mg, K and Na	H, Al and BC2 (=Ca+Mg)
Sulphate adsorption	Langmuir equation	Langmuir equation	Langmuir equation
Phosphate adsorption	Langmuir equation	-	-
Complexation reactions	Equilibrium equations	-	-

[1] In NUCSAM, these processes are also described as a function of temperature

[2] In RESAM and NUCSAM the maintenance uptake equals it the sum of litterfall, root turnover and foliar exudation minus foliar uptake.

[3] In RESAM and NUCSAM there is also the option to include a dependence of pH on the weathering rate.

Calibration and validation

In this thesis *calibration* is used in a broad sense, i.e. the determination of model input data, e.g. parameters, initial and boundary conditions, by using available measurements. Some authors use the term *parameterisation* either with or without a fitting procedure based on measurements (cf. Addiscott *et al.*, 1995). Following this definition, calibration, as it is used here, equals parameterisation with a fitting procedure. In order to cope with ill-defined and information-poor situations where data are sparse and uncertain, calibration can be helpful in order to reduce the prediction uncertainty.

The basic question whether we can *validate* a model is both a philosophical and a scientific one. Addiscott *et al.* (1995) stated in an evaluation on both questions that from a philosophical point of view 'although we may be able to discriminate between models, we can never *validate* a model in the sense of *proving* that it is correct'. On the other hand *validation* is derived from *validus*, meaning strong, whereas in legal and theological parlance it also means *efficacious* or 'producing the intended effect'. In a modelling context validation can be defined as 'the art of the applicable' (cf. Addiscott *et al.*, 1995). In this thesis *validation* is used in a more operational way (cf. Konikow and Bredehoeft, 1992), i.e. the goodness of fit of simulations to measurements or even the confrontation of the model output(s) with expert judgement or personal experience.

A widely accepted approach of calibration and validation, is, after the model has been calibrated successfully to a particular data set, the model is (in)validated by comparing model outputs with an independent data set. In practice, however,

validation is in fact a sort of evaluation of an applied model. In this context Janssen and Heuberger (1995) distinguished:

- the *ability* of the model to reproduce the system behaviour
- the *suitability* of the model for the intended use
- the *robustness* of the model for model input data

Furthermore, model validation is not a *once-and-for-all* activity leading to an absolute and definite judgement on the model's adequacy. Rather it is an ongoing process, which is always performed in a certain evolving context against which the statements should be expressed and interpreted (cf. Janssen and Heuberger, 1995). In many situations, a thorough validation will be impossible or limited, usually due to a lack of data or time, where both are often a result of limited financial resources.

Uncertainty analysis

Although models for regional scale assessments have great potentials, they should be used with caution, because both models and data often have a high and variable level of associated uncertainty (cf. Loague *et al.*, 1998). Consequently, it is crucial that these uncertainties are quantified. However, knowledge and information on these problems is typically limited, uncertain and poor. For reliable development and application of such models, a thorough *sensitivity* and *uncertainty* analysis is essential. These help to clarify the origins and effects of model uncertainties. In literature the distinction between uncertainty analysis and sensitivity analysis is not always clear. Sensitivity analysis is primarily concerned with the question how model outputs are affected by (small) variations in values of model input data (i.e. parameters, initial conditions, inputs). This provides useful information for model calibration and further model development (cf. Janssen, 1994). In an uncertainty analysis situations are considered where uncertainty and/or risk play a crucial role. This is achieved by assuming that values of model input data and the model as such are uncertain, due to uncertainty sources, and how these uncertainty affect the model outputs. The uncertainty in model outputs of a dynamic model originates from errors or misspecification of (i) model structure, (ii) parameters, (iii) initial conditions, (iv) model inputs and (v) model operation, due to incomplete knowledge, data or natural variability.

A variety of techniques for uncertainty analyses has been reported (cf. Iman and Helton, 1988 and Janssen *et al.*, 1990). Roughly, we can distinguish (i) Monte Carlo based methods and (ii) analytically based techniques. For the analysis of process-oriented dynamic models Monte Carlo methods are preferred, since they are simple and straightforward. They rely on the assumption that the uncertainty in model input data can be described by specifying probability distributions and mutual correlations. From these probability distributions, multivariate sets of model input data are drawn. These samples are used to run the model, i.e. a Monte Carlo simulation. This results in a multivariate set of model outputs that are stored for further analysis. This analysis consists of calculating (i) the basic statistical information of the model outputs and (ii) the uncertainty contribution of the various uncertainty sources to the model outputs. Monte Carlo methods, however, also have drawbacks, including huge computational loads. In order to cope with this problem several more sophisticated Monte Carlo

methods are available, e.g. Latin Hypercube Sampling (McKay *et al.*, 1979) and Controlled Random Search (Price, 1983).

Examples of uncertainty analyses in the field of biogeochemical modelling at the plot scale are the quantification of uncertainties for pesticide leaching for one generic soil landuse combination (Tiktak *et al.*, 1994) or for one mapping unit in a region (Finke *et al.*, 1996). In regional scale assessments, model input data are usually derived from generally available data, e.g. soil and landcover maps, using (pedo)transfer functions (Bouma *et al.*, 1986; Tiktak *et al.*, 1998). Finke *et al.* (1996) quantified the output uncertainty resulting from both spatial variability and the uncertainty in pedotransfer functions by a Monte Carlo analysis and analysed how much these sources contributed to the total variance.

Model comparison

Comparison of outputs of various models provides insight in the uncertainty due to the model structure. This can be either a comparison between models that totally differ in the modelling concept or models that differ in degree of detail. Among modellers the benefit of model comparison is widely recognised. Several studies on this topic have been performed, e.g. in 1993 during a workshop 16 forest-soil-atmosphere models were compared, using a long-term data-set from Solling, Germany (Tiktak and Van Grinsven, 1995).

To compare model outputs either with data or with outputs from other models, both qualitative and quantitative methods should be used. Qualitative methods are based on visual inspection of the model results in conjunction with the associated data using, e.g. scatter plots, time series, distribution functions. Quantitative methods try to express the degree of agreement numerically, i.e. by a performance measure (Janssen and Heuberger, 1995).

1.5 Research questions of this thesis

Until now in the Netherlands a lot of research has been performed on modelling nutrient cycling and soil acidification (cf. De Vries, 1994; Van der Salm, 1999). The model RESAM has been applied for the Netherlands (De Vries *et al.*, 1994a) and on a site scale (Van der Salm *et al.*, 1999). The same is true for the precursor of the model SMART2 (cf. De Vries *et al.* (1989) for a site application and De Vries *et al.* (1994b) for a European application). This previous research focussed on (i) process identification, (ii) data derivation and (iii) model development. At that time, these models were also used for scenario evaluation without rigorous validation, calibration and uncertainty analysis. This implies that the validity of the results could not be presented, but only the plausibility. Ever since, however, more and more attention has been paid to model evaluation. A selection of the research on evaluation of these models forms the core this thesis. It aims at the evaluation of the reliability and validity of a set of

biogeochemical models developed for various spatial and temporal scales. The research summarised in this thesis was based on the following hypotheses:

- Adequate simulation of temporal responses in soil solution chemistry on a daily basis at various depth requires a detailed muli-layer biogeochemical model;
- Annual average responses in soil solution chemistry at the bottom of the root zone can be adequately simulated with a simple, one-layer biogeochemical model;
- Simulation of soil solution chemistry on a regional scale requires a simplified model;
- Adequate simulation of soil solution chemistry on a regional scale requires parameterisation, calibration, validation and uncertainty analysis on that scale.

More specifically, I will try to answer the following questions:

- What is the adequacy of a detailed terrestrial biogeochemical model in predicting soil solution chemistry at short time interval and various soil depth? (cf. Chapter 2.1)?
- Is uncertainty analyses, which give insight in the relative contribution of processes to the model outputs, beneficial in simplifying a detailed terrestrial biogeochemical model (cf. Chapter 2.2)?
- What is the adequacy of a simple one-layer terrestrial biogeochemical model in simulating soil solution chemistry (cf. Chapter 2.3)?
- What is the change in model performance at various soil depth and time scales due to model simplification, including spatial and temporal aggregation of a terrestrial biogeochemical model in simulating soil solution chemistry (cf. Chapter 2.4)?
- What is the applicability of a simplified model on a regional scale in view of data availability (cf. Chapter 3.1)?
- What is the prediction uncertainty due to uncertainty in geographical data and model parameters when applying a model on a regional scale? (cf. Chapter 3.2)?
- What is the gain in model performance on a regional scale after regional model calibration (cf. Chapters 3.3)?
- What is the adequacy of simple biogeochemical models as a tool for policy makers. (cf. Chapter 4)?

Figure 1 illustrates the steps taken in this thesis in the transition from modelling on a site scale towards application on regional scales.
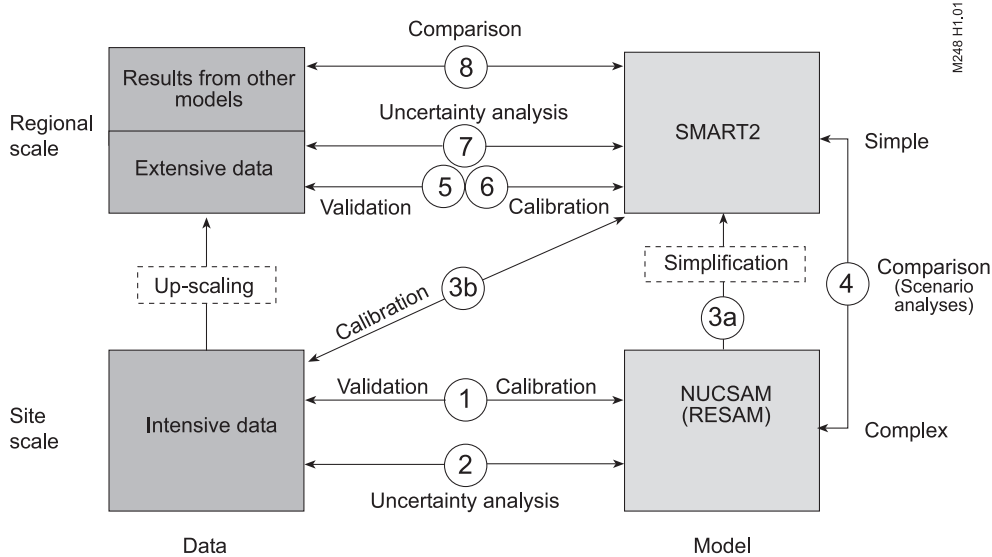
Figure 1 Outline of the model evaluation procedure used in this thesis. Numbers refer to the actions listed in the text

On a site scale:
1. Develop a quantitative mechanistic site-scale model with a high degree of process knowledge, spatial (vertical) and temporal resolution. Calibrate and validate the site-scale model on high resolution data, (in depth and time) of intensively monitored sites by (cf. Chapter 2.1):
   - Minimising the uncertainty and difference between observations and model results by calibrating poorly defined model parameters (calibration)
   - Comparing model results with (another) high resolution data-set (validation)
2. Perform a sensitivity and uncertainty analysis to determine the most important model parameters and associated processes (cf. Chapter 2.2)
3. Simplify the site-scale model (3a) into a regional-scale model by (i) aggregation of processes and input data based on the desired temporal resolution at regional scale (temporal aggregation) and (ii) aggregation of soil layers (spatial aggregation). Calibrate the regional scale model (3b) at an (intensively) monitored site, and validate at another site (cf. Chapter 2.3). Preferably, the simplification of the process description is based on the sensitivity analysis of the detailed model. (cf. Chapter 2.2)
4. Compare the performance of the site-scale and regional-scale model on the same intensively monitored sites, using (i) the original high resolution data and (ii) aggregated data at the same temporal resolution as the model. Compare predicted long-term trends of the site-scale and regional-scale model for the appropriate temporal resolution (cf. Chapter 2.4)

On a regional scale:

5. Validate the regional-scale model on low resolution (spatial) data at a coarse spatial scale (cf. Chapter 3.1)
6. Reduce the uncertainty by calibrating poorly defined model parameters at a large spatial scale (cf. Chapter 3.3)
7. Specify the uncertainty in the model results at a regional scale (perform an uncertainty analysis of the regional-scale model in a spatial context) (cf. Chapter 3.2)
8. Compare the results of the regional scale model with other models (cf. Chapter 3.4)

1.6   Outline of this thesis

The research questions will be answered in chapters II and III, where chapter II addresses the evaluation and reliability at the site scale and chapter III at the regional scale. Both chapters subsequently conduct (i) model validation and calibration, (ii) uncertainty analysis and (iii) model comparison (cf. Table 3).

Table 3 Outline of the thesis in terms of reliability action and scale, numbers refer to Chapter numbers

Reliability action	Scale	
	Local scale	Regional scale
Validation and calibration	2.1, 2.3	3.1, 3.3
Uncertainty analysis	2.2	3.2
Model comparison	2.4	3.4

Part II starts with a detailed description of the soil acidification and nutrient cycle model NUCSAM and a validation of the model on the Dutch experimental forest site at Speuld (Chapter 2.1). As a next step the uncertainty in model predictions due to the uncertainty in input data at a site scale was investigated using a simpler version of the NUCSAM model, the model RESAM (Chapter 2.2). The regional scale model SMART2, derived from NUCSAM, is described in Chapter 2.3. This chapter also presents the calibration and validation of this model at a manipulated monitoring site (Risdalsheia, Norway). In Chapter 2.4 all three models (NUCSAM, RESAM and SMART2) are applied and compared at one intensively monitored location (Solling, Germany). In order to increase the confidence of long-term predictions of the simplified regional scale model, also long-term predictions of the three models are compared.

Part III of this thesis starts with the application and validation of the regional-scale model SMART2 for the Netherlands (Chapter 3.1). The uncertainty associated with the SMART2 application at a large spatial scale is presented in Chapter 3.2. Chapter 3.3 shows how the uncertainty in model results at a national scale can be reduced by performing a calibration using regional scale data. In Chapter 3.4 the performance of the SMART2 model on the national scale is compared with two other models.

This thesis concludes with part IV where the results and conclusions of the model evaluation are summarised and evaluated with respect to the research questions.

I Introduction

II Evaluation on a site scale

2.1 Nutrient cycling and soil acidification modelling on a site scale
A revised version of:
- NUCSAM: a model for evaluating nutrient cycling and soil acidification in forest ecosystems
  By: J. Kros, J.E. Groenenberg, C. van der Salm, W. de Vries and N. van Breemen
  Submitted to Ecological Modelling

2.2 The uncertainty in forecasting trends of forest soil acidification
A slightly revised version of:
- The uncertainty in forecasting trends of forest soil acidification
  By: J. Kros, W. de Vries, P.H.M. Janssen and C.I. Bak
  Published in: Water, Air and Soil Pollution, 66:29-58

2.3 Modelling effects of acid deposition and climate change on soil and runoff chemistry
A combination of revised versions of:
- SMART2: Modelling of soil acidity and nitrogen availability in natural soil ecosystems in response to changes in acid deposition and hydrology
  By: J. Kros, J.P. Mol-Dijkstra, W. de Vries and G.J. Reinds
  Submitted to Ecological Modelling
- Modelling effects of acid deposition and climate change on soil and runoff chemistry at Risdalsheia, Norway
  By: Janet P. Mol-Dijkstra and Hans Kros
  Published in: Hydrology and Earth System Sciences: 5:487-498.

2.4 Validation and comparison of soil acidification models with different degrees of process aggregation on a site scale
A combination of revised versions of:
- Application of soil acidification models with different degrees of process aggregation on an intensively monitored spruce site
  By: C. van der Salm, J. Kros, J.E. Groenenberg, W. de Vries and G.J. Reinds, 1995
  Published in: S.T. Trudgill (Ed.): Solute modelling in catchment systems, John Wiley, Chichester, UK: 327-346.
- Uncertainties in long-term predictions of forest soil acidification due to neglecting seasonal variability
  By: J. Kros, J.E. Groenenberg, W. de Vries and C. van der Salm
  Published in: Water, Air, and Soil Pollution: 79:353-375.

II Evaluation on a site scale

2.1 Nutrient cycling and soil acidification modelling on a site scale

Abstract

A detailed soil and nutrient cycling model for forest ecosystems (NUCSAM) is described here. The model integrates the hydrological- and nutrient cycle and soil chemical processes, while including all relevant processes in the forest canopy, organic surface layer, mineral soil and soil solution, that are known according to current knowledge. The hydrological cycle is modelled by a separate Darcy-law-based hydrological model. Nutrient cycling involves nutrient uptake, litterfall, root turnover and mineralisation. Forest growth is described by a logistic growth function. Equilibrium and rate limiting chemical reactions are explicitly modelled in a chemical module. Chemical reactions rates depend on temperature, whereas biochemical processes depend on temperature, moisture content and pH.

The NUCSAM model was applied to the Speulderbos Douglas fir stand, and validated using measured data on soil and soil solution chemistry. Results mostly showed a reasonable to good agreement with observations. However, the pH was overestimated in the topsoil and underestimated in the subsoil. The Ca concentration in the topsoil and Cl in the subsoil was slightly underestimated. Long-term (60 a) impacts of acid deposition of three deposition scenarios on two generic forest soil combinations were also evaluated with NUCSAM. Scenario analyses showed a fast response of the Al and SO_4 concentration after a decrease in SO_x deposition and a time-delay in decrease of the NO_3 concentration resulting from a decrease in NO_x deposition and higher soil solution concentrations below Douglas fir.

2.1.1 Introduction

There has been a continuous interest in developing and using detailed process-oriented ecosystem models for the simulation of vegetation and soil processes, cf. reviews by Ågren *et al.* (1991), Tiktak and Van Grinsven (1995) and Ryan *et al.* (1996). Such models are of interest for linking experimental data and hypotheses testing in view of: general ecosystem research, acidification, eutrophication, biodiversity and climate change. A detailed ecosystem model must integrate the hydrological cycle, nutrient cycling, and other soil processes. Furthermore, such a model must include all relevant environmental factors that affect these processes.

Several hypotheses that link forest growth and forest vitality to air pollution, atmospheric deposition, soil acidification and disturbed nutrient cycling have been developed. Examples are the Al-toxicity hypothesis (Ulrich, 1983) and the nitrogen saturation hypothesis (Skeffington, 1988). Such hypothetical effect relationships can be tested by applying mechanistic and comprehensive simulation models. As a first step, the integrated Dutch Acidification Systems model (DAS) has been developed during the Dutch Priority Programme on Acidification (Heij and Schneider, 1991). This model aims at evaluating the long-term effectiveness of acidification abatement strategies on a number of receptor systems (forests, forest-soils, heathland and aquatic ecosystems). The model describes the complete causality chain from emissions to

effects in a regionalised way. An important effect module within DAS is the forest soil model RESAM (De Vries *et al.*, 1995a; Chapter 2.2), which has a temporal resolution of one year. Later on, within the context of the national planning bureau's (NPB, MPB), an even more integrated simulation model was developed, the Natuurplanner (Alkemade *et al.*, 1998). This required a more simplified biogeochemical model, for which we developed the model SMART2 (see Chapter 2.3).

The regional models RESAM and SMART2 include various simplifications such as a yearly time scale, single soil layer (SMART2) and lumped process formulations. Validation of such regional models is, however, cumbersome, as most measurements are carried out at the stand level. Validation at that level of detail is problematic since the model outputs of these models is in the form of yearly average concentrations that cannot be compared directly to (biweekly or monthly) monitoring measurements, which show high temporal dynamics. Furthermore, RESAM and SMART2, which aim at predicting long-term changes, cannot be validated with results from relatively short (3-10 a) monitoring programmes. To overcome this limitation we built a detailed stand-level model with a high degree of process knowledge and a higher temporal resolution: the Nutrient Cycling and Soil Acidification model (NUCSAM). Besides the necessity of having a detailed biogeochemical model as a research tool, the most important reason for developing NUCSAM was validation and scientific justification for the regional models RESAM and SMART2. The model NUCSAM has been applied previously to the Solling experimental forest in Germany (Groenenberg *et al.*, 1995) and to a roofing experimental site Speuld, the Netherlands (Van der Salm *et al.*, 1998).

In this Chapter, a comprehensive description of the model NUCSAM is given together with a validation of the model to a Dutch Douglas fir stand in the Speulderbos. Data on forest hydrology, soil chemistry and tree growth were available for the period 1986-1990 (Heij and Schneider, 1991; Evers *et al.*, 1987). Furthermore, the results of scenario analyses are presented.

2.1.2   Model description

Model structure

NUCSAM is a process-oriented model that simulates the major hydrological and biogeochemical processes in the forest canopy, organic surface layer, and mineral soil. It considers evapotranspiration, heat transport, canopy processes, litterfall, mineralisation, below and above ground nutrient uptake, soil processes and solute transport. The change in soil solution and solid phase chemistry is calculated from a set of mass balance equations, describing the input, output and interactions in each compartment. Vertical heterogeneity is taken into account by differentiating between soil layers. Each soil layer is a completely mixed homogeneous compartment of constant density.

Processes in the model are generally described by zero-order and first-order rate equations and equilibrium equations. To incorporate the effect of environmental changes, most process parameters are described as a function of temperature, soil

moisture content and pH. The model includes all major ions playing an important role in nutrient cycling and soil acidification: H, Al, Na, K, Mg, Ca, NH_4, NO_3, PO_4, SO_4, Cl and organic anions (RCOO). The model is specially developed for application at forest stands that are intensively monitored for atmospheric deposition, precipitation (meteorological conditions), litterfall and soil solution chemistry. The model inputs include atmospheric deposition, global radiation, precipitation and air temperature. Ideally, the model requires these inputs on a daily basis. However, less detailed input is also conceivable. This is especially true for deposition, which is generally available at a larger time scale. The model computes fluxes and concentrations in the vegetation compartments and the soil layers on a daily basis. The basic structure of the model is given in Figure 1.
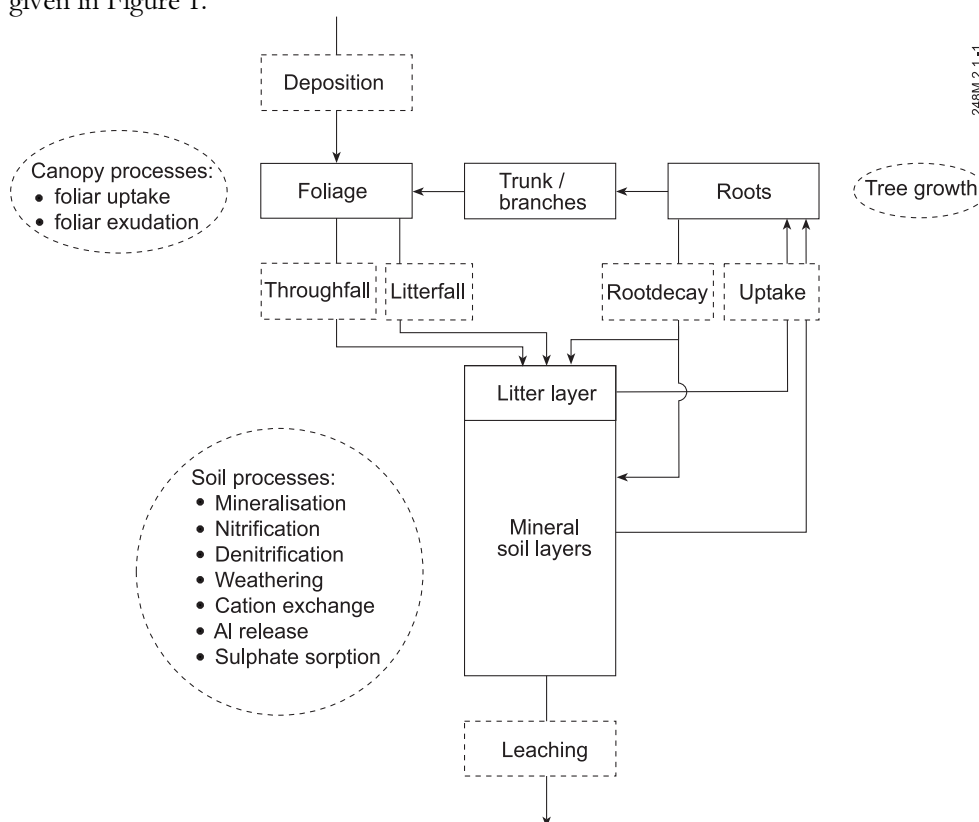
Figure 1 The basic structure of NUCSAM, showing the key pools and fluxes

Biochemical processes

Nutrient cycling

Nutrient cycling includes the daily uptake of nutrients by the growing forest and the return of nutrients to the soil by means of litterfall and root turnover. This cycle is

19

closed by mineralisation. The vegetation removes nutrients from the soil solution and through above ground uptake in order to produce biomass. Losses of nutrients from the vegetation are caused by litterfall, root turnover and foliar exudation. Litterfall is deposited onto the organic surface layer of the soil, whereas roots are decomposed in the organic surface layer and deeper soil layers. Nutrients return to the soil solution by mineralisation of litter and dead roots.

Canopy interactions

The solute fluxes to the soil surface by throughfall are calculated in NUCSAM from the total deposition corrected for canopy interactions, i.e. foliar uptake and foliar exudation. In NUCSAM the total input through atmospheric deposition is derived from the input through dry deposition en bulk deposition. Dry deposition must be specified as model input, whereas bulk deposition is derived from precipitation fluxes and precipitation chemistry. Total deposition of NH_4, NO_3, SO_4 is calculated from the input by dry deposition and bulk deposition:

$$FX_{td} = ffX_{dd} \cdot FX_{dd} + P \cdot cX_i \tag{1}$$

where FX (mol_c ha^{-1} d^{-1}) refers to the flux of element X, ffX_{dd} (-) is the forest filtering factor for dry deposition of element X, P the precipitation (m d^{-1}), c the concentration of element X in wet deposition (mol_c m^{-3}) and where the subscript td refers to total deposition, dd to dry deposition.

The total deposition of the base cations Ca, Mg, K, Na as well as Cl is calculated from the input by bulk deposition solely:

$$FX_{td} = ff_{dd} \cdot FX_{bd} \tag{2}$$

where FX (mol_c ha^{-1} d^{-1}) refers to the flux of element X, ff_{dd} (-) is the forest filtering factor for bulk deposition for base cations and Cl. Note that contrary to ffX_{dd}, ff_{dd} implicitly correct for the input of dry deposition. This is because there is only data available on the bulk deposition of base cations and Cl. Deposition of Al and P is assumed to be negligible, and not included in the model.

Foliar uptake of NH_4, NO_3, SO_4 and H is described as a linear function of the dry deposition of these elements:

$$FX_{fu} = frX_{fu} \cdot FX_{dd} \tag{3}$$

where FX (mol_c ha^{-1} d^{-1}) refers to the flux of element X, frX_{fu} (-) is the uptake fraction of element X and where the subscript fu refers to foliar uptake and dd to dry deposition.

Foliar uptake of NH_4 and H is counterbalanced by exchange with Ca, Mg and K (Draayers, 1993):

$$FCa_{fe} + FMg_{fe} + FK_{fe} = FNH_{4,fu} + FH_{fu} \tag{4}$$

where the subscript *fe* refers to foliar exudation and *fu* refers to foliar uptake. The foliar exudation flux of each individual cation, FX_{fe} (mol_c ha^{-1} a^{-1}) is calculated as:

$$FX_{fe} = frX_{fe} \cdot (FNH_{4,fu} + FH_{fu}) \tag{5}$$

where frX_{fe} (-) is the foliar exudation fraction of Ca, Mg and K. The sum of these fractions equals 1.

Accumulation and leaching from the canopy

To calculate the fluxes and concentrations in the leachate from the canopy (throughfall), it is necessary to determine the throughfall volume and the interception capacity ($A_{wc,mx}$ (m)). The calculation of the throughfall waterflux (*TF*) is described in Section *Canopy interception*. When precipitation exceeds the interception capacity ($A_{wc,mx}$ (m)), accumulated dry deposition and exudated base cations are leached from the canopy. This is modelled by a first order equation.

The accumulation and leaching of constituents form the canopy is calculated from the following mass balance:

$$\frac{dV_c}{dt} = P \cdot cX_{in} + ffX_{dd} \cdot FX_{dd} + FX_{fe} - TF \cdot cX_{out} \tag{6}$$

where V_c is the amount of accumulated deposition in the canopy (mol_c m^{-2}), *P* and *TF* are the daily precipitation and throughfall (m d^{-1}) respectively, cX_{in} and cX_{out} are the constituent concentration in the solute entering and leaving the canopy respectively (mol_c m^{-3}). Integration of Eq. (6) leads to:

$$cX_{out}(t) = \frac{P(t)}{TF(t)} \cdot cX_{in} + (cX_{out} \cdot (t-1) - \frac{P(t)}{TF(t)} \cdot cX_{in}) \cdot \exp\left(-(\frac{TF}{A_{wc,max}}) \cdot t\right) \tag{7}$$

The daily throughfall is then calculated by:

$$FX_{tf}(t) = TF(t) \cdot cX_{out}(t) \tag{8}$$

Litterfall and root turnover

Litterfall and root turnover are the input to the organic pools of N, P, Ca, Mg, K and S. Both processes are described by first-order rate reactions:

$$FX_{lf} = (1 - frX_{re,lv}) \cdot kX_{lf} \cdot Am_{lv} \cdot ctX_{lv} \tag{9}$$

$$FX_{rd} = (1 - frX_{re,rt}) \cdot kX_{rd} \cdot Am_{rt} \cdot ctX_{rt} \tag{10}$$

where k_{lf} and k_{rd} (a^{-1}) are the rate constants for litterfall and root turnover, Am_{lv} and Am_{rt} (kg ha^{-1}) are the amounts of leaves and fine roots, ctX_{lv} and ctX_{rt} (mol$_c$ kg^{-1}) are the contents of element X in leaves and roots, and $frX_{re,lv}$ and $frX_{re,rt}$ (-) are the reallocation fractions for element X in leaves and fine roots, respectively. Am_{lv} and Am_{rt} are directly derived from the given maximum amounts of leaves and roots (see Section *Forest Growth*). The contents of P, Ca, Mg, K and S in leaves and fine roots are assumed to be constant in time. As high contents of nitrogen are caused by high nitrogen deposition rates, the nitrogen content in stems, branches, leaves and fine roots is calculated as a function of nitrogen deposition by:

$$ctN = \begin{cases} ctN_{mn} & \text{for } N_{td} \leq N_{td,mn} \\ ctN_{mn} + (ctN_{mx} - ctN_{mn}) \cdot \dfrac{N_{td} - N_{td,mn}}{N_{td,mx} - N_{td,mn}} & \text{for } N_{td,mn} < N_{td} < N_{td,mx} \\ ctN_{mx} & \text{for } N_{td} \geq N_{td,mx} \end{cases} \tag{11}$$

where ctN_{mn} and ctN_{mx} (mol$_c$ kg^{-1}) are the minimum and the maximum nitrogen content in stems, branches, leaves or fine roots, respectively and $FN_{td,mn}$ and $FN_{td,mx}$ (mol$_c$ ha^{-1} a^{-1}) are the minimum and the maximum deposition levels between which the nitrogen content in biomass is affected. Furthermore, a certain delay period between deposition change and change in N content is considered in NUCSAM.

The resulting annual litterfall and root turnover is distributed over the year, using a monthly varied coefficient to derive monthly variable fluxes.

Mineralisation

To describe the dynamics and mineralisation of organic matter we consider three organic matter pools. Models with only one pool are not able to describe the long-term dynamics of mineralisation, because of the apparent change of the decay constant with time. Several models, such as SOM (Jenkinson and Rayner, 1977), CENTURY (Parton *et al.*, 1987), NICCE (Van Dam and Van Breemen, 1995) and MERLIN (Cosby *et al.*, 1997), distinguish two or more organic matter pools with different decay rates. A similarity of these models is that the organic matter pools are only discernible conceptually and not physically or chemically. A drawback of the use of such a concept is that the pools of organic matter and nutrients are hardly measurable. Consequently, within NUCSAM we choose for pools that can be related with field observations (cf. Groenenberg *et al.*, 1998).

In NUCSAM the three pools: litter, fermented material and humic material were assigned to three morphological distinguishable pools i.e. the L, F and H horizons of the organic surface layer. These morphologically distinguishable pools can be sampled

in the field separately in order to measure pools of organic matter and contents of nutrients. The pools represent successive stages in the decomposition of organic matter, of which the litter compartment is the most easy decomposable compartment and humus, the most refractory compartment. Besides litter input from above ground material the F and H horizon also derive organic matter by the turnover of fine roots, as described before (Eq. 14). Decomposition of roots is described analogous to the decomposition of above ground litter.

Figure 2 gives a schematic presentation of the organic mater pathways in NUCSAM. (cf. Groenenberg *et al.*, 1998).

mi_{lt} = mineralisation of filter
tr_{lt} = transformation of litter to fermented material
mi_{fm} = mineralisation of fermented material
tr_{fm} = transformation of fermented to humic material
mi_{hu} = mineralisation of humic material
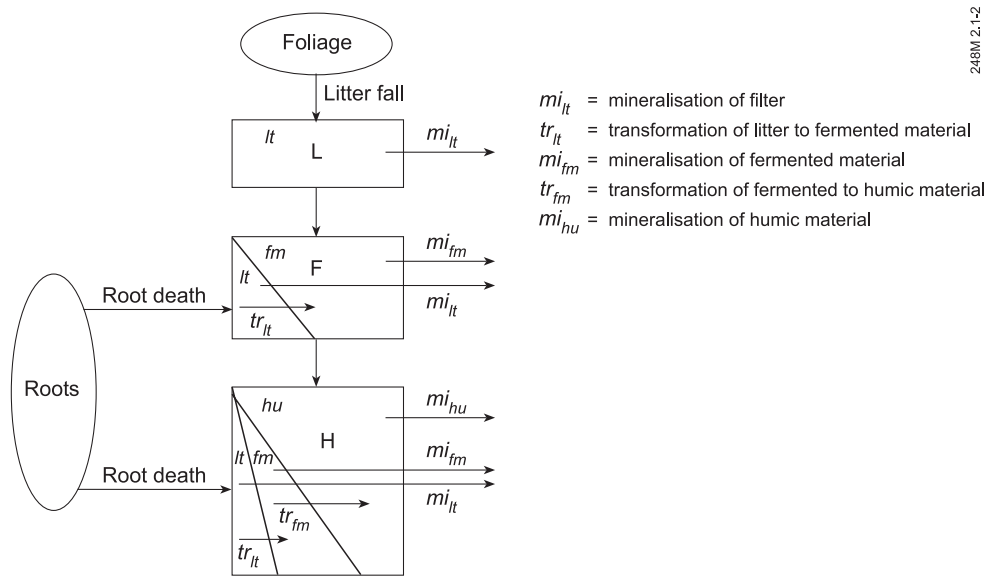
Figure 2 Organic matter pathways in NUCSAM

Fresh organic material (litterfall and root turnover) is added to the litter compartment. Material from the litter compartment is mineralised to CO_2 and DOC (mi_{lt}) and transformed to fermented material (tr_{lt}). Fermented material is mineralised to CO_2 and DOC (mi_{fm}) and transformed to humic material (tr_{fm}). Humic material is the final stage of organic matter decay and therefore is only mineralised (mi_{hu}). Part of the humic material from the organic surface layer may be transferred to the mineral soil as a result of bio-turbation. Organic matter in living biomass is lumped with death organic material because living biomass is only a small fraction of organic matter in soils.

Mass balances of carbon in the various organic pools are determined by the input to the compartment either by addition of fresh organic material (litter compartment) or by transformation of organic matter (fermented and humus compartment) and by the output due to mineralisation and further transformation. Mineralisation and transformation of the organic carbon, nitrogen, phosphorous and

base cations in the pools are modelled as first order processes. For the litter and fermentation layer, the mass balances (mol_c ha^{-1} a^{-1}) thus equal:

$$\frac{d(Am_{lt} \cdot ctX_{lt})}{dt} = (1 - fr_{le}) \cdot FX_{lf} - (k_{mi,lt} + k_{hu,lt}) \cdot Am_{lt} \cdot ctX_{lt} \tag{12}$$

$$\frac{d(Am_{fe} \cdot ctX_{fe})}{dt} = k_{hu,lt} \cdot A_{lt} \cdot ctX_{lt} - (k_{mi,fe} + k_{hu,fe}) \cdot Am_{fe} \cdot ctX_{fe} \tag{13}$$

where fr_{le} (-) is the leaching fraction, this fraction represents the immediate release of nutrients (usually mainly K and Na) to soil solution $k_{mi,lt}$ (a^{-1}) is the mineralisation constant for the litter layer, $k_{hu,lt}$ (a^{-1}) is the humification constant for the litter layer, $k_{mi,fm}$ (a^{-1}) is the mineralisation constant for the fermentation layer and $k_{hu,fe}$ (a^{-1}) is the humification constant for the fermentation layer, ctX_{lt} and ctX_{fe} (mol_c kg^{-1}) are the contents of N, P, K, Ca, Mg and S in the litter and fermentation layers, and Am_{lt} and Am_{fm} (kg ha^{-1}) are the amounts of litter and fermented material, respectively.

In the model the carbon content of organic matter does not change with ongoing decomposition i.e. $ctC_{om} = ctC_{lt} = ctC_{fm} = ctC_{hu}$, this according to the similar carbon content found in bulked samples of the L and F horizons compared to H horizons as determined in a field inventory of 150 forest stands (De Vries *et al.*, 1995b). The contents of other components are dynamic through differences in mineralisation rate (only for N) and the differences in element contents in litterfall and root turnover. The input flux of fresh organic material (root turnover and litterfall) depends on the amount of leaves and roots according to (see Eqs. 9 and 10).

For each soil layer within NUCSAM, a mass balance (mol_c ha^{-1} a^{-1}) can be written for soil organic matter:

$$\frac{d(A_{hu,t} \cdot ctX_{hu,t})}{dt} = \tag{14}$$
$$fr_{hu,t} \cdot (Am_{fm} \cdot ctX_{fm} + k_{mi,rn} \cdot Am_{rn} \cdot ctX_{rn} - k_{mi,hu} \cdot Am_{hu,t} \cdot ctX_{hu,t})$$

where $fr_{hu,i}$ (-) is fraction of soil organic matter in soil layer i, $k_{hu,fm}$ (a^{-1}) is humification constant for the fermentation layer, $k_{mi,rn}$ (a^{-1}) is mineralisation constant for the root necromass, and $k_{mi,hu}$ (a^{-1}) is mineralisation constant for the humus layer. The flux of organic anions, $RCOO_{mi}$, produced during mineralisation of all distinguished organic matter compartments (mol_c ha^{-1} a^{-1}) is calculated from charge balance considerations:

$$RCOO_{mi} = NH_{4,mi} + Ca_{mi} + Ca_{mi} + K_{mi} - SO_{4,mi} - H_2PO_{4,mi} \tag{15)}$$

Part of the organic matter from the humus compartment may be transferred to the mineral soil by bio-turbation. In NUCSAM this is modelled by transferring a constant fraction of the newly formed humus over the mineral soil. layers according to the root distribution.

Mineralisation and transformation rates depend on temperature and moisture content. In NUCSAM maximum rate constants are corrected for non-optimal temperature and moisture effects by multiplying the rate constants with correction factors.

Mineralisation of nitrogen in each organic matter compartment was coupled with carbon mineralisation. At low N contents the rate of nitrogen mineralisation is reduced by multiplying the actual mineralisation rate constant with a C/N ratio dependent reduction factor ($rf_{mi,CN}$) to account for nitrogen immobilisation. This reduction factor is calculated as (Janssen, 1984; De Vries *et al.*, 1994a):

$$rf_{mi,CN} = \begin{cases} 1 & \text{for } CN_s \leq CN_{mo} \\ 1 - \dfrac{CN_s - CN_{mo}}{DA_{mo} \cdot CN_{mo}} & \text{for } CN_{mo} < CN_s < (1 + DA_{mo}) \cdot CN_{mo} \\ 0 & \text{for } CN_s \geq (1 + DA_{mo}) \cdot CN_{mo} \end{cases} \tag{16}$$

with CN_s the C/N ratio of the incoming organic material by leaf fall, root turnover or transformation of the litter or fermented compartment, CN_{mo} is the C/N ratio of the micro-organisms decomposing the substrate (-) and DA_{mo} is the dissimilation to assimilation ratio of the decomposing microbes (-).

Actual values for the mineralisation rate constants are also reduced by factors such as soil moisture. In NUCSAM, the same reduction functions where used as for the SMART2 model (see Chapter 2.3).

Nitrogen transformations

Nitrification (mol_c ha^{-1} a^{-1}) is described as a first-order reaction by:

$$FNH_{4,ni} = -f_c \theta \cdot TL \cdot k_{ni} \cdot cNH_4 \tag{17}$$

where θ (m^3 m^{-3}) is the volumetric water content, TL (m) is thickness of the soil layer, k_{ni} (a^{-1}) is the nitrification rate constant. As with mineralisation, the nitrification rate constant is adjusted on the basis of soil temperature, water content and pH (De Vries, 1988). The nitrification rate constant is reduced at high water contents.

Denitrification (mol_c ha^{-1} a^{-1}) is also described as a first-order reaction by:

$$FNO_{3,de} = -f_c \theta \cdot TL \cdot k_{de} \cdot cNO_3 \tag{18}$$

As with mineralisation, the maximum values for the nitrification and denitrification rate constant, k_{ni} and k_{de}, are adjusted by the moisture content and pH: In NUCSAM, the same reduction functions where used as for the SMART2 model (see Chapter 2.3).

Uptake of nutrients by roots

Total uptake of NH_4, NO_3, Ca, Mg, K, PO_4^{3-} and SO_4 (mol_c ha^{-1} a^{-1}) is described in NUCSAM by a demand function, which consists of maintenance uptake and growth uptake in stems and branches according to:

$$FX_{ru} = FX_{gu} + FX_{lf} + FX_{fe} + FX_{rd} + FX_{fu}$$
(19)

where the subscript *ru* refers to root uptake, *lf* to litter fall, *rd* to root turnover, *fe* to foliar exudation, *fu* to foliar uptake and *gu* to growth uptake. The growth uptake is directly related to stem and branch growth:

$$FX_{gu} = dAm_{st} \cdot (ctX_{st} + fr_{gu,br} \cdot ctX_{br})$$
(20)

where $fr_{gu,br}$ (-) is the fraction of growth uptake for branches, kr_{gl} (kg ha^{-1} a^{-1}) is a logistic rate constant, dAm_{st} (kg ha^{-1} a^{-1}) is the stem growth, $Am_{st,mx}$ (kg ha^{-1}) is the maximum amount of stemwood, ctX_{st} (mol_c kg^{-1}) is content of element X in stemwood, ctX_{br} (mol_c kg^{-1}) is content of element X in branches, t (a) is time, t_{50} (a) is time at which the amount of stemwood is $0.5 \cdot Am_{st,mx}$ and *age* (a) is the stand age at the start of the simulation. The contents of P, Ca, Mg, K and S in stemwood are assumed to be constant in time. The concentration of nitrogen in stems is described as a function of the nitrogen deposition according to Eq. (11).

The nutrient uptake from a given soil layer i is determined by the given root distribution:

$$FX_{ru,i} = FX_{ru} \cdot fr_{rti}$$
(21)

where $FX_{ru,i}$ (mol_c ha^{-1} a^{-1}) is uptake of element X from soil layer i, FX_{ru} (mol_c ha^{-1} a^{-1}) is total uptake of element X, fr_{rti} is the root fraction in soil layer i. The uptake of nutrients for each layer will be extracted from the soil solution. When there is a shortage in a particular layer, this can be compensated by additional uptake from other layers. When there is a shortage for the whole soil profile uptake will be reduced, resulting in lower contents in the vegetation compartments.

Preferential uptake of NH_4 over NO_3 is calculated according to (Gijsman, 1990):

$$FNH_{4,ru} = \cfrac{1}{1 + \cfrac{1}{f_p NH_{4,ru}}} \cdot FN_{ru}$$
(22)

where $f_p NH_{4,ru}$ (-) is a preference factor for the uptake of NH_4 over NO_3. NO_3 uptake is calculated as the difference between total nitrogen uptake and NH_4 uptake:

$$FNO_{3,ru} = FN_{ru} - FNH_{4,ru} \tag{23}$$

The resulting nutrient demand is distributed over the year, using a monthly varied coefficient to derive monthly uptake fluxes from the annual uptake (cf. litterfall and root turnover distribution over the year):

$$FX_{ru,month} = fr_{up,month} FX_{ru,annual} \tag{24}$$

With:

$$\sum_{month=1}^{12} fr_{up,month} = 1 \tag{25}$$

Forest growth

Forest growth is simulated by a logistic growth function. There is no feedback of nutrient cycling on growth rate. Stem growth and canopy growth are calculated as annual fluxes. The model uses monthly varied coefficients to relate annual growth fluxes to monthly nutrient uptake fluxes and litterfall fluxes. Growth constants are taken from available field and literature data. Stem growth, dAm_{st} (kg ha^{-1} a^{-1}), is described with a logistic growth function:

$$dAm_{st} = \frac{Am_{st,mx}}{1 + \exp(-kr_{grl} \cdot (age + t - t_{50}))} \tag{26}$$

where (kr_{grl}, kg ha^{-1} a^{-1}) is a logistic rate constant, dAm_{st} (kg ha^{-1} a^{-1}) is the stem growth, $Am_{st,mx}$ (kg ha^{-1}) is the maximum amount of stemwood, t (a) is time, t_{50} (a) is time at which the amount of stemwood is $0.5 \cdot Am_{st,mx}$ and age (a) is the stand age at the start of the simulation.

Growth of branches (kg ha^{-1} a^{-1}) is derived from the stem growth using a fixed branch to stem ratio fr_{brst} (-):

$$dAm_{br} = fr_{brst} \cdot dAm_{st} \tag{27}$$

The actual amounts of leaves and roots (kg ha^{-1}) are described as a fraction of the maximum amounts:

$$Am_{lv/rt} = \frac{Am_{st}}{Am_{st,mx}} \cdot Am_{lv/rt,mx} \tag{28}$$

where $Am_{lv/rt}$ (kg ha^{-1}) is the actual amount of foliage (lv) or roots(rt) and $Am_{lv/rt,mx}$ (kg ha^{-1} a^{-1}) is the given maximum amounts of foliage (lv) or roots(rt). Generally the maximum amount of leaves and roots is achieved several decades earlier than the maximum amount of stems, but this was not considered in this version of NUCSAM. The nutrient contents of base cations and sulphur remain constant in all biomass compartments, whereas the nitrogen contents are calculated as a function of the atmospheric deposition. In NUCSAM we used the same relation between N content in leaves and N deposition as used in RESAM (cf. De Vries *et al.*, 1995a) and in SMART2 (see Chapter 2.3).

Geochemical process

Rate limited reactions

Protonation of organic anions and weathering are described by rate-limited first-order reactions. Protonation (the association of organic anions with H) is described according to:

$$FRCOO_{pr} = -\theta \cdot TL \cdot k_{pr} \cdot cRCOO \tag{29}$$

where k_{pr} (a^{-1}) is a pH dependent protonation rate constant, θ the volumetric moisture content (m m^{-3}), TL the thickness of the soil layer (m) and cRCOO the concentration of organic anion in the soil solution.

Weathering (dissolution) fluxes of Al and base cations from carbonates, silicates (primary minerals) and aluminium hydroxides (mol$_c$ ha^{-1} a^{-1}) are described by first-order rate reactions and Elovich reactions respectively. The flux of calcium from dissolution of carbonates is described by:

$$FCa_{we,cb} = \rho \cdot TL \cdot kCa_{we,cb} \cdot ctCa_{cb} \cdot (cCa_e - cCa) \tag{30}$$

where ρ (kg m^{-3}) is the bulk density, $kCa_{we,cb}$ (m^3 mol$_c^{-1}$ a^{-1}) is a weathering rate constant, $ctCa_{cb}$ (mol$_c$ kg^{-1}) is the content of Ca in carbonates, and cCa and cCa_e (mol$_c$ m^{-3}) are the concentration and equilibrium concentration of calcium (cf. Eq. 30), respectively. When the soil solution is supersaturated with respect to calcite, equilibrium is enforced. The flux of base cations from silicates (primary minerals) is described by (Van Grinsven, 1988):

$$FX_{we,pm} = \rho \cdot TL \cdot kX_{we,pm} \cdot ctX_{pm} \cdot cH^{\alpha(X)} \tag{31}$$

where $kX_{we,pm}$ (m^3 mol$_c^{-1}$ a^{-1}) is a weathering rate constant, ctX_{pm} (mol$_c$ kg^{-1}) is the content of base cation X in primary minerals, cH (mol$_c$ m^{-3}) is the H concentration and α (-) is a parameter. The weathering of aluminium from primary minerals is described by:

$$FAl_{we,pm} = 3FCa_{we,pm} + 0.6FMg_{we,pm} + 3FK_{we,pm} + 3FNa_{we,pm} \tag{32}$$

This equation comes down to congruent weathering of Anorthite (Ca), Chlorite (Mg), Microcline (K) and Albite (Na). When the solution is under saturated with respect to natural gibbsite, the release of aluminium from hydroxides is described by an Elovich equation:

$$FAl_{we,ox} = \rho \cdot TL \cdot kEl_1 \cdot \exp(kEl_2 \cdot ctAl_{ox}) \cdot (cAl_e - cAl) \tag{33}$$

with cAl and cAl_e (mol_c m^{-3}) as the actual and equilibrium concentration of aluminium in the soil solution, and $kEl1$ (m^3 mol_c^{-1} a^{-1}) and $kEl2$ (kg mol_c^{-1}) as Elovich constants. As with calcite, equilibrium is enforced with respect to Al hydroxide when the soil solution is supersaturated (cf. Eq. 33).

Weathering of P is described by the rate-limited equation:

$$FP_{we} = \rho \cdot TL \cdot kP_{we} \cdot ctP_t \cdot (cP_e - cP) \tag{34}$$

where ϱ (kg m^{-3}) is the bulk density, kP_{we} (m^3 mol_c^{-1} a^{-1}) is the weathering rate constant for P, ctP_t (mol_c kg^{-1}) is the total phosphate content, cP (mol_c m^{-3}) is the actual phosphate concentration in the soil solution, and cP_e (mol_c m^{-3}) is the equilibrium concentration of phosphate with apatite, variscite or strengite.

Equilibrium reactions

We assume chemical equilibrium for the dissociation of CO_2, the concentration of Ca in the presence of Ca carbonate, the concentration of Al in contact with Al hydroxide, adsorption/desorption of SO_4 and cation exchange. The concentration of Ca in equilibrium with Ca carbonate is calculated as:

$$cCa_e = KCa_{cb} \cdot \frac{pCO_2}{(cHCO_3^-)^2} \tag{35}$$

where KCa_{cb} (mol^3 L^{-3} bar^{-1}) is the equilibrium constant for Ca carbonate dissolution and pCO_2 (bar) is the partial CO_2 pressure in the soil. In NUCSAM we assumed the pCO_2 in the soil to constant. The bicarbonate concentration in the soil solution (mol_c m^{-3}) is calculated from:

$$cHCO_3^- = \frac{(KCO_2 \cdot pCO_2)}{cH^+} \tag{36}$$

where KCO_2 (mol^2 L^{-2} bar^{-1}) is the product of Henry's law constant for the equilibrium between CO_2 in soil water and soil air, and the dissociation constant of H_2CO_3. The concentration of Al in equilibrium with natural gibbsite is calculated by:

$$cAl_e = KAl_{ox} \cdot cH^3 \tag{37}$$

where KAl_{ox} (mol^{-2} L^2) is the equilibrium constant for aluminium hydroxide dissolution.

Cation exchange is described by Gaines-Thomas equations with Ca as reference ion according to:

$$\frac{frX_{ac}^2}{frCa_{ac}^{z_x}} = KX_{ex} \cdot \frac{cX^2}{cCa^{z_x}} \tag{38}$$

with z_x (-) as the valence of cation X, KX_{ex} ((mol L^{-1})$^{z_x-2}$) as the Gaines-Thomas selectivity constant for exchange of cation X against Ca, frX_{ac} (-) is the fraction of cation X on the adsorption complex. X equals H, Al, Fe, Mg, K, Na or NH_4.

frX_{ac} is calculated by:

$$frX_{ac} = \frac{ctX_{ac}}{CEC} \tag{39}$$

where CEC (mol$_c$ kg^{-1}) is the cation exchange capacity. The sum of all fractions is equal to 1.

SO_4 and H_2PO_4 sorption in each soil layer are described with a Langmuir equilibrium equation according to:

$$ctX_{ad} = \frac{XSC \cdot cX}{\dfrac{1}{KX_{ad}} + cX} \tag{40}$$

where ctX_{ad} (mol$_c$ kg^{-1}) is the sorbed amount of anion X, XSC (mol$_c$ kg^{-1}) is the sorption capacity for X (cf. Eq. 75 for S and Eq. 76 for P), and KX_{ad} (m^3 mol$_c^{-1}$) is the equilibrium constant for sorption of anion X.

NUCSAM also includes ion speciation, such as the hydrolysis of Al and complexation of aluminium with organic anions. All equilibrium reactions are calculated with the chemical equilibrium program EPIDIM (Rijtema et al., 1999). In EPIDIM the chemistry of soil solution is defined by a set of chemical components (such as H and NO_3) and a set of ion species or complexes (such as HCO_3 and $AlSO_4$) with associated specific formation constants. The formation of a certain species out of the components can be written as:

$$A_i = \sum_{j=1}^{M_B} a_{i,j} B_j \quad \text{for } i=1,\ldots,N \tag{41}$$

where $a_{i,j}$ is the stoichiometric coefficient of component $\boldsymbol{A}_i$ in the formation of species B_j, and M_B the number of species B and N the number of components.

The concentration of each species can be expressed in the concentration of the components according to:

$$B_j = K_j \prod_{i=1}^{N} A_i^{a_{i,j}} \quad \text{for } j=1,\ldots,M_B \tag{42}$$

where B_j is the concentration of species j, A_i is the concentration of component i and N the number of components, K_j the formation constant of species j. $a_{i,j}$ is the stoichiometric coefficient and M_B the number of species B. For each component the total concentration is calculated as:

$$A_k^T = \sum_{j=1} \left(a_{i,j} K_j \prod_{i=1}^{N} A_i^{a_{i,j}} \right) \tag{43}$$

where A_k^T is the total concentration of component k.

The total concentrations (A_k^T) are known from the mass balance calculations (see Eq. 68). This results in a set of N equations with N unknowns, i.e. the component concentration. This set of equations is then solved numerically with a Newton Raphson iteration scheme.

To correct for the non ideal behaviour of ions, the formation constants K_j used are the conditional constants, corrected for the ionic strength in the soil solution. These modified constants are calculated from the thermodynamic formation constants of the species and activity coefficient of the species and components:

$$K_j = K_j^0 \frac{\displaystyle\prod_{i=i}^{N} \gamma_i^{a_{i,j}}}{\gamma_j} \tag{44}$$

where γ_i and γ_j are the activity coefficient of the component i and species j respectively, K_j the corrected formation constant and K_j^0 the standard formation constant. Activity constants are calculated with a Davis approximation (cf. Stumm and Morgan, 1981).

Water, heat and solute transport

Water transport

To simulate evaporation, transpiration, soil water fluxes and soil water contents, an adapted version of the SWATRE model (Belmans *et al.*, 1983) was used as hydrological submodel, as described below.

Potential evapotranspiration

Potential transpiration is calculated by multiplying the reference evapotranspiration according to Makkink (1957) by an empirical, season dependent crop factor. For conditions in the Netherlands, the Makkink equation is written as:

$$E_r = \frac{\beta}{\lambda} \cdot \frac{s}{s + \gamma} \cdot K \downarrow \cdot f_s \tag{45}$$

in which E_r (m d^{-1}) is the Makkink reference evapotranspiration, s (g g^{-1} K^{-1}) is derivative of the saturation water vapour pressure temperature curve, γ (g g^{-1} K^{-1}) is psychrometer constant, $K\downarrow$ (W m^{-2}) is global radiation, λ (J g^{-1}) is specific heat of evaporation and β (-) is empirical constant related to the geographical latitude, which for conditions in the Netherlands is equal to 0.65.

Canopy interception

Water is supplied to the canopy by precipitation and lost by throughfall and evaporation of intercepted water. The daily throughfall is calculated as:

$$TF = P - E_i \tag{46}$$

where P (m d^{-1}) is daily precipitation, TF (m d^{-1}) is daily throughfall and E_i (m d^{-1}) is evaporation of intercepted water. The amount of water intercepted is calculated by using a coefficient of free throughfall in combination with a threshold value. A relatively simple empirical one-layer canopy-interception submodel is used in order to calculate the throughfall flux (*TF*).

   The calculation of the interception evaporation is based on Gash (1979). An analytical approximation is used to calculate daily interception. However, unlike the original Gash model, NUCSAM uses daily evaporation rates instead of yearly average evaporation rates and takes in to account the changes in the amount of water stored in the canopy. As evaporation rates are lower during rainfall, empirical correction factors have been introduced for the dry and wet part of the day. First the amount of rainfall required to saturate the canopy, P_s (m), is calculated:

$$P_s = -A_{wc} \frac{\overline{R}}{E_r \cdot fE_{wet}} \cdot \ln\left(1 - \frac{E_r \cdot fE_{wet}}{\overline{R}} \cdot \frac{1}{sc}\right). \tag{47}$$

where sc (-) the soil cover fraction, E_r (m d^{-1}) the reference evapotranspiration, fE_{wet} (-) a correction factor for the evaporation rate during rainfall, $\overline{R}$ (m d^{-1}) the average rainfall intensity, P (m) the precipitation and A_{wc} (m) the maximum amount of water stored in the canopy:

$$A_{wc} = A_{wc,\max} - A_{wc}(t-1) \tag{48}$$

with $A_{wc.max}$ is the maximum amount of water that can be stored in the canopy and $A_{wc}(t-1)$ is the amount of water in the canopy at the previous time step.

The maximum interception evaporation ($E_{i,max}$) is calculated as:

$$E_{i,\max} = \begin{cases} P \cdot sc & \text{if } P < P \\ P_s \cdot sc + \dfrac{E_r \cdot fE_{wet}}{\overline{R}} \cdot (P - P_s) & \text{if } P \geq P_s \end{cases} \tag{49}$$

The amount of water stored in the canopy directly after rainfall equals:

$$A_{wc,0} = A_{wc}(t-1) + E_{i,\max} \tag{50}$$

The canopy water storage at the end of the day is calculated as:

$$A_{wc}(t) = A_{wc,0} \cdot e^{-\frac{E_r \cdot fE_{dry}}{A_{wc,\max}} \cdot t_d} \tag{51}$$

where A_{wc} (m) is the water storage at the end of the day, $A_{wc,0}$ (m) the water storage at the start of the dry part of the day, fE_{dry} (-) a correction factor for the evaporation rate during the dry part of the day, and t_d (d) the length of the dry part of the day, which is calculated from the precipitation and average rainfall intensity:

$$t_d = 1 - \frac{P}{\overline{R}} \tag{52}$$

The actual daily interception evaporation equals the maximum interception evaporation minus the change in water storage in the canopy:

$$E_i = E_{i,\max} - \frac{A_{wc}(t) - A_{wc}(t-1)}{\Delta t} \tag{53}$$

Transpiration and soil evaporation

Potential transpiration and potential soil evaporation are calculated by partitioning the potential evapotranspiration on the basis of the available energy by a method equivalent to Van Grinsven *et al.* (1987) and Tiktak and Bouten (1992):

$$
\begin{aligned}
E_{pl}^{*} &= f_c \cdot \left(sc \cdot E_r - f_i \cdot E_i \right) \\
E_s^{*} &= (1 - sc) \cdot E_r
\end{aligned}
\tag{54}
$$

where E_{pl}^{*} (m d^{-1}) is the potential transpiration, E_s^{*} (m d^{-1}) is the potential soil evaporation, f_c (-) is an empirical factor that accounts for crop characteristics, sc (-) is the soil cover fraction, E_i (m d^{-1}) is evaporation of intercepted water, and f_i (-) is the fraction of the daily interception that reduces the potential transpiration. The soil cover is calculated on the basis of the leaf area index.

The actual soil evaporation rate is calculated as a function of time since the last rainfall event according to Black *et al.* (1969):

$$
E_s = \varepsilon \cdot \left(\sqrt{t_d + 1} - \sqrt{t_d} \right) \cdot E_s^{*}
\tag{55}
$$

where E_s (m d^{-1}) is actual soil evaporation, t_d (d) is time from the start of a drying cycle and ε (d$^{-1/2}$) is an empirical parameter. The potential transpiration is distributed among soil layers on the basis of the root length distribution. Reduction of water uptake occurs when soil water pressure heads drop below or exceed a threshold value. The root water uptake fluxes are summed to get the actual transpiration.

Snow accumulation and snowmelt

A snow module based on the Birkenes model (Christophersen *et al.*, 1983) was included in NUCSAM. Precipitation is partitioned into snow and rain as a function of the average daily temperature:

$$
P_r = = \begin{cases} P & \text{if } T_r \geq T_s \\ P \cdot \dfrac{T - T_s}{T_r - T_s} & \text{if } T_r < \overline{T} < T_s \\ 0 & \text{if } T_r \geq T_s \end{cases}
\tag{56}
$$

where P_r is the total amount of rainfall (mm d^{-1}), P is the total daily precipitation (snow and rain, expressed as the total amount of water) in mm d^{-1}, T the mean daily temperature, T_r the temperature above which all precipitation is rainfall and T_s the temperature below which all precipitation is snow. The snow part P_s (mm d^{-1}) follows then from:

$$
P_s = P - P_r
\tag{57}
$$

Snowmelt (S_m) was calculated according to Bergström (1975), which included a degree-day approach combined with a parameter that allows an increasing effect of temperature on the snowmelt as the snowmelt proceeds:

$$S_m = C_0 (1 + C_{eff} \cdot \sum M_s)(T - T_0)$$
(58)

where C_0 is the initial degree-day factor (mm °C^{-1} day^{-1}), C_{eff} the rate of increase of the degree-day factor (mm^{-1}), $\sum M_s$ the accumulated melt during a period of snowcover (mm), T the mean daily temperature and T_0 the threshold temperature for snowmelt.

Sublimation of snow is calculated as:

$$S_b = f_{snsb} \cdot E_r$$
(59)

where f_{snsb} is a factor to calculate snow sublimation form the potential evapotranspiration.

Snow accumulation is calculated in terms of the amount of water in the snow pack, by:

$$S = S_0 + (P_s - S_b + S_m) \cdot \Delta t$$
(60)

where S and S_0 are the amount of water in the snow pack in the actual and former time step (mm), P_S the amount of snowfall (mm d^{-1}), S_b the sublimation rate (mm d^{-1}), S_m the snowmelt rate (mm d^{-1}) and ΔT the time step, which is one day. Sublimation of snow was calculated as a fraction of daily evapotranspiration.

The concentration in snowmelt is included in the as first-order process (see Chen *et al.*, 1983):

$$cX_{sn} = cX_{sn,t-1} e^{-k_{sn} \cdot S_m \Delta t}$$
(61)

where k_{sn} is the leaching coefficient (-), $cX_{sn,t-1}$ is the concentration of X in the snowpack at the beginning of the time step and cX_{sn} at the end of the time step (mol$_c$ m^{-3}).

Soil water transport

Transport of water through the soil is calculated with a numerical solution of Richard's equation:

$$\frac{\partial \theta}{\partial t} = \frac{\partial}{\partial z} \left[k(h) \cdot (\frac{\partial h}{\partial z} + 1) \right] - s(h)$$
(62)

where θ (m³ m⁻³) is volumetric water content, t (d) time, z (m) vertical position in the soil, h (m) soil water pressure head, K (m d⁻¹) hydraulic conductivity and S (d⁻¹) sink term accounting for root water uptake. The model allows for upward water transport.

Soil heat transport

Soil temperature influence the rate of the biogeochemical processes and the chemical equilibrium constants. The soil temperature module in NUCSAM is almost identical as used in the ILWAS-model (Gherini *et al.*, 1985). In the simulation of soil temperature, it is assumed that the forest floor is covered by canopy such that the direct solar radiation reaching the soil is negligible. The heat fluxes over the soil layers are driven by advection through the infiltration of water and conductance by the soil media. Each layer has a heat capacity that is a function of the soil moisture content:

$$Q_i = (1 - \theta_i^s)C_s + \theta_i(t)C_W \tag{63}$$

where Q_i is the heat capacity of layer i (kJ m⁻³ °C⁻¹), C_s is the heat capacity of the solid phases: 2500 kJ m⁻³ C⁻¹ for organic matter and 2000 kJ m⁻³ C⁻¹ for mineral phase (values taken from Koorevaar *et al.*, 1983), C_W is the heat capacity of water, θ_i^S the porosity of the soil (m³ m⁻³) and $\theta_i(t)$ the actual soil moisture content at t=t. The heat capacity of air is negligible.

The thermal conductivity of the soil media is also calculated as a function of the actual soil moisture content, as an average per soil layer (t):

$$\lambda_i = \frac{\theta_i(t)\lambda_W + f_{tc}(1 - \theta_S)\lambda_S}{\theta_i(t) + f_{tc}(1 - \theta_S)} \tag{64}$$

where λ_S and λ_W are the thermal conductivity (kJ m⁻³ °C⁻¹) if soil layer i (that includes organic matter and mineral phase, 0.25 and 8.8 J m⁻¹ s⁻¹ °C⁻¹ for and water respectively and f_{tc} a weighing factor dependent on the bulk density of the soil.

With the heat capacity and conductivity of the soil media, the soil heat input flux ($F_{Q,in,i}$) and output flux ($F_{Q,out,i}$) (kJ d⁻¹) per soil layer reads:

$$F_{Q,in,i} = F_{W,i-1}(t)T_{i-1} + \lambda_{i-1}(T_i - T_{i-1}) \tag{65}$$

$$F_{Q,out,i} = F_{W,i}(t)T_i + \lambda_i(T_i - T_{i+1}) \tag{66}$$

where $F_W(t)$ is the water input flux from layer i-1 (m³ d⁻¹), T_{i-1} and T_i the temperature of layer i-1 and i (°C), and λ_i the thermal conductivity of layer i.

The heat balance for each soil layer is defined by:

$$F_{Q,in,i} - F_{Q,out,i} = Q_i(T_i(t-1) - T_i(t)) \tag{67}$$

where Q_i is the heat capacity of layer i (kJ m^{-3} °C^{-1}) and $T_i(t\text{-}1)$ and $T_i(t)$ the temperature (°C) of layer i at the beginning and at the end of the time step respectively. The heat balance equation for each soil layer can be written in a tridiagonalmatrix with the temperature (T_i) of each layer on the diagonal. From this system the temperature for each layer is solved using an implicite solution method. For the upper boundary, the temperature of the ambient air is used. The lower boundary is set to a constant temperature of 10 °C, which is the average temperature of groundwater in the Netherlands.

Solute transport

Solute transport within NUCSAM is calculated by the solute transport module TRANSOL (Rijtema *et al.*, 1999). The basic equation of TRANSOL is the convection-dispersion equation:

$$\frac{\partial \theta c}{\partial t} = -\frac{\partial J_s}{\partial z} + \Delta (R_{source} - R_{sink}) \tag{68}$$

where θ is the soil moisture content (m m^{-3}), c the concentration of a constituent in the soil solution (mol$_c$ m^{-3}), J_s the vertical solute flux (mol$_c$ m^{-2} d^{-1}), z the soil depth (m), R_{source} and R_{sink} the source and sink terms (mol$_c$ m^{-3} d^{-1}) respectively. Within TRANSOL the convection-dispersion equation is solved semi-analytically. Since the incoming and outcoming fluxes are constant with time during a time-step, the soil moisture content varies linear with time, according to:

$$\theta(t) = \theta(t_0) + \varphi t \tag{69}$$

where $\theta(t_0)$ is the moisture content at the beginning of the time-step t and φ the rate of change of θ within the time-step. The value of φ is calculated every time-step on the basis of θ's from the two previous time-steps. Using the left hand side of Eq. 68, the rate of change in the soil solution is defined by:

$$\frac{\partial \theta c}{\partial t} = \left(\theta(t_0) + \varphi t\right)\frac{\partial c}{\partial t} + \varphi c \tag{70}$$

When neglecting the second order term of diffusion/dispersion, the remaining first order equation can be solved analytically. The transport term is numerically approximated by:

$$-\frac{\partial J_s}{\partial z} = \frac{\partial}{\partial z}\left(qc - \theta \, D_{dd} \frac{\partial c}{\partial z}\right) \approx \frac{q_{i-\frac{1}{2}}}{\Delta z}c_{i-1} - \frac{q_{i+\frac{1}{2}}}{\Delta z}c_i \tag{71}$$

where q is the waterflux (m d^{-1}) and D_{ss} diffusion/dispersion coefficient (m^2 d^{-1}). The diffusion/dispersion is then mimicked by numerical dispersion by choosing an appropriate layer thickness.

2.1.3   Data used for the NUCSAM application to the Speulder forest

Site description

Input data were derived mainly from the data set of the Speuld location as described in Tiktak *et al.* (1995). The Speuld site is located in a 2.5 ha Douglas fir stand at an altitude of 50 m. The stand is surrounded by a large forest of approximately 50 km^2; the nearest edge is at a distance of about 1.5 km. The soil is a well-drained Typic Dystochrept (USDA) or Cambic podzol (FAO, 1988) on heterogeneous sandy loam and loamy sand textured ice-pushed river sediments. A full soil profile description is included in Tiktak *et al.* (1988). The water-table is at a depth greater than 40 m throughout the year. In 1988, the start of the monitoring period, the stand was 29 years old.

The characteristics of the data-set

Measurements were carried out at different spatial scales and at different positions within the stand. Most soil hydrological measurements were carried out at one plot of 30×30 m^2, although an attempt has been made to scale these measurements to stand average values (Bouten *et al.*, 1992). Soil chemical measurements are 'point' measurements. Samples were taken from three plots and the volume of soil sampled is small. Also the tree physiological measurements were carried out at one point within the forest stand. On the other hand, eddy correlation measurements of deposition and transpiration are representative at a scale which is larger than the stand. Measurements of throughfall amounts, throughfall quality and of forest growth, although point measurements, were scaled to average values. However, all these measurements were carried out at the Eastern half of the stand, possibly leading to a deviation from stand average values.

Due to these different spatial scales it is almost impossible to combine all measurements within one data-set. Consider the following example: If the hydrological part of NUCSAM is calibrated using the average transpiration measured by eddy correlation as a criterion, the hydrological regime will be different from the hydrological regime at the soil chemical sampling points. For this reason, the hydrological part of NUCSAM (i.e. an adapted version of the model SWATRE, cf. Section *Water transport*) was calibrated using data from the soil monitoring plot only. This calibration is not representative for the stand as a whole, but can be used in combination with the soil chemical data-set. For the derivation of the geo-chemical input parameters of NUCSAM, the data-set for plot B was used (see Tiktak *et al.*, 1995).

Hydrological data

Vegetation dependent properties

The most important vegetation dependent hydrologic parameters are presented in Table 1. Interception capacity and efficiency are based on measurements with a microwave transmission technique and calibration of detailed interception models (Bouten, 1992). Soil cover fraction, reduction point and wilting point and crop factor are based on calibration of the hydrological model SWIF on the Speuld site (Tiktak and Bouten, 1990, 1994). Average precipitation intensity and evaporation factors are based on the calibration of the measured amount of throughfall. Root density data are based on measurements in June 1989 (Olsthoorn, 1991).

Table 1 Vegetation dependent hydrologic parameter values for the Speulderbos site

Parameter	Symbol	Value	Unit
Soil cover fraction [1]	sc	0.9	-
Average precipitation intensity [2]	R	10.0	mm
Interception capacity [2]	$A_{wc,max}$	2.1	mm
Factor for evaporation [4]			
during dry part of day:	fE_{dry}	1.5	-
during wet part of day:	fE_{wet}	0.5 - 9.0	-
Reduction point [1]	$b_{r,d}$	-600	cm
Wilting point [1]	$b_{r,w}$	-6000	cm
Crop factor [1]	f_c	0.85	-
Root density distribution[3]:			
Litter	R_i	0.05	-
0-20 cm	R_i	0.30	-
20-40 cm	R_i	0.34	-
40-60 cm	R_i	0.15	-
60-80 cm	R_i	0.08	-
> 80 cm	R_i	0.08	-

[1] Based on Tiktak and Bouten (1990; 1994).

[2] Measured by Bouten (1992).

[3] Based on root length distribution measurements by Olsthoorn (1991).

[4] Based on the calibration of SWATRE to Speuld.

Soil physical characteristics

Water retention characteristics were obtained from simultaneously measured average water contents and pressure heads at a plot of 30×30 m². The physical characteristics are valid for the same plot as the monitoring data. To extrapolate the retention characteristics outside the range of pressure heads that can be measured with tensiometers the measured data were fitted to the Mualem-Van Genuchten functions (Van Genuchten, 1980):

$$\theta(h) = \theta_r + \frac{\theta_s - \theta_r}{[1 + (\alpha \cdot |h|)^n]^m} \tag{72}$$

where θ_s (m³ m⁻³) is saturated volumetric water content, θ_r (m³ m⁻³) residual water content, h (m) pressure head, a (m⁻¹) reciprocal of the air entry value, n (-) a fitting parameter and $m = 1-1/n$. Table 2.3 summarises the results of the fitting. Conductivity characteristics were not measured for the Speuld site because of the high spatial variability of the Speuld site and the associated large number of samples which have to be analysed to obtain representative conductivity data. Alternatively, theoretical conductivity characteristics were used according to the Mualem model (Van Genuchten, 1980):

$$K(h) = K_s + \frac{[(\alpha \cdot |h|)^{n-1} \cdot (1 + (\alpha \cdot |h|)^n)^{-m}]^2}{[1 + (\alpha \cdot |h|)^n]^{\frac{m}{2}}} \tag{73}$$

where, K_s (m d⁻¹) is the hydraulic conductivity. Values for the saturated hydraulic conductivity were based on calibration on the Speuld data set during the winter period when evapotranspiration is small (Tiktak and Bouten, 1990).

Table 2 Parameters of the Mualem-Van Genuchten functions to describe the soil physical properties. Source: Tiktak and Bouten (1992)

Depth	θ_s (m³ m⁻³)	θ_r (m³ m⁻³)	a (cm⁻¹)	n (-)	K_s (cm d⁻¹)
litter	0.50	0.00	0.10	1.25	800
0-60 cm	0.33	0.00	0.10	1.25	800
> 60 cm	0.21	0.00	0.04	1.40	100

Snow parameters

Unlike the previous parameters, snow parameters were not based on measurements at Speuld, since they were not available. Most snow parameters (Table 3) were taken from Bergström (1975), except for the rate of increase of the degree-day factor (C_{eff}) the snowmelt rate (S_m) which was calibrated on data from an experimental forest stand in Solling, Germany (cf. Groenenberg *et al.*, 1995) and the leaching coefficient (k_{sn}) which was set to 1.

Table 3 Parameters used to calculate snow processes

Parameter	Value	Unit
T_s	-1.5	˚C
T_r	1.6	˚C
T_o	0.0	˚C
C_{eff}	0.25	mm^{-1}
C_0	0.1	mm ˚C^{-1} day^{-1}
k_{sn}	1	-

Geochemical data

Measured soil data used for the derivation of geochemical parameters were often available for different depths in the soil profile. In order to obtain a coherent set of parameters and initial conditions of variables, input data were scaled to the same depths according to:

$$\hat{X}_z = \frac{\Delta z_2 X_1 + \Delta z_1 X_2}{\Delta z_1 + \Delta z_2} \tag{74}$$

where X_z is the estimated value of state variable X at depth z, $X_{1/2}$ is the measured value of state variable X at depth $z_{1/2}$, and $z_{1/2}$ is the nearest depth with measurement $z_1 < z < z_2$. For state variables related to a soil layer with thickness Δz, z is the depth in the middle of that layer.

Exchange constants

Gaines-Thomas exchange coefficients were calculated from the long-term average soil solution concentrations extracted with cups (plot B; Tiktak *et al.*, 1995) and the measured amount of exchangeable cations (Tiktak *et al.*, 1995). From the concentrations, activities were calculated with the chemical equilibrium program EPIDIM (Rijtema *et al.*, 1999). Coefficients were calculated with Eq. (33) using Ca as the reference ion. As the content of exchangeable base cations was below the detection limit, the exchangeable fractions (fraction of total CEC) of all base cations were set to 0.01 to calculate Gaines-Thomas exchange coefficients and to initialise the model. Results are shown in Table 4.

Table 4 Gaines-Thomas exchange coefficients (mol l^{-1})$^{z-2}$ and cation exchange capacity (mmol$_c$ kg^{-1})

Depth (cm)	Gaines-Thomas exchange coefficient relative to Ca (mol l^{-1})$^{z-2}$						CEC (mmol$_c$ kg^{-1})
	H	Na	K	NH$_4$	Mg	Al+Fe	
-9-0	4.00×10^4	42.9	151.9	1890.9	3.4	561.7	245.7
0-5	1.70×10^4	22.3	128.3	289.1	2.5	813.7	96.9
5-10	0.57×10^4	6.7	80.6	13.6	1.2	127.5	58.3
10-20	0.13×10^4	6.0	120.8	6.7	1.1	73.0	57.1
20-30	0.87×10^4	8.6	267.0	11085.1	1.4	32.2	42.8
30-40	6.66×10^4	5.1	162.5	2136.4	0.9	1.8	29.0
40-50	2.50×10^5	3.3	93.7	1624.7	0.7	0.4	26.9
50-60	2.95×10^5	3.1	69.6	10526.7	0.7	0.4	25.7
60-70	2.43×10^5	3.5	59.2	19454.1	0.8	0.7	27.7
70-80	2.33×10^5	4.5	56.5	3625.4	1.0	1.4	28.8
80-100	2.83×10^5	6.6	52.5	0.0	1.2	2.5	39.7

Weathering rate parameters

Parameters for weathering of silicates (Eq. 31) were calculated from results of batch experiments (De Vries, 1994) for a generic Cambic Podzol (Table 5). They estimated the total weathering flux for a 70 cm profile by dividing the fluxes derived from the batch experiments by 50. This factor was introduced to account for differences between field and laboratory conditions. The fluxes presented by De Vries (1994) were multiplied by a factor 10/7 to calculate the weathering fluxes for a 1 m profile. The weathering rate constant for the Speuld profile, $kX_{we,pm}$, is calculated as follows. The coefficients a and $kX_{we,pm}$ are assumed to be layer independent. Parameter a was taken directly from De Vries (1994). The average pH value as measured for plot B by Van der Maas and Pape (1990) was substituted. Total element contents and the bulk density were taken from Tiktak *et al.* (1988). Equation (26) can be written down for each soil layer. By substituting all parameters into equation (26), and by assuming that the total weathering fluxes calculated by this equation equals the weathering flux by De Vries (1994), the weathering rate constant can be calculated. The results of the calculations are presented in Table 5.

Parameters for weathering of secondary Al compounds (Table 6) were taken from batch experiments as described by De Vries (1994). They investigated a total number of 15 sites throughout the Netherlands. For the model applications, we selected the soil horizons that showed most resemblance to Speuld. These included the Ah, Bhs, BCs and C horizons.

Table 5 Parameters for weathering of silicates (Eq. 31)

Cation	Total weathering flux[1] (mol$_c$ ha^{-1} a^{-1})	pH dependent		pH independent
		$kX_{we,pm}$ (a^{-1})	α (-)	$kX_{we,pm}$ (a^{-1})
Na	80	8.43×10^{-2}	0.87	4.19×10^{-5}
K	75	2.33×10^{-1}	1.02	4.87×10^{-2}
Ca	45	2.26×10^{-1}	0.85	7.11×10^{-3}
Mg	20	1.92×10^{-1}	1.54	8.81×10^{-1}

[1] source: De Vries (1994)

Table 6 Parameters for the calculation of weathering of oxalate extractable Al (De Vries, 1994)

Depth (cm)	$kEl1$ (kg^{-1} a^{-1})	$kEl2$ (m^3 mol$_c$$^{-1}$)	Horizon in De Vries (1994)
0-10	1.13×10^{-6}	11.4	Ah
10-40	2.04×10^{-4}	9.1	Bhs
40-80	7.49×10^{-4}	7.3	Bcs
80-100	1.67×10^{-4}	9.8	C

Sulphate and phosphate sorption parameters

The sulphate sorption capacity, SSC (mmol$_c$ kg^{-1}), was calculated from the oxalate extractable amount of secondary Al according to (Johnson and Todd, 1983):

$$SSC = 0.02 \cdot ctAl_{ox} \tag{75}$$

The phosphate sorption capacity, PSC (mol$_c$ kg^{-1}), was calculated from the equation (Van der Zee, 1988):

$$PSC = 0.2 \cdot (ctAl_{ox} + ctFe_{ox}) \tag{76}$$

Contents of oxalate extractable Al were taken from Tiktak *et al.* (1988) and contents of oxalate extractable Fe from measurements on comparable Cambic podzols (De Vries, unpublished results). Results on SSC and *PSC* are shown in Table 7. The Langmuir adsorption constant for SO$_4$, $KeSO_{4\ ad}$, was set to 2 m^3 mol^{-1}, which was taken from the RESAM database (De Vries *et al.*, 1994a). The Langmuir adsorption constant for phosphate, $KeH_2PO_{4\ ad}$ was set to 12 m^3 mol^{-1}, which was determined from cH_2PO_4 (phosphate in soil solution) and ctP_{ad} (oxalate extractable phosphate) as determined in 150 forest stands in the Netherlands ($KeH_2PO_{4\ ad} = ctP_{ad}/(cH_2PO_4 (PSC-ctP_{ad}))$, see Eq. (40)).

Table 7 Sulphate and phosphate sorption capacities for the different soil layers

Depth (cm)	SSC (mmol$_c$ kg^{-1})	PSC [1] (mmol$_c$ kg^{-1})
0-5	3.3	59
5-10	3.4	60
10-20	5.7	99
20-30	8.1	123
30-40	9.8	140
40-50	7.6	118
50-60	6.3	106
60-70	5.6	98
70-80	5.2	94
80-100	5.4	66

[1] Derived from generic data for a Cambic Podzol

Soil layer independent parameters

The Al equilibrium constant and parameters for nutrient cycling are presented in Table 8.

Table 8 Values for soil-layer independent model parameters

Process	Parameter	Value	Unit
Foliar uptake[1]	$frNH_{4,fu}$	0.21	-
	frH_{fu}	0.58	-
Foliar exudation[1]	$frCa_{fe}$	0.18	-
	$frMg_{fe}$	0.11	-
	frK_{fe}	0.71	-
Nitrification[2]	k_{ni}	100.0	a^{-1}
Al dissolution[3]	KAl_{ox}	5.0×10^8	l^2 mol^{-2}

[1] Based on throughfall data over the period 1987-1990 (Van der Maas and Pape, 1990).
[2] Obtained by calibration. The generic value for k_{ni} is 40 a^{-1}.
[3] Average IAP for Al(OH)$_3$ at 90 cm over the period 1987-1990, activities calculated from measured concentrations (Van der Maas and Pape, 1990).

Forest growth data

The main ecophysiological research and growth analysis was carried out from 1987 until 1989 (Evers *et al.*, 1991) in a plot adjacent to the plot where most of the soil research was done. The ecophysiological subplot had a somewhat lower stand density compared to the soil research plot (765 *vs.* 812 trees ha^{-1}). After 1989, the biomass analysis was moved to the soil research plot, causing a discontinuity in the data series. Table 9 gives an overview of basic stand data for the soil plot and for the tree physiological plot as measured in December 1988.

Table 9 Tree growth parameters as derived from the ecophysiological plot 1 (Jans *et al.*, 1991) and the soil research plot (Olsthoorn, 1991)

Parameter	Symbol	Unit	Value
Stand age	age_{lt}	a	30
Logistic growth constant	kr_{grl}	a^{-1}	0.094
Maximum amount of stems	$Amst_{mx}$	Mg ha^{-1}	543.8
Amount of foliage	Am_{lv}	Mg ha^{-1}	19.5
Half life time growth function	$t05$	a^{-1}	38
Branch stem ratio	fr_{brst}	-	0.11
Litterfall rate[1]	klf	a^{-1}	0.15

[1] Litterfall was measured directly using 12 litter traps with a surface area of 1 m^2 (Van der Maas and Pape, 1990).

State variables that must be known at the beginning of the simulation include the element contents in needles, stems, branches, roots and litter. Data related to these compartments are given in Table 10. Data are given for the end of the year 1988.

Table 10 Data on biomass and element contents of needles, roots and stems of Speuld stand

Compartment	Biomass	Element content (% of dry weight)					
	(Mg ha^{-1})	N	P	K	Ca	Mg	S
Foliage (Am_{lv})[1]	18.5	1.84	0.11	0.58	0.33	0.09	0.14
Branches (Am_{br})[2]	14.0	0.30	0.04	0.10	0.05	0.03	0.05
Stems (Am_{st})[2]	60.0	0.20	0.01	0.10	0.05	0.01	0.05
Fine roots (Am_{rt})[3]	3.2	1.00	0.10	0.08	0.16	0.04	0.10
Litter (Am_{lt})[4]	35.0	-	-	-	-	-	-

[1] Measured in the ecophysiological research (Evers *et al.*, 1991).

[2] Nutrient contents in branches, wood and roots inferred from general data (Berdowski *et al.*, 1991).

[3] Measured in the soil research plot by Olsthoorn (1991).

[4] Measured by Tiktak and Bouten (1992). The litter mass is an average value for 485 samples. Element contents in litter are calculated by the model using the foliage contents as initial values.

2.1.4 Model calibration procedure

The applied model contains parameters, initial and boundary conditions, which are incompletely known. More information on these quantities, which are often not measurable, is required to improve the model performance. Hence, model calibration is required to determine these values accurately from the available measurements, taking into account the intended model use and available prior knowledge.

Model calibration thus becomes a critical phase in the modelling process. Despite its importance, the required activities for calibration are often given little consideration, and in many cases the model is calibrated using non-structured arbitrary methods. As the model under consideration contains a large number of parameters, a well-structured and systematic calibration approach is needed, supported by useful guidelines.

Strategy

Janssen and Heuberger (1995) present a general outline of the calibration process, and distinguish various important steps:
- Identify the characteristics of the data-set.
- Identify the parameters that need calibration, preferably by performing model analyses (sensitivity and uncertainty analyses).
- Specification of model performance criteria, which express the discrepancy between measurements and model results.
- Solution of the calibration problem, which often consists of adjusting the model parameters such that the model results match the measurements adequately (e.g. minimal misfit).

The calibration process is usually completed by assessing the accuracy and quality of the obtained model (validation aspects; cf. Janssen and Heuberger (1995)). In the sequel it is briefly addressed how the above mentioned issues were used for the calibration of the NUCSAM model to the Speuld data-set.

Parameters that need calibration

The choice of the model parameters that need calibration was based on an uncertainty analysis for the model RESAM (Chapter 2.2 and Kros *et al.*, 1993). Table 11 summarises the parameters for which the solute concentrations were most sensitive, uncertain or hard to derive.

Table 11 NUCSAM model parameters that were calibrated

Calibration order	Parameter	Description	Affects concentration of:
1	$ffSO_{2dd}$	forest filtering factor $SO_{2\,dd}$	SO_4
2	$ffNO_{xdd}$	forest filtering factor $NO_{x\,dd}$	NO_3 and NH_4
3	$ffNH_{xdd}$	forest filtering factor $NH_{x\,dd}$	NO_3 and NH_4
4	ff_{dd}	forest filtering dry deposition base cations and Cl	Na, K, Ca, Mg and Cl
5	kr_{ni}	nitrification rate constant	NO_3 and NH_4
6	kEl_1	Elovich constant	Al and H
7	$ctNlv_{mx}$	Maximum N-content of leaves	NO_3 and NH_4
8	$krCa_{we}$	rate constant for Ca-weathering	Ca
9	$krMg_{we}$	rate constant for Mg-weathering	Mg

These parameters have been chosen for model calibration. To calibrate soil chemistry, simulated soil chemical variables were compared with measured soil chemical variables using statistical measures. For the calibration only concentrations in the soil solution were used since these were the only variables measured in time, soil contents (e.g. oxalate extractable Al) were only measured once. Solute concentrations were measured with cups and plates at different depths for three plots (cf. Tiktak *et al.*, 1995). Because of the large variation in measured concentrations between these three plots (cf. Tiktak *et al.*, 1995) it was decided to choose one plot for calibration (plot 5) because otherwise no trends in soil chemistry would be visible. Model outputs used

for calibration are: pH and the concentrations of Al, Ca, Mg, K, NO₃, NH₄, SO₄ and Cl at 10, 20 and 90 cm depth, two depths for the topsoil and one in the subsoil below the root zone. The choice of the hydrological parameters to be calibrated (not shown in Table 11) was based on Tiktak and Bouten (1992).

Performance criteria

For the evaluation of model performance in relation to observation data in Speuld, two different performance measurements were used (Janssen and Heuberger, 1995):

$$NME = \frac{\overline{P_i} - \overline{O_i}}{\overline{O_i}} \tag{77}$$

$$NMAE = \frac{\frac{1}{N}\sum_{i=1}^{N}|P_i - O_i|}{\overline{O_i}} \tag{78}$$

where, NME (-) is the Normalised Mean Error, $NMAE$ (-) is the Normalised Mean Absolute Error, P_i is the predicted value, O_i is the observed value, $\overline{O}$ and $\overline{P}$ are the averages for the observed and predicted values and N is the number of observations. The NME compares predictions and observations on an *average* basis (i.e. over the whole time-span). The NME thus expresses the bias in average values of model predictions and observations and gives a rough indication of overestimation ($NME >$ 0) or underestimation ($NME <$ 0). The $NMAE$ is an absolute indicator for the discrepancy between model predictions and observations. The $NMAE$ does not allow for compensation of positive and negative discrepancies. An $NMAE$ of zero is considered optimal.

These criteria can be defined and evaluated for various model quantities, individually as well as jointly. For a fair comparison between model results and observations, their temporal and spatial scale should be compatible. For model calibration, model results were compared with accumulated throughfall amounts, soil water contents and soil solution composition.

Solution of the calibration problem

Several automated and objective calibration procedures are available for the calibration of time-series resulting from dynamic models e.g. the Rotated Random Scan method (Janssen and Heuberger, 1995). Such automated calibration procedures have been applied to a simplified regional scale models e.g. MACAL, a steady state soil-vegetation model (Kros *et al.*, 1994a) and SMART2, a dynamic soil-vegetation model (Chapter 3.2; Kros *et al.*, 1999). However, even for these simplified models identification problems occurred and some additional assumptions were necessary in order to achieve a solution. Considering the large number of model parameters and

their mutual interaction in Nucsam, it will definitely result in identification problems. Consequently, we decided to calibrate the different Nucsam parameters manually and sequentially by comparing model output and measurements using performance criteria (cf. Eq. 77 and 78). Therefore we followed the subsequent sequential steps:

- Calibration of the hydrological submodule using time series of throughfall and soil watercontent measurements
- Calibration of the biogeochemical modules using soil solution concentrations.

Table 11 gives the order in which parameters of biogeochemical modules were calibrated. Comparison between model output for different parameter values with measured data was done by comparing the statistical measures for the most effected (sensitive) model output (cf. Table 11). In case of an (almost) equal model performance with respect to the most sensitive variables, differences in model performance for other model outputs were taken into account to choose the most optimal parameter value.

The presented misfit criteria consider only specific aspects of the system under study, and express the agreement between model data and data in a very condensed form, i.e. in one number. Therefore, the use of these quantitative criteria has been supplemented by qualitative techniques (e.g. visual comparison of measurements and model results).

2.1.5 Scenario analyses

Nucsam was also used to assess the long-term development of soil solution chemistry, in particular Al concentration in the soil solution, Al/Ca ratio, the content of secondary aluminium compounds and the soil nutrient status. This goal was achieved by performing scenario analyses for two generic forest-soil combinations, i.e. Douglas fir on a Cambic podzol (DFCP) and Scots pine on a Haplic Arenosol (SPHA). The combination DFCP was chosen because this acts as a reference, whereas the combination SPHA is a very common tree soil combination in the Netherlands. Model simulations were carried out with deposition scenarios that are representative for Dutch regions with low, average and high deposition rates, respectively. It was assumed that in a clean region, the target acid deposition load of 1400 mol_c ha^{-1} a^{-1} is reached in 2010, whereas in average and polluted regions these loads are reached in 2050 and 2100, respectively (Keizer, 1994). Recently, the deposition targets has been adjusted (see Chapter 3.1). This scenario is a rather optimistic one with respect to the reduction of deposition. Weather data were randomly selected by a statistical model of historically observed weather data (Richardson and Wright, 1984). The results of these scenario analyses were primarily meant as an example of model use for predictive purposes, as only one deposition scenario and one realisation of weather data was evaluated.

Table 12 presents the deposition scenarios for the six combinations evaluated.

Table 12 Total acid deposition (mol$_c$ ha^{-1} a^{-1}) for generic Scots pine (SP) and Douglas fir (DF) stands in the Veluwe (Central Netherlands)

Year	Total acid deposition (mol$_c$ ha^{-1} a^{-1})	
	SP	DF
1980 [1]	8300	8700
1990 [1]	5400	6400
2000 [2]	2600	3000
2010 [2]	2000	2300
2050 [2]	1400	1600

[1] Inferred from DEADM calculations (see further text).
[2] Deposition target (Keizer, 1994). These target has been adjusted recently (cf. Chapter 3.1)

For the period between 1980 and 1991, the deposition of acidifying components was estimated with the DEADM model (Erisman, 1993). The DEADM model was used to generate data for an average stand, based on meteorological measurements and measurements of concentrations in the atmosphere and precipitation. For the period before 1980, concentration measurements were not available and the deposition was inferred from historical deposition data which were based on emissions in those years (Thomas *et al.*, 1988). The historical deposition was scaled to the DEADM deposition, using the following equation:

$$Ac = Ac_{td,hist} \cdot \left(\frac{\overline{Ac_{td,DEADM}}}{\overline{Ac_{td,hist}}} \right) \tag{79}$$

where Ac_{td} (mol$_c$ ha^{-1} a^{-1}) is the total deposition of acidity, $Ac_{td,hist}$ (mol$_c$ ha^{-1} a^{-1}) is the deposition based on emissions, $\overline{Ac_{td,DEADM}}$ (mol$_c$ ha^{-1} a^{-1}) is the average deposition of acidity calculated with DEADM for the period 1980-1991 and $\overline{Ac_{td,hist}}$ (mol$_c$ ha^{-1} a^{-1}) is the average deposition of acidity based on emission data for 1980-1991. Future deposition data of acidity (1992-2050) were inferred from average DEADM results for 1989-1991 and the deposition targets (Table 12) by linear interpolation. Moreover, it was assumed that the relative contributions of SO$_x$, NO$_x$ and NH$_x$ were constant and equal to the contributions for 1991. The average deposition figures were converted to deposition figures for Douglas fir and Scots pine by applying filter factors (De Vries, 1991). Scots pine was assumed to behave as an average tree with respect to dry deposition, so the calculated deposition figures directly apply to Scots pine. Dry deposition for generic Douglas fir was inferred from the DEADM results using a dry deposition filter factor of 1.2. Finally, the deposition of base cations was calculated using a filter factor of 2.5 for Scots pine, and 3.0 for Douglas fir.

An overview of the used generic hydrological, soil chemical and forest growth data is given in Kros *et al.* (1996).

2.1.6   Results of model calibration

Hydrology

Interception and throughfall

The hydrological submodel was calibrated in two steps: (i) calibrating the interception losses using measured throughfall values and (ii) calibrating the transpiration and soil evaporation fluxes using measured water contents. The interception fluxes were calibrated using data for the year 1988 only, because for this year the differences between the daily precipitation at station Drie and the weekly site measurements where the smallest. The transpiration and soil evaporation fluxes were calibrated by using data for the year 1989, because frequent measurements on water content were available for that year only.

Simulated throughfall amounts for the years 1988 and 1989 are presented in Figure 3. Table 13 presents the annual water balances for the period 1987-1989. The calibrated NUCSAM model overestimated the accumulated throughfall amount for 1989 and underestimated the throughfall amount for 1987. For 1988, throughfall amounts are in close agreement with measured throughfall values (maximum deviation < 10% of observed value). The overestimation of throughfall for 1987 and 1989 are partly caused by deviations between the precipitation at station Drie and the on-site precipitation (see Table 13). A second explanation for the deviations in 1987 and 1989 are differences in average rainfall intensity. In 1989, rainfall mainly occurred as large storms. After such storms, a large part of the total precipitation drains instantaneously from the canopy and evaporation loss is relatively small. In 1987, however, a large part of the annual precipitation was in the form of small storms and evaporation losses were high. Since NUCSAM uses an average rainfall intensity (R), this may also lead to deviations.
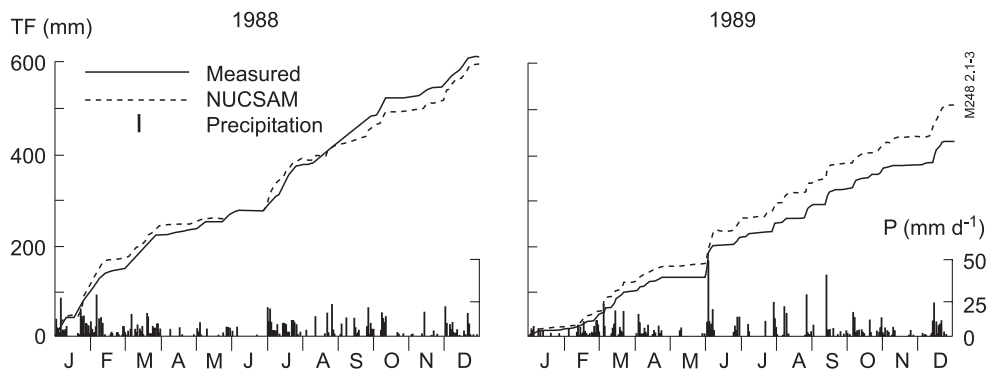
Figure 3 Accumulated simulated and measured throughfall (TF) and measured daily precipitation (P) for the years 1988 and 1989

Table 13 Simulated water balance terms for the Speuld experimental forest

	1987		1988		1989	
	Observed	NUCSAM	Observed	NUCSAM	Observed	NUCSAM
	Fluxes (mm a^{-1})					
Precipitation	950 [1]	976 [2]	935 [1]	933 [2]	710 [1]	806 [2]
Interception	-	357	-	331	-	285
Throughfall	660	619	618	602	449	521
Evaporation	-	55	-	56	-	66
Transpiration	-	365	-	323	-	371
Drainage	-	199	-	221	-	84
Transpiration reduction (%)	-	0.8	-	13	-	16

[1] On-site measured precipitation. These values were not used by NUCSAM, because on-site measurements were not carried out daily.

[2] Precipitation measured at station Drie was used as input to NUCSAM.

Soil water contents

Simulated soil water contents for 1989 are shown in Figure 4. Table 14 gives an overview of performance criteria for the discrepancy between the observed and measured soil water contents. The performance for the 0-50 cm soil layer appeared to be reasonably good, whereas for the 50-100 cm soil layer, soil water contents are underestimated. However, differences mainly occur in autumn, indicating that rewetting of the soil occurs too late. NUCSAM was not able to predict the dynamic behaviour of measured soil water contents correctly, probably indicating that fingered flow is a relevant hydrological process for Speuld.
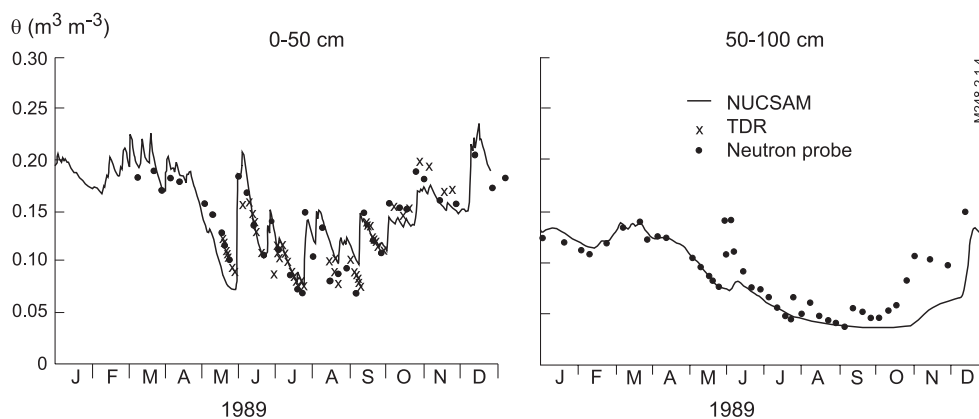
Figure 4 Comparison of observed and simulated water contents in the 0-50 and 50-100 cm soil layers for the year 1989

Table 14 NUCSAM Performance criteria for the discrepancy between observed and measured soil water contents

Layer	NME [1]	NMAE [2]
0-50 cm[3]	0.10	0.25
50-100 cm[4]	-0.13	0.17

[1] Normalised Mean Error (see Eq. 77)
[2] Normalised Mean Absolute Error (see Eq. 78)
[3] Model output compared with TDR measurements (n = 88).
[4] Model output compared with neutron probe measurements (plot B; n = 43).

Soil solution concentrations

Results of the calibration are shown for 20 cm and 90 cm depth in Figure 5. Table 15 shows the NME and NMAE (Eq. 77 and 78) for the major components for 10, 20 and 90 cm depth.

Simulated pH values are calculated from the charge balance in NUCSAM, implying that they are affected by virtually all biogeochemical processes in the model. Simulated pH values showed to be over estimated for 20 cm and slightly under estimated for 90 cm. At 10 cm depth the agreement was good (figure not shown). This is also reflected by the performance criteria, i.e. the Normalised Mean Absolute Error (NMAE) for H concentration at these depths (Table 15).

Table 15 Performance of NUCSAM during the observation period

Parameter	Performance measurement (-) and number of observations (-)								
	H	Al	Ca	Mg	K	NO$_3$	NH$_4$	SO$_4$	Cl
Depth 10 cm									
N [1]	48	37	37	37	37	41	44	41	41
NMAE [2]	0.39	0.60	0.52	0.86	0.83	0.54	0.84	0.62	0.65
NME [2]	-0.37	-0.30	-0.45	-0.86	0.80	-0.37	-0.82	-0.60	-0.65
Depth 20 cm.									
N	48	41	40	40	40	46	44	46	46
NMAE	0.81	0.49	0.63	0.86	2.16	0.41	4.70	0.44	0.47
NME	-0.81	0.10	-0.63	-0.86	2.16	-0.24	3.94	-0.33	-0.40
Depth 90 cm.									
N	48	35	35	35	35	43	34	43	43
NMAE	0.32	0.57	0.40	0.54	0.84	0.53	0.97	0.40	0.52
NME	0.20	0.28	-0.34	-0.54	-0.84	0.02	-0.90	0.02	0.04

[1] N is number of observations
[2] NMAE is Normalised Mean Absolute Error and NME is Normalised Mean Error (see Eq. 77 and 78).
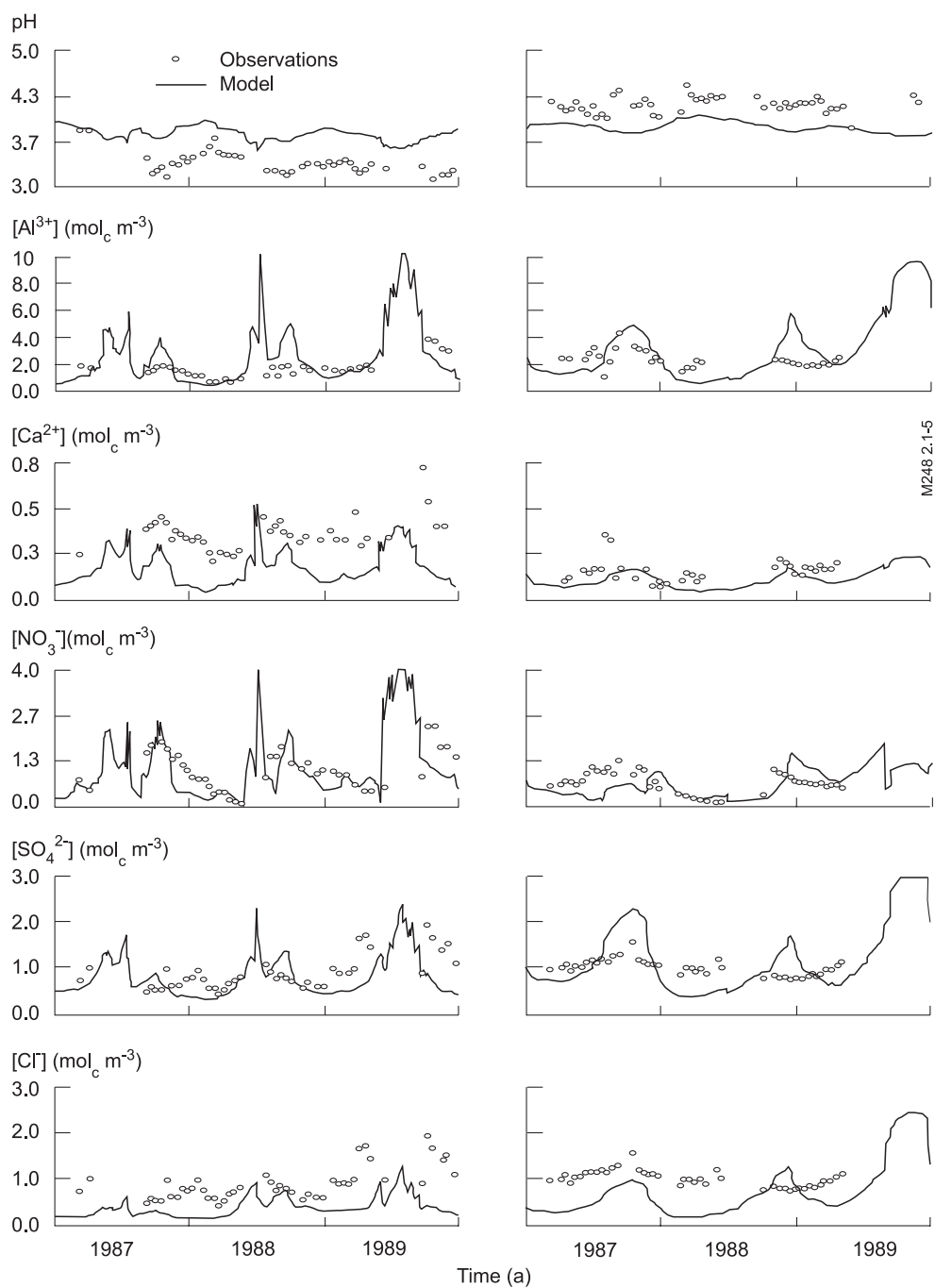
Figure 5 Simulations of soil water chemistry by NUCSAM for 20 cm (left) and 90 cm (right) depth

The Al concentration was simulated fairly well at both depths. Regarding the calibration results for both the pH and the Al concentration, it can be concluded that the pH and Al behaviour in Speuld cannot be described adequately with a combination of the Al-hydroxide equilibrium model (Eq. 33) and rate-limited dissolution of Al-hydroxides (Eq. 37). This was also noticed in a model comparison study for the Solling site in Germany (Groenenberg *et al.*, 1995; Kros and Warfvinge, 1995). Wesselink and Mulder (1995) could also not reproduce both pH and Al concentrations by Al oxide solubility. They attributed this to Al complexation with dissolved organic matter.

The Ca concentration at 20 cm depth was underestimated. This is also reflected by the *NME*, which is ≤ -0.50. At 90 cm depth, Nucsam gives a slight underestimation. The underestimation of the Ca concentration at 20 cm depth is probably due to either an overestimation of the calcium root uptake in the topsoil or an underestimation of the return of calcium by litterfall. Changing the internal cycling of base cations within the system will lead to higher calcium concentrations in the topsoil, without affecting the calcium concentrations below the root zone (i.e. > 90 cm). Because of the reasonable fit of the Ca concentration at 90 cm depth (i.e. below the root zone), we assume that the calcium input by weathering and deposition is correct.

NO$_3$ concentrations were reasonably well reproduced by Nucsam (*NMAE* = 0.41 - 0.54). This is in contrast with a previous application of the Nucsam model within a model comparison study at Solling, Germany (Groenenberg *et al.*, 1995; Kros and Warfvinge, 1995), from which it appears that the behaviour of nitrogen could not be simulated reasonably well. SO$_4$ concentrations were also predicted reasonably well. Cl concentrations, however, were clearly underestimated, especially at 90 cm depth for the years 1987 and 1988. This is striking because are rather conservative anions in Dutch forest soils. The poor performance for these anions is most likely caused by the strong spatial variability of throughfall fluxes and spatial patterns of water uptake by roots. This indicated that the hydrological calibration, which was based on another plot (see *Site description*), is not valid for the soil chemical monitoring plot.

2.1.7 Model predictions in response to a deposition scenario

Hydrology

Table 16 shows the long-term average simulated water balance for Douglas fir on a Cambic podzol and Scots pine on a Haplic Arenosol in the 'Veluwe' region. Some general conclusions can be drawn from the table:

- Nucsam simulates a lower average interception evaporation for Scots pine than for Douglas fir, which is in line with Molchanov (1960). who found an interception fractions of the precipitation of 37 % for Spruce forest and 21% for pine forest.
- Actual transpiration for Douglas fir is much higher than for Scots pine due to a higher potential transpiration. This is mainly because of the higher crop factor and

the lower canopy gap factor for Douglas fir. This demonstrates that feed-backs between the hydrological submodel and the forest-growth submodel should be considered during forest succession. Compared to transpiration values given by Roberts (1983) for an average forest in Europe (330 mm a^{-1}), values for Douglas fir are higher and for Scots pine lower.
- Soil evaporation is lower under Douglas fir than under Scots pine. This is mainly caused by the lower Leaf Area Index and higher canopy gap fraction for Scots pine.
- Variation in time of potential transpiration, interception evaporation, actual transpiration and soil evaporation is much smaller than variation in time of precipitation.
- There is hardly any reduction of soil evaporation calculated by NUCSAM. This is the consequence of using the approach by Black *et al.* (1969), which is only sensitive to the length of the period with a daily precipitation less than 0.3 mm. The generated meteorological dataset contains correct drought intervals but apparently underestimates the length of periods without precipitation.
- The average precipitation surplus for Douglas fir is very small.

The actual transpiration for Douglas fir is almost similar to that for Speuld. The actual transpiration simulated by NUCSAM for Scots pine (268 mm a^{-1}) compares well with that from previous SWATRE simulations by De Visser and De Vries (1989) (281 mm a^{-1}). For Douglas fir, however, the NUCSAM flux (371 mm a^{-1}) is substantially higher than that simulated by De Visser and De Vries (1989), viz 328 mm a^{-1}.

Table 16 Average simulated water balance for Douglas fir on a Cambic podzol and Scots pine on a Haplic Arenosol in region 'Veluwe' for the period 1980-2050

Tree/Soil Combination	Fluxes and standard deviation (mm a^{-1}) [1]					α (-) [2]
	P	I	E_{pl}	E_s	PS	
Douglas/Podzol	804±98	304±35	371±20	59±3	74±40	0.96±0.06
Pine/Arenosol	804±98	288±34	268±11	95±4	188±38	0.99±0.03

[1] P (mm a^{-1}) is precipitation, I (mm a^{-1}) is interception loss, E_{pl} (mm a^{-1}) is transpiration, E_s is soil evaporation, and PS (mm a^{-1}) is precipitation surplus.
[2] α (-) is ratio of actual transpiration over potential transpiration (E_{pl}/E_{pl}')

Soil chemistry

Figure 6 shows the simulated yearly average soil solution concentrations for the 'Veluwe' region. Concentrations of sulphate and Al are higher and the pH is lower in the soil under Douglas fir than under Scots pine due to higher filtering of air pollutants by Douglas fir, and a lower precipitation surplus. NUCSAM simulates a fast response of the sulphate concentration after a reduction in SO$_x$ deposition, whereas the response of Al shows a considerable time delay. The pH increase under Douglas fir is clearly higher than the increase under Scots pine. This difference is mainly due to the use of a log scale. When inspecting the H concentration (not shown), the decrease in H concentration was more or less comparable.
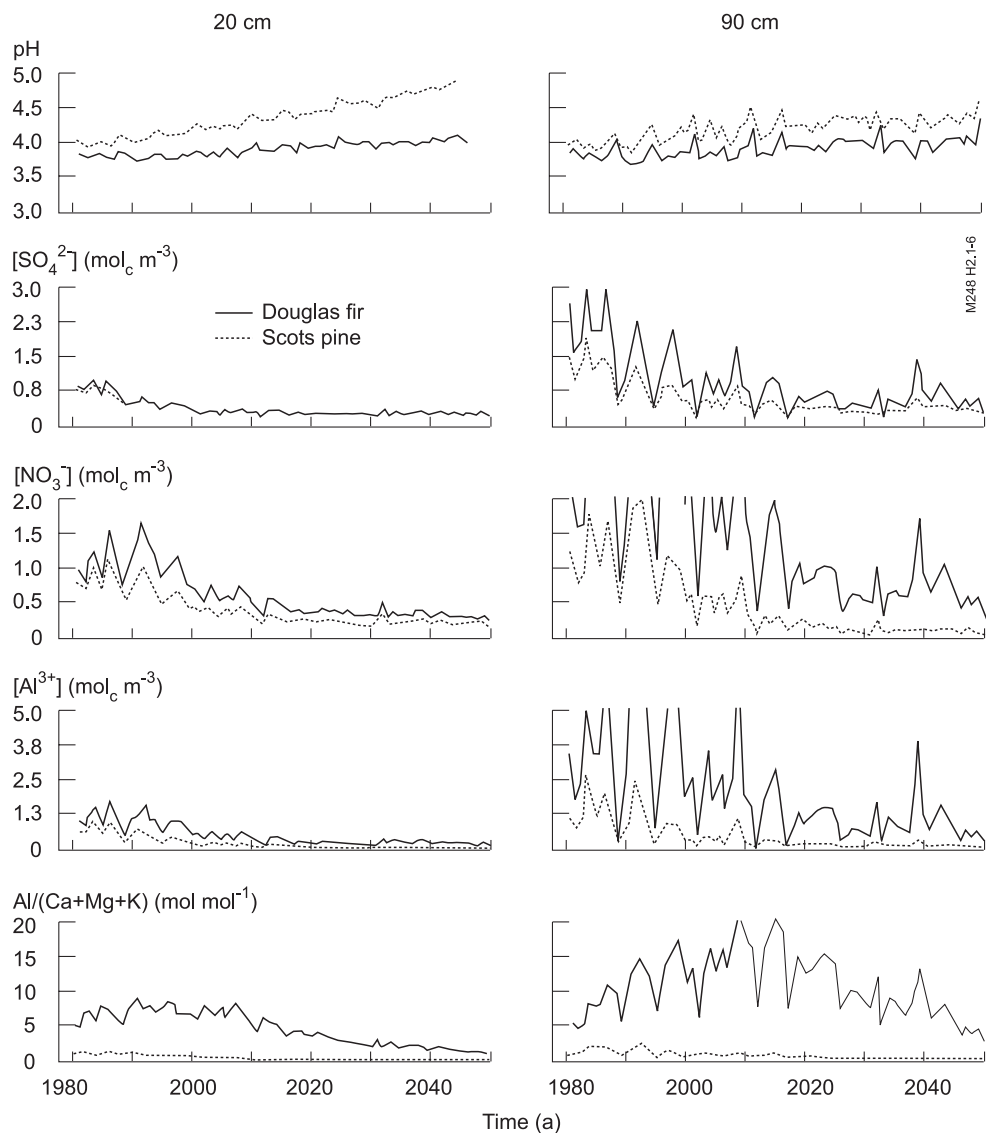
Figure 6 Simulated soil water chemistry at for Douglas fir on a Cambic podzol and for Scots pine on a Haplic Arenosol (right) in the 'Veluwe' region at 20 cm depth (left) and at 90 cm depth (right) for a reducing deposition scenario

Results showed a higher concentration of NO_3 under Douglas fir than under Scots pine. As with sulphate, this is caused by higher filtering of NO_x and NH_x by Douglas. NUCSAM also simulates a time delay for the decrease of the NO_3 concentration in the soil solution after a decrease in NH_x and NO_y deposition, caused by the release of nitrogen previously stored in living biomass and litter. The NO_3

leaching fluxes at 90 cm depth show the same behaviour as the NO_3 concentrations at 90 cm depth.

Table 17 shows that root uptake of NH_4 and NO_3 in 2010 is approximately 66% of the uptake in 1990. There is a clear reduction in N root uptake flux in 2010. This is caused by a fast decrease of the nitrogen content in needles simulated by this model, which in turn is a result of the assumed empirical relationship between the nitrogen content in needles and the nitrogen deposition (see Section *Forest growth*). As these results apply to two individual years, conclusions with respect to time-trends must be drawn carefully. This is especially true with respect to mineralisation.

Table 17 Annual simulated fluxes of NO_3 and NH_4 for Douglas fir on a Cambic Podzol for the 'Veluwe', for 1990 and 2010

Process	Fluxes [1] (mol_c ha^{-1} a^{-1})			
	NH_4		NO_3	
	1990	2010	1990	2010
Throughfall	3.20	1.09	1.42	0.54
Mineralisation	6.57	3.05	0.00	0.00
Root uptake	-3.92	-1.68	-2.61	-1.12
Leaching [2]	-0.15	-0.49	-2.92	-2.53

[1] Positive fluxes indicate an increase in the soil solution concentration

[2] Refers to 1 m depth

Differences between Douglas and Scots pine showed again to be large. A considerable time delay was found for the Al/(Ca+Mg+K) ratio, which continues to rise for a short time after deposition reduction. This phenomenon was also observed in an application on a Norway Spruce stand at Solling, Germany (Groenenberg *et al.*, 1995). It can be explained by exchange of Ca from the soil solution against sorbed Al. This is less pronounced in this study than in Solling, due to the smaller CEC of the soils used in this study. Both the Al/(Ca+Mg+K) ratio and the time-delay for decrease of this ratio is larger for Douglas compared to Scots pine, which is caused by the higher acid load for a soil under Douglas. Regarding the criteria for indirect effects on forest stress several criteria have been propagated. Sverdrup and Warfvinge (1993) showed that based on laboratory experiments a critical Al/(Ca+Mg+K) ratio can be derived above which harmful effects on root and shoot growth occur. For a spruce forest the critical value for the Al/(Ca+Mg+K) is 2 and for pine 0.8. The results show that at 20 cm depth an Al/(Ca+Mg+K) ratio < 0.8 for pine was reached in 2000 and an Al/(Ca+Mg+K) ratio < 2 occurred around 2040. In the subsoil the criteria were met about 10 years later.

In conclusion, results show a fast response of the sulphate and aluminium concentrations after a decrease in SO_x deposition, a time-delay for the NO_3 concentration following a decrease in deposition, and higher soil solution concentrations for Douglas.

2.1.8   Discussion and conclusions

Major conclusions

NUCSAM could reproduce the general magnitude of measured quantities. The scenario analyses showed a fast response of the sulphate and aluminium concentrations in the soil solution after a decrease of the SO_x deposition, time-delay for the NO_3 concentration following a decrease in nitrogen deposition, and depletion of the pool of secondary aluminium compounds in regions with high deposition.

Model validation

A major conclusion arising from this exercise should be that the detailed NUCSAM model is now thoroughly tested against a common data-sets (Speuld), and that it provides a wealth of opportunities to test hypotheses about the interactions between forest, soil and atmosphere. Furthermore, the long-term results from the scenario analysis show plausible results. It is, however, not absolutely proven whether the model is a suitable instrument for long-term predictions and scenario analyses. It is obvious that the Speuld data-set was too short for 'true' model-validation. Moreover, due to the large spatial variability of throughfall, soil solution chemistry and stand structure, it was almost impossible to build a meaningful and representative data-set. A major reason for this was that the monitoring at Speuld followed a 'disciplinary' approach, with separate subplots for hydrology, soil chemistry and forest growth. Either was the number of sampling replicates too small to calculate stand averages (soil chemistry), or it was impossible to select more or less homogeneous subplots (hydrology and biomass inventory). Furthermore, individual monitoring groups came with different data for some model parameters. Nevertheless, NUCSAM could reproduce the general magnitude of measured quantities, such as soil water contents and soil solution chemistry. However, NUCSAM was not always successful in simulating measured seasonal dynamics and the Al chemistry.

Uncertainties

One of the problems with calibrating a complicated model is that it is difficult, if not impossible, to find a unique set of model parameters. One way to improve the uniqueness of the obtained calibration is using automated and objective calibration procedures. In view of the large number of model parameters that need calibration, such a calibration procedure is very time-consuming. For this reason, automated calibration procedures have not been applied to NUCSAM, but strict (manual) calibration procedures have been postulated. However, if the uniqueness of the calibration remains questionable, results of scenario analyses are also uncertain. Model uncertainty can be assessed by performing thorough and systematic uncertainty analyses. Confidence in predictions from an individual model will also increase when other models predict the same magnitude and trends of model outputs. Therefore, NUCSAM was used in two model comparison studies (Van Grinsven *et al.*, 1995 and

Tiktak *et al.*, 1995). Results showed that the compared models were able to identify the general trends and levels of ion concentrations and fluxes. Arguably, stress factors (cf. pH, Al and Al/Ca ratios) may be modelled with a level of detail corresponding to the uncertainties in how the trees reacts to chemical stress in the rhizosphere (Sverdrup *et al.*, 1994). Problems remain, however, when inspecting the details (e.g. seasonalility) especially for modelling of Al, pH and N behaviour. Most probably the Al behaviour can be improved by taking the Al complexation with dissolved organic matter into account.

Scenario analyses

Scenario analyses were carried out for a Douglas fir and a Scots pine on an Haplic Arenosol. The most important trend were a fast response of the sulphate and aluminium concentrations after a decrease in SO_x deposition, time-delay for the NO_3 concentration following a decrease in nitrogen deposition, higher soil solution concentrations in the soil below Douglas fir, and depletion of the pool of secondary aluminium compounds.

Recommendations for future research

After application of the integrated model NUCSAM at the stand-level, some uncertainties still remain. Despite these uncertainties progress was made. This exercise clearly shows that for further hypothesis testing and validation of the model NUCSAM, there is a need to continue intensive monitoring programs, but the balance between data acquisition in the various compartments of the ecosystem should be emphasised. Moreover, much more attention should be paid to bridging the gap between models and experimental data. NUCSAM should be used to select the most important parameters to be monitored. Furthermore, NUCSAM can be used to set-up sampling strategies (in particular sampling frequencies). Another major point of concern should be the issue of *quality control*. The current exercise shows that both the model and the dataset were poorly adjusted. Perhaps the only way to guarantee that integrated data-sets become and remain available is by building databases, which are maintained by a small group of researchers that consists of both modeller and field scientists. Besides long-term monitoring of important model parameters, there is a need for measurement campaigns aimed at reducing the uncertainty in the model results. However, such campaigns should be directed by the requirements of integrated models, and not follow a disciplinary line. Besides intensive monitoring programs there is a need for extensive monitoring on a larger number of locations. Such extensive monitoring programs are mandatory for calibration of regional models (see Part III of this thesis). However, as with the intensive monitoring programs, much more attention should be paid to bridging the gap between models and measurements. In extensive monitoring, the need for using models to set-up measurements campaigns is even more evident than in intensive monitoring programs.

After the application and validation of the stand-level model NUCSAM, some uncertainties still remain, and new uncertainties arose. For further hypothesis testing

and validation the model has been applied to a roofing experimental site Speuld (Van der Salm *et al.*, 1998). Results of that study were comparable with a NICCCE application to Speuld (Koopmans and Van Dam, 1998). However, NUCSAM should be used to further explore available manipulation experiments, which serves two goals (i) further validation and testing of the model and (ii) use the model to integrate and interpret the data records collected at those sites.

Finally, present site calibrations could be used to assess the uncertainty of predictions for Speuld, and the deposition scenarios. This will be presented in the next Chapter. Instead of using NUCSAM in order to assess the uncertainty in long-term predictions the simplified version RESAM was used.

Acknowledgement

2.2 The uncertainty in forecasting trends of forest soil acidification

Abstract

A Regional Soil Acidification Model (RESAM) has been developed to gain insight in long-term impacts of deposition scenarios on forest soils in The Netherlands. Model predictions of such large-scale environmental effects of acid deposition require extrapolation of site specific data to large geographical regions. The major aim of this study is to quantify the uncertainty in model response to a given deposition scenario, due to uncertainty and spatial variability in data. Furthermore, the uncertainty analysis was performed to determine which additional data will most likely improve the reliability of predictions. An efficient Monte Carlo technique was used in combination with regression analysis. The analysis was restricted to one forest soil ecosystem: a leptic podzol with Douglas fir, subject to a scenario of decreasing atmospheric deposition. The investigated output variables were pH, Al/Ca ratio and NH_4/K ratio in the root zone, which are generally used as indicators of forest soil acidification and of potential forest damage. In most cases the relation between the parameters and model output can be satisfactorily described by a linear regression model. The contribution of the uncertainty of various parameters to the uncertainty of the considered output variable depends on soil compartment and time. The uncertainty, as measured by the coefficient of variation, appears to be high for the NH_4/K and Al/Ca ratios, whereas it was relatively low for pH. Results show that the uncertainty in the depositions of SO_x, NO_x and NH_x in a receptor area and the uncertainty in the parameters and variables determining the nitrogen and aluminium dynamics contribute most to the resulting uncertainty of the considered model output.

2.2.1 Introduction

The long-term impact of acid deposition on soils is an important ecological problem. The development of unfavourable Al/Ca ratios and NH_4/K ratios, either by the mobilisation of Al (acidification) or the accumulation of ammonium (eutrophication), may lead to forest deterioration induced by the inhibition of the uptake of nutrients such as Ca and Mg (Ulrich and Matzner, 1983; Roelofs *et al.*, 1985; Boxman *et al.*, 1988).

Several process-oriented models have been developed to predict the long-term effects of acid deposition on soil (e.g. Arp, 1983; Chen *et al.*, 1983; Reuss and Johnson, 1986; Cosby *et al.*, 1985; Bloom and Grigal, 1985; Levine and Ciolkosz, 1988). However, most of these models do not include the effect of the nutrient cycle, although this is very important for making predictions of the Al/Ca and NH_4/K ratios in the upper soil horizons. A notable exception is the ILWAS model developed by Chen *et al.* (1983), but this model is difficult to apply on a regional scale, because of its extensive data input requirements. Therefore, a Regional Soil Acidification Model (RESAM) has been developed for analysing long-term soil responses to acid deposition on a regional scale (De Vries *et al.*, 1994a). It is used for predicting the annual average

61

fluxes and concentrations of the major elements in characteristic forest/soil ecosystems in the Netherlands.

For its regional application RESAM has been linked as a submodel in an overall framework predicting environmental impacts of S and N emissions to evaluate the effectiveness of abatement strategies: the integrated Dutch Acidification Simulation (DAS) Model (Olsthoorn *et al.*, 1990). The regional application has been performed for 20 predefined deposition regions (De Vries *et al.*, 1995a). For each region the long-term impact of acid deposition on the most relevant combinations of soil and vegetation has been evaluated by RESAM. The deposition scenario for each region is delivered by the deposition module of the DAS model.

As part of the DAS model, RESAM holds a central place in the analysis of the acidification problems and the evaluation of abatement strategies. In connection with such policy applications it is imperative that the uncertainty of the model results is analysed, particularly since the lack of long-term series of observations to calibrate a model makes it difficult to indicate the reliability of long-term predictions.

Uncertainty in long-term predictions is mainly due to: (i) insufficient knowledge of the investigator, (ii) uncertainty of data and (iii) model implementation. Insufficient knowledge is reflected by the model structure which includes several assumptions and simplifications with respect to the modelled processes. Essential processes in acidifying systems which are imperfectly known include (Jenkins *et al.*, 1989): (i) the dynamics of organic matter, including the behaviour of dissolved organic matter; (ii) the dynamics of solid phase Al including complexation of inorganic Al by organics; (iii) N cycling through the vegetation, especially nitrification/denitrification, and (iv) the dynamics of forest growth in relation to the acidification status of the soil. Although the model structure is possibly an important uncertainty source, it is very difficult or even impossible to asses. An indication may for instance be obtained by model comparison or by comparing different process formulations.

Apart from the model structure (and implementation), the uncertainty in model outputs is also due to uncertainties in data, viz source terms, initial conditions of model variables, and model parameters (e.g. Hornberger *et al.*, 1986; Alcamo and Bartnicki, 1987). The uncertainty in data is due to natural variability and inaccurate and insufficient measurements. In order to represent the natural variability (spatial and/or temporal) of the processes under consideration, one usually specifies a (joint) probability distribution for the associated model inputs, reflecting the expected range of values (see e.g. Hettelingh, 1989). Similarly, in situations where the uncertainties in model inputs are mainly due to inaccurate and/or insufficient data, one usually also applies probability distributions to specify the possible range of values which one expects (i.e. reflecting the 'degree of belief'). Both situations are closely related and can be approached through an analysis of how model output depends upon model inputs (Hornberger *et al.*, 1986). The difference is, however, that (spatial) variability is a fact of nature whereas poorly defined inputs can be constrained by additional data to reduce the uncertainty in model predictions.

Several publications analysed the effects of uncertain inputs, initial conditions and model parameters in the field of environmental modelling, for instance in the fields of long-range air pollution transport (Alcamo and Bartnicki, 1987), watershed

acidification (Hornberger *et al.*, 1986; Kämäri *et al.*, 1986; Hettelingh, 1989), and water quality modelling (Beck and Van Straten, 1983). In most cases, a Monte Carlo analysis approach was used. One of the underlying premises in nearly all these studies is that the model structure is 'correct' or at least represents current knowledge adequately. The same assumptions have been made in our study. An indication of the influence of model structure is planned to be published later by a comparison with other models which differ in complexity and type of process formulations (see Chapter 2.4).

The major aim of this study is to gain insight into: (i) the uncertainty in RESAM output variables due to uncertainties in the model inputs; (ii) the importance of the model inputs in order to have a guideline as to which additional data will most likely improve the reliability of predictions; (iii) whether average model inputs produce adequate average model outputs, to verify whether simulation with average model inputs, as will be used in a regional application to limit the computation time, is acceptable. The analysis is restricted to one forest soil, a leptic podzol with Douglas fir, subject to a scenario with decreasing deposition. The investigated output variables are pH, NH_4/K and Al/Ca ratios in the root zone, which are generally used as indicators of soil acidification and of potential forest damage.

2.2.2 Model structure of RESAM

The acidification process in RESAM is conceptualised as a disturbance in forest element cycling. The model structure is based on this concept. RESAM simulates the major biogeochemical processes occurring in the forest canopy, litter layer and mineral soil horizons. The biogeochemical processes accounted for in the model are: foliar uptake and foliar exudation, litterfall and root decay, mineralisation, root uptake, nitrification and denitrification, protonation of organic anions, carbonate dissolution/precipitation, weathering of primary minerals containing Al and base cations (Ca, Mg, K, Na), aluminium hydroxide dissolution/precipitation, cation exchange of H, Al, base cations and NH_4, SO_4 adsorption/desorption and dissolution/speciation of inorganic C. Here we used a simplified version of RESAM in order to limit computation time. The simplification mainly concerns the use of a steady-state nutrient cycle instead of a dynamic one.

Table 1 gives a brief overview of the model formulations used. The general construction of the notation of the source terms, variables and parameters used in RESAM is given in Table 2.

Table 1 Description of the most important processes included in the model

---

1. Foliar uptake and foliar exudation

$$FNH_{3,fu} = fNH_{3,fu} \cdot FNH_{3,dd}$$

$$FX_{fe} = kX_{fe} \cdot A_{lv} \cdot ctX_{lv} \qquad \text{X = Ca, Mg, K}$$

2. Litterfall and root decay

$$FX_{lf} = kX_{lf} \cdot A_{lv} \cdot ctX_{lv} \qquad \text{X = M, S, Ca, Mg, K}$$

$$FX_{rd} = k_{rd} \cdot A_{rt} \cdot ctX_{rt} \qquad \text{X = N, S, Ca, Mg, K}$$

3. Mineralisation (steady-state option)

$$FX_{mi} = FX_{lf} + FX_{rd} \qquad \text{X = N, S, Ca, Mg, K}$$

4. Root uptake (steady-state option)

$$FX_{ru} = FX_{gu} + FX_{lf} + FX_{fe} - FX_{fu} + FX_{rd} \qquad \text{X = N, S, Ca, Mg, K}$$

Distribution of N over NO_3 and NH_4 :

$$FNH_{4,ru} = fr_{fr}NH_{4,ru} \cdot \frac{cNH_4}{cNH_4 + cNO_3} \cdot FN_{ru}$$

$$FNO_{3,ru} = FN_{ru} - FNH_{4,ru}$$

5. Nitrification and denitrification

$$FNH_{4,ni} = \theta \cdot D \cdot k_{ni} \cdot cNH_4$$

$$FNO_{3,ni} = \theta \cdot D \cdot k_{de} \cdot cNO_3$$

6. Protonation

$$FRCOO = \theta \cdot D \cdot k_{pr} \cdot cRCOO$$

7. Carbonate dissolution/precipitation

$$FCa_{we,cb} = \rho \cdot D \cdot kCa_{we,cb} \cdot ctCa_{cb} \cdot (cCa_e - cCa)$$

$$cCa_e = KeCa_{cb} \cdot \frac{pCO_2}{cHCO_3}$$

with:
cCa_e = equilibrium concentration
pCO_2 = partial CO_2 pressure

8. Weathering of primary minerals

$$FX_{we,pm} = \rho \cdot D \cdot kX_{we,pm} \cdot ctX_{pm} \qquad \text{X = Ca, Mg, K, Na}$$

$$FAl_{we,pm} = 3 \cdot FCa_{we,pm} + 0.6 \cdot FMg_{we,pm} + 3 \cdot K_{we,pm} + 3 \cdot Na_{we,pm}$$

i.e. congruent weathering of equal amounts of anorthite (Ca), chlorite (Mg), microcline (K) and albite (Na)

9. Aluminium hydroxide dissolution/precipitation

$$FAl_{we,ox} = \rho \cdot D \cdot kAl_{ox} \cdot ctAl_{ox} \cdot (cAl_e - cAl)$$

$$cAl_e = kAl_{ox} \cdot cH^3$$

with: cAl_e = equilibrium concentration

Table 1 (continued)

---
10. Cation exchange

$$\frac{frX_{ac}}{frCa_{ac}^{\tilde{z}_x}} = KeX_{ex} \cdot \frac{cX^2}{cCa^{\tilde{z}_x}} \; ;$$

with: $fX_{ac} = \frac{ctX_{ac}}{CEC}$

$_x$ valence of cation X

$X = H, Al, Mg, K, Na, NH_4$

---
11. SO$_4$ adsorption

$$ctSO_{4,ad} = \frac{SSC \cdot KeSO_{4,ad} \cdot cSO_4}{1 + KeSO_{4,ad} \cdot cSO_4}$$

---
12. Dissolution/speciation of inorganic C

$$cHCO_3 = KCO_2 \cdot \frac{pCO_2}{cH}$$

Table 2 Notation of RESAM source terms, variables and parameters

Entity		Constituent	Process		Compartment	
A	amount [kg ha^{-1}]	N	dd	dry deposition	ac	adsorption complex
c	concentration in the soil solution [mol$_c$ m^{-3}]	NO$_2$	de	denitrification	ad	sorption site
ct	content [mmol$_c$ kg^{-1}]	NO$_3$	dw	wet deposition	cb	carbonates
CEC	cation exchange capacity [mmol$_c$ kg^{-1}]	NH$_3$	ex	exchange	lv	leaves/ needles
D	layer thickness [m]	NH$_4$	fe	foliar exudation	ox	oxides
f	fraction [-]	S	fu	foliar uptake	pm	primary minerals
fpr	preference factor [-]	SO$_2$	gu	net (growth) uptake	rt	roots
F	flux [mol$_c$ ha^{-1} a^{-1}]	SO$_4$	lf	litterfall	st	stems
k	rate constant [a^{-1}]	Ca	mi	mineralisation		
K	equilibrium constant [mol^x 1^y]	Mg	pr	protonation		
rho	bulk density [kg m^{-3}]	K	rd	root decay		
SSC	sulphate sorption capacity [mmol$_c$ kg^{-1}]	Na	ru	root uptake		
θ	volumetric moisture content [m^3 m^{-3}]	Cl	we	weathering		
		H				
		Al				
		HCO$_3$				
		RCOO				
		CO$_2$				

Foliar exudation, litterfall, root decay, nitrification, denitrification, protonation and weathering are described by first-order reactions. Foliar uptake is considered a fraction of the dry atmospheric deposition. Root uptake is equal to the sum of

litterfall, foliar exudation and root decay minus foliar uptake plus a given net growth. Net growth is either described by a logistic function or as a constant increase. Here we used the latter option. Root uptake per soil layer is assumed to be proportional to the transpiration per soil layer. The dissolution of Ca and Al from carbonates and hydroxides respectively, is described as a first-order reaction, which is rate-limited by the degree of undersaturation. If supersaturation occurs, the Ca or Al concentration is set to equilibrium. Cation exchange and sulphate sorption are treated as equilibrium reactions, using Gaines-Thomas equations and a Langmuir isotherm, respectively. Speciation/dissolution of inorganic C is computed from equilibrium equations. A complete overview of the model structure of RESAM is given in De Vries *et al.* (1994a). The model input includes atmospheric deposition and hydrological data. Initial concentrations of cations and anions in the soil solution and the adsorption complex are calculated from an assumed equilibrium with the present atmospheric deposition.

2.2.3 Methodology

Monte Carlo simulation

There are various techniques available for performing uncertainty analysis (e.g. Janssen *et al.*, 1990). The most commonly used method for evaluating the uncertainty associated with parameter uncertainty in environmental modelling is related to Monte Carlo simulation. Monte Carlo methods suppose that the uncertainty of the various sources of uncertainty i.e. source terms, variables and parameters (in the following all these 'model inputs' will be referred to as parameters) can be characterised by their distribution functions and their correlations. Next, simulations are carried out with a randomly selected set of parameter values from the distribution functions. From the results, the distribution functions and the variance for the particular output variables can be estimated.

In performing uncertainty analysis with Monte Carlo techniques we distinguish two major steps: (i) sampling of model parameters followed by model simulation, and (ii) quantifying the (overall) uncertainty in the model output variables and determining the contribution of the model parameters to this uncertainty by using statistical techniques.

Sampling method

The number of Monte Carlo simulations needed for accurate estimates depends on the applied sampling method and on the number of considered sources of uncertainty. Especially in the case of RESAM, Monte Carlo analysis with straightforward drawings will lead to numerous and unnecessary computer runs.

An efficient sampling method has been developed named 'Latin Hypercube Sampling' (LHS) (McKay *et al.*, 1979; Iman and Conover, 1980). The principle of this method is a combination of two common statistical techniques. First, for each input parameter the parameter range is divided into N strata with equal probability $1/N$,

where N is a specified number equal to the number of Monte Carlo simulations. In each stratum a value is randomly sampled. Second, the values for each parameter are combined randomly, or with a specified correlation, with values of the other parameters to form a multivariable sample of N parameter combinations. Consequently it uses a relatively small number of model simulation runs. This method has been used successfully in various applications (Downing *et al.*, 1985; Iman and Helton, 1985, 1988; Gardner *et al.*, 1983; Kämäri *et al.*, 1986; Hettelingh, 1989).

In this study we have applied an adapted version of the software package PRISM (Gardner *et al.*, 1983). This is a package for performing uncertainty analyses by using Monte Carlo simulations with Latin Hypercube Sampling (LHS) in combination with statistical techniques.

Statistical analysis

The first purpose of the analysis is to quantify the overall uncertainty in the response variables by computing means, variances, percentiles, frequency distributions etc.

The second purpose is to identify which sources of uncertainty contribute most to the overall uncertainty/variability in the output variable. In general this is done by correlation and regression analyses. An extended overview of these techniques is given by Janssen *et al.* (1990). Here we restrict to a short summary of regression analysis. Linear regression analysis is applied to explain variability in a response variable (say $\mathbf{y}$) by considering a set of potential explanatory variables (say $\mathbf{x}_1,...,\mathbf{x}_p$). In this context the response variable is the output variable of RESAM and the explanatory variables are the sources of uncertainty. The linear regression model has e.g. the following form:

$$\mathbf{y} = \hat{\beta}_0 + \hat{\beta}_1 \cdot \mathbf{x_1} + \hat{\beta}_2 \cdot \mathbf{x_2} + \cdots + \hat{\beta}_p \cdot \mathbf{x_p} + \hat{e} \tag{1}$$

where: $\hat{\beta}_k$ ($k = 0,1,..., p$) denote the estimated regression coefficients (using the least-squares method) and ê denotes the residual term which is left unexplained by linear regression.

The coefficient of determination (COD) (also called R^2) of this regression is equal to:

$$R^2 = COD = 1 - \frac{S_{\hat{e}}^2}{S_y^2} \tag{2}$$

where S is the standard deviation of the regression residual, and S_y is the standard deviation of the response variable. COD is a number between 0 and 1. It measures the fraction of the variance in the response variable which is explained by the linear regression model. In fact, COD expresses the validity of the linear model to approximate (fit) the original model output $\mathbf{y}$ (COD $\approx$ 1 means a good fit).

When the regression model gives a good fit (COD $\approx$ 1), the coefficients $\hat{\beta}_k$ appropriately express the sensitivity of the model output $\mathbf{y}$ to variations in the parameters $\mathbf{x}_k$. $\hat{\beta}_k$ however does not account for the uncertainty in the explanatory variable $\mathbf{x}_k$. In order to include this uncertainty, it is useful to scale the original regression model (Eq. 1) with respect to the mean values and the standard deviations of $\mathbf{y}$ and $\mathbf{x}_k$.

This results in the standardised regression model (Draper and Smith, 1981):

$$\frac{\mathbf{y} - \overline{y}}{S_y} = \hat{\beta}_1^{(s)} \cdot \frac{\mathbf{x_1} - \overline{x}_1}{S_{x_1}} + \cdots + \hat{\beta}_p^{(s)} \cdot \frac{\mathbf{x_p} - \overline{x}_p}{S_{x_p}} + \hat{e}^{(s)} \tag{3}$$

where $\hat{\beta}_k^{(s)}$ ($k = 1, ..., p$) represent the estimated standardised regression coefficients (SRC), which are related to the coefficients $\hat{\beta}_k$ by:

$$SRC_k = \hat{\beta}_k^{(S)} = \hat{\beta}_k \cdot \frac{S_{x_k}}{S_y} \tag{4}$$

Here S_{x_k} and S_y denote the standard deviations of $\mathbf{x}_k$ and $\mathbf{y}$. The subscript $_k$ denote the average values of $\mathbf{y}$ and $\mathbf{x}_k$.

From Eq. (3) it is obvious that the standardised regression coefficients (SRC) indicates the increase or decrease in the model output y (in terms of its standard deviation S_y) due to an increase in parameter $\mathbf{x}_k$ (in terms of its standard deviation S_{x_k}), while the other parameters $\mathbf{x}_j$ remain unchanged. Therefore the SRC can be used to assess the importance of each parameter $\mathbf{x}_k$ in explaining the uncertainty of the considered model output. Usually this is done by ranking the sources of uncertainty on the basis of the SRC. This method has the following disadvantages: (i) the SRC can be misleading in case of strong non-linearity in the relation between $\mathbf{x}_k$ and $\mathbf{y}$; and (ii) the SRC does not account for the influence of other parameters on $\mathbf{y}$ besides $\mathbf{x}_k$.

Ad. (i): The SRC is only a measure for the linear relationship between parameters and the associated model output. Therefore it is always important to inspect the COD. When the COD is low, there are strong non-linear relationships and the use of the SRC is not justified. When strong non-linearity occurs, it is worthwhile to apply data transformation (e.g. a logarithmic transformation) to the parameters and/or the model output. However, an appropriate data transformation is sometimes hard to find. Generally rank transformation is used, which is shown to be a robust and powerful transformation (Iman *et al.*, 1981). The uncertainty contribution is then analysed by studying the standardised rank transformed regression coefficients (SRRC). In fact, rank transformed regression analysis only gives information about the monotony of the relationship between parameters and associated model output.

Ad. (ii): Although the SRC and/or SRRC are recommended in literature (Dale *et al.*, 1988; Iman and Helton, 1988), it is shown by Janssen *et al.* (1990) that they are imperfect when the parameters are correlated. For this reason Janssen *et al.* (1990) introduced a new improved measure, which determines the relative change in the uncertainty (S_y) of the model output **y** as a result of a (small) relative change in the uncertainty (S_{x_k}) of the parameter **x**$_k$, taking the influence of the correlated sources into account. This results in a compound measure named the partial uncertainty contribution (PUC):

$$PUC_k = \sum_{j=1}^{p} \hat{\beta}_j^{(S)} \cdot r_{x_j y} \cdot r_{x_k x_j}^2 = \sum_{j=1}^{p} SRC_j \cdot LCC_j \cdot r_{x_k x_j} \tag{5}$$

where $r_{x_j y}$ and $r_{x_k x_j}$ are the correlation coefficients between **x**$_j$ and **y**, and **x**$_k$ and **x**$_j$ respectively. The quantity $r_{x_j y}$ will in the sequel also be denoted as LCC$_j$ (Linear Correlation Coefficient).

When there are no correlations, the PUC can be simplified to (Janssen *et al.*, 1990):

$$PUC_k = SRC_k \cdot LCC_k = SRC_k^2 \tag{6}$$

In this specific case the SRC is equal to the root of the PUC (C), which we will call the root of the (partial) uncertainty (coefficient) (RTU). When the SRC differs from the RTU, this is an indication for a correlation between the parameters considered. Contrary to the SRC, the RTU is always positive.

In this study we use the RTU as a measure for the uncertainty contribution, unless the COD appears to be very low. In that case we perform rank analysis and use the SRRC.

Apart from using regression analysis in quantifying the uncertainty distributions, we have applied this technique to get a justification for using averaged parameter values in a regional application: if the COD is close to 1 during the simulation period, the model has a strong linear behaviour, and the average output of all the Monte Carlo simulations will be close to the output of a simulation carried out with average parameter values.

Furthermore, we have used the results of the regression analysis to see whether the (linear) regression models, that can be seen as a model simplification of the 'real' model (i.e. a so-called meta model; Kleijnen, 1987; Rotmans *et al.*, 1988), could possibly replace RESAM for a regional application.

2.2.4 Uncertainty in model input

Restrictions

The investigated output variables have been restricted to the pH, NH_4/K ratio and Al/Ca ratio in the root zone of a leptic podzol covered by Douglas fir. The soil profile consists of four horizons (layers): O (litter layer, 4 cm), A (15 cm), Bh (25 cm) and C (20 cm). For this soil profile, with four layers, RESAM needs about 200 source terms, variables and parameters, which have to be estimated on the basis of rather uncertain *a priori* information.

In order to restrict the number of (uncertain) parameters, and consequently also the number of Monte Carlo simulations, we have assumed a steady-state nutrient cycle with a constant net uptake (i.e. tree growth), which implies that the total uptake (foliar uptake and root uptake) is equal to the sum of litterfall, foliar exudation, root decay and net uptake. Consequently, there is no accumulation of N and S in needles, roots and/or litter layer. Furthermore, a feedback between reducing depositions of N and S and their contents in the needles is not considered. Especially for N this might be an important mechanism. It is likely that in the long run the assumption of a stationary nutrient cycle will lead to an overestimation of both the NH_4/K ratio and the Al/Ca ratio and to an underestimation of pH for the decreasing-deposition scenario considered (see Section *Data*).

Furthermore, we have assumed a constant hydrology, by taking a constant annual precipitation volume. Finally, uncertainties in various parameters which were *a priori* considered as insignificant of the investigated model output, have not been investigated. Examples of these are: Ca, Mg, K and Na contents in primary minerals; exchangeable fractions of NH_4, Ca, Mg, K and Na, and the selectivity constants of Mg and Na. Using these assumptions, the number of parameters for which probability distributions have to be specified has been reduced to 70.

Data

Deposition data (source terms)

Uncertainty in deposition is related to spatial variability caused by concentration gradients and variation in filtering dry deposition. The uncertainty and spatial variability in wet and dry depositions is restricted to one receptor area in the centre of the Netherlands with intensive animal husbandry. The source terms consist of both dry and wet deposition of SO_2, NO_2, and NH_3 and wet deposition of base cations (Ca, Mg, K, Na) and chloride. The dry deposition of base cations, chloride and sea salt sulphate is described by a dry deposition factor (f_{dd}). This is a factor by which the wet deposition must be multiplied to determine the dry deposition.

The deposition values used are given in Table 3. Data have been derived from wet deposition and throughfall measurements of SO_4, NO_3, NH_4 and Na in 27 coniferous forest stands in the Netherlands (Tiktak *et al.*, 1988; Ivens *et al.*, 1988; Kleijn *et al.*, 1989; Houdijk, 1993). The ratio of Na in throughfall minus bulk

deposition to Na in bulk deposition was used to estimate f_{dd} (Bredemeier, 1988). The values for NH_4 and SO_4 were considered representative of a deposition region with intensive animal husbandry.

Table 3 Ranges and distributions of deposition fluxes (mol_c ha^{-1} a^{-1}) and the dry deposition factor (-)

Input	Mean	SD	Min.	Max.
$FSO_{2\ dw}$	875	225	690	1410
$FSO_{2\ dd}$	2965	1025	1650	4260
$FNO_{2\ dw}$	440	35	370	470
$FNO_{2\ dd}$	530	230	320	1100
$FNH_{3\ dw}$	1310	220	945	1730
$FNH_{3\ dd}$	2885	1050	1530	4810
FCa_{dw}	240	125	135	490
FMg_{dw}	190	65	130	360
FK_{dw}	240	60	150	340
FNa_{dw}	730	165	495	970
FCl_{dw}	1125	315	640	1610
f_{dd}	0.98	0.55	0.31	1.96

The deposition scenario used is based on the emission reduction policy in the Netherlands (Schneider and Bresser, 1988). Although the intended reductions are subject to various uncertainties, which are mainly due to political and technical factors, we do not consider them here. The emission scenario is divided into two periods: 1987-2000 and 2000-2010; the corresponding reduction fractions are given in Table 4. The reduction during these two periods is considered linear. The reduction is only applied on SO_x, NO_x and NH_x; the depositions of the base cations and Cl remain constant.

Table 4 Reduction fractions for total deposition fluxes of SO_x, NO_x and NH_x

Period	SO_x	NO_x	NH_x
1987-2000	0.63	0.40	0.58
2000-2010	0.58	0.29	0.40

Here we restrict the uncertainty in the source terms to the initial (i.e. 1987) values as specified in Table 3. The deposition scenario for each Monte Carlo simulation is obtained by multiplying the by LHS sampled initial deposition value for SO_x, NO_x and NH_x by the corresponding reduction factor.

Initial values of variables

An overview of the distributions specified for the initial values is given in Table 5.

Table 5 Distributions of initial conditions

Variable	Unit	Distribution type	Mean	SD	Min.	Max.
A_{lv}	kg ha⁻¹	normal	9500.0	3135.0	3400.0	16000.0
A_{rt}	kg ha⁻¹	uniform	3750.0	-	1350.0	6300.0
$f_{rt\,1}$	-	normal	0.39	0.13	0.06	0.66
$f_{rt\,2}$	-	normal	0.41	0.12	0.04	0.78
ctN_{st}	%	normal	0.11	0.015	0.08	0.12
$ctCa_{st}$	%	normal	0.07	0.035	0.04	0.13
ctK_{st}	%	normal	0.04	0.016	0.02	0.07
ctS_{st}	%	normal	0.02	0.008	0.01	0.04
ctN_{lv}	%	normal	2.80	0.59	1.49	3.71
$ctCa_{lv}$	%	normal	0.32	0.14	0.13	0.79
ctK_{lv}	%	normal	0.36	0.08	0.20	0.66
ctS_{lv}	%	normal	0.24	0.05	0.17	0.36
ctN_{rt}	%	normal	0.34	0.05	0.25	0.40
$ctCa_{rt}$	%	normal	0.25	0.07	0.16	0.34
ctK_{rt}	%	normal	0.22	0.07	0.13	0.44
ctS_{rt}	%	normal	0.05	0.01	0.03	0.07
rho_0	kg m⁻³	normal	150.0	60.0	22.0	454.0
rho_1	kg m⁻³	normal	1310.0	139.0	790.0	1530.0
rho_2	kg m⁻³	normal	1450.0	48.0	1300.0	1540.0
rho_3	kg m⁻³	normal	1540.0	35.0	1300.0	1600.0
$ctAl_{ox\,1}$	mmol$_c$ kg⁻¹	lognormal	4.18 (65.0)[1]	0.66	2.46 (12.0)	5.21 (184.0)
$ctAl_{ox\,1}$	mmol$_c$ kg⁻¹	lognormal	5.11 (156.0)	0.61	2.95 (19.0)	6.65 (777.0)
$ctAl_{ox\,1}$	mmol$_c$ kg⁻¹	lognormal	4.98 (145.0)	0.41	3.77 (42.0)	6.01 (406.0)
SSC_1	mmol$_c$ kg⁻¹	lognormal	0.26 (1.3)	0.47	-1.42 (0.25)	1.31 (3.7)
SSC_2	mmol$_c$ kg⁻¹	lognormal	3.30 (1.2)	0.48	-7.0 (0.0)	2.74 (15.5)
SSC_3	mmol$_c$ kg⁻¹	lognormal	2.90 (1.1)	0.32	-7.0 (0.0)	2.09 (8.1)
CEC_0	mmol$_c$ kg⁻¹	normal	282.0	68.0	108.0	700.0
CEC_1	mmol$_c$ kg⁻¹	lognormal	3.4 (30.0)	0.72	0.69 (2.0)	5.2 (186.0)
CEC_2	mmol$_c$ kg⁻¹	lognormal	2.4 (11.1)	0.67	0.0 (1.0)	3.8 (43.0)
CEC_3	mmol$_c$ kg⁻¹	lognormal	1.6 (4.8)	0.68	0.0 (1.0)	2.9 (19.0)
$fAl_{ac\,0}$	-	normal	0.05	0.03	0.02	0.11
$fAl_{ac\,2}$	-	normal	0.53	0.15	0.37	0.78
$fAl_{ac\,3}$	-	normal	0.73	0.15	0.52	0.89

[1] For lognormal distributions values in brackets denote the nominal values; the other values concern the log-transformed counterparts

The initial values that must be specified with respect to the tree species are amounts and element contents in needles, roots and stems and the root distribution. The needle biomass (A_{lv}) and element contents in stems (ctX_{st}, X = N, S, Ca, K) and roots (ctX_{rt}, X = N,S,Ca,K) are based on literature data (a.o. Kimmins et al., 1985). Element contents in needles (ctX_{lv}, X = N,S,Ca,K), root biomass (A_{rt}) and root distribution data ($f_{rt\,n}$, n = layer number) are based on field research in eight Douglas forest stands in the centre of the Netherlands (Oterdoom et al., 1991). Note that extremely high N contents occur in the needles, up to 3.7% (Table 5). They are due to the high NH$_x$ input in the investigated area. A decreasing deposition may lead to a decrease in the N content, but this is not included in this model analysis. Data for the root biomass (A_{rt}) and the root distribution fractions ($f_{rt\,n}$, n=1,2,3) are related to the fine roots (< 2 mm), which are active in water and nutrient uptake. Naturally, in the

case of three layers only two fractions are independent. We calculated the fraction in layer 3 from the other two: $f_{rt\,3} = 1 - f_{rt\,1} - f_{rt\,2}$. Afterwards we checked whether the distribution of $f_{rt\,3}$ matched with the measured one. The field survey of Oterdoom *et al.* (1991) gave no information about roots in the litter layer. Consequently, we did not include roots in the litter layer; however, it is likely that the litter layer contains a considerable amount of (fine) roots (Grier *et al.*, 1981; Persson, 1983).

Investigated variables related to the soil are bulk density (*rho*), content of aluminium hydroxides ($ctAl_{ox}$), sulphate sorption capacity (*SSC*), cation exchange capacity (*CEC*), and fraction of exchangeable aluminium (fAl_{ec}). The distributions of *rho* and *CEC* in the litter layer (layer 0) were derived from the field survey in eight Douglas stands mentioned earlier (Kleijn *et al.*, 1989). Values for $ctAl_{ox}$ and *SSC* in the litter layer were assumed to be zero. For the mineral layers *rho*, $ctAl_{ox}$ and *CEC* were derived from the soil information system available at the Winand Staring Centre. *SSC* was related to $ctAl_{ox}$ using literature data (Johnson and Todd, 1983). The aluminium occupation of the exchange complex ($fAl_{ec\,n}$, n=0...3) was derived from the field survey in eight Douglas stands (Kleijn *et al.*, 1989).

Model parameters

A summary of the relevant model parameters is given in Table 6. The investigated model parameters related to the vegetation are the foliar uptake factor of NH_3 ($fNH_{3\,fu}$), the preference factor for the NH_4 uptake by roots ($f_{pr}NH_{4\,ru}$), foliar exudation constants (kX_{fe}, X=Ca, K, Mg), litterfall (k_{lf}) and root decay (k_{rd}) constants. The distributions used for the foliar uptake fraction and the root uptake preference factor of NH_4 are more or less arbitrary. Foliar uptakes of SO_2 and NO_2 were considered negligible. Distributions of the foliar exudation of Ca, K and Mg were derived from the differences between throughfall and estimated total deposition in 15 Douglas stands (Tiktak *et al.*, 1988; Kleijn *et al.*, 1989; Houdijk, 1993). Total deposition was estimated by adding the measured bulk deposition (*dw*) to the dry deposition, calculated by multiplying the f_{dd} factor with the bulk deposition (see Table 3). Litterfall values were based on a national inventory of the forest vitality in the Netherlands (P. van der Tweel, pers. comm.). The distribution of the root decay constant was derived from data given by Santantonio and Hermann (1985).

Investigated model parameters related to the soil are the nitrification constants ($k_{ni\,n}$, n=0,1,2,3), protonation constant (k_{pr}), weathering rate constants of primary minerals ($kX_{we\,pm}$, X=K/Na, Ca/Mg) and aluminium hydroxides ($kAl_{we\,ox\,n}$ n=1,2,3), the aluminium hydroxide equilibrium constant (KAl_{ox}), the sulphate adsorption constant ($KSO_{4\,ad}$) and the exchange constants taking Ca as the reference ion (KX_{ex}, X=H, Al, NH_4, K).

Table 6 Distributions of model parameters

Parameter	Unit	Distribution type	Mean	SD	Min.	Max.
$fNH_{3\,fu}$	-	uniform	0.1	-	0.0	0.2
$f_{pr}NH_{4\,ru}$	-	uniform	1.5	-	0.0	2.0
kCa_{fe}		normal	0.14	0.05	0.08	0.23
kMg_{fe}	a^{-1}	normal	0.26	0.04	0.19	0.31
kK_{fe}	a^{-1}	normal	0.22	0.08	0.09	0.32
k_{rd}	a^{-1}	uniform	2.0	-	1.5	2.5
$k_{ni\,0}$	a^{-1}	uniform	85.0	-	50.0	120.0
$k_{ni\,1}$	a^{-1}		20.0	-	10.0	30.0
$k_{ni\,2}$	a^{-1}	uniform	2.0	-	0.0	5.0
$k_{ni\,3}$	a^{-1}	uniform	2.0	-	0.0	5.0
k_{pr}	a^{-1}	uniform	50.0	-	25.0	75.0
$kK/Na_{we\,pm}$	a^{-1}	uniform	$1.1 \cdot 10^{-4}$	-	$2.0 \cdot 10^{-5}$	$2.0 \cdot 10^{-4}$
$kCa/Mg_{we\,pm}$	a^{-1}	uniform	$5.25 \cdot 10^{-4}$	-	$5.0 \cdot 10^{-5}$	$1.0 \cdot 10^{-3}$
$kAl_{we\,ox\,1}$	a^{-1}	uniform	0.02	-	0.01	0.03
$kAl_{we\,ox\,2}$	a^{-1}	uniform	0.20	-	0.10	0.30
$kAl_{we\,ox\,3}$	a^{-1}	uniform	0.20	-	0.10	0.30
KAl_{ox}	$(mol\,l^{-1})^{-2}$	uniform	$10^{8.77}$	-	$10^{8.11}$	$10^{9.35}$
$KH_{ex\,0}$	$(mol\,l^{-1})^{-1}$	lognormal	3.50 (33.0)[1]	1.00	1.50 (4.5)	5.50 (2.5)
$KH_{ex\,1}$	$(mol\,l^{-1})^{-1}$	lognormal	6.79 (889.0)	1.29	4.76 (117.0)	9.19 (9800.0)
$KH_{ex\,2}$	$(mol\,l^{-1})^{-1}$	lognormal	7.83 (2515.0)	1.96	4.01 (55.0)	10.3 (2533.0)
$KH_{ex\,3}$	$(mol\,l^{-1})^{-1}$	lognormal	7.72 (2252.0)	3.52	2.62 (14.0)	12.2 (98789.0)
$KAl_{ex\,0}$	$mol\,l^{-1}$	lognormal	4.30 (74.0)	1.00	2.30 (10.0)	6.30 (545.0)
$KAl_{ex\,1}$	$mol\,l^{-1}$	lognormal	-1.18 (0.3)	1.32	-2.98 (0.1)	0.9 (0.6)
$KAl_{ex\,2}$	$mol\,l^{-1}$	lognormal	-0.18 (0.8)	1.38	-2.19 (0.1)	1.6 (0.1)
$KAl_{ex\,3}$	$mol\,l^{-1}$	lognormal	-0.14 (0.9)	1.44	-1.80 (0.2)	2.7 (5.5)
$KNH_{4\,ex\,0}$	$(mol\,l^{-1})^{-1}$	lognormal	1.40 (4.1)	0.20	1.00 (2.7)	1.80 (6.0)
$KNH_{4\,ex\,1}$	$(mol\,l^{-1})^{-1}$	lognormal	1.69 (5.4)	1.33	-0.5 (0.6)	3.58 (36.0)
$KNH_{4\,ex\,2}$	$(mol\,l^{-1})^{-1}$	lognormal	5.23 (187.0)	1.91	1.64 (5.2)	8.06 (3165.0)
$KNH_{4\,ex\,3}$	$(mol\,l^{-1})^{-1}$	lognormal	7.62 (2039.0)	1.93	4.79 (120.0)	10.6 (3478.0)
$KK_{ex\,0}$	$(mol\,l^{-1})^{-1}$	lognormal	2.50 (12.0)	0.70	1.10 (275.0)	3.90 (49.0)
$KK_{ex\,1}$	$(mol\,l^{-1})^{-1}$	lognormal	3.60 (37.0)	0.69	2.40 (11.0)	4.4 (6.0)
$KK_{ex\,2}$	$(mol\,l^{-1})^{-1}$	lognormal	4.77 (118.0)	0.63	3.61 (37.0)	5.5 (52.0)
$KK_{ex\,3}$	$(mol\,l^{-1})^{-1}$	lognormal	6.17 (478.0)	0.87	5.02 (151.0)	7.4 (772.0)
$KSO_{4\,ad}$	$m^3\,mol_c^{-1}$	lognormal	0.00 (1.0)	1.15	-2.30 (0.1)	2.3 (10.0)

[1] For lognormal distributions, values in brackets denote the nominal values; the other values concern the log-transformed counterparts.

The distributions of the nitrification, protonation and aluminium hydroxide weathering rate constants were chosen somewhat arbitrary around a calibrated value, since very little is known about the uncertainty/variability of these parameters. The distribution type was assumed to be uniform. The distributions of the base weathering constants were based on information in De Vries and Breeuwsma (1986), whereas the aluminium hydroxide equilibrium constant distribution was derived from Lindsay (1979) and May *et al.* (1979). Distributions of the selectivity constants were derived from a field survey by Kleijn *et al.* (1989). Contrary to other soil parameters, the distribution type of the selectivity constant was assumed to be lognormal.

Correlations

Naturally, various parameters are correlated. Here we only consider those correlations for which we have obvious indications, i.e. those with a correlation coefficient greater than 0.5. Correlations for deposition parameters, turnover parameters of roots and needles and selectivity constants included in the analysis are given in Table 7.

Table 7 Correlations used

Parameter 1	Parameter 2	Correlation coefficient
$FSO_{2\,dd}$	$FNO_{2\,dd}$	0.77
$FSO_{2\,dd}$	$FNH_{3\,dd}$	0.89
$FNO_{2\,dd}$	$FNH_{3\,dd}$	0.51
FCl_{dw}	FNa_{dw}	0.80
k_{lf}	A_{lv}	-0.80
k_{rd}	A_{rt}	-0.60
$f_{rt\,1}$	$f_{rt\,2}$	-0.67
KH_{ex}	KAl_{ex}	0.52
KK_{ex}	$KNH_{4\,ex}$	0.76

Especially, the dry deposition fluxes of SO_x and NH_x appear to be strongly correlated. The same is true for the wet deposition fluxes of Na and Cl. The correlations between deposition parameters are based on bulk precipitation and throughfall data in the 27 coniferous stands mentioned before (Houdijk, 1993; Ivens *et al.*, 1988; Kleijn *et al.*, 1989). The correlation between k_{lf} and A_{lv} is based on the knowledge that the product $k_{lf} \cdot A_{lv}$ lies between $1\cdot10^3$ and $4\cdot10^3$ kg ha^{-1} a^{-1} (Kimmins *et al.*, 1985; Tiktak *et al.*, 1988). The correlation coefficient used was determined by trial and error. The same holds for the correlation between k_{rd} and A_{rt}. The correlation between the root distribution parameters ($f_{rt\,1}$ and $f_{rt\,2}$) was based on the field survey of Oterdoom *et al.* (1991). A correlation with $f_{rt\,3}$ was introduced implicitly by the relation $f_{rt\,3} = 1 - f_{rt\,1} - f_{rt\,2}$ (see Initial values of variables). The correlations between the selectivity constants of Al and H, which together occupied about 90% of the exchange complex, and between K and NH_4 were based on the field survey of Kleijn *et al.* (1989).

2.2.5 Results

Introduction

The presentation of the uncertainty in model output is restricted to the pH, NH_4/K ratio and Al/Ca ratio in two layers of the leptic podzol soil profile: the top of the root zone (A, 15 cm) and the bottom of the root zone (C, 20 cm).

The uncertainty in the model output is presented by:

- the mean, the standard deviation (SD) and the coefficient of variation (CV) (i.e. SD/mean) at the beginning (1987), halfway (2000) and at the end (2010) of the simulation period;

- the trajectory of the mean, median (50 percentile), 97.5 percentile and 2.5 percentile during the simulation period (i.e. 1987-2010).

Furthermore, we give the model output of a simulation carried out with mean parameter values, referred to as reference run, in order to investigate the correspondence between this result and the mean of all the Monte Carlo simulations. With this we can check if one simulation with mean parameter values suffice for a regional application, planned in the near future.

The contribution of the model parameters to the uncertainty is presented by the trajectory of the root of the (partial) uncertainty (coefficient) (RTU) of the three most important parameters either at the beginning or at the end of the simulation period.

pH

The mean, the standard deviation (SD) and the coefficient of variation (CV) of the pH in layers 1 and 3 in 1987, 2000 and 2010 are given in Table 8. The model results show that the absolute uncertainty (SD) in the pH in the subsoil is slightly higher than that in the topsoil, whereas the opposite is true for the relative uncertainty (CV). Both the absolute and the relative uncertainty remain fairly constant in both layers during the simulation period. The pH in both layer 1 and layer 3 increases during the simulation period, due to the decreasing deposition.

Table 8 Mean, *SD* and *CV* of the pH in layers 1 and 3 in 1987, 2000 and 2010

Layer	Year	Mean	SD	CV
1	1987	3.0	0.11	0.04
1	2000	3.1	0.11	0.04
1	2010	3.2	0.13	0.04
3	1987	4.1	0.13	0.03
3	2000	4.2	0.13	0.03
3	2010	4.3	0.14	0.03

Figure 1 shows the trajectories of the mean, various percentile values, and the reference run in both layers during the simulation period. At the initiation of each simulation, model outputs are in steady state with respect to deposition. This is done by running the model 25 years in advance while keeping all the 'capacity' variables constant.

The reference run and the mean correspond very well. In the reference run the pH is only about 0.01 to 0.08 lower than the mean. There is a slight difference between the median and the mean in layer 3 (median > mean), which indicates that the pH distribution is skewed to the left.
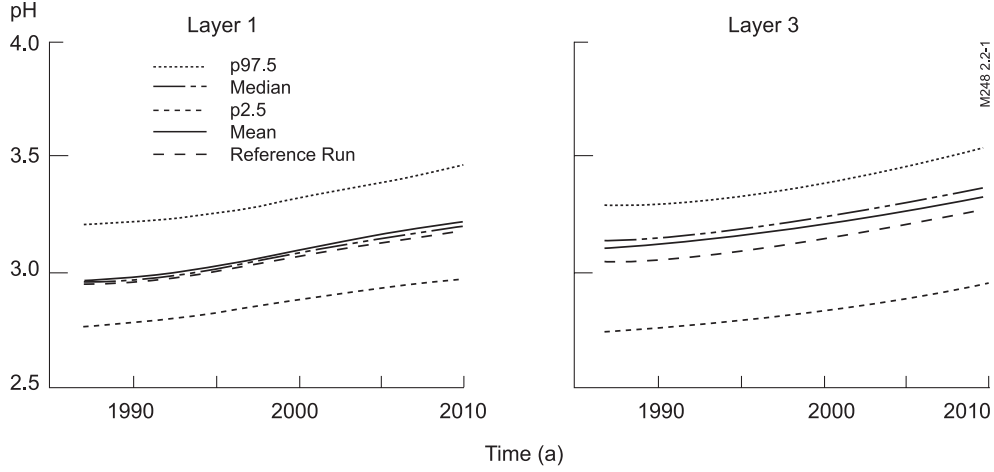
Figure 1 Temporal evolution of the mean, the median, the 97.5 and 2.5 percentiles, and the reference run of the pH in layers 1 and 3.

The temporal evolution of the three parameters with the highest RTU with respect to the pH in layers 1 and 3, either at the beginning or at the end of the simulation period, is shown in Figure 2. During the simulation period, the coefficient of determination (COD or R^2) of the regression models lies between 0.92 and 0.96 in layer 1, and between 0.87 and 0.88 in layer 3.
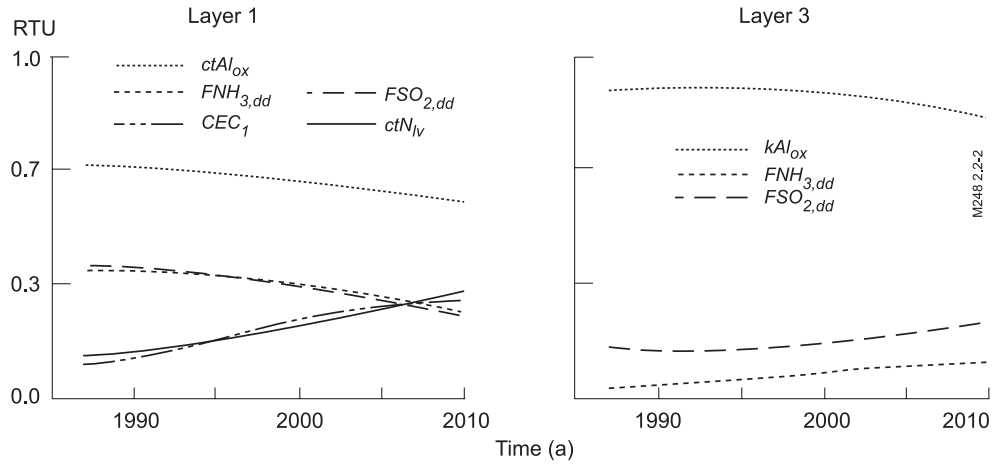
Figure 2 Temporal evolution of the RTU between model parameters and the pH in layers 1 and 3

Figure 2 shows that the uncertainty of the pH in layer 1 is mainly determined by uncertainty in the amount of aluminium hydroxide ($ctAl_{ox\ 1}$) in that layer, whereas the uncertainty in the equilibrium constant of aluminium hydroxide (KAl_{ox}) mainly determines the uncertainty of the pH in layer 3. Both $ctAl_{ox}$ and KAl_{ox} determine the H

buffering by aluminium hydroxides. The fact that $ctAl_{ox}$ is important in layer 1 is due to a strong undersaturation with respect to aluminium hydroxides. In this layer the KAl_{ox} hardly affects the Al dissolution. However, in layer 3 saturation occurs with respect to aluminium hydroxide, thus explaining the importance of KAl_{ox}. Both the uncertainty contributions of $ctAl_{ox}$ and KAl_{ox} decrease during the simulation period, which is due to the decreasing deposition.

Next to the Al dissolution parameters, the dry deposition of NH_3 ($FNH_{3\,dd}$) and SO_2 ($FSO_{2\,dd}$), which are the main contributors to the acid load, determine the uncertainty of the pH in both layers. It must be noted, that the high RTU value of $FSO_{2\,dd}$ is mainly due to the correlation between $FSO_{2\,dd}$ and $FNH_{3\,dd}$. This is confirmed by inspecting the standardised regression coefficients (SRC), a measure which does not account for correlations (see Section *Statistical Analysis*). The SRC of $FSO_{2\,dd}$ in layer 1 lies between -0.21, in 1987, and -0.01, in 2010, and the SRC of FNH_3 between -0.18, in 1987, and -0.22, in 2010. For layer 1 the N content in needles (ctN_h) and the CEC in that layer (CEC_1) also appear to be important, especially as the simulation period proceeds. For ctN_h, this is due to the increase in the relative contribution of the internal N cycle to the acid load. It must be noted, however, that the N content in the needles has been kept constant over the simulation period (see Section *Restrictions*), whereas it will most probably decrease as a result of the decreasing N deposition (Van den Burg *et al.*, 1988; Van den Burg and Kiewiet, 1989). The uncertainty contribution of ctN_h might thus be overestimated. The increase in the uncertainty contribution of CEC_1 with time, is also caused by the change in deposition: a decrease in H load leads to less aluminium dissolution resulting in Al desorption and H adsorption. However, the contribution of the CEC is temporal: when the deposition level remains constant after the deposition reduction period, a new equilibrium is installed. Consequently the uncertainty contribution will decrease.

Molar NH₄/K ratio

The mean, the SD and the CV of the molar NH_4/K ratio in 1987, 2000 and 2010 are given in Table 9.

Table 9 Mean, *SD* and *CV* of the molar NH_4/K ratio in layers 1 and 3 in 1987, 2000 and 2010

Layer	Year	Mean	SD	CV
1	1987	3.4	1.2	0.35
1	2000	1.8	0.7	0.40
1	2010	1.2	0.6	0.45
3	1987	0.5	0.6	1.1
3	2000	0.2	0.3	1.6
3	2010	0.0	0.1	3.2

These model results show that the absolute uncertainty (SD) of the NH_4/K ratio in the topsoil (layer 1) is greater than in the subsoil (layer 3), whereas the opposite is true for the relative uncertainty (CV). In both layers the absolute

uncertainty decreases during the simulation period, due to the decrease in (N) deposition. On the other hand, the relative uncertainty increases, especially in layer 3. The deposition reduction leads to a depression of the mean molar NH_4/K ratio in both layers. The molar NH_4/K ratio in layer 3 is permanently about 1 to 2 units lower than in layer 1. This is mainly caused by nitrification and to a lesser extent by NH_4 uptake. During the entire simulation period the molar NH_4/K ratio in the topsoil remains below 5, which is generally considered to be an acceptable ratio (Roelofs *et al.*, 1985; De Vries, 1988).
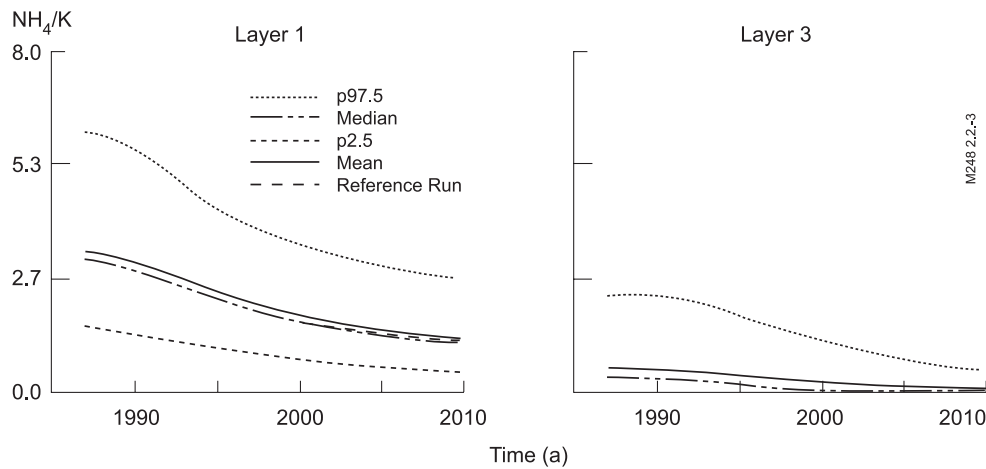
Figure 3 Temporal evolution of the mean, the median, the 97.5 and 2.5 percentiles, and the reference run of the NH_4/K mol ratio in layers 1 and 3

Figure 3 shows the time evolution of the mean, various percentile values and the reference run of the molar NH_4/K ratio. Figure 3 clearly confirms the difference in absolute uncertainty between layers 1 and 3 shown in Table 9 In layer 1 the reference run lies somewhat lower than the mean, but the similarity is striking. In layer 3 the difference is more substantial. The median lies also below the mean, which implies that the distribution is skewed to the right.

Figure 4 shows the RTU trajectories of the three parameters with the highest RTU either at the beginning or at the end of the simulation period. During the simulation period the COD of the regression models lies between 0.92 and 0.94 in layer 1, whereas it decreases from 0.82 at the beginning to 0.46 in layer 3. Although the COD at the end of the simulation period is low, we still use the RTU for the analysis, because data transformations did not improve the COD. However, one should bear in mind, that the COD in layer 3 is decreasing at the end of the simulation period to an unacceptably low value, which means that the RTU is no longer an optimal measure to quantify the uncertainty.
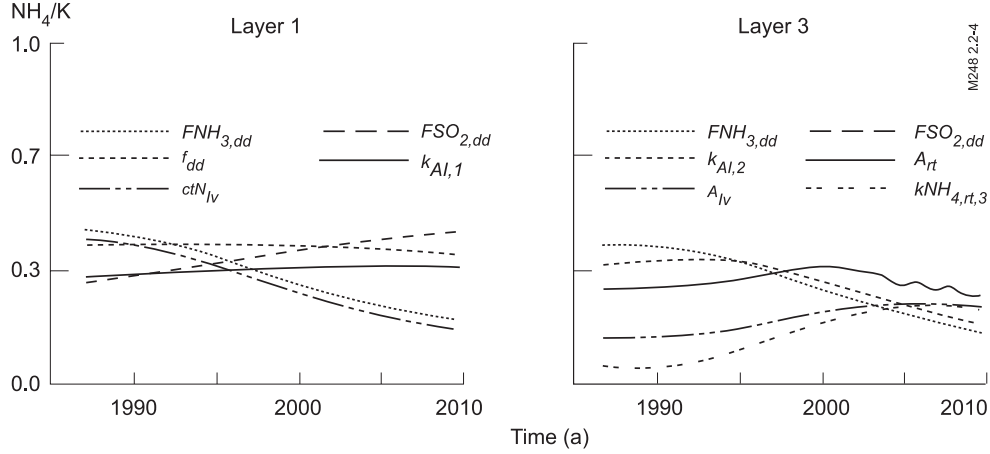
NH$_4$/K

Figure 4 Temporal evolution of the RTU between model parameters and the NH$_4$/K mol ratio in layers 1 and 3

At the beginning of the simulation period the uncertainty in the molar NH$_4$/K ratio in layer 1 is mainly determined by the dry depositions of NH$_3$ (*FNH$_{3\ dd}$*) and SO$_2$ (*FSO$_{2\ dd}$*) and the dry deposition factor (*f$_{dd}$*). During the simulation period, the uncertainty contribution of the deposition parameters decreases, whereas the influence of the N content in needles (*ctN$_{lv}$*) and the nitrification rate constant (*k$_{ni\ 1}$*) increase. This means that the uncertainty contribution of the internal N cycle becomes greater than the contribution of the external N load (compare the pH). The uncertainty contribution of *f$_{dd}$* remains more or less constant.

Contrary to layer 1, the uncertainty in layer 3 is mainly determined by parameters influencing the NH$_4$ concentration. As in layer 1, *FNH$_{3\ dd}$* and *FSO$_{2\ dd}$* mainly determine the uncertainty at the beginning of the simulation period, whereas their influence decreases when the simulation period proceeds. For both layers it is remarkable that *FSO$_{2\ dd}$* strongly contributes to uncertainty in the molar NH$_4$/K ratio. This is caused, however, by the predefined correlation between *FSO$_{2\ dd}$* and *FNH$_{3\ dd}$* (see Section *Correlations*). Similar to layer 1, the influence of the internal N cycle increases with time. In the year 2010 the biomass amounts of roots (*A$_{rt}$*) and needles (*A$_{lv}$*) contribute strongly to the uncertainty of the NH$_4$/K mol ratio. Remarkable is also the relatively high uncertainty contribution of the NH$_4$ selectivity constant in layer 3 (*KNH$_{4\ se\ 3}$*). As in layer 1, the impact of the deposition parameters decreases, whereas, unlike in layer 1, the nitrification rate parameter in layer 2 (*k$_{ni\ 2}$*) decreases too.

Molar Al/Ca ratio

The mean, the SD and the CV of the molar Al/Ca ratio in 1987, 2000 and 2010 are given in Table 10.

Table 10 Mean, *SD* and *CV* of the molar Al/Ca ratio in layers 1 and 3 in 1987, 2000 and 2010

Layer	Year	Mean	SD	CV
1	1987	2.3	1.2	0.53
1	2000	1.5	0.9	0.59
1	2010	1.0	0.6	0.59
3	1987	9.8	5.0	0.51
3	2000	10.5	11.6	1.1
3	2010	5.3	6.5	1.2

From these model results it is clear that both the absolute (SD) and the relative (CV) uncertainties in layer 3 are much greater than the uncertainties in layer 1. The absolute uncertainty in layer 1 decreases with time, whereas the relative uncertainty remains fairly constant. On the other hand in layer 3 there is a dramatic increase in uncertainty, especially in the period between 1990 and 2000 both in the relative and the absolute uncertainty. Furthermore the mean also increases during this period. This is caused by changes in the adsorption complex. As a result of the decreasing deposition, the concentrations of H and the Al decrease too. This leads to exchange of Ca against H, which results in a relatively stronger decrease in the Ca concentration than the decrease in the Al concentration, leading to a temporal increase in the molar Al/Ca ratio.
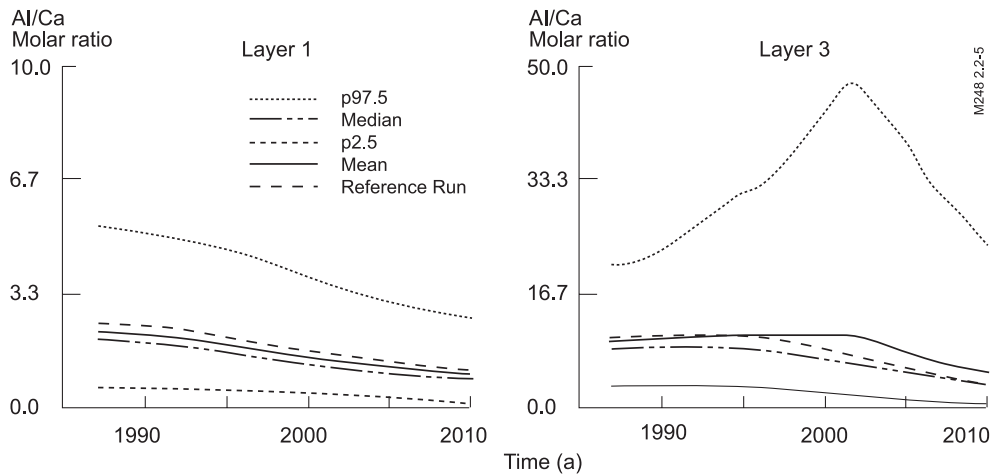
Figure 5 Temporal evolution of the mean, the median, the 97.5 and 2.5 percentiles, and the reference run of the Al/Ca mol ratio in layers 1 and 3

Figure 5 shows the time evolution of the mean, various percentile values, and the reference run of the molar Al/Ca ratio. In layer 1 the reference run is more or less equal to the mean. In layer 3, however, the reference trajectory clearly deviates from the mean after 1996.

It is clear that eventually the decrease in deposition has a positive effect on the molar Al/Ca ratio. In both layers the mean molar Al/Ca ratio decreases by about 50%. However, when a dynamic nutrient cycle would have been considered, the decrease in molar Al/Ca ratio would probably have been less. As a result of decreasing N contents in the needles, the acid production caused by the N mineralisation followed by nitrification would be lower.

It is remarkable that, in spite of the strong reduction in deposition, the mean Al/Ca ratio in layer 3 remains above 1, which can be considered an acceptable value (De Vries, 1988). However, simulations over a longer time period showed that the mean Al/Ca ratio in layer 3 will decrease further by 3 units in the period 2010 to 2030, due to a decrease in Ca adsorption.

Contrary to the other analysed model outputs, we used the rank transformed data of the molar Al/Ca ratio in layer 3. This is done, because a linear regression with the original data resulted in a bad 'fit' (low COD), which was highly improved by rank transformation as shown in Figure 6. The COD in layer 1 lies, during the entire simulation period, between 0.94 and 0.96.
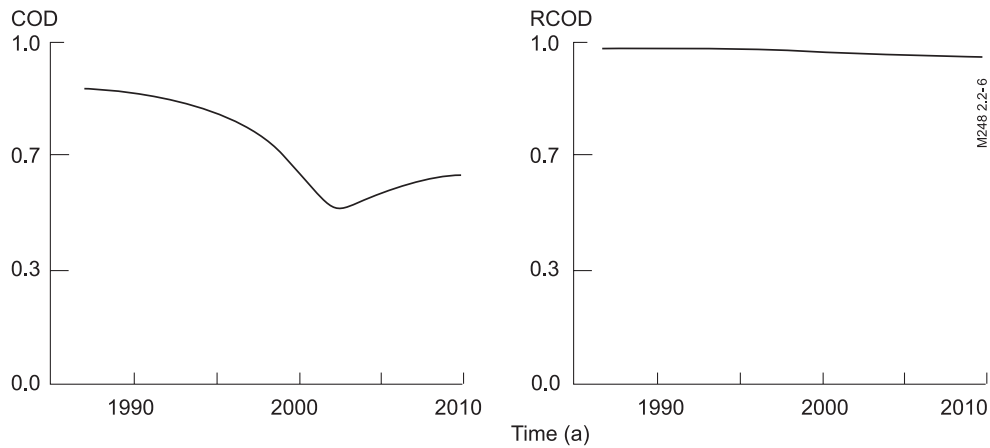
Figure 6 The COD and the RCOD in layer 3 during the simulation period

Figure 7 shows trajectories of the three parameters with the highest RTU in layer 1 and the highest standardised rank transformed regression coefficient (SRRC) in layer 3, either at the beginning or at the end of the simulation period. The uncertainty of the Al/Ca ratio in layer 1 is mainly determined by the content of aluminium hydroxide ($ctAl_{ox\ 1}$), the deposition of Ca (FCa_{dw}), and the Ca content in the needles ($ctCa_{lv}$). The uncertainty contribution of $ctAl_{ox\ 1}$ slightly increases with time, which is a result of a decrease in $ctAl_{ox\ 1}$ during the simulation (dissolution of aluminium hydroxide due to acid deposition). When simulations are carried out over a period of 100 a (De Vries and Kros, 1989) the uncertainty in the Al/Ca ratio is almost completely determined by the uncertainty in $ctAl_{ox\ 1}$. The influence of FCa_{dw} and $ctCa_{lv}$ on the uncertainty remains fairly constant during the simulation period.
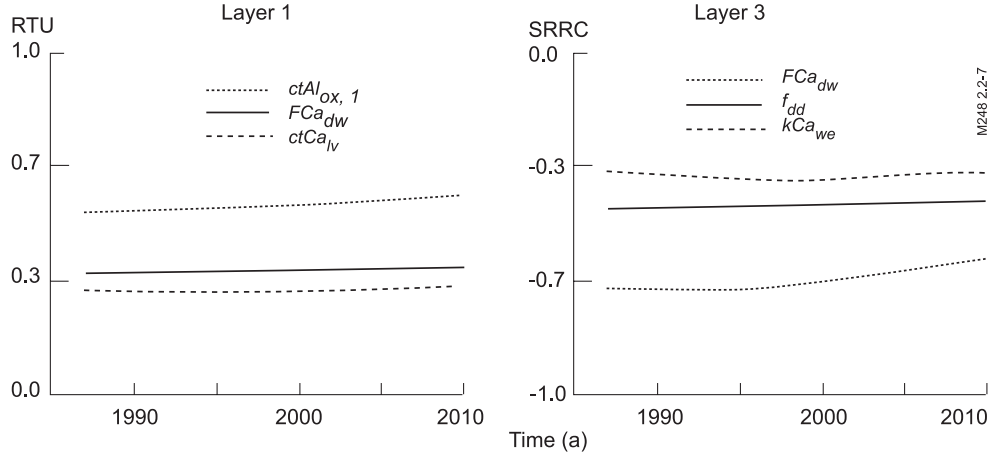
Figure 7 Temporal evolution of the RTU between model parameters and the Al/Ca mol ratio in layers 1 and 3

At the bottom of the root zone, it is mainly the Ca deposition (FCa_{dn}, f_{dd}) which determines the uncertainty in the Al/Ca ratio, although it slightly decreases during the simulation period. Remarkable is that also the Ca weathering constant of primary minerals (kCa_{we}) significantly contributes to the uncertainty. In this context, it is important to note that the values of the SRRC in layer 3 are negative, since higher values of FCa_{dn}, f_{dd} and kCa_{we} result in higher Ca concentrations and thereby in lower Al/Ca ratios. The RTU is always positive (see Section *Statistical Analysis*).

2.2.6   Discussion and conclusion

Discussion

The information provided by the uncertainty analysis can be used as a basis for further model development and data collection. The processes related with the relatively certain parameters could be aggregated. However, one should be aware that the uncertainty depends strongly on the considered output. For example, the uncertainty contribution of kMg_{fe} would be more pronounced when the Mg concentration was considered. In order to reduce the uncertainty of the most critical parameters, it is necessary to make a distinction between uncertainty due to natural variability and uncertainty due to a poorly defined model parameter distribution. Important parameters whose uncertainties mainly originate from inaccurate and/or insufficient data are KAl_{ox}, f_{dd}, k_{ni}. The uncertainty related with these parameters can be reduced by additional data collection and/or calibration on relevant field measures. The uncertainty of the other group of important parameters originates mainly from natural variability, i.e. mainly $ctAl_{ox}$, $FNH_{3\ dd}$, $FSO_{2\ dd}$, ctN_{lr}. The uncertainty related to those parameters is simply a fact of nature.

In general, the model outputs of a simulation with average parameter values correspond quite well with the average of the outputs from all the Monte Carlo simulations. This is related to the linear behaviour of most model outputs, which is expressed by a COD value close to 1 for most regression models. However, replacing the original RESAM by these linear regression models (frequently called 'meta-model') in further studies is not suitable.

The regression models are mainly descriptive and have not much explanatory value. The coefficients in these models are highly time-dependent. Moreover, their values depend on the specific deposition scenario considered in this study. The relation with the important processes at hand does not show up clearly and explicitly, and therefore their use for further in-depth studies is rather limited.

Conclusions

A decrease in deposition leads almost directly to a strong decrease in NH_4/K ratio, a slight decrease in Al/Ca ratio, and a slight increase in pH. When a non-stationary nutrient cycle had been considered, the observed effects would probably have been stronger, since the assumption of a stationary nutrient cycle may have led to an overestimation of the NH_4/K and the Al/Ca ratio, and an underestimation of the pH.

The relative uncertainty, determined by the variation coefficient, strongly depends on the considered model output, soil layer and time and is:
- high for the NH_4/K ratio and the Al/Ca ratio and low for the pH;
- always larger in the subsoil than in the topsoil;
- nearly constant for the pH in both topsoil and subsoil and for the NH_4/K and Al/Ca ratios in the topsoil, whereas it strongly increases with time for both ratios in the subsoil.

The uncertainty contribution of model parameters on model outputs depends on the considered model output, soil layer, and time as shown in Table 11.

Table 11 The most important uncertainty sources for the pH, NH_4/K and Al/Ca ratios in the topsoil and the subsoil at the beginning (1987) and at the end (2010) of the simulation period.

Model output	pH		NH_4/K		Al/Ca	
	Begin	End	Begin	End	Begin	End
Top soil	$ctAl_{ox}$	$ctAl_{ox}$	$FNH_{3\,dd}$	ctN_{lt},	$ctAl_{ox}$	$ctAl_{ox}$
	$FSO_{2\,dd}$	ctN_{lt},	$FSO_{2\,dd}$	f_{dd}	FCa_{dw}	FCa_{dw}
	$FNH_{3\,dd}$	CEC	f_{dd}	k_n	$ctCa_{lt}$	$ctCa_{lt}$
Sub soil	KAl_{ox}	KAl_{ox}	$FNH_{3\,dd}$	A_{rt}	FCa_{dw}	FCa_{dw}
	$FNH_{3\,dd}$	$FNH_{3\,dd}$	$FSO_{2\,dd}$	A_{lt}	f_{dd}	f_{dd}
	$FSO_{2\,dd}$	$FSO_{2\,dd}$	k_n	$KNH_{4,\,se}$	kCa_{w}	kCa_{w}

The uncertainty in pH is mainly determined by the content of aluminium hydroxides ($ctAl_{ox}$) in the topsoil and the aluminium hydroxide equilibrium constant (KAl_{ox}) in the subsoil. Furthermore, the dry depositions of NH_3 ($FNH_{3\,dd}$) and SO_2 ($FSO_{2\,dd}$) also contribute strongly to the uncertainty of the pH in both the topsoil and

subsoil. However, at the end of the simulation period, at a low acid deposition load, the uncertainty contribution of the deposition decreases (external N cycle) and the contribution of the N content in needles (ctN_{lr}) increases (internal N cycle).

At the beginning of the simulation period, the uncertainty in the NH$_4$/K ratio, is mainly determined by the dry deposition of NH$_3$ ($FNH_{3\ dd}$) for both the topsoil and the subsoil, the dry deposition factor of base cations (f_{dd}) for the topsoil, and the nitrification constant (k_{ni}) for the subsoil. At the end of the simulation period, the influence of the dry deposition of ammonia decreases (external N cycle), and the uncertainty contribution of the nitrification constant (k_{ni}, topsoil), the N content in needles (ctN_{lr}, topsoil), and the amounts of roots and needles (A_{rt}, A_{lr}, subsoil) increase (internal N cycle).

The uncertainty in the Al/Ca ratio in the topsoil is mainly determined by the content of aluminium hydroxide ($ctAl_{ox}$), followed by the wet deposition of Ca (FCa_{dn}) and the Ca content in needles ($ctCa_{lr}$). In the subsoil it is mainly the total deposition of Ca (FCa_{dn}, f_{dd}), followed by the Ca weathering rate constant of primary minerals (kCa_{we}), which determines the uncertainty. The uncertainty contribution of these parameters remains more or less constant during the simulation period.

The parameters that hardly influence the uncertainty of the considered model outputs are the bulk density (rho) of all soil layers, the S content in leaves (ctS_{lr}), stems (ctS_{st}) and branches (ctS_{br}), the foliar exudation rate constant of Mg (kMg_{fe}) and the foliar uptake constant of NH$_3$ ($fNH_{3\ fu}$).

II Evaluation on a site scale

2.3 Modelling effects of acid deposition and climate change on soil and runoff chemistry

Abstract

Elevated CO_2 levels, caused by anthropogenic emissions of CO_2 to the atmosphere, and higher temperatures may also lead to increased plant growth and uptake of N, but increased temperature may lead to increased N mineralisation, causing enhanced N-leaching. The overall result of both counteracting effects, particular in the long run, is largely unknown. To gain insight in those long-term effects, the geochemical model SMART2 was applied, using data from the catchment-scale experiments of the RAIN and CLIMEX projects, conducted on boreal forest ecosystems at Risdalsheia (southern Norway). These unique series of experiments at the ecosystem scale provides information on the short-term effects and interactions of N deposition and increased temperature and CO_2 on C and N cycling and especially the runoff chemistry. To predict changes in soil processes in response to climate change, the model was extended, by including the temperature effect on mineralisation, nitrification, denitrification, Al dissolution and mineral weathering. The extended model was tested on the two manipulated catchments at Risdalsheia and long-term effects were evaluated by performing long-time runs. The effects of climate change treatment, which resulted in increased N fluxes at both catchments, were slightly overestimated by SMART2. The temperature dependency of mineralisation was simulated adequately, but the temperature effect on nitrification was slightly overestimated. Monitored changes in base cation concentrations and pH, though were simulated quite well with SMART2. The long-term simulations, indicate that the increase in N runoff is only a temporal effect; on the long-term, no effect on total N-leaching is predicted. At higher deposition level the temporal increase in N-leaching lasts longer than at low deposition level. Contrary to N leaching, a temperature increase leads to a permanent decrease in Al concentrations and pH.

2.3.1 Introduction

Emissions of CO_2 and other greenhouse gases to the atmosphere may lead to an increase in global temperature over the next decades. Largest changes are expected at high latitudes (Houghton *et al.*, 1990). Primary productivity in boreal ecosystems has increased in large regions of northern Europe and eastern North America due to enhanced N deposition, since these systems are N-limited (Kauppi *et al.*, 1992). Higher CO_2 concentrations may lead to increased plant growth, C sequestration and uptake of N. Increased temperatures, on the other hand may lead to increased mineralisation (Stanford *et al.*, 1973; Edwards, 1975), causing CO_2 production and enhanced N-leaching. The overall result and in particular the long-term effects are largely unknown.

Large-scale whole-ecosystem experiments provide one of the tools to study the response of the ecosystem and to evaluate geochemical models that include global change processes. At Risdalsheia, southern Norway, the effects and interactions of N deposition and increased temperature and CO_2 on C and N cycling and especially the runoff chemistry have been examined at catchment-scale experiments on boreal forest

ecosystems (Van Breemen *et al.*, 1998; Wright, 1998). Runoff chemistry is of particular interest. It provides a sensitive integrated signal of change in terrestrial catchments; while changes in the internal N cycle are often difficult to discern directly due to spatial and temporal variability.

To quantify the impacts of acid deposition, land use and climate change at large (regional to national) scale, simulation models are being used. The models MERLIN (Wright *et al.*, 1998b) and MAGIC7 (Wright *et al.*, 1998a) have been applied at Risdalsheia to test effects of climate change on runoff chemistry. In this paper we evaluate the enhanced SMART2 model (Mol-Dijkstra and Kros, 2001) using the control and the manipulated catchments at Risdalsheia. SMART2 has been developed in order to integrate soil acidification processes and nutrient cycling, and to predict long-term effects of acid deposition scenarios on a national and continental scale. To quantify the effects of climate change on soil processes, we included the effect of temperature on these processes to integrate effects of climate change, acid deposition and nutrient cycling in a quantitative way. This extended version of SMART has also been applied on the European scale (Ferrier and Helliwell, 2000). The Risdalsheia experimental catchments are very suitable for application of SMART2, because the experimental design of the experimental catchments corresponds with the temporal and spatial resolution of the model output. We used annual fluxes of solutes in runoff (Wright *et al.*, 1998a), corresponding to the time steps of one year that is used by SMART2.

The major aims of this paper are to (i) test the hypothesised temperature effects by calibration and validation of the model on a manipulated catchment and (ii) evaluate long-term effects of climate change on C and N cycling and especially on N runoff. To test the temperature effect in SMART2, we first calibrated the model at the control catchment ROLF, and next, after the incorporation of the temperature effect, at the EGIL catchment where soil temperature was increased. Finally, we evaluated the model at the KIM catchment which was subjected to elevated air temperature and CO_2-pressure. The effect of deposition reduction was only evaluated at the KIM catchment. Long-term effects of deposition reduction, temperature rise and increase of CO_2-pressure were evaluated by extrapolating the existing treatments at Risdalsheia for 30 years.

2.3.2 Modelling approach

Model structure

SMART2 is a simple, single-layer soil acidification and nutrient cycling model. It includes the major hydrological and biogeochemical processes in the vegetation, litter and mineral soil. The model simulates changes in H, Al, divalent base cations (BC2=Ca+Mg), K, Na, NH_4, NO_3, SO_4, HCO_3 and Cl concentrations in the soil solution. In addition, it simulates changes in solid phase characteristics connected to the acidification status, i.e. carbonate content, base saturation and amorphous Al precipitates. The SMART2 model consists of a set of mass balance equations, describing the soil input-output relationships, and a set of equations describing the rate-limited and equilibrium soil processes. SMART2 is an extension of the SMART

model (De Vries *et al*., 1989). Since the (original) SMART model does not include a complete nutrient cycle, it is not suitable for calculating N availability. Furthermore, it does not include upward solute transport. Therefore, the model SMART was extended with a nutrient cycle (litterfall, mineralisation and uptake) and an improved modelling of hydrology, including runoff, upward and downward solute fluxes. Most of the extensions were derived from the dynamic multi-layer model RESAM (De Vries *et al*., 1995a) and the steady-state multi-layer model MACAL (De Vries *et al*., 1994c). Figure 1 gives a schematic representation of the SMART2 model. The included processes are summarised in Table 1.
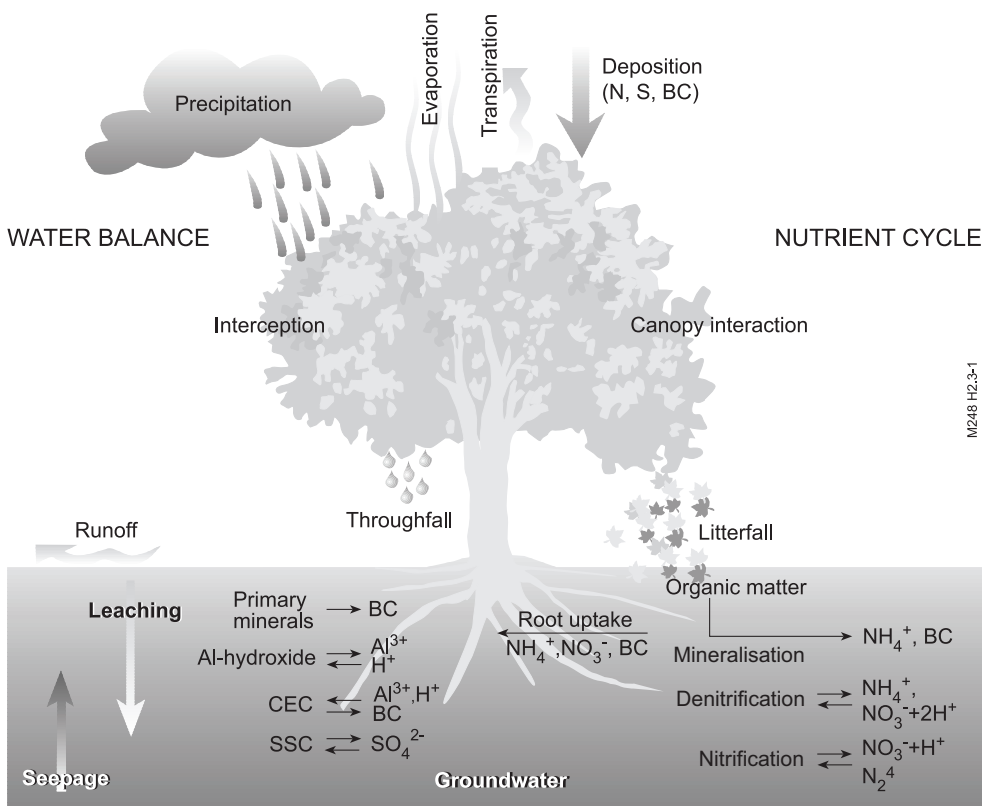
Figure 1 Schematic representation of the processes included in the SMART2 model

Table 1 Overview of processes included in SMART2

Process	Element	Process description
Input:		
Total deposition	SO_4, NO_3, NH_4, BC2 [1]), Na, K, Cl	Inputs; deposition fluxes are multiplied by an element- and vegetation-dependent filtering factor[2])
Upward seepage	SO_4, NO_3, NH_4, BC2 [1]), Na, K, Cl	Inputs
Water Balance	-	Inputs: precipitation, upward seepage, evapotranspiration
Rate-limited reactions:		
Foliar uptake	NH_4	Linear function of total deposition
Foliar exudation	BC2 [1]), K	Equals foliar uptake
Litterfall	BC2 [1]), K, NH_4, NO_3	Logistic growth
Root decay	BC2 [1]), K, NH_4, NO_3	Linear function of litterfall
Mineralisation	BC2 [1]), K, NH_4, NO_3	First-order reaction and a function of pH, Mean Spring Water table (MSW) and C/N ratio of the litter
N immobilisation	NH_4, NO_3	Proportional to N deposition and a function of the C/N ratio soil organic matter
Growth uptake	BC2 [1]), K, NH_4, NO_3	Logistic growth
Nitrification	NH_4, NO_3	Proportional to net NH_4 input and a function of pH, Mean Spring Water table (MSW) and C/N ratio
Denitrification	NO_3	Proportional to net NO_3 input and a function of pH, Mean spring water table (MSW) and C/N ratio
Silicate weathering	Al, BC2 [1]), Na, K	Zero order reaction
Equilibrium reactions:		
CO_2 Dissociation	HCO_3	CO_2 equilibrium
Dissociation of organic acid	RCOO	Oliver equation
Carbonate weathering	BC2 [1])	Carbonate equilibrium
Al hydroxide weathering	Al	Gibbsite equilibrium
Cation exchange	H [3]), Al, BC2 [1])	Gaines-Thomas equations
Sulphate sorption	H [3]), SO_4	Langmuir equation

[1]) BC2 stands for the sum of divalent base cations (Ca + Mg)

[2]) The vegetation-dependent filtering factor takes the roughness length of the canopy into account

[3]) Implicitly, H is affected by all processes. This is accounted for by the charge balance

SMART2 was constructed using a process-aggregated approach to minimise input data requirements for applications on a regional scale. This implied the following simplifying assumptions:

i. The various ecosystem processes have been limited to a few key processes:

The soil solution chemistry in SMART2 depends solely on the net element input from the atmosphere (deposition), groundwater (upward seepage), nutrient cycling processes (uptake, litterfall, mineralisation and immobilisation) and the geochemical interaction in the soil ((de)nitrification, CO_2 equilibria, weathering of carbonates, silicates and/or Al-hydroxides and cation exchange). Processes that are not taken into

account, are: (i) N fixation and NH_4 exchange, (ii) uptake, immobilisation and reduction of SO_4 and (iii) complexation of Al with OH, SO_4 and RCOO.

ii. The included processes have been represented by simplified conceptualisations:

Soil interactions are either described by simple rate-limited reactions (e.g. uptake and silicate weathering) or by equilibrium reactions (e.g. carbonate and Al-hydroxide weathering and cation exchange). Influence of environmental factors such as pH on rate-limited reactions and rate-limitation of weathering and exchange reactions are ignored. Solute transport is described by assuming complete mixing of the element input within one homogeneous soil compartment with a constant density and a fixed depth (at least the root zone). Because SMART2 is a single layer soil model neglecting vertical heterogeneity, it predicts the concentration of the soil water leaving the root zone. The annual water flux percolating from this layer is taken equal to the annual precipitation plus upward seepage minus evapotranspirations, which terms must be specified as a model input. The time step of the model is one year, so seasonal variations are not considered. Justifications for the various assumptions and simplifications have been given by De Vries *et al.* (1989). Furthermore, Chapter 2.4 of this thesis will address the consequences of model simplification into more detail.

Process descriptions

In this section an overview of the process descriptions used in the SMART2 is given. An explanation of the symbols used is given in Annex 1.

Mass balances

For each of the cations (Na, K, BC2=Mg+Ca, NH_4, Al) and strong acid anions (SO_4, NO_3, Cl) considered in SMART2 the mass balance equation for a compartment with depth z, is given by:

$$\frac{d}{dt} \cdot X_{tot}(z) = X_{in} + X_{int}(z) - PE(z) \cdot [X](z) + X_{sen}(z) \tag{1}$$

where $X_{tot}(z)$ is the total amount of ion X in the soil solution (mol_c m^{-2}) of a soil compartment with depth z (m). X_{in} is the sum of all input fluxes to the soil (mol_c m^{-2} a^{-1}). $X_{int}(z)$ is the sum of all interaction fluxes (mol_c m^{-2} a^{-1}) in the soil at depth z (m). $X_{sen}(z)$ is the net seepage flux (mol_c m^{-2} a^{-1}) entering a soil compartment with depth z (see Eq. 6). $[X](z)$ is the concentration of ion X (mol_c m^{-3}) in the soil compartment with depth z. In SMART2 the precipitation excess at depth z, $PE(z)$ is calculated as:

$$PE(z) = P \cdot (1 - f_{int}) - fr_{ru}(z) \cdot Tr \tag{2}$$

where P is the precipitation, Tr the actual transpiration, f_{int} the interception fraction (-) and $fr_{ru}(z)$ the cumulative transpiration (water uptake by roots) fraction (-) in the root zone at depth z, which is calculated as:

$$fr_{ru}(z) = \begin{cases} 1 - \left(\dfrac{T_{rz} - z}{T_{rz}} \right)^{ru_{exp}} & \text{for } z \le T_{rz} \\ 1 & \text{for } z > T_{rz} \end{cases} \tag{3}$$

where T_{rz} is the thickness of the root zone (m) and ru_{exp} is an exponent determining the water uptake pattern.

Upward seepage

Upward seepage is included in the mass balance, Eq. (1), as a net term, i.e. the input of the upward seepage flux (X_{sen}) minus the lateral output flux (X_{la}). Figure 2 gives an overview of the water balance in the soil system, including seepage.
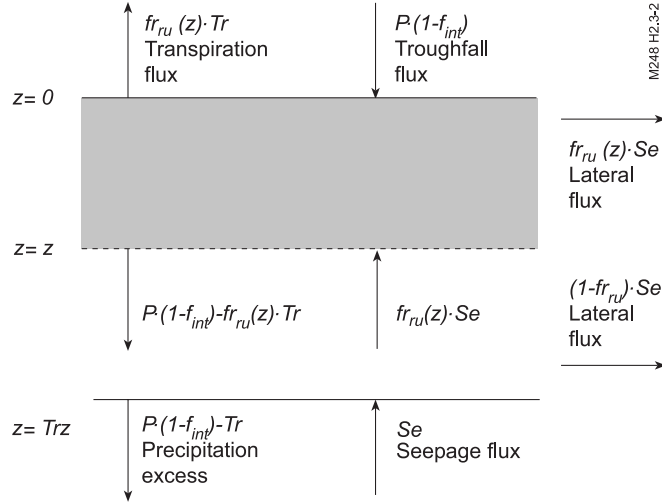
Figure 2 Water balance in SMART2

The input to the soil system consists of the throughfall flux, $P \cdot (1 - f_{int})$ and the upward seepage flux, Se. In SMART2, upward seepage is defined as the flux at the bottom of the root zone. The upward seepage flux is assumed to be reduced at shallower depth. For the sake of simplicity for seepage input into the root zone, the same reduction function with depth is used as for transpiration, i.e. $fr_{ru}(z)$, cf. Eq. (3). Consequently, the seepage input to the compartment with depth z equals: $fr_{ru}(z) \cdot Se$. The seepage flux of ion X is described as:

$$X_{se}(z) = fr_{ru}(z) \cdot Se \cdot [X]_{se} \tag{4}$$

where $[X]_{se}$ stands for the concentration of ion X in the seepage water (mol$_c$ m^{-3}) and Se the upward seepage flux (m a^{-1}). Because it is stated that the transpiration is independent of the upward seepage flux, Se, there must be a lateral output flux which equals the seepage input: $- fr_{ru}(z) \cdot Se$.

The concentration of ion X in the lateral output flux at depth z equals the concentration in the soil compartment, $[X](z)$. Consequently, the lateral output flux of ion X is described as:

$$X_{la}(z) = - fr_{ru}(z) \cdot Se \cdot [X](z) \tag{5}$$

where Se is the upward seepage flux (m a^{-1}). The net effect of seepage at depth z, $X_{sen}(z)$, is thus:

$$X_{sen}(z) = fr_{ru}(z) \cdot Se \cdot ([X_{se}] - [X](z)) \tag{6}$$

From Eq. (6) it is follows that the influence of upward seepage on the concentration in the considered soil compartment is larger as the concentration of ion X in the upward seepage water deviates more from the concentration in the soil solution. Note that the remaining part of the upward seepage flux that does not reach depth z is draining laterally. This lateral flux equals: $- (1 - fr_{ru}(z)) \cdot Se \cdot [X_{se}]$.

Input fluxes

The external input by atmospheric deposition to the soil compartment is influenced by the total deposition (*td*), foliar uptake (*fu*), foliar exudation (*fe*) and mineralisation of litter (*mi*). Their presence depends on the component involved:

$$Al_{in} = 0 \tag{7}$$
$$BC2_{in} = BC2_{td} + BC2_{fe} + BC2_{mi} \tag{8}$$
$$K_{in} = K_{td} + K_{fe} + K_{mi} \tag{9}$$
$$Na_{in} = Na_{td} \tag{10}$$
$$NH_{4,in} = NH_{4,td} - NH_{4,fu} + N_{mi} \tag{11}$$
$$NO_{3,in} = NO_{3,td} \tag{12}$$
$$SO_{4,in} = SO_{4,td} \tag{13}$$
$$HCO_{3,in} = 0 \tag{14}$$
$$RCOO_{in} = 0 \tag{15}$$
$$Cl_{in} = Cl_{td} \tag{16}$$

And the input of H is calculated from the charge balance:

$$H_{in} = SO_{4,in} + NO_{3,in} + HCO_{3,in} + Cl_{in} + RCOO_{in} - \\ - NH_{4,in} - Al_{in} - BC2_{in} - K_{in} - Na_{in}$$

(17)

Canopy interactions

The canopy interactions included in SMART2 were taken from the RESAM model (De Vries *et al.*, 1995a). Foliar uptake of NH_4 and H is described as:

$$X_{fu} = frX_{fu} \cdot X_{td}$$

(18)

where frX_{fu} is the foliar uptake fraction of H or NH_4. For H_{fu} the deposition of free H (H_{td}) is calculated from the charge balance:

$$H_{td} = SO_{4,td} + NO_{3,td} + Cl_{td} - NH_{4,td} - BC2_{td} - K_{td} - Na_{td}$$

(19)

Foliar exudation of the cations (K, BC2) is taken equal to foliar uptake of NH_4 and H (cf. De Vries *et al.*, 1995a), and is assumed to be triggered by exchange with these ions (Roelofs *et al.*, 1985; Ulrich, 1983). The foliar exudation of each individual cation is calculated as:

$$X_{fe} = frX_{fe} \cdot (NH_{4,fu} + H_{fu})$$

(20)

with $X=K, BC2$, frX_{fe} is the foliar exudation fraction of K and BC2 (-), and sum of frK_{fe} and $frBC2_{fe}$ equals 1.

Litterfall and root decay

The inputs by litterfall and root decay in SMART2 affecting the mineralisation flux, were also taken from the RESAM model (De Vries *et al.*, 1995a). In SMART2, litterfall is the input to an organic pool containing N, BC2 and K. Contrary to RESAM, SMART2 does not include a physical litter layer in which a separate concentration is calculated. Only an organic pool is modelled, which has the same soil solution concentration as the mineral soil. Input fluxes of N, BC2 and K by litterfall, X_{lf} are described as:

$$X_{lf} = (1 - frX_{re}) \cdot Am_{lf} \cdot ctX_{lv}$$

(21)

where Am_{lf} is the amount of litterfall (kg ha^{-1} a^{-1}), ctX_{lv} is the contents of element X in leaves (mol$_c$ kg^{-1}) and frX_{re} are reallocation fractions for element X in leaves (-). Reallocation of K and BC2 in leaves prior to litterfall is considered negligible (i.e. $frK_{re} = frBC2_{re} = 0$). The amount of stems and litterfall are described by a logistic growth

94

function (see Eq. 54 and 55). High contents of N in leaves and fine roots in Dutch forests are caused by the high N deposition level. To account for this effect, the N content in leaves is calculated as a function of the N deposition according to:

$$ctN_{lv} = \begin{cases} ctN_{lv,mn} & for\ N_{td} \leq N_{td,mn} \\ ctN_{lv,mn} + (ctN_{lv,mx} - ctN_{lv,mn}) \cdot \dfrac{N_{td} - N_{td,mn}}{N_{td,mx} - N_{td,mn}} & for\ N_{td,mn} < N_{td} < N_{td,mx} \\ ctN_{lv,mx} & for\ N_{td} \geq N_{td,mx} \end{cases} \qquad (22)$$

where $ctN_{lv,mn}$ and $ctN_{lv,mx}$ are the minimum and maximum N content in leaves (mol_c kg^{-1}) and $N_{td,mn}$ and $N_{td,mx}$ are the minimum and maximum total deposition levels of N (mol_c ha^{-1} a^{-1}) between which the N content of leaves is influenced. For the Netherlands $N_{td,mn}$ = 1500 mol_c ha^{-1} a^{-1} and $N_{td,mx}$ = 7000 mol_c ha^{-1} a^{-1} were used. Contrary to RESAM the reallocation fraction (frX_{re}) is not considered as a function of the N content in the foliage, frX_{re} remains constant during the simulation period.

The dynamic turnover of fine roots is coupled with the amount of litterfall and divided between the litter compartment (depth independent) and the mineral soil (depth dependent). The root decay flux in the litter compartment ($X_{rd,lt}$) is described as:

$$X_{rd,lt} = X_{lf} \cdot ncf \cdot fr_{rt,lt} \qquad (23)$$

where ncf is the nutrient cycling factor (-), which is defined as the ratio of the root turnover (related to nitrogen) and the above ground nitrogen cycle (litterfall flux), and $fr_{rt,lt}$ is the fraction of fine roots in the litter layer (-). The depth-dependent root decay flux in the mineral soil ($X_{rd,ms}(z)$) is described as:

$$X_{rd,ms}(z) = fr_{ru}(z) \cdot X_{lf} \cdot ncf \cdot (1 - fr_{rt,lt}) \qquad (24)$$

Mineralisation

As with canopy interactions, litterfall and root decay, mineralisation in SMART2 is also taken from the RESAM model. For the simulation of the decomposition of above-ground organic matter (litter, including dead roots in the litter layer) a distinction is made between a rapidly decomposing pool of fresh litter (less than one year old) and a slowly decomposing pool of old litter (more than one year) (Janssen, 1984). The mineralisation flux of N (during mineralisation N is released as NH4), K and BC2 (mol_c ha^{-1} a^{-1}) from fresh litter, $X_{mi,fl}$, is described as a fraction of the input of X by litterfall and root decay in the litter compartment according to:

$$X_{mi,fl} = \left[frX_{le} + fr_{mi} \cdot (1 - frX_{le}) \right] \cdot X_{lf} \cdot (1 + ncf \cdot fr_{rt,lt}) \qquad (25)$$

where fr_{mi} is a mineralisation fraction (-) and frX_{le} is a litter leaching fraction (-). Leaching only refers to the release of BC2 (=Ca+Mg) and K from fresh litter just after litterfall, a process which is especially important for K. Litter leaching is a process which differs from mineralisation because organic matter is not decomposed.

Fresh litter which is not mineralised is transferred to the old litter (humus) pool. The mineralisation flux of NH_4, K and BC2 from this litter pool, $X_{mi,lt}$, is described by first-order kinetics (Van Veen, 1977):

$$X_{mi,lt} = k_{mi,lt} \cdot Am_{lt} \cdot ctX_{lt}$$
(26)

where $k_{mi,lt}$ is the mineralisation rate constant from old litter (a^{-1}), Am_{lt} is the amount of old litter (kg ha^{-1}) and ctX_{lt} is the content of element X in old litter (mol$_c$ kg^{-1}). At present, mineralisation of organic matter in the mineral soil layers is not considered in SMART2, except for the mineralisation from root necro-mass, which is fed by root decay as described before. The total input by mineralisation (X_{mi}) in the litter layer consists of the sum of mineralisation of fresh litter, old litter and the root decay in the litter layer:

$$X_{mi} = X_{mi,lt} + X_{mi,fl} + X_{rd,lt}$$
(27)

Root decay in the mineral soil is considered to be mineralised completely. The total mineralisation flux at depth z becomes equal to:

$$X_{mi,tot}(z) = X_{mi,lt} + X_{mi,fl} + X_{rd,lt} + X_{rd,ms}(z)$$
(28)

The flux of organic anions, $RCOO_{mi,tot}$, produced during mineralisation from both fresh and old litter and from dead root (mol$_c$ ha^{-1} a^{-1}) is calculated from charge balance considerations:

$$RCOO_{mi,tot}(z) = N_{mi,tot}(z) + BC2_{mi,tot}(z) + K_{mi,tot}(z)$$
(29)

Actual values for the mineralisation fraction ($fr_{mi,fl}$ and $fr_{mi,lt}$) and mineralisation rate constant ($k_{mi,fl}$ and $k_{mi,lt}$) are described in SMART2 as maximum values, which are reduced by factors such as soil moisture (water-table), pH and the C/N ratio. For all constituents the maximum value ($k_{mi,mx}$ and $f_{mi,mx}$) is influenced by the mean water-table during spring time (Mean Spring Water table, MSW) and the pH. The N mineralisation is also influenced by the C/N ratio:

$$fr_{mi} = fr_{mi,mx} \cdot rf_{mi,MSW} \cdot rf_{mi,pH} \cdot rf_{mi,CN}$$
(30)

$$k_{mi} = k_{mi,mx} \cdot rf_{mi,MSW} \cdot rf_{mi,pH} \cdot rf_{mi,CN}$$
(31)

where $rf_{mi,MSW}$, $rf_{mi,pH}$ and $rf_{mi,CN}$ are the reduction factors for water-table, pH and N content (C/N ratio) respectively (-). For BC2 and K, $rf_{mi,CN} = 1$. The reduction

functions for water-table and pH were partly taken from RESAM (cf. De Vries *et al.*, 1988):

$$rf_{mi,MSW} = \begin{cases} 0.25 & \textit{for } MSW \leq 0.45 \\ \log_{10}(4 \cdot MSW) & \textit{for } 0.45 < MSW < 2.50 \\ 1 & \textit{for } MSW \geq 2.50 \end{cases} \tag{32}$$

$$rf_{mi,pH} = \begin{cases} 0 & \textit{for } pH \leq 2.5 \\ \dfrac{pH - 2.5}{2} & \textit{for } 2.5 < pH < 3.5 \\ \dfrac{pH - 1}{5} & \textit{for } 3.5 \leq pH < 6 \\ 1 & \textit{for } pH \geq 6 \end{cases} \tag{33}$$

The N mineralisation values are reduced at low N contents (high C/N ratios) to account for immobilisation by microbes according to (Janssen, 1984):

$$rf_{mi,CN} = \begin{cases} 1 & \textit{for } CN_s \leq CN_{mo} \\ 1 - \dfrac{CN_s - CN_{mo}}{DA_{mo} \cdot CN_{mo}} & \textit{for } CN_{mo} < CN_s < (1 + DA_{mo}) \cdot CN_{mo} \\ 0 & \textit{for } CN_s \geq (1 + DA_{mo}) \cdot CN_{mo} \end{cases} \tag{34}$$

where CN_{mo} is the C/N ratio of the micro-organisms decomposing the substrate (-), CN_s is the C/N ratio of the substrate (fresh litter ($s=fl$), old litter ($s=lt$)) and DA_{mo} is the dissimilation to assimilation ratio of the decomposing microbes (-). Values for DA_{mo} and CN_{mo} are related to fungi because they are mainly responsible for mineralisation of forest litter.

N immobilisation

Besides implicitly modelled immobilisation by mineralisation, SMART2 includes also a description of N immobilisation by soil organic matter, which has also been included in the SMART model (De Vries *et al.*, 1994b). The description of N immobilisation is based on the assumption that the amount of organic matter (carbon) is constant. Consequently, immobilisation of carbon and base cations is not accounted for the mineral soil.

N immobilisation is described by an increase in N content in organic matter. When the C/N ratio of the soil (CN_{om}) varies between a critical (CN_{cr}) and a minimum value (CN_{mn}), the immobilisation rate is assumed to decrease according to:

$$N_{im} = \begin{cases} 0 & \text{for } CN_{om} \leq CN_{mn} \\ (N_{td} - N_{gu} - N_{le,mn}) \cdot \dfrac{CN_{om} - CN_{mn}}{CN_{cr} - CN_{mn}} & \text{for } CN_{mn} < CN_{om} < CN_{cr} \\ N_{td} - N_{gu} - N_{le,mn} & \text{for } CN_{om} \geq CN_{cr} \end{cases} \tag{35}$$

The minimum N leaching rate ($N_{le\ mn}$) is calculated by multiplying the precipitation excess by a natural background NO_3 concentration in drainage water of $0.02 \text{ mol}_c \text{ m}^{-3}$ (Rosén, 1990). During the simulation, the C content is fixed whereas the N content is annually updated, by adding the amount of N immobilised during each time step to the N amount in the mineral topsoil. The C/N ratio is in turn updated by dividing the fixed C pool by the variable N pool according to:

$$CN_{om} = \frac{\rho_{rz} \cdot T_{iz} \cdot ctC_{iz}}{AmN_{iz} + N_{im}} \tag{36}$$

Because N immobilisation mainly occurs in the humus layer and the upper mineral soil (Tietema, 1992), the thickness of the zone where N immobilisation (T_{iz}) occurs is taken at 20 cm.

Interaction fluxes

The interaction fluxes for Al, BC2, K, Na, NH_4 and NO_3 accounted for in SMART2 are base cation and Al weathering (*we*), root uptake (*ru*), nitrification (*ni*), denitrification (*de*) and rootdecay in the mineral soil (*rd mi*). For nitrification and denitrification reduction functions as a function of pH and groundwater level are included (see Eq. 60 and 61). The interaction fluxes for a compartment with depth z are described as:

$$Al_{int}(z) = Al_{we} \cdot z \tag{37}$$

$$BC2_{int}(z) = BC2_{we} \cdot z - fr_{ru}(z) \cdot BC2_{ru} \tag{38}$$

$$K_{int}(z) = K_{we} \cdot z - fr_{ru}(z) \cdot K_{ru} \tag{39}$$

$$Na_{int}(z) = Na_{we} \cdot z \tag{40}$$

$$NH_{4,int}(z) = -fr_{ru}(z) \cdot (NH_{4,ni} + NH_{4,ru}) \tag{41}$$

$$NO_{3,int}(z) = fr_{ru}(z) \cdot (NH_{4,ni} - NO_{3,ru} - NO_{3,de}) \tag{42}$$

$$SO_{4,int}(z) = 0 \tag{43}$$

$$HCO_{3,int}(z) = 0 \tag{44}$$

$$RCOO_{int}(z) = 0 \tag{45}$$

$$Cl_{int}(z) = 0 \tag{46}$$

$$H_{int}(z) = SO_{4,int}(z) + NO_{3,int}(z) + HCO_{3,int}(z) + Cl_{int}(z) + RCOO_{int}(z) - \\ NH_{4,int(z)} + Al_{int}(z) - BC2_{int}(z) - K_{int}(z) - Na_{int}(z) \tag{47}$$

Mineral weathering

Weathering of divalent base cations (BC2=Ca+Mg) and monovalent base cations (Na, K) is include as a zero-order reaction. The weathering of Al is related to BC2 weathering according to:

$$Al_{we} = r \cdot BC2_{we} \tag{48}$$

where r is the stoichiometric equivalent ratio of Al to BC2 in the congruent weathering of silicates. In SMART2 this value is fixed to 2, which is based on an average for Ca and Mg (cf. De Vries *et al.*, 1995a).

Nutrient uptake

Nutrient uptake is taken from the MACAL model (De Vries *et al.*, 1994c). Total root uptake of NH₄, NO₃, BC2=Ca+Mg, K is described as a demand function, which consists of maintenance uptake, to re-supply the needles/leaves/shoots and roots (steady-state situation), and net (growth) uptake in stems and branches. The total root uptake fluxes for NH₄, NO₃, BC2 and K (mol$_c$ ha^{-1} a^{-1}) are thus described as:

$$NO_{3,ru} = (N_{lf} - N_{fu} + N_{gu}) \cdot \frac{NO_{3,in}}{N_{in}} \tag{49}$$

$$NH_{4,ru} = (N_{lf} - N_{fu} + N_{gu}) \cdot \frac{NH_{4,in}}{N_{in}} \tag{50}$$

$$BC2_{ru} = BC2_{lf} + BC2_{fe} + BC2_{gu} \tag{51}$$

$$K_{ru} = K_{lf} + K_{fe} + K_{gu} \tag{52}$$

where *gu* stands for growth uptake, and N = NH₄+NO₃. In case of nutrient shortage the nutrient contents in the foliage are reduced according to the maximum available nutrients. However, the model does not include a feedback of nutrient shortage on growth.

Growth uptake is calculated as:

$$X_{gu} = (Am_{st}(t) - Am_{st}(t-1)) \cdot ctX_{st} \tag{53}$$

where $Am_{st}(t) - Am_{st}(t-1)$ is the increment in amount stems for the current year (=time step) (kg ha^{-1} a^{-1}) and ctX_{st} is the content of element X in stems (mol$_c$ kg^{-1}). The current amount stems and branches is forced by a logistic growth function:

$$Am_{st}(t) = \frac{Am_{st,mx}}{1 + \exp(-k_{gl} \cdot (age_{vg} + t - t_{1/2}))} \tag{54}$$

where $Am_{st}(t)$ is the amount of stems (and branches) for simulation year t (kg ha^{-1}), $Am_{st,mx}$ the maximum amount of stems (kg ha^{-1}), age_{vg} the initial age of the vegetation (forest), $t_{1/2}$ the half life-time (a), k_{gl} is the logistic growth rate constant (a^{-1}).

In the model the amount of litterfall is linked to the stem growth parameters by assuming that the maximum amount of litterfall is reached with a three times higher growth constant than the maximum amount of stems:

$$Am_{lf}(t) = \frac{Am_{lf,mx}}{1 + \exp(-3 \cdot k_{gl} \cdot (age_{vg} + t - t_{1/2}))} \tag{55}$$

where $Am_{lf,mx}$ is the maximum amount of litterfall (kg ha^{-1} a^{-1}).

Nitrification and denitrification

Nitrification and denitrification for the complete soil layer (mol$_c$ ha^{-1} a^{-1}) are described in SMART2 as a fraction of the net input:

$$NH_{4,ni} = fr_{ni} \cdot \left(NH_{4,in} - NH_{4,ru} + \frac{NH_{4,in}}{N_{in}} \cdot \left(N_{mi,tot} - N_{im} \right) \right) \tag{56}$$

$$NO_{3,de} = fr_{de} \cdot \left(NO_{3,in} - NO_{3,ru} + NH_{4,ni} - \frac{NO_{3,in}}{N_{in}} \cdot N_{im} \right) \tag{57}$$

where fr_{ni} and fr_{de} are the nitrification and denitrification fractions (-), NH$_{4,in}$ and $NO_{3,in}$ stand for the gross input fluxes of NH$_4$ and NO$_3$, respectively, cf. Eqs. (11) and (12), $NH_{4,ru}$ and $NO_{3,ru}$ stands for the root uptake fluxes of NH$_4$ and NO$_3$ respectively, cf. Eqs. (47) and (48), $NH_{4,im}$ and $NO_{3,im}$ stands for the immobilisation fluxes in the mineral soil of NH$_4$ and NO$_3$ respectively, Eq. (15), $N_{mi,tot}$ is the total mineralisation flux, cf. Eq. (28) and $NH_{4,ni}$ is the nitrification flux, cf. Eq. (56). As with mineralisation, the maximum values for the nitrification and denitrification rate constant, $fr_{ni,mx}$ and $fr_{de,mx}$, are adjusted by the mean water-table and pH:

$$fr_{ni} = fr_{ni,mx} \cdot rf_{ni,MSW} \cdot rf_{ni,pH} \tag{58}$$

$$fr_{de} = fr_{de,mx} \cdot rf_{de,MSW} \cdot rf_{de,pH} \tag{59}$$

where $rf_{ni/de,MSW}$ and $rf_{ni/de,pH}$ are the nitrification and the denitrification reduction factors for the water-table and pH respectively (-). Maximum values are reduced with a decreasing mean spring water-table for nitrification, because this process is restricted to aerobic conditions, whereas the opposite is true for denitrification. Both rate constants are also reduced with decreasing pH.

The nitrification reduction functions for mean spring water-table is described as:

$$rf_{ni,MSW} = \begin{cases} rf_{ni,MSW,mn} & \text{for } MSW \leq z_1 \\ rf_{ni,MSW,mn} + (rf_{ni,MSW,mx} - rf_{ni,MSW,mn})\dfrac{MSW - z_1}{z_2 - z_1} & \text{for } z_1 < MSW < z_2 \\ rf_{ni,MSW,mx} & \text{for } MSW \geq z_2 \end{cases} \quad (60)$$

were $rfr_{ni,MSW,mn}$ is the soil dependent minimum value of the reduction function (-), and z_1 and z_2 are soil dependent MSW (m) values where the reduction function is changed.

The nitrification reduction function for pH is described as:

$$rf_{ni,pH} = \frac{1}{1 + \exp(4 \cdot (2.75 - pH))} \tag{61}$$

The denitrification reduction function for mean spring water-table is described as:

$$rf_{de,MSW} = \begin{cases} rf_{de,msw,mx} & \text{for } MSW \leq 0m \\ rf_{de,msw,mx} + (rf_{de,msw,mn} - rf_{de,msw,mx}) \cdot \dfrac{MSW}{z_{de}} & \text{for } 0 < MSW < z_{de} \\ rf_{de,msw,mn} & \text{for } MSW \geq z_{de} \end{cases} \tag{62}$$

where z_{de} (m) is the soil-dependent depth of the MSW below which the reduction by $rf_{de,MSW}$ (-).

The denitrification reduction function for mean pH is described as:

$$rf_{de,pH} = \begin{cases} 0 & \text{for } pH \leq 3.5 \\ \dfrac{pH - 3.5}{3} & \text{for } 3.5 < pH < 6.5 \\ 1 & \text{for } pH \geq 6.5 \end{cases} \tag{63}$$

Cation Exchange and chemical equilibria

Cation exchange is included for H, Al and BC2 described by Gaines-Thomas equations using concentrations instead of activities (cf. De Vries *et al.*, 1989):

$$\frac{fr\,H_{ac}^{\;2}}{fr\,BC2_{ac}} = KH_{ex} \cdot \frac{[\mathrm{H}^+]^2}{[\mathrm{BC}^{2+}]} \tag{64}$$

$$\frac{fr\!Al_{ac}^{\;2}}{fr\!BC2_{ac}^{\;3}} = KAl_{ex} \cdot \frac{[\mathrm{Al}^{3+}]^2}{[\mathrm{BC}^{2+}]^3} \tag{65}$$

The charge balance for the exchange complex requires that:

$$frH_{ac} + frBC2_{ac} + frAl_{ac} = 1 \tag{66}$$

Sulphate adsorption is described by a Langmuir equation:

$$ctSO_{4,ac} = \frac{SSC \cdot [\mathrm{SO}_4^{2-}]}{C_{1/2} + [\mathrm{SO}_4^{2-}]} \tag{67}$$

where $ctSO_4$ (mol_c kg^{-1}) is the sorbed amount of SO_4, SSC (mol_c kg^{-1}) the sulphate sorption capacity and $C_{1/2}$ the half-saturation constant (mol_c m^{-3}). The dissociation of CO_2, the dissolution of Ca carbonate (calcareous soils only) and the dissolution of Al hydroxide is described as (cf. De Vries *et al.*, 1988):

$$[\mathrm{HCO}_3^-] = K_{CO_2}\,\frac{pCO_2}{[\mathrm{H}^+]} \tag{68}$$

$$[\mathrm{BC}^{2+}] = \frac{K_{Ca_{cb}} \cdot pCO_2}{[\mathrm{HCO}_3^-]^2} \tag{69}$$

$$[\mathrm{Al}^{3+}] = \mathrm{K}_{Al_{ox}} \cdot [\mathrm{H}^+]^3 \tag{70}$$

The dissociation of organic acids (humic +fulvic acids) is modelled as (cf. Posch *et al.*, 1993):

$$[\mathrm{RCOO}^-] = [\mathrm{RCOO}_{tot}] \cdot \frac{K_a}{K_a + [\mathrm{H}^+]} \tag{71}$$

where K_a is a pH dependent dissociation constant, according to (Oliver *et al.*, 1983):

$$-\log_{10} K_a = a + b \cdot pH - c \cdot pH^2 \tag{72}$$

where the a, b and c are based on experimental data. Oliver *et al.* derived the values $a=$ 0.96, $b=$0.90 and $c=$0.039 for surface water.

The H concentration is determined by charge balance, Eq. (14), because the model structure of SMART2 is based on the anion mobility concept (Reuss and Johnson, 1986). The charge balance for the soil solution concentrations equals:

$$[H^+] = [SO_4^{2-}] + [NO_3^-] + [HCO_3^-] + [Cl^-] + [RCOO^-] - $$
$$[BC^{2+}] - [NH_4^+] - [Na^+] - [K^+] - [Al^{3+}] \tag{73}$$

Concentrations of K, Na, NH_4, NO_3 and Cl are fully determined by the mass balance equation, cf. Eq. (1). The concentration of base cations in non-calcareous soils is determined by both the mass balance equation and a change in the adsorbed amount of base cations determined by cation exchange equilibrium reactions, Eqs. (62) and (63). The concentrations of HCO_3 and Al are determined by both the mass balance equations and an equilibrium with H, cf. Eqs. (66), (67) and (68). The concentration of divalent base cations in calcareous soils is determined by both the mass balance equation and a change in carbonate content. In these soils carbonate weathering is included, Eq. (67), but silicate weathering, Al hydroxide weathering and cation exchange are neglected (the Al concentration is thus set to zero). The dissociation of organic acids is modelled by Eq. (69). Sulphate sorption is described by a Langmuir isotherm, Eq. (65). The pH is thus influenced by all rate-limited and equilibrium processes causing proton production or consumption.

The dissolved and adsorbed concentrations are calculated by solving fourteen equations with fourteen unknowns, i.e. ten concentrations ($[H^+]$, $[Al^{3+}]$, $[K^+]$, $[Na^+]$, $[BC^{2+}]$, $[SO_4^{2-}]$, $[NO_3^-]$, $[Cl^-]$, $[HCO_3^-]$, $[RCOO^-]$), three exchangeable fractions (*frH$_{ac}$, frBC2$_{ac}$, frAl$_{ac}$*) and adsorbed SO_4 (*ctSO$_{4,ac}$*). The numerical solution procedure is given in Posch *et al.* (1993).

Inclusion of the effect of temperature

The effect of temperature was considered for (i) the mineralisation of old litter, nitrification and denitrification, (ii) Al hydroxide dissolution and (iii) weathering of primary minerals. A direct temperature effect on growth was not included because observations did not clearly indicate a change in growth (Van Breemen *et al.*, 1998) and the effects of temperature rise and increase of CO_2 on growth are still ambiguous (Mohren, pers. comm.). There might be, however, an indirect effect of temperature on growth because of a larger N availability due to increased mineralisation. In SMART2, this would increase N uptake, but not biomass, so, the N-content in biomass would increase until a given maximum nitrogen content.

We choose the same dependency for mineralisation, nitrification and denitrification, as the temperature dependencies of these processes are similar. The temperature effect on N mineralisation is often described by a Q_{10} function. Kätterer *et al.* (1998) and Stanford *et al.* (1973) found Q_{10} values between 2.0 and 2.5. Kirschbaum (1995) found a temperature dependent Q_{10} for mineralisation with higher values at lower temperatures, which is in agreement with Ross and Bridger (1978).

The temperature dependency of nitrification (cf. Grundmann *et al.*, 1995; Stark, 1996) and denitrification (Grant, 1991; Nômmik and Larson, 1989) are mostly described by an Arrhenius equation. A Q_{10}-function is, however, also used (e.g. Knowles, 1982 who gives in a review Q_{10} values of 1.5 to 3.0 for denitrification). To have a comparable description, we choose a Q_{10} function for all three microbiological processes as (cf. Kirschbaum, 1995):

$$k(T) = k(T_{ref}) \cdot Q_{10}^{\frac{T - T_{ref}}{10}} \tag{74}$$

where k represents either the mineralisation rate constant of old litter (a^{-1}), or the nitrification factor (-) or the denitrification factor (-), T is the temperature (K) and T_{ref} is the reference temperature (K). For all these nitrogen transformation processes, we obtained a fitting Q_{10} value of 1.6. The temperature effect on mineralisation refers to the mineralisation of old litter, because the decomposition rate of fresh litter did not change under the different treatments (Verburg, 1998).

For the Al oxide dissolution the temperature dependency was described by Van 't Hoff's equation (e.g. Stumm and Morgan, 1981):

$$K_{Al_{ox}}(T) = K_{Al_{ox}}(T_{ref}) \cdot \exp\left(\frac{\Delta H^{\circ}}{R} \cdot (\frac{1}{T_{ref}} - \frac{1}{T}) \right) \tag{75}$$

where $K_{Al\ ox}$ is the Al oxide dissolution constant ($mol^{-2}\ L^2$), ΔH° is the reaction enthalpy (= -95.5 kJ mol^{-1}) and R is the universal gas constant ($8.3 \cdot 10^{-3}$ kJ mol^{-1} K^{-1}). Temperature rise will lead to a decrease of $K_{Al\,ox}$.

The temperature effect on weathering rates was described as (Sverdrup, pers. com.):

$$X_{we}(T) = X_{we}(T_{ref}) \cdot \exp\left(3600 \cdot \left(\frac{1}{T_{ref}} - \frac{1}{T} \right) \right) \tag{76}$$

where X_{we} is weathering rate (mol_c m^{-3} a^{-1}). A temperature increase from 5 °C to 8.7 °C implies an increase in weathering of 20%.

The effect of increased CO_2 pressure was not included for the biochemical processes, but for the geochemical equilibria pCO_2 is included. The pCO_2 in soil air is calculated as a multiple of the pCO_2 in the atmosphere. Consequently, increase in CO_2 pressure in the atmosphere directly implies an increase in pCO_2 in soil air.

2.3.3 Site description and manipulation experiments

Site description

Risdalsheia is located near Grimstad, southern Norway (58°23'N, 8°19'E) at 300 m above sea level (Wright *et al.*, 1998a). The site is representative for large areas of upland southern Norway. Mean annual precipitation is 1400 mm, runoff 1200 mm and mean annual temperature is 5°C (mean of –3°C in January and +16°C in July). Vegetation is mainly a sparse cover of pine (*Pinus sylvestris* L.) and birch (*Betula pubescens* L.) with heather (*Calluna vulgaris* L.) and blueberry (*Vaccinium myrtillus* L.) as dominant ground species. Risdalsheia receives relatively high levels of acid deposition with mean values for 1984–1992 of 113 $mmol_c$ S m^{-2} a^{-1} and 132 $mmol_c$ N m^{-2} a^{-1}. (Wright *et al.*, 1993).

Manipulation experiments

Two sets of manipulation experiments have been conducted at Risdalsheia (Table 2). The first set of experiments (the RAIN-project: Reversing Acidification In Norway) entailed exclusion of ambient N and S deposition (Wright *et al.*, 1993) at the roofed KIM catchment from June 1984 until August 1999. The roofed EGIL catchment received recycled ambient acid rain. The uncovered catchment ROLF served as outside control. The decrease in S and N deposition resulted in a strong decrease of SO_4 and N concentrations in the runoff, accompanied by decrease in base cation concentrations, and increase in acid neutralising capacity (ANC) (Wright *et al.*, 1993; Wright and Jenkins, 2001).

Table 2. Overview of the treatments at the catchments at Risdalsheia in the CLIMEX project

Name	Treatment	Deposition[1]	Climate[2]
ROLF	Control	Ambient	none
EGIL	Control	Ambient	none
	Treatment	Ambient	Soil warming
KIM	Control	Clean	none
	Treatment	Clean	CO_2 + air warming

[1] Deposition manipulation started in 1984
[2] Climate manipulation started in 1994

The second set of experiments (the CLIMEX-project: CLIMate change EXperiment) began April 1994 and involved manipulation of CO_2 and temperature. These new treatments (Dise and Jenkins, 1995) were superimposed on the ongoing RAIN treatments. Both the KIM catchment and the EGIL catchment were divided in a treatment section and a control section. At the KIM catchment, CO_2 was added to the air during the growing season at target concentration of 560 ppm and the air was warmed by +5°C in January and +3°C in July, with intermediate temperature during the intervening months. Runoff chemistry of both treatment sections was analysed. Wright (1998) found increased NO_3 and NH_4 concentrations in runoff in response to

elevated temperature. At the EGIL catchment, the soil was warmed by means of electric heating cables placed beneath the litter in the treatment section, resulting in an average soil temperature rise of 3.7°C at 5 cm depth during the first 3 years of treatment. The runoff chemistry was analysed only in the treatment section of the EGIL catchment. Lükewille and Wright (1997) found a significant increase in N concentrations in runoff in response to elevated soil temperature during the first 15 months of treatment.

At the EGIL catchment, there was no change in growth or biomass of the shrubs or pine trees, and no change in N concentrations in the shrub foliage (Arp, pers. com.). Beier and Rasmussen (1997) found a small increase in N concentrations in pine needles at both catchments. Arp and Berendse (1997) found a small increase in growth of the shrubs at the KIM catchment.

Mineralisation and nitrification measurements were performed for 3 years: one control year (1994) and two treatment years (1995 and 1996). Verburg (1998) and Verburg *et al.* (1999) found an increase in net N-mineralisation and nitrification due to climate change, but variability was high. At the EGIL catchment there was no significant change in mineralisation and nitrification. At the KIM catchment the increase in net mineralisation was significant. Decomposition rates of fresh litter were not affected by temperature and CO_2 treatments.

Model parameterisation

To test the model and the included temperature dependencies, the SMART2 model was applied to two catchment experiments at Risdalsheia. For the simulation of the concentrations of different elements in the runoff the model was calibrated at the ROLF catchment. The Al oxide dissolution constant, the mineralisation constant and the nitrification factor were calibrated manually, using the concentrations of NO_3, NH_4, BC2 and Al and pH in the runoff . The inclusion of temperature-dependencies of N-processes and of the Al oxide dissolution constant was tested as from 1995, the year the temperature rise started, at the EGIL catchment. The SMART2 model was validated for both temperature and deposition changes by applying it at the KIM catchment.

The soil parameters were either derived from measurements (Wright *et al.*, 1993) or from the MAGIC7 calibration at Risdalsheia (Wright *et al.*, 1998a) (Table 3). The selectivity constant for Al-BC exchange (KAl_{ex}) and H-BC exchange (KH_{ex}) were calculated by using Gaines-Thomas equations (see Eq. 64 and 65). The adsorbed fractions and runoff concentrations were derived from Wright *et al.* (1993). Averages of measured absorbed fractions and concentrations at the three catchments were taken.

The vegetation parameters (Table 3) were either taken from measurements or from estimates.

Table 3. Fixed parameters for KIM and EGIL used in calibration of SMART2.

Parameters				Derived	Reference
Soil parameters	ROLF	EGIL	KIM		
Soil depth (m)	0.10	0.10	0.10	measured	(Wright *et al.*, 1998a)
Bulk density (g cm^{-3})	0.66	0.53	0.73	measured	(Wright *et al.*, 1993)
Porosity (m m^{-1})	0.5	0.5	0.5	measured	(Wright et *al.*, 1998a)
CEC (mmol$_c$ kg^{-1})	87.0	97.0	97.0	measured	(Wright *et al.*, 1993)
Organic matter (kg kg^{-1})	0.25	0.26	0.24	measured	(Wright *et al.*, 1993)
Initial C/N (-)	25.	25.	25.	calibrated	(Wright *et al.*, 1998a)
SO$_4$-ads. Half saturation (mol$_c$ m^{-3})	60.	60.	60.	measured	(Wright *et al.*, 1998a)
SO$_4$-ads. Max. capacity (mol$_c$ m^{-3})	6.0	6.0	6.0	measured	(Wright *et al.*, 1998a)
Solubility Al(OH)$_3$ (log$_{10}$)	7.2	7.2	7.2	calibrated	This study
Sel. constant Al-BC exchange (log$_{10}$)	-1.63	-1.63	-1.63	calculated	Required data from Wright *et al.* (1993)
Sel. constant H-BC exchange (log$_{10}$)	2.85	2.85	2.85	calculated	Required data from Wright *et al.* (1993)
Total organic acid (mol$_c$ m^{-3})	0.12	0.12	0.12	measured	(Wright *et al.*, 1998a)
pCO$_2$ (multiple of pCO$_2$ in air) (-)	6.32	6.32	6.32	measured	(Wright *et al.*, 1998a)
BC2-weathering (mol$_c$ m^{-3} a^{-1})	0.005	0.005	0.005	calibrated	(Wright *et al.*, 1998a)
Na-weathering (mol$_c$ m^{-3} a^{-1})	0.001	0.001	0.001	calibrated	(Wright *et al.*, 1998a)
K-weathering (mol$_c$ m^{-3} a^{-1})	0.000	0.000	0.000	calibrated	(Wright *et al.*, 1998a)
Vegetation parameters [1]					
Ammonium foliar uptake fraction (-)	0.4		0.4	estimated	(Kros *et al.*, 1995a)
Proton foliar uptake fraction (-)	0.4		0.4	estimated	(Kros *et al.*, 1995a)
K foliar exudation fraction (-)	0.65		0.65	estimated	(Kros *et al.*, 1995a)
Max. amount of litterfall (kg m^{-2} a^{-1})	0.175		0.209	measured	(Arp, pers comm.; Beier, pers comm.)
Reallocation fraction (-)	0.10		0.10	estimated	(Kros *et al.*, 1995a)
BC$_2$ leaf contents (%)	0.81		0.61	measured	(Arp and Berendse, 1997)
K leaf contents (%)	0.73		0.53	measured	(Arp and Berendse, 1997)
N contents in litterfall (%)	0.96		0.84	measured	(Arp, pers comm.; Beier, pers comm.)
Logistic growth rate constant (a^{-1})	0.15		0.15	derived	(Kros *et al.*, 1995a)
Growth half time (a)	10.		10.	derived	(Kros *et al.*, 1995a)
Max. amount of biomass (kg m^{-2})	3.2		3.1	estimated	(Arp, pers comm.; Beier, pers comm.)
N nutrient content (%)	1.13		0.63	measured	(Arp and Berendse, 1997)
BC$_2$ nutrient content (%)	0.002		0.002	measured	(Arp and Berendse, 1997)
K nutrient content (%)	0.002		0.002	measured	(Arp and Berendse, 1997)
Mineralisation factor fresh litter (-)	0.4		0.4	estimated	(Kros *et al.*, 1995a)
Min. rate constant old litter (a^{-1})	0.16		0.16	calibrated	this study
Fraction roots in litter layer (-)	0.75		0.75	estimated	(Kros *et al.*, 1995a)
Nutrient cycling factor (-)	1.77		1.82	calculated	Data from Arp and Beier, pers. comm.

[1] For ROLF and EGIL the same vegetation parameters were used

For shrubs we derived data from Arp and Berendse (1997) and Arp (pers. comm.), while for trees the data were based on Beier and Rasmussen (1997) and Beier (pers. comm.). Parameters that were not measured or estimated at Risdalsheia were taken from Kros *et al.* (1995a), using the values for heather. The measured aboveground litterfall of shrubs (Arp, pers. com.) and of the trees Beier (pers. com.) were summed. The root turnover was calculated using the measured litterfall and assuming a nutrient cycling factor (*ncf,* see Eq. 23) of 0.5 for trees and a *ncf* of 3.0 for shrubs (Kros *et al.*, 1995a). These amounts of litterfall in combination with these nutrient cycling factors resulted in a biomass weighted average *ncf* of 1.8. At the EGIL catchment, N-mineralisation fluxes were 10 – 15 % higher than the measured N mineralisation fluxes. (Table 4). The total litterfall values are much lower (approximately less than half) than the values mentioned in Wright *et al.* (1998b), who only used estimates since measurements were not available at that time.

We excluded the influence of soil solution pH on mineralisation, because it had a too strong a positive feedback: increased pH which in turn increased mineralisation, causing an unrealistic overestimation of the nitrogen concentration. Furthermore, experimental support for the positive feed back of pH on mineralisation is rather weak.

2.3.4   Results

Model calibration

The calibration of the simulated runoff chemistry without temperature effect was performed by comparing simulated concentrations with observed concentrations from the ROLF catchment (Figure 3). The temperature effect was calibrated at the EGIL catchment from 1995 (Figure 4).

Calibration at the ROLF control catchment

Cl concentrations were reproduced very well, indicating a well-simulated hydrology (Figure 3). The NO_3 and the NH_4 concentrations were reproduced quite well too. The dynamics in SO_4 and BC2 concentrations were not fully reproduced by SMART2. The fluctuations of SO_4 concentrations were underestimated, as was also found by Van der Salm *et al.* (1995), who attributed this effect to the lack of vertical heterogeneity of the model. SMART2 considers the mineral soil as one-layer neglecting vertical heterogeneity and consequently it underestimates the retardation of absorbing compounds. The pH was overestimated for the years before 1990, whereas the Al concentrations were overestimated during the entire simulation period. Changing the Al oxide dissolution constant leads either to increased or decreased both of pH and Al concentrations, so calibration of the Al oxide dissolution constant cannot improve predictions of pH and Al concentrations at the same time. The same problem was found by Wesselink and Mulder (1995), who could not reproduce both pH and Al concentrations by Al oxide solubility. They attributed this to Al complexation with dissolved organic matter. We calibrated the value of the Al oxide dissolution constant,

such that it resulting satisfactory pH values and BC2 concentrations. Taking into account Al complexation with organic compounds might lead to better results.
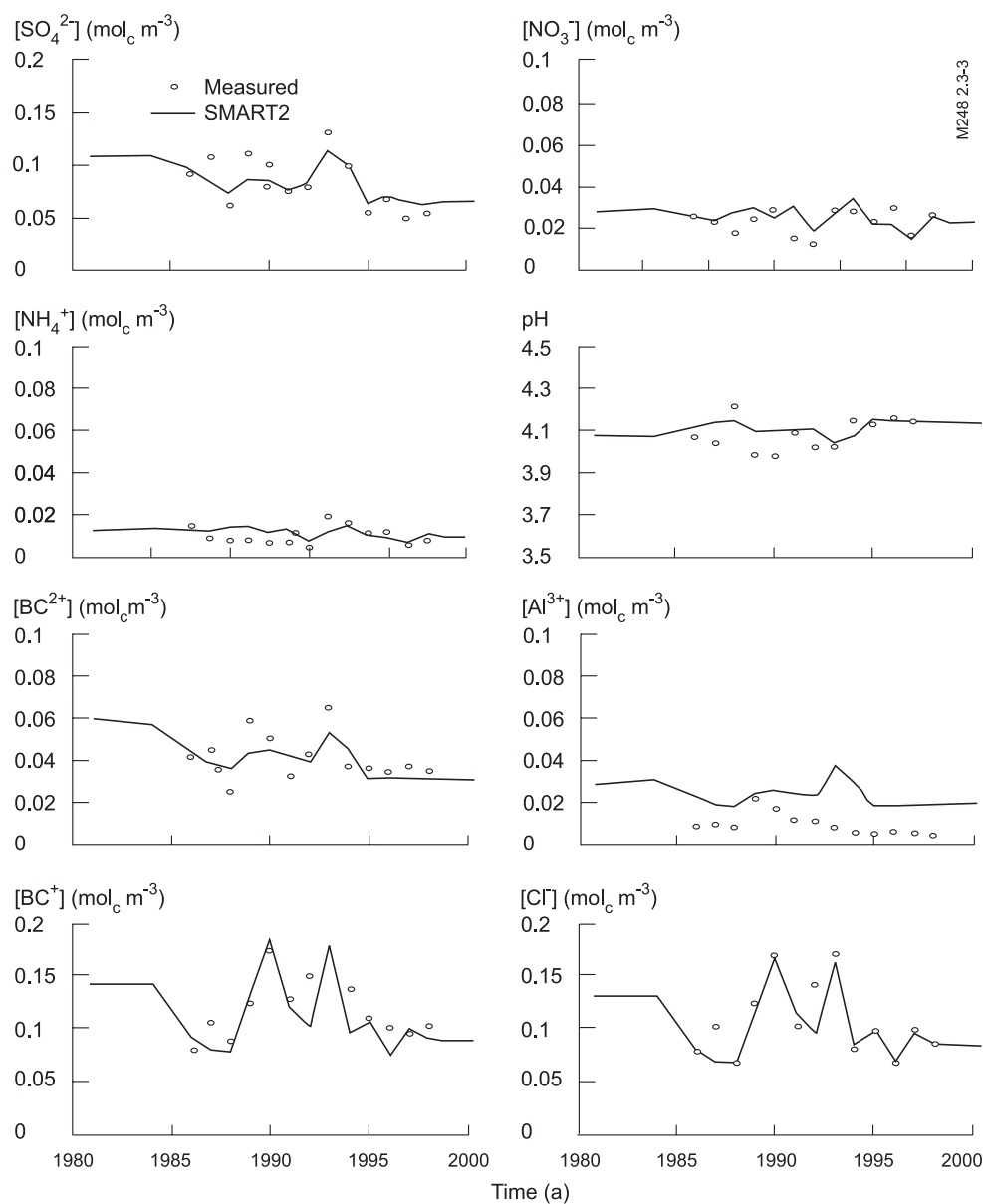
Figure 3 Measured and simulated concentrations of SO₄, NO₃, NH₄, pH, BC2, Al, BC and Cl for the ROLF control catchment
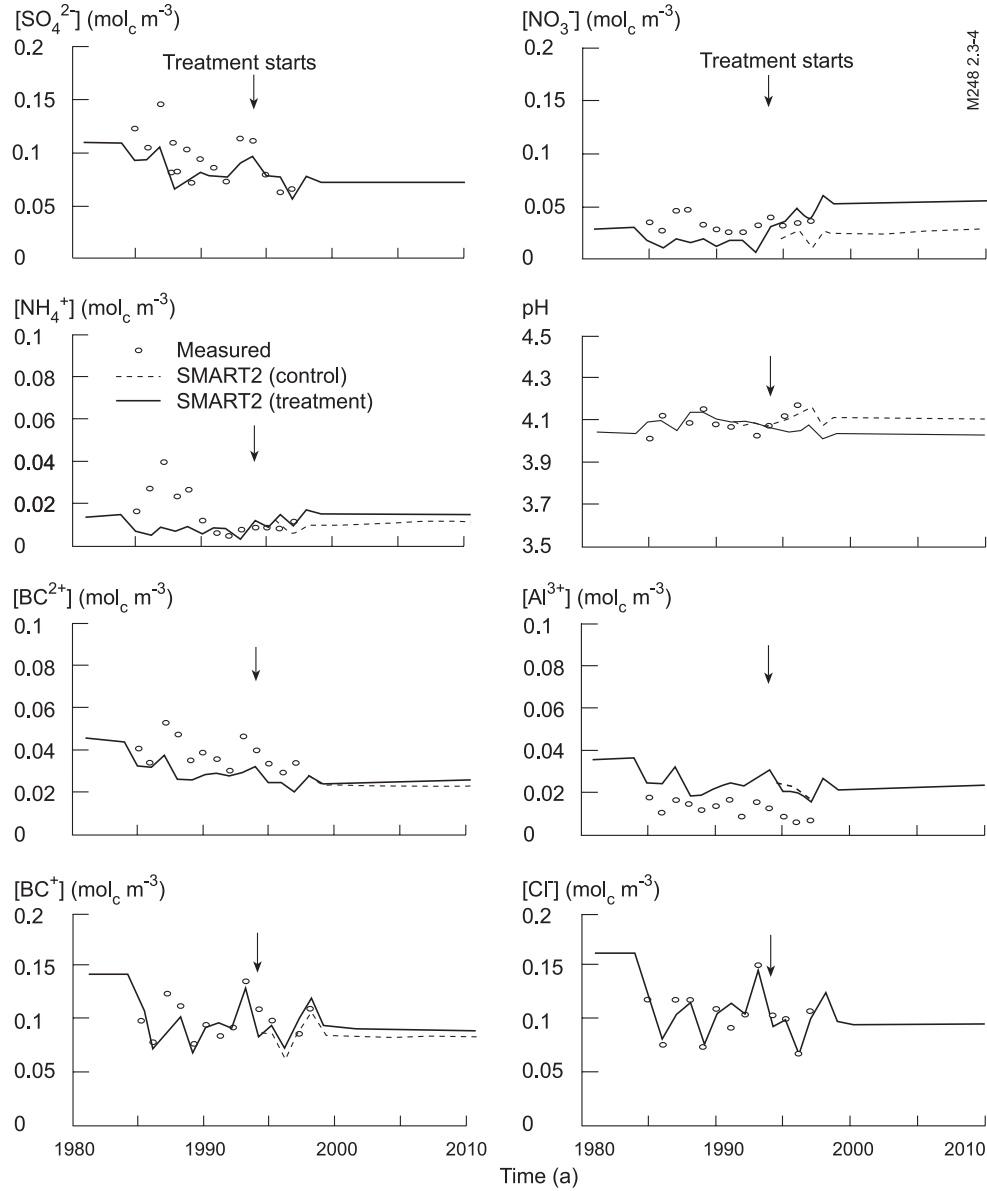
Figure 4 Measured and simulated concentrations of SO$_4$, NO$_3$, NH$_4$, pH, BC2, Al, BC and Cl for the EGIL catchment with a soil temperature increase starting in 1994

Calibration of the temperature effect at the EGIL catchment

The incorporation of the temperature effect was calibrated at the EGIL catchment, using the measured mineralisation and nitrification rates (see section 3.2). The observed and the simulated relative increase in N-mineralisation were comparable,

about 10% (Table 4). The nitrification at EGIL was underestimated, but the relative temperature effect was overestimated, which is an indication that the Q_{10} for nitrification might be too high. Figure 4 shows an increase in simulated NO_3 and NH_4 concentrations starting from 1995. This is also found for the observed concentrations, though to a less extent. The concentrations before 1995 were clearly underestimated, resulting in an underestimation of the 3 years pre treatment N-leaching fluxes. This was probably caused by an overestimation of N-uptake, since N-mineralisation was slightly overestimated (Table 4). The relative increase in N leaching due to temperature rise was overestimated by SMART2. The observed increase was 68% whereas the simulated increase was 200 % (Table 4).

The higher measured N-contents in needles (Beier and Rasmussen, 1997) indicate a higher N-uptake after temperature rise, which was not predicted by SMART2. Even though SMART2 calculates a higher mineralisation and therefore a higher N availability, the N-uptake did not increase, because the N-content in the biomass had already reached the maximum value before the temperature rise. In SMART2, N uptake can only increase if the N content in biomass is not maximal.

The lower actual Al hydroxide dissolution constant due to temperature rise (see Eq. 75) caused a decrease in calculated Al concentrations and pH with temperature rise. Furthermore, BC2 and BC concentrations increased due to higher weathering rates. This effect, however, was not sufficient to compensate the pH decrease due to a shift in the Al hydroxide equilibrium and the increase in NO_3 concentration due to enhanced mineralisation.

Evaluation at the KIM catchment

Deposition reduction (1984 – 1994)

After calibration the model was evaluated to the KIM catchment, using the same parameter set for the soil, except for bulk density, CEC and organic matter (Table 3). The vegetation related parameters differed at the two catchments: at the KIM catchment the ground vegetation was mainly *Calluna vulgaris* L., whereas at the EGIL catchment it was *Vaccinium myrtillus* L. The predicted trends in SO_4, NO_3 and NH_4 concentrations in runoff corresponded well to the observed trends, but SMART2 underestimated the SO_4, NO_3, NH_4 and BC2 concentrations and overestimated pH (Figure 5), Al, BC and Cl concentrations were predicted well. The underestimation of the concentration of SO_4, NO_3, NH_4 and BC2 might be caused by a too strong response to the reduction in deposition, which may be caused by an underestimation of sulphate desorption and a too fast release of nitrogen. Divalent base cation concentrations are strongly correlated to SO_4 input. Higher acid input due to higher SO_4 input induces an exchange of base cations by H and Al, resulting in higher BC2 concentrations.
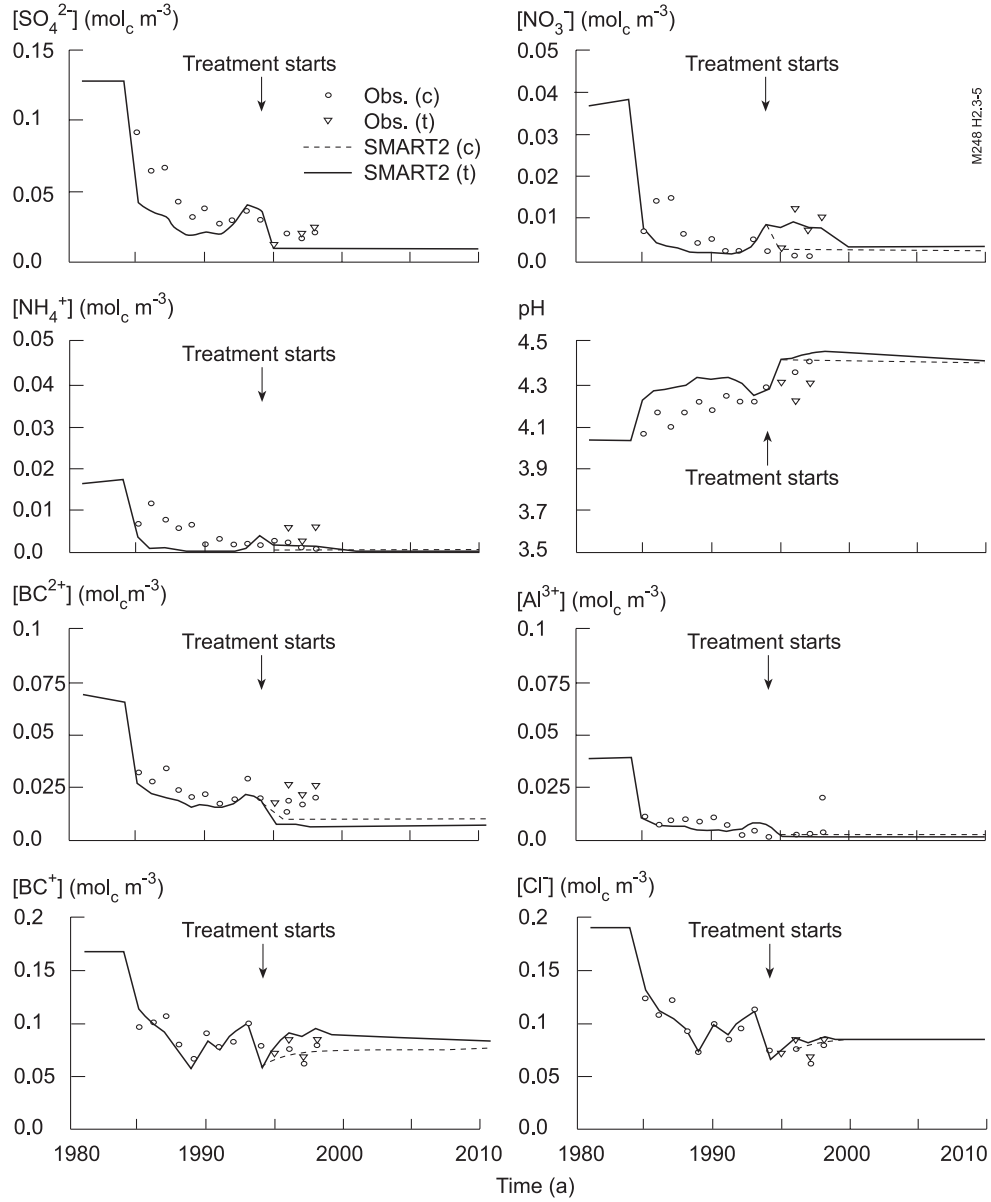
Figure 5. Measured and simulated concentrations of SO_4, NO_3, NH_4, pH, BC2, Al, BC and Cl for KIM catchment with deposition reduction as from 1984 and a CO_2 and air temperature increase starting in 1994.
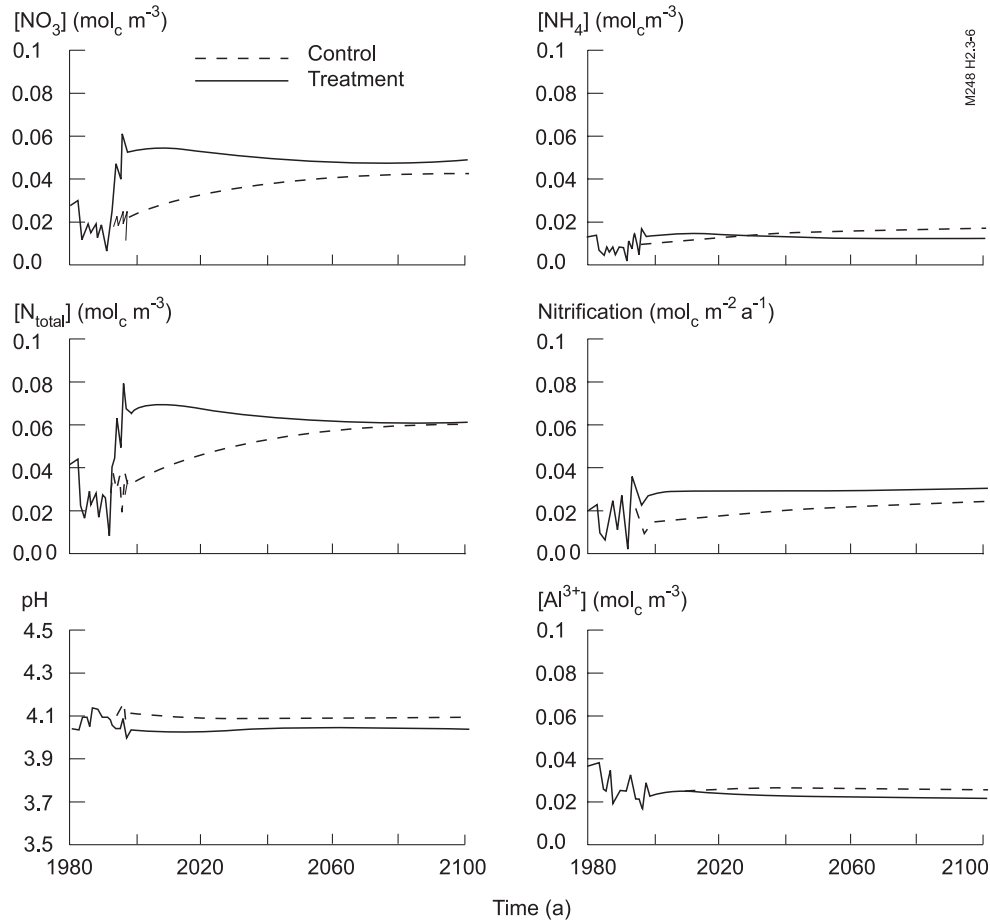
Figure 6 Simulated concentrations of NO₃, NH₄, total N and nitrification for the EGIL catchment in the long-term

Temperature rise

The response of N concentrations to temperature rise after 1994 was simulated fairly well (Figure 5), especially the increase in nitrate concentrations was reproduced well. In contrast to the EGIL catchment, SMART2 simulated an increase of N uptake due to temperature rise (Table 4). At the KIM catchment, the N content in the leaves increased, because the maximum N content was not reached yet, which resulted in a higher N uptake (see Eq. 22).

The field experiments show a little treatment response to BC2 concentrations and no response to SO₄ concentrations, whereas the model gave a decrease in BC2 concentrations and no response to SO₄ concentrations (Figure 5). SMART2 predicted a pH increase in response to temperature rise, whereas the observed pH actually fell. The Al concentrations were adequately simulated both before and after the temperature rise, although the effect was small. Both simulated and measured Al

concentrations decreased due to temperature rise. The respond of BC concentrations on temperature rise was simulated well. Both the simulated and observed BC concentrations increased in response to temperature rise.

Since the short-term effect of the soil heating was rather small, we decided to evaluate the possible long-term effect of temperature rise. Therefore the soil heating treatment of EGIL was simulated for a period of 200 years. The deposition during this 200 year period was taken as the average of 1995-1998. SMART2 predicts the climate change effect on N-leaching to be temporal (Figure 6). After 100 years, the N leaching in the treatment run is equal to that of the control run. At the actual temperature it took more than 100 years to reach a steady state (N saturation), whereas at the elevated temperature it took less than 50 years. At higher temperature less N was accumulated in the soil, because of a higher mineralisation rate. The NO_3/NH_4 ratio changed, due to increased nitrification. In the long-term, NO_3 concentrations increased whereas NH_4 concentrations decreased. At the KIM catchment (low deposition) a new steady state was already reached within 5 years (Figure 5). Due to the lower Al oxide dissolution constant at 8.7 °C than at 5 °C, the Al concentrations after temperature rise were lower than before, resulting in lower pH values.

2.3.5   Discussion and conclusions

In general, the observed time-series in runoff chemistry in response to deposition reduction and temperature rise were well reproduced by the model SMART2. At the roofed sites, however, SMART2 tended to underestimate the concentrations of SO_4, NO_3, NH_4 and BC2, though the simulated trends were reproduced well. Mol-Dijkstra *et al.* (1998) tested the performance of SMART2 in response to deposition reduction at a spruce forest (Speuld) in the Netherlands, where bi-weekly soil solution samples were taken with 4 replicates. The SMART2 results were compared with flux-weighted averaged concentrations obtained from observed soil solution chemistry and modelled hydrology. This uncertainty in fluxes due to high soil variability at Speuld thwarted the model validation. In contrast to the observations at Speuld, the observations at the Risdalsheia catchments are 'real' annual average concentrations from the runoff of the whole catchment, which means that the time and space resolutions of measurements and modelling are similar. This application, with quite a long observation period, contributes to an increase in confidence in using SMART2 at the regional scale, especially to evaluate deposition scenarios.

The inclusion of the climate change effect in SMART2 was restricted to the temperature effect on mineralisation of old litter, nitrification, denitrification, weathering and Al oxide dissolution constant. For the N related processes we obtained a Q_{10} value of 1.6. Kätterer *et al.* (1998), however, found Q_{10} values for mineralisation of about 2.5 for comparable soil and vegetation types. Kirschbaum (1995), even, found a Q_{10} value of 5.0 at a temperature of 5 °C. Although there was an indication that N-uptake increased, the temperature effect on growth was not included because the effect on growth is not clear and the temperature dependency as well as the CO_2 dependency of growth is not well known. An increase in N availability,

however, induced an increase in N-uptake at the KIM catchment, which was caused by an increase in N content in the biomass. This increase was possible since at that low N input, the N content in the biomass was below its maximum. At the EGIL catchment the maximum N content was already reached due to higher N input, so there was no response of N uptake. The inclusion of the temperature dependencies gave satisfactory results. The observed increase in N-runoff was reproduced well by the model, just like the observed increase in mineralisation and nitrification. Still, there is a need to pay attention to the N-cycling in SMART2, considering the adaptation of the pH influence on mineralisation in this application.

Table 4 Three years average pre and post treatment N-fluxes as calculated by SMART2, MERLIN and observed (mmol m^{-2} a^{-1}). The standard deviations are given in brackets

	N-flux	SMART2		MERLIN		Observed	
		pre	post	pre	post	pre	post
EGIL	Deposition	77 (22)	83 (21)	76	59	77 (22)	83 (21)
	Litterfall	262 (6)	257 (1)	485	487	-	-
	Mineralisation	269 (1)	312 (3)	418	456	245 (-)[1]	271 (57)[2]
	Uptake	307 (6)	301 (3)	486	485	-	-
	Nitrification	10 (7)	30 (7)	-	-	45 (-)[1]	67 (11)[2]
	Denitrification	0 (0)	2 (0)	-	-	-	-
	Leaching	18 (13)	54 (12)	28	48	28 (6)	47 (10)
KIM	Deposition	21 (8)	0 (-)	14	0	21 (8)	0 (-)
	Litterfall	195 (4)	197 (3)	469	477	-	-
	Mineralisation	225 (2)	256 (2)	437	472	147 (-)[1]	201 (7)[2]
	Uptake	238 (2)	247 (3)	470	482	-	-
	Nitrification	4 (3)	8 (2)	-	-	2 (-)[1]	3 (0)[2]
	Denitrification	0 (0)	0 (0)	-	-	-	-
	Leaching	5 (5)	8 (3)	4	9	3 (1)	9 (4)

[1] n = 1
[2] n = 2

Wright *et al.* (1998b) applied MERLIN at Risdalsheia. This model is of comparable complexity as SMART2 and gave comparable results. MERLIN is a simple process-orientated model focused on simulation of concentrations of inorganic nitrogen in soil leachate and runoff in terrestrial ecosystems (Cosby *et al.*, 1997). The model links the C and N cycles. The ecosystem is simplified to one plant compartment and two soil organic matter compartments (labile and refractory organic matter), the effect of temperature was included by changing the decomposition rate in 1995, the year the temperature treatment started. MERLIN calculated a higher N turnover than SMART2, due to a higher N input via litterfall (Table 4). Wright *et al.* (1998b) used estimated litterfall fluxes for shrub vegetation, whereas we used recently measured litterfall fluxes (Arp, pers. com.). However, both models calculated comparable N leaching fluxes. Considering the 3 years pre and the 3 years post treatment, MERLIN calculated the increase of N leaching very well, but the year-to-year variations were not well reproduced. As with SMART2, MERLIN predicted increased N runoff in response to temperature rise. On the long-term, however,

MERLIN predicted an enduring higher N runoff in response to temperature rise (Wright *et al.*, 1998b), while SMART2 predicted only a temporal increase.

The length of the period with increased N runoff in response to elevated temperature depends on deposition level. The SMART2 simulations indicate that with high deposition levels, the temporal effect of increased N leaching is longer than with lower deposition levels. Due to increased nitrification, the ratio between NO_3 and NH_4 concentrations changes. NO_3 concentrations increase and NH_4 concentrations decreased.

It seems that the biochemical processes give a temporal response to temperature rise, whereas the geochemical processes change is permanent. To test the model more rigorously in its suitability to predict responses to climate change, additional years of treatment would be needed. For instance, the strong temporal variability in the mineralisation and nitrification measurements makes it difficult to test the model behaviour in response to temperature rise over such a short period. Application to other soil warming experiments (Rustad *et al.*, 2001) would be additional to test the prediction climate change response of the model. The long-term runs showed a temporal effect of temperature rise dependent on deposition level. It would be recommendable to test this effect in the field.

2.4 Validation and comparison of soil acidification models with different degrees of process aggregation on a site scale

Abstract

A one-layer (SMART2) and a multi-layer (RESAM) soil acidification model with a resolution of one year and a multi-layer soil acidification model with a temporal resolution of one day (NUCSAM) were applied to an intensively monitored spruce site at Solling, Germany. SMART2 was specially developed for the application on a national and European scale, RESAM for application on the regional to national scale, whereas NUCSAM is a typical site-scale model. Contrary to SMART2 and RESAM, NUCSAM takes seasonal variability into account since it simulates solute transport and biogeochemical processes on a daily basis. Consequently, NUCSAM accounts for seasonal variation in deposition, precipitation, transpiration, litterfall, mineralisation and root uptake.

The major aim was to study the influence of model simplifications, in terms of process detail, number of soil layers and temporal variability, on the modelled of soil solution concentrations and leaching fluxes. To that aim, the models where first validated by comparing simulated concentrations and leaching fluxes with measured values at the Solling site during the period 1973-1989. Next, long-term soil and soil solution response simulated with three models were compared using two deposition scenarios for the period 1990-2090. Input parameters were derived from measured data at the Solling site. Outputs from the one-layer model SMART2 were compared with measured soil solution concentration averaged over depth.

All models were able to simulate most of the concentrations during the examined period reasonably well. However, the one-layer model, SMART2, had some difficulties to simulate strong changes in soil solution concentrations due to a lower retardation in the soil system. RESAM simulated a somewhat stronger rise and fall in base cation and SO_4 concentrations in the subsoil.

Although both the seasonal and the interannual variation in the soil solution concentrations as modelled by the three models showed large differences, the long-term trends corresponded quite well and the leaching fluxes were almost similar. Generally it appeared that the uncertainty due to time resolution and vertical heterogeneity in long-term predictions was relatively small. So, the use of the simplified model SMART2, that neglects seasonal variation and vertical heterogeneity, is in most aspects acceptable for the evaluation of long-term trends in soil and soil solution chemistry.

2.4.1 Introduction

Various models have been developed to analyse the long-term response of surface waters and soils to acid deposition. These models have been designed for use on a continental to national scale, such as MAGIC (Cosby *et al.*, 1985) and SMART (De Vries *et al.*, 1989), SMART2 (Chapter 2.3; Kros *et al.*, 1995a,b) and RESAM (Chapter 2.2; De Vries *et al.*, 1995a) or for use on a catchment or site scale, such as ILWAS (Chen *et al.*, 1983) and NUCSAM (Chapter 2.1; Groenenberg *et al.*, 1995).

Models designed for regional predictions tend to be more simplified than site scale models to minimise input requirements. Simplification may involve (i) less detailed process formulations, (ii) reduce temporal resolution, for example using an

annual time resolution, thereby neglecting variability within a year of both model input and processes and (iii) reduced vertical resolution, by using a smaller number of soil compartments. These simplifications may cause errors in predictions. Seasonal variability is generally driven by climatic (e.g. precipitation, deposition, evaporation, snowmelt) and biotic factors (e.g. litterfall, mineralisation, nutrient uptake). Georgakakos *et al.* (1989) indicated that the neglect of such natural day-to-day variability, may significantly affect long-term predictions of lake alkalinity. Similarly, Warfvinge and Sandén (1992) showed that the long-term trend in soil solution ANC is affected by time resolution.

Another problem with long-term large scale (soil) acidification models is the lack of sufficient long-term (> 50 years) series of observations, which makes these models difficult to calibrate and validate. A thorough calibration and validation on short-term (< 10 years) series is hardly possible because these models do not account for seasonal variability which plays an important role in short-time data records. However, results of the long-term large scale models can be compared with results of more detailed models which are validated on relatively short-term data sets.

The objective of this study is to characterise the effect of model simplifications on soil solution response, with emphasis on the influence of temporal and vertical resolution. For that purpose, we compared the results derived with SMART2 (one soil layer, annual resolution), RESAM (multi-layer, annual resolution), and NUCSAM (multi-layer, daily resolution). The three models were first tested and validated using measured concentrations of an intensively monitored spruce site at Solling, Germany. At this site inputs, solute concentrations and solid phase element contents have been measured continuously for more than twenty years (1973-1990), along with plant physiological, hydrological, micrometeorological and soil biological monitoring programmes. Next, we characterise the effect of model simplification on long-term predictions of soil and soil solution response. The long-term simulations with the three models were performed for two atmospheric deposition scenarios over a 100-year period.

2.4.2 Models used

SMART2 is a one-layer model, whereas RESAM and NUCSAM distinguish a litter layer and several mineral soil layers. SMART2, RESAM and NUCSAM all simulate the major biogeochemical processes in the canopy, litter layer and mineral soil horizons. SMART2 was especially developed for the application on a national to the European scale. RESAM has been developed to analyse the long-term soil response to acid deposition on a regional scale. NUCSAM accounts for seasonal variation in deposition, precipitation, transpiration, litterfall, mineralisation and root uptake and all the biochemical and geochemical processes are modelled as a function of temperature, and is especially designed for application on a site-scale.

NUCSAM

NUCSAM (Chapter 2.1; Groenenberg *et al.*, 1995) includes hydrological processes, i.e. (i) partitioning of precipitation into rainfall and snowfall, (ii) snowpack accumulation and snowmelt, (iii) interception evaporation from the forest canopy and soil evaporation, (iv) transpiration and snowmelt, and (v) one-dimensional vertical transient water flow.

Water fluxes and soil water contents are calculated with an adapted version of the SWATRE (Belmans *et al.*, 1983) model, a finite difference solution to the Richard's equation. The adapted version includes an interception evaporation based on Gash (1979), a snow module and divides root uptake over the different soil layers according to a fixed root distribution (see Chapter 2.1).

The biogeochemical processes accounted for in NUCSAM are basically the same as used in RESAM except for mineralisation. In NUCSAM (i) litterfall, root decay, mineralisation and root uptake are distributed over the year by given monthly coefficients, (ii) both upwards and downwards solute transport is simulated and (iii) speciation of inorganic carbon is computed from known equilibrium equations. All chemical equilibrium and rate-limited equations are solved with a separate chemical equilibrium module EPIDIM (Rijtema *et al.*, 1999), which calculates aluminium complexation with organic and inorganic anions.

RESAM

RESAM (Chapter 2.2; De Vries *et al.*, 1995a) simulates all processes occurring the forest canopy, litter layer and mineral soil horizons which significantly influence the concentration of major ions in the soil solution. The model consists of a set of mass balance equations, kinetic equations and equilibrium equations. Mass balance equations describe the input-output relationship in each soil layer for all ions, except for H and HCO_3. The concentration is determined by the CO_2 equilibrium equation (cf. Chapter 2.2), whereas the H concentration is determined from the charge-balance. Model input includes atmospheric deposition and hydrological data.

The soil layers are considered as homogeneous compartments of constant density and the constituent input mixes completely within each soil layer. The time resolution is one year. However, the time-step of the model is one to five days to avoid numerical instability and to minimise numerical dispersion.

SMART2

The one-compartment soil acidification and nutrient cycling model SMART2 (Chapter 2.3; Kros *et al.*, 1995a,b), includes the major hydrological and biogeochemical processes in the vegetation, litter and mineral soil. Apart from pH, the model also predicts changes in aluminium (Al), divalent base cation (BC2, i.e. Ca+Mg), sodium (Na), potassium (K), nitrate (NO_3) and sulphate (SO_4) concentrations in the soil solution, and solid phase characteristics restricted to the acidification status, i.e. carbonate content, base saturation and amorphous Al precipitates. SMART2 was

developed from the dynamic soil acidification model SMART (De Vries *et al.*, 1989), by including a nutrient cycling and improving modelling of hydrology. The SMART2 model consists of a set of mass balance equations, describing the soil input-output relationships, and a set of equations describing the rate-limited and equilibrium soil processes.

Methodology

General Approach

To objectively compare differences in predictions by these three models differences in parameterisation must be minimised. Data for the models were derived from the Solling data set (Bredemeier *et al.*, 1995). Where the models used the same state variables and process parameters with the same vertical or temporal resolution, we simply used the same values for the three models. Parameters for SMART2 were derived by depth-averaging of the values which were used for RESAM and NUCSAM (input mapping: Rose *et al.*, 1991). Annual deposition and water fluxes, which are input to the model RESAM and SMART2, were derived by accumulating the daily NUCSAM values to annual values.

Vertical configuration and simulation period

At the Solling site NUCSAM and RESAM considered a litter layer of 7 cm (at the start of the simulations) and seven mineral soil layers to a depth of 90 cm (Table 1). For SMART2 two separate simulations were performed: (i) with a single mineral soil layer of 10 cm thickness and (ii) with a single layer of 90 cm thickness.

All models were run for the period 1971-1990. The period 1961-1970 was used as an initialisation period to estimate solute concentrations in 1970 and to equilibrate solute concentrations with exchangeable cations and adsorbed SO_4. During that period, amounts of exchangeable cations and adsorbed amounts of SO_4 were continuously updated while pools of cations in primary minerals and of Al in amorphous precipitates were kept constant.

Model adaptations

In regional applications, SMART2 and RESAM use annual average hydrological fluxes, which are kept constant throughout the simulation period in order to study focuses on the influence of differences in biogeochemical process descriptions and their vertical and temporal resolution (one day versus one year). SMART2 and RESAM were slightly adapted to account for variations in hydrological fluxes between the years.

The SMART2 model is normally applied to calculate concentrations at the bottom of the root zone. To apply the SMART2 model at shallow depth (10 cm), the calculation of N-immobilisation was slightly adapted. In the standard version of SMART2, N-immobilisation is supposed to occur in the upper 20 cm of the soil. For

the simulation of concentrations at 10 cm depth, the total N immobilisation flux was multiplied by the ratio of the amount of organic C in the considered layer and the amount up to 20 cm depth.

Model comparison

The modelled flux-weighted annual averaged concentrations by SMART2 and RESAM can not be directly compared with the monthly measured soil solution concentration. Possibilities to compare the results of the three models with observation data are comparing: (i) monthly observed concentrations with estimated monthly concentrations derived from RESAM and SMART2 output by linear interpolation between annual values, or (ii) estimated flux-weighted annual averaged measured concentrations (or leaching fluxes) with simulated values. Annual leaching fluxes can be obtained by multiplying measured monthly concentrations with monthly simulated water fluxes (see *Hydrological data*). Flux-weighted annual averaged concentrations were derived by dividing the 'measured' leaching flux by the annual water fluxes.

In this study, a combined approach was used: simulated concentrations were compared with measured concentrations (according to (i) and simulated cumulative annual leaching fluxes were compared with (calculated) measured annual leaching fluxes. A comparison of measured concentrations with simulated concentrations and cumulative fluxes gives a good impression of the performance of the models and the ability of the models to simulate trends and extreme values.

For a more objective comparison of the model outputs two statistical measures were calculated, i.e. the Normalised Mean Absolute Error (*NMAE*) and the Normalised Mean Error (*NME*) (cf. Janssen and Heuberger, 1995 and Chapter 2.1):

$$NMAE = \frac{\frac{1}{N} \sum_{i=1}^{N} |P_i - O_i|}{\overline{O_i}} \tag{1}$$

$$NME = \frac{\frac{1}{N} \sum_{i=1}^{N} (O_i - P_i)}{\overline{O_i}} \tag{2}$$

where P_i is the modelled value, O_i is the observed value, $\overline{O}$ is the average of the observations, and N is the number of observations. *NMAE* quantifies the average deviation between model prediction and measurements. *NME* indicates of the tendency of the model to underestimate (positive value) or overestimate (negative value) the observation data. *NMAE* and *NME* for the three models were calculated using monthly concentrations for model results and measurements.

Model input data

Hydrological data

For all models hydrological fluxes and water contents were calculated by an adapted version of the SWATRE model (cf. Chapter 2.1). Drainage fluxes, root uptake fluxes and water contents from SWATRE were directly used by NUCSAM. For RESAM and SMART2 annual root uptake fluxes were derived by accumulating the daily root uptake fluxes to annual values. To keep water contents constant throughout the simulation period, annual drainage fluxes were calculated by subtracting the root uptake fluxes from the input flux for each layer. For RESAM, water contents for each layer were averaged over the simulation period. The data for SMART2 were derived by depth averaging the water contents that were used for RESAM. An overview of the main hydrological fluxes and water contents is given in Table 1.

Table 1 Average drainage fluxes and water contents used in NUCSAM, RESAM and SMART2

Layer (cm)	Average drainage flux (cm a^{-1})		Average soil water content (m^3 m^{-3})	
	NUCSAM/RESAM	SMART2	NUCSAM/RESAM	SMART2
0-10	73.6	73.6	0.40	0.40
10-20	70.1	-	0.39	-
20-30	64.0	-	0.36	-
30-40	55.7	-	0.36	-
40-60	47.7	-	0.37	-
60-80	43.0	-	0.34	-
80-90 [1]	41.0	41.0	0.34	0.36

[1] SMART2 soil layer 0-90 cm

Biological data

An overview of the biological data and their derivation is given in Table 2. The parameters for N cycling in NUCSAM/RESAM and SMART2 were derived independently from the Solling data set as the process description in the models is different. RESAM/NUCSAM use an overall nitrification rate, which is reduced by moisture content, pH and organic matter content. For SMART2 separate nitrification fractions, based on input-output budgets, were derived for the run with the 10 cm soil layer and the run with the 90 cm soil layer. The relationship between moisture content, pH, organic matter content and nitrification rate, which was used in NUCSAM/RESAM was not calibrated on the site data.

Table 2 Values for soil layer independent model parameters used in the simulation based on the Solling data set (Bredemeier *et al.*, 1995)

Process	Parameter	Unit	Value	Model
Foliar uptake[a]	$fr\,NH_{4,fu}$	-	0.11	NUCSAM, RESAM
	$fr\,H_{fu}$	-	0.33	NUCSAM, RESAM
Foliar exudation[a]	$fr\,Ca_{fe}$	-	0.49	NUCSAM, RESAM
	$fr\,Mg_{fe}$	-	0.09	NUCSAM, RESAM
	$fr\,K_{fe}$	-	0.42	NUCSAM, RESAM
	$fr\,BC2_{fe}$	-	0.58	SMART2
Tree growth[b]	k_{rgrl}	a^{-1}	0.10	NUCSAM, RESAM, SMART2
	A_{stmax}	kg ha^{-1}	3.8x10^5	NUCSAM, RESAM, SMART2
	t_{05}	a	69.2	NUCSAM, RESAM, SMART2
Litterfall[c]	k_{lf}	a^{-1}	0.19	NUCSAM, RESAM
Root decay	kr_{rd}	a^{-1}	1.4	NUCSAM, RESAM
Nutrient cycling factor	ncf	-	0.5	SMART2 [d]
Root uptake pattern	ru_{exp}	-	6.58	SMART2 [e]
Mineralisation	$fr_{mi\,fl}$		0.4	NUCSAM, RESAM, SMART2
	$k_{mi\,lt}$		0.05	NUCSAM, RESAM, SMART2
Nitrification[f]	$k_{ni,mx}$	a^{-1}	100.0	NUCSAM, RESAM
	$fr_{ni,mx}$	-	4.5	SMART2
Denitrification[g]	$k_{de.mx}$	a^{-1}	10.0	NUCSAM, RESAM
	fr_{de}	-	0.10	SMART2
N immobilisation[h]	C/N	-	19.5	SMART2

[a] Based on average throughfall and deposition data over the period 1974-1990
[b] Derived by curve fitting of the biomass measurements, which were corrected for thinning (62.9%).
[c] Average needlefall rate over the period 1967-1973, taking into account that 92.5% of the litterfall is needlefall
[d] *ncf* refers to the ratio of root decay to litterfall (see Chapter 2.3). This ratio was derived from the annual average root decay (1.49) to litterfall (2.96) in Solling
[e] *ru$_{exp}$* refers to the exponent determine the water and nutrient uptake pattern in SMART2 (see Chapter 2.3). This ratio was derived by assuming that 50%.of the nutrient uptake take place in the top 10 cm of the soil profile.
[f] *k$_{ni,max}$* is derived from average throughfall and mineralisation fluxes over the period 1970-1985, assuming that all mineralised N is released as NH$_4$. *fr$_{ni}$* is derived form average throughfall and average drainage fluxes and calculated average root uptake fluxes for the period 1973–1990
[g] Derived from De Vries *et al.* (1995a).
[h] Based on 1973 data for C$_{org}$ and N$_{org}$

Growth uptake in all three models was calculated by multiplying a given (logistic) growth rate (see Chapter 2.1, 2.2 and 2.3) by the element content in 1968 in stems and branches respectively. N content is calculated with a linear relationship between N content and N deposition. N content is minimal at a N deposition of 1500 mol$_c$ ha^{-1} a^{-1} and maximal at a N deposition of 7000 mol$_c$ ha^{-1} a^{-1}. Element contents of other nutrients were assumed to remain constant. Growth uptake fluxes in SMART2 at 10 cm depth were automatically generated in the model by the depth dependent root uptake function (see Chapter 2.3). This root uptake function is calibrated such that 50% of the nutrients are taken up in the upper 10 cm of the soil profile. Parameters related to forest growth were kept constant, the stand remains a mature forest with a very low net growth and a relatively high nutrient cycling

throughout the simulation period. The monthly distribution fractions for litterfall, root decay, mineralisation and root uptake as used in NUCSAM are given in Table 3. In RESAM and SMART2 these fractions were equally distributed over the year.

Table 3 Monthly distribution fractions (-) for litterfall (*lf*), root decay (*rd*), mineralisation (*mi*) and root uptake (*ru*) as used in NUCSAM

Month	*lf*	*rd*	*mi*	*ru*
January	0.00	0.00	0.00	0.01
February	0.00	0.00	0.00	0.01
March	0.00	0.00	0.10	0.05
April	0.00	0.00	0.15	0.08
May	0.10	0.10	0.15	0.15
June	0.10	0.10	0.20	0.15
July	0.10	0.10	0.20	0.15
August	0.10	0.10	0.15	0.15
September	0.20	0.20	0.05	0.10
October	0.20	0.20	0.00	0.09
November	0.10	0.10	0.00	0.05
December	0.10	0.10	0.00	0.01

Geochemical data

NUCSAM and RESAM

Geochemical data for NUCSAM and RESAM as given in Table 4 to Table 6, were directly derived from the Solling data set (Bredemeier *et al.*, 1995). Gaines-Thomas exchange constants (for all three models) were based on average soil solution concentrations measurements in 1983 and solid phase analyses in the same year (Table 6). Sulphate adsorption constants for NUCSAM and RESAM (Table 6) were derived from data in Meiwes (1979).

Table 4 Soil properties used for NUCSAM, RESAM and SMART2. Bulk density (ϱ), cation exchange capacity (*CEC*), amorphous Al (hydr)oxide content ($ctAl_{ox}$) and sulphate sorption capacity (*SSC*)

Soil layer (cm)	ϱ (kg m^{-3})	CEC (mmol$_c$ kg^{-1})	$ctAl_{ox}$ (mmol$_c$ kg^{-1})	*SSC* (mmol$_c$ kg^{-1})
NUCSAM and RESAM				
0-10	930	132	97	1.0
10-20	1140	79	97	4.5
20-30	1190	58	185	4.5
30-40	1390	45	185	4.5
40-60	1390	56	185	4.5
60-80	1690	56	176	6.7
80-90	1690	76	94	6.7
SMART2				
0-10	930	132	97	1.0
0-90	1389	66	156	5.1

Weathering fluxes of primary minerals in NUCSAM and RESAM were described by a first-order equation (see Chapter 2.1 and 2.2). Rate constants for this equation (Table 5) were derived from a budget study (Wesselink *et al.*, 1994). Dissolution parameters of Al-hydroxides (Elovich equation; see Chapter 2.1) in RESAM and NUCSAM, are given in Table 5 together with their derivation.

SMART2

Most data for SMART2 were derived by depth averaging the data that were used for NUCSAM and RESAM (Table 5 and Table 6). Some parameters that were only used in SMART2 were directly obtained from the Solling data set. Soil properties which were used in SMART2, i.e. bulk density (ρ), cation exchange capacity (*CEC*), sulphate sorption capacity (*SSC*), amorphous Al (hydr)oxide content (*ctAl$_{ox}$*) (Table 4) were derived by depth averaging the data used in NUCSAM and RESAM (Table 4). To calculate Gaines-Thomas exchange constants for SMART2 (Table 6) concentrations and solid phase analyses were depth averaged for the 10 cm and 90 cm soil compartment. A depth weighted sulphate adsorption constant for SMART2 was derived in three steps. First adsorbed amounts of sulphur were calculated for all layers, considered in NUCSAM/RESAM, using a Langmuir equation (see Chapter 2.1, Eq. 67) and the sulphate adsorption constants from Meiwes (1979), assumed the same range in dissolved SO$_4$ concentrations with depth. Next, the calculated adsorbed amounts were depth-weighted. Finally, the depth-weighted sulphate adsorption constant was derived by fitting the depth-weighted adsorbed SO$_4$ amounts against the SO$_4$ concentration range.

Table 5 Weathering rate constants of amorphous Al (hydr)oxides and primary minerals used in the simulation by NUCSAM and RESAM

Layer (cm)	$krEl_1$ [1] (m^3 kg^{-1} a^{-1})	$krEl_2$ [2] (kg mol$_c^{-1}$)	KAl_{ox} [3] (l^2 mol^{-2})	Weathering rate constants [4] (10^{-3} a^{-1})			
				Ca	Mg	K	Na
0-10	0.6 x10^{-7}	750	3.5×10^8	6.5	93.6	0.011	0.021
10-20	2.0 x10^{-7}	750	3.5×10^8	6.0	73.2	0.008	0.015
20-30	5.1 x10^{-7}	750	3.5×10^8	5.6	66.9	0.007	0.013
30-40	5.1 x10^{-7}	750	3.5×10^8	5.4	63.7	0.006	0.010
40-60	5.1 x10^{-7}	750	3.5×10^8	5.3	61.8	0.005	0.011
60-80	5.1 x10^{-7}	750	3.5×10^8	6.2	51.7	0.005	0.011
80-90	5.1 x10^{-7}	750	3.5×10^8	10.9	25.8	0.003	0.011

[1] Elovich constant, see Eq. (33), Chapter 2.1. Derived from average soil solution concentrations of H and Al in 1983, assuming KAl_{ox}=3.5x10^8 and $krEl_2$=7.5x10^{-2}.

[2] Elovich constant, see Eq. (33), Chapter 2.1. The average of values given in De Vries (1994).

[3] Al (hydr)oxide equilibrium constant, see Eq. (37), Chapter 2.1. Average IAP for Al(OH)$_3$ at 90 cm over the period 1973-1991. The value given, is the value at 25 ^{o}C, which is derived from the value at field temperature (10 ^{o}C).

[4] Based on total analysis and weathering fluxes of base cations from Wesselink *et al.* (1994) and average H concentration in 1983.

Table 6 Gaines-Thomas exchange constants and SO_4 sorption constants used in the simulation by NUCSAM and RESAM

Soil layer (cm)	Exchange constants [1] $(mol\ l^{-1})^z\ x^{-2}$						KSO_{4ad} [2] $(l\ mol^{-1})$
	H	Al	Mg	K	Na	NH_4	
0-10	5180	0.97	1.60	647	8.4	1.05	0.5×10^{-3}
10-20	57.5	26.2	2.56	3660	29.1	6.53	7.6×10^3
20-30	15.3	8.75	65.3	7470	21.2	30.7	1.5×10^3
30-40	15.3	7.37	0.42	18700	32.0	30.7	1.5×10^3
40-60	15.3	7.37	1.25	16900	36.2	30.7	2.4×10^3
60-80	15.3	26.2	1.25	16900	36.2	30.7	2.4×10^3
80-90	15.3	26.2	1.25	16900	36.2	30.7	2.4×10^3

[1] Based on average soil solution concentration measurements in 1983 and solid phase analyses in the same year except for NH_4 which is taken from De Vries *et al.* (1995a)

[2] Derived from Meiwes (1979).

In SMART2 weathering fluxes are input to the model and were directly derived from the above mentioned budget study (Table 7) and dissolution of Al-hydroxide was described by equilibrium with an Al-hydroxide. Solubility products for the Al-hydroxide at 10 and 90 cm depth were derived from average soil solution concentrations of H and Al in 1983 at these depths. The solubility product for Al-hydroxide at 90 cm depth was also used in RESAM and NUCSAM to calculate the Al concentration at equilibrium.

Table 7 Geochemical parameters for SMART2

Parameter	Unit	Values	
		10 cm	90 cm
KAl_{ox} [1]	$l^2\ mol^{-2}$	4.0×10^7	2.0×10^9
$FBC2_{we}$ [2]	$mol_c\ m^{-3}\ a^{-1}$	0.039	0.043
$FBC1_{we}$ [2]	$mol_c\ m^{-3}\ a^{-1}$	0.011	0.012
KAl_{ex}	$l\ mol^{-1}$	0.7	3.5
KH_{ex}	$mol\ l^{-1}$	4786	1862
KSO_{4ad}	$l\ mol^{-1}$	4.2×10^3	3.9×10^3

[1] Average IAP for $Al(OH)_3$ at 10 and 90 cm based on measured Al and H concentrations in the period 1973-1990

[2] For 10 cm based on NUCSAM weathering rates and average H concentrations at 10 cm depth for the period 1973-1990, for 90 cm depth directly based on weathering fluxes from Wesselink *et al.* (1994)

Deposition data and scenarios

For the deposition during the observation period 1973-1990 we used yearly values for wet and dry deposition as described in Bredemeier *et al.* (1995).

For the long-term application of the three models, we used two atmospheric deposition scenarios for the period 1990-2090, i.e. (i) *Business as Usual* (*BU*): deposition values from the Solling data set in 1990 were kept unchanged for the period 1990-2090; (ii) *Improved Environment* (*IE*): deposition of SO_x, NO_x and NH_x were reduced linearly with time between 1990 and 2000 by 75% and kept constant afterwards. For all other constituents the values of 1990 were kept constant, except for H, which is calculated from the charge balance. The values for the total deposition fluxes (in mol_c $ha^{-1}\ a^{-1}$) used for 1990 were: 1473 for NH_4, 1410 for NO_3 and 3641 for SO_4. For base

cations and Cl the total deposition fluxes were 458 for Ca, 344 for Mg, 44 for K, 875 for Na and 1052 for Cl.

2.4.3 Results and discussion

Validation and testing

To characterise the effects of differences in the models, the simulated concentrations and leaching fluxes were compared with measured concentrations and leaching fluxes in the topsoil (10 cm) and subsoil (90 cm) for SO_4, Cl, NO_3, NH_4, Al and BC2 (divalent base cations). Simulated and measured concentrations are shown in Figure 1 (SO_4 and Cl), Figure 2 (NO_3 and NH_4) and Figure 3 (Al and BC2). An overview of the statistical measures, *NMAE* and *NME*, for the various substances in topsoil and subsoil is given in Table 8. All models simulated the measured concentrations reasonably well. Differences between the output of the models SMART2, RESAM and NUCSAM were rather small. A notable difference occurred for the SO_4 concentration in the subsoil. During the first five years SMART2 clearly performed less than RESAM and NUCSAM, whereas during the period 1980-1985 the opposite is true. Another remarkable result from the performance measures (Table 8) is that SMART2 showed in most cases the lowest values for both *NMAE* and *NME* (i.e. the best performance), whereas NUCSAM showed the highest values (i.e. the worse performance). A more detailed discussion on the performance of the models to simulate the individual ions is held in the following sections where the influence of the model differences is presented.

Table 8 Normalised Mean Absolute Error (*NMAE*) and Normalised Mean Error (*NME*) for simulated concentrations

Component	Depth	*NMAE*			*NME*		
		SMART2	RESAM	NUCSAM	SMART2	RESAM	NUCSAM
SO_4	10	0.25	0.24	0.37	0.17	0.05	-0.01
	90	0.29	0.24	0.25	0.06	0.12	0.18
NO_3	10	0.49	0.50	0.62	0.19	0.09	-0.04
	90	0.53	0.63	0.76	0.23	0.36	-0.25
NH_4	10	1.6	6.0	5.0	-0.26	-6.0	-4.9
	90	1.0	0.93	0.88	0.99	0.93	0.80
BC2	10	0.29	0.25	0.41	0.03	0.21	-0.21
	90	0.29	0.16	0.46	-0.23	0.02	-0.43
Al	10	0.33	0.33	0.52	0.32	0.12	0.02
	90	0.34	0.37	0.33	0.19	0.34	0.30
H	10	0.47	0.47	0.53	0.47	0.45	0.51
	90	0.40	0.49	0.49	0.36	0.48	0.47
Cl	10	0.26	0.28	0.41	0.11	0.03	-0.04
	90	0.25	0.16	0.23	0.06	0.06	0.16

Influence of vertical resolution

The influence of vertical resolution is best illustrated by the SO_4 concentrations and leaching fluxes (Figure 1), as deposition and adsorption of SO_4, was described in all

models in practically the same way. The trends in SO_4 concentrations, as simulated by NUCSAM and RESAM, were generally in good agreement with the observation data. SMART2, however, overestimated SO_4 concentrations at 90 cm depth from 1972-1978, during that period a strong rise in SO_4 concentrations took place at this depth. This overestimation is caused by a larger dispersion of the SO_4 front in a one-layer system compared to a multi-layer system. In a multi-layer system elevated atmospheric input of SO_4 initially stores the absorbed SO_4 in the upper soil layers only. In a one-layer system, elevated input immediately leads to a (small) rise in the absorbed amounts and concentrations for the whole soil profile. Although concentrations were overestimated by SMART2 in the subsoil, from 1973-1975, the performances for SO_4 in both layers for the whole trajectory were comparable with the other multi-layer models. SMART2 even showed the lowest value for the *NME* (Table 8). Cumulative leaching fluxes for SO_4 and Cl at 10 cm depth were simulated rather well. Leaching fluxes at 90 cm were slightly overestimated for Cl by all three models and slightly underestimated for SO_4 by RESAM and NUCSAM.

As a result of the smoothed SO_4 front, the rise in Al due to weathering in the period 1972-1978 is less pronounced in SMART2. This causes a lower exchange of adsorbed base cations against Al compared to the other models. This lower BC2 desorption in turn leads to a lower rise of the BC2 concentrations in the subsoil, as simulated by SMART2 (see Figure 3).

Influence of process description

The main differences in process description between the models occur in the description of processes involving the nitrogen dynamics. All three models account for storage of N in the litter layer and for mineralisation. However, SMART2 and RESAM only made a distinct between old and fresh litter, whereas NUCSAM includes a three compartment model (see Chapter 2.1). Furthermore, (de)nitrification in SMART2 is described in a different way than it is in RESAM and NUCSAM.

Nevertheless comparable results for the NO_3 concentrations in both soil layers were obtained (Figure 2). This is confirmed by the *NMAE* and NME (see Table 8). The NH_4 concentrations in the topsoil (Figure 2) were clearly overestimated by NUCSAM and RESAM (*NME* < 0), whereas SMART2 underestimate this concentration. In the subsoil, all models simulated comparable NH_4 concentrations, which were underestimated with respect to the measurements (see *NME* values, Table 8). The relatively good agreement between observed and simulated concentrations with SMART2 in the topsoil, is partly due to the fact that in SMART2 different nitrification constants at 10 and 90 cm depth were used, which were directly derived from the Solling data set. RESAM and NUCSAM, however, used one overall nitrification parameter.
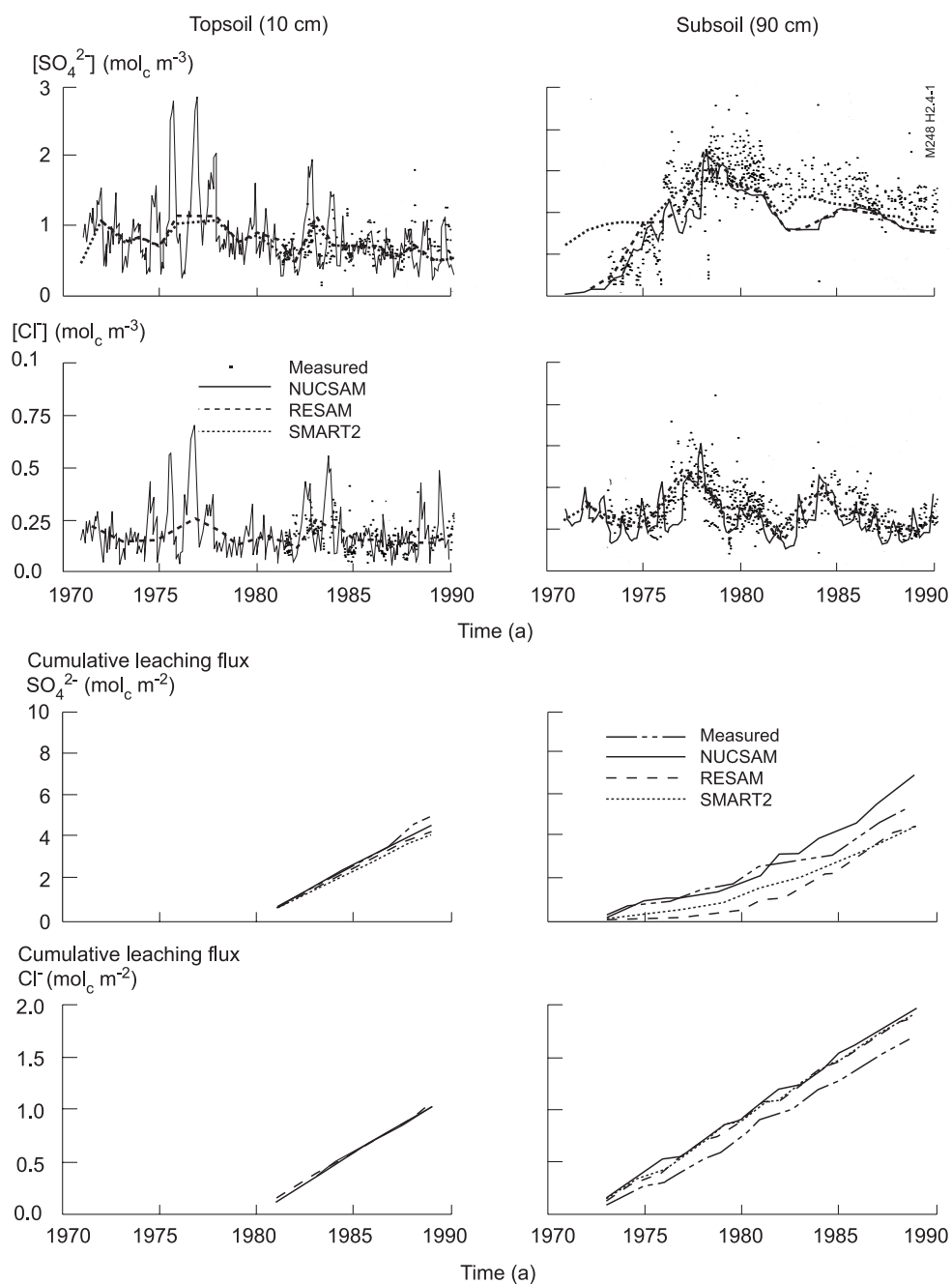
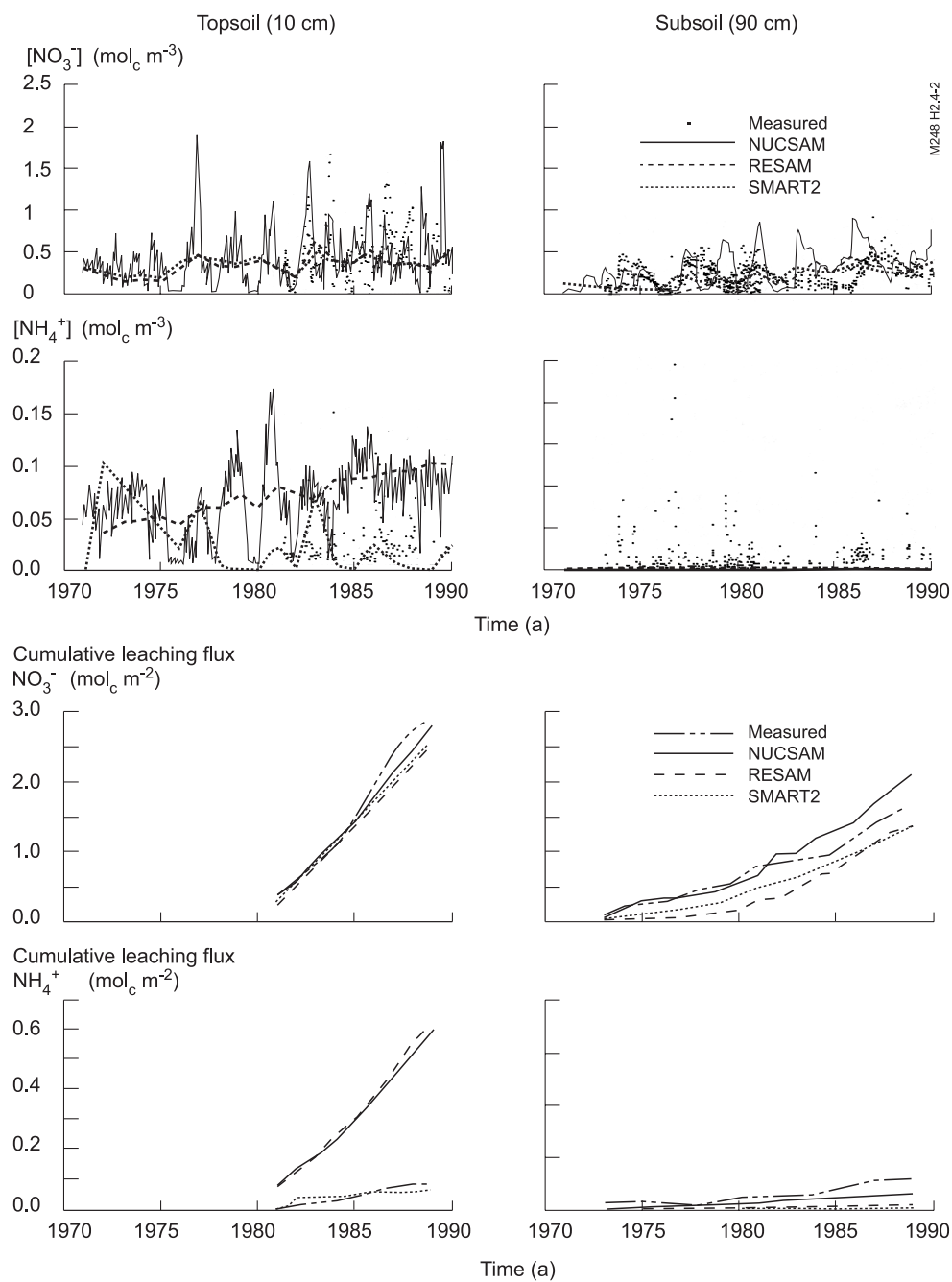Figure 1 Measured and simulated SO₄ and Cl concentrations and leaching fluxes at 10 (left) and 90 cm depth (right)

Figure 2 Measured and simulated NO₃ and NH₄ concentrations and leaching fluxes at 10 (left) and 90 cm depth

Another difference between SMART2 and RESAM/NUCSAM is the way in which Al concentrations are calculated. SMART2 assumes equilibrium with Al-hydroxide, whereas RESAM and NUCSAM use a kinetic description (see Chapter 2.1 and 2.2). Figure 3 shows that results for the simulation of Al (main cation) were comparable with those for the main anion SO_4. The way in which Al concentrations were calculated appears to have hardly any influence on the results for the chosen period, both in the topsoil and the subsoil. In long-term predictions NUCSAM/RESAM and SMART2 may give different Al concentrations, particularly in the topsoil where the dissolved Al is far from equilibrium with gibbsite. Exhaustion of solid Al-compounds, will lead to a lower simulated Al concentration by NUCSAM/RESAM, whereas that simulated by SMART2 will remain constant. This effect, however, does not occur in this case, see Figure 4.

Influence of temporal resolution

The influence of neglecting seasonal fluctuations on solute fluxes can best be identified by comparing RESAM and NUCSAM, models with a comparable process description and a difference in temporal resolution. The most direct influence of the chosen temporal resolution is on Cl concentrations and fluxes. For example, NUCSAM with daily up- and downward water fluxes gives stronger fluctuations in concentrations than RESAM (Figure 1). *NMAE* values for the Cl concentrations, however, showed that the simulation of the Cl concentrations by NUCSAM was not better than for the other models. In the topsoil, the simulated fluctuation of the Cl concentration was sometimes out of phase with the measured fluctuation. In the subsoil, NUCSAM underestimated Cl concentrations in wet periods (Table 8).

The influence of the chosen temporal resolution can particularly strong for the NO_3, NH_4 and base cations concentrations, which are strongly influenced by seasonal processes as nutrient uptake and mineralisation. NO_3 concentrations (Figure 2, Table 8) simulated with NUCSAM and RESAM were in close agreement with the measurements in the topsoil. Although, NUCSAM simulated the seasonal peaks in NO_3 concentrations *NMAE* values in the topsoil were somewhat higher for NUCSAM compared to RESAM. NO_3 concentrations in the subsoil were poorly simulated by RESAM up to 1980. From 1980 onwards concentrations simulated by NUCSAM and RESAM were in the same range as measured values (relatively low *NMAE* and *NME*). However, fluctuations in simulated concentrations by NUCSAM occurred more frequent than the measured multi-year fluctuations in concentrations. The differences in simulated NO_3 concentrations in the subsoil, between NUCSAM and RESAM is caused by the fact that in NUCSAM total N uptake is lower. N uptake in NUCSAM is lower due to a restriction of the N uptake to the growing-season, which leads in certain years to a higher N demand than available in the soil solution, causing a lower total N uptake in that year.

Cumulative leaching fluxes for NO_3 in the topsoil (Figure 2) were in close agreement with measured leaching fluxes both for NUCSAM and RESAM. Cumulative leaching fluxes in the subsoil, were underestimated (-0.3 mol_c m^{-2}) by RESAM, due to the underestimation of the concentrations (positive *NME*) in the period up to 1980

and overestimated ($+0.4$ mol$_c$ m^{-2}) by NUCSAM due to the overestimation of seasonal peak concentrations (negative *NME*).

The correspondence between simulated and measured NH$_4$ concentrations (Figure 2) was poor for RESAM and NUCSAM. The periodical fluctuations in concentrations in the subsoil were not simulated by NUCSAM and in general NH$_4$ concentrations were overestimated in the topsoil. Although, both measured and simulated NH$_4$ concentrations were relatively low, the deviation between measured and simulated values leads to a serious overestimation (about 0.5 mol$_c$ m^{-2}) in the period 1983 to 1989.
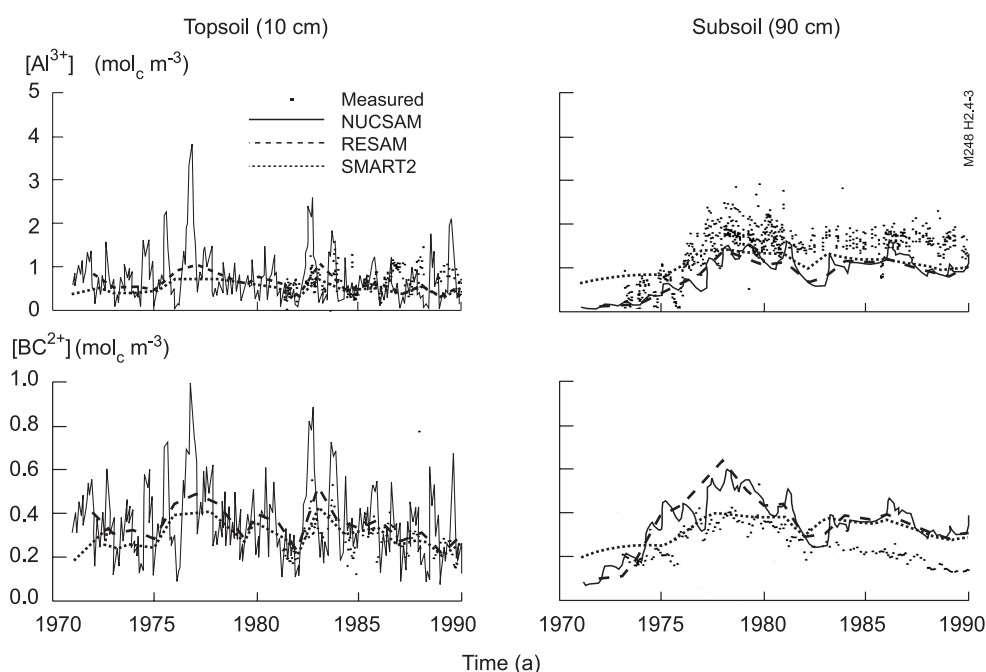
Figure 3 Measured and simulated Al and BC2 concentrations at 10 (left) and 90 cm depth (right)

Base cation concentrations (Figure 3) are influenced both by processes with a strong seasonal magnitude, such as mineralisation, solute transport and ion-exchange. The general trend in divalent base cation concentrations in the topsoil was reasonably simulated both by NUCSAM and RESAM. NUCSAM and RESAM overestimated the rise in BC2 concentrations in the subsoil up to 1978. From 1982 onwards all models overestimated BC2 concentrations, probably due to an underestimation of tree growth during this period. RESAM produced a somewhat stronger rise and fall in BC2 concentrations in the subsoil than NUCSAM. This is caused by a stronger desorption of BC2 in RESAM. The same phenomenon, can be observed for SO$_4$, albeit to a lesser extent (Figure 1). RESAM simulated slightly higher SO$_4$ concentrations than NUCSAM from 1975-1980. The deviation between RESAM and NUCSAM is induced by slight

differences in hydrology as reflected by the differences in simulated Cl concentrations in the subsoil.

Long-term predictions with NUCSAM, RESAM and SMART2

Model performance using annual average concentrations

Contrary to the *Validation and testing* section, we quantified the long-term model performance by comparing the flux-weighted annual averaged simulated concentrations with the corresponded observed ones. Figure 4 presents the long-term flux-weighted annual average concentrations as simulated by the three models for the *Business as Usual (BU)* scenario. Results for the *Improved Environment (IE)* scenario are given in Figure 5. Figure 4 and Figure 5 also include the observed flux-weighted annual average values. These values were calculated from the observed concentrations which were weighted with simulated soil waterfluxes that correspond with the period between the current and previous sampling date.

Regarding the performance of the three models to simulate the observed concentrations and ratio in terms of the *NMAE* (Table 9), we can conclude that the results for all models are quit comparable. Notable exceptions are, however, the Al/BC ratio at 10 cm and the SO_4 concentration at 10 cm for SMART2 and the NO_3 concentration at 90 cm for NUCSAM. Inspecting the individual values of the *NMAE* (the closer to zero the better the predictions), results appeared to be good (*NMAE* ≤ 0.30) for the SO_4 concentrations in the topsoil and subsoil and the Al concentration in the subsoil for all models, for the NO_3 concentration in the topsoil for NUCSAM, and for the Al concentration in the topsoil for RESAM, moderate (0.30 < *NMAE* < 0.60) for the NO_3 concentration in the topsoil and subsoil for SMART2 and RESAM, and the Al concentration in the topsoil for SMART2, and bad (*NMAE* ≥ 0.60) for the NO_3 concentration in the subsoil for NUCSAM and the Al/BC2 ratio in the topsoil and subsoil for all models.

Concerning the performance of the model SMART2, Table 9 shows that for the SO_4, NO_3 and Al concentrations in the subsoil the performance is always either better than RESAM or better NUCSAM. The performance of SMART2 for these concentration in the topsoil is always less than the performance of RESAM and NUCSAM, although the deviations were small. For the Al/BC2 ratio the performance of SMART2 is always the poorest. However, RESAM and NUCSAM also showed a rather poor performance, which is not much better than that of SMART2. The bad performance of this compound model output was due to an overestimation of the Al concentration and an underestimation of the BC2 concentration (see Figure 3).

Also from this comparison based on the annual average concentration, it can be concluded that the performance of the regional scale model SMART2 yield to comparable performance as obtained for the models RESAM and NUCSAM. This is an important result, since the annual average concentration is usually the temporal aggregation level used in national assessments by the Environmental and Nature Policy Assessment Office.

133

Table 9 Performance of the two models during the observation period expressed as the Normalised Mean Absolute Error (*NMAE*)

	NMAE							
	SO$_4$		NO$_3$		Al		Al/BC2	
	10 cm	90 cm	10 cm	90 cm	10 cm	90 cm	10 cm	90 cm
NUCSAM	0.16	0.15	0.26	0.70	0.30	0.21	4.0	12.7
RESAM	0.14	0.10	0.32	0.57	0.21	0.25	3.9	13.2
SMART2	0.26	0.11	0.38	0.39	0.36	0.24	4.2	21.2

Scenario analysis

General features

Under the *BU* scenario (Figure 4) the Al concentration gradually increased in the subsoil. In the topsoil, however, Al concentration decreased. This is due to a depletion of the Al hydroxide pool in topsoil. As a result of the depletion of the Al hydroxide pool, which highly determines the buffer capacity, the pH decreased (cf. De Vries *et al.*, 1994a). Under the *IE* scenario, the Al concentration (Figure 5) strongly decreased in both the topsoil and subsoil, due to deposition reductions.

Under the *IE* scenario SO$_4$ and NO$_3$ strongly decreased in response to the decrease in atmospheric deposition. Due to SO$_4$ desorption and N mobilisation from the humus, there was a retardation in the concentration response, especially in the subsoil. Afterward, the SO$_4$ and NO$_3$ concentrations showed a constant level for both scenarios.

The molar Al/BC2 ratio in the topsoil showed a similar trend as the Al concentration. For both scenarios the molar Al/BC2 ratio decreased below 2, i.e. the critical value for spruce forest. Under the *BU* scenario this decrease was accompanied by a decrease in pH due to depletion of Al (hydr)oxides, and the pH buffering it provides. In the subsoil the Al/BC2 ratio gradually increased with the *BU* scenario. Under the *IE* scenario the Al/BC2 ratio initially showed a delayed response to the decrease in deposition. The delay time for the multi-layer models, RESAM and NUCSAM, was considerably shorter than for the single-layer model SMART2.

Differences between SMART2, RESAM and NUCSAM predictions

The agreement between flux weighted annual averaged concentration simulated by SMART2, RESAM and NUCSAM, was generally good for all presented constituents. The most remarkable difference between the two model results was that the NUCSAM outputs strongly fluctuating while the SMART2 and RESAM outputs were smoothed. This is, of course, inherent to the temporal resolution of the models; daily based versus annual average based. From 1970-1990, however, the SMART2 and RESAM results also showed a slightly fluctuating behaviour, which was caused by using the measured yearly values for deposition during this period.
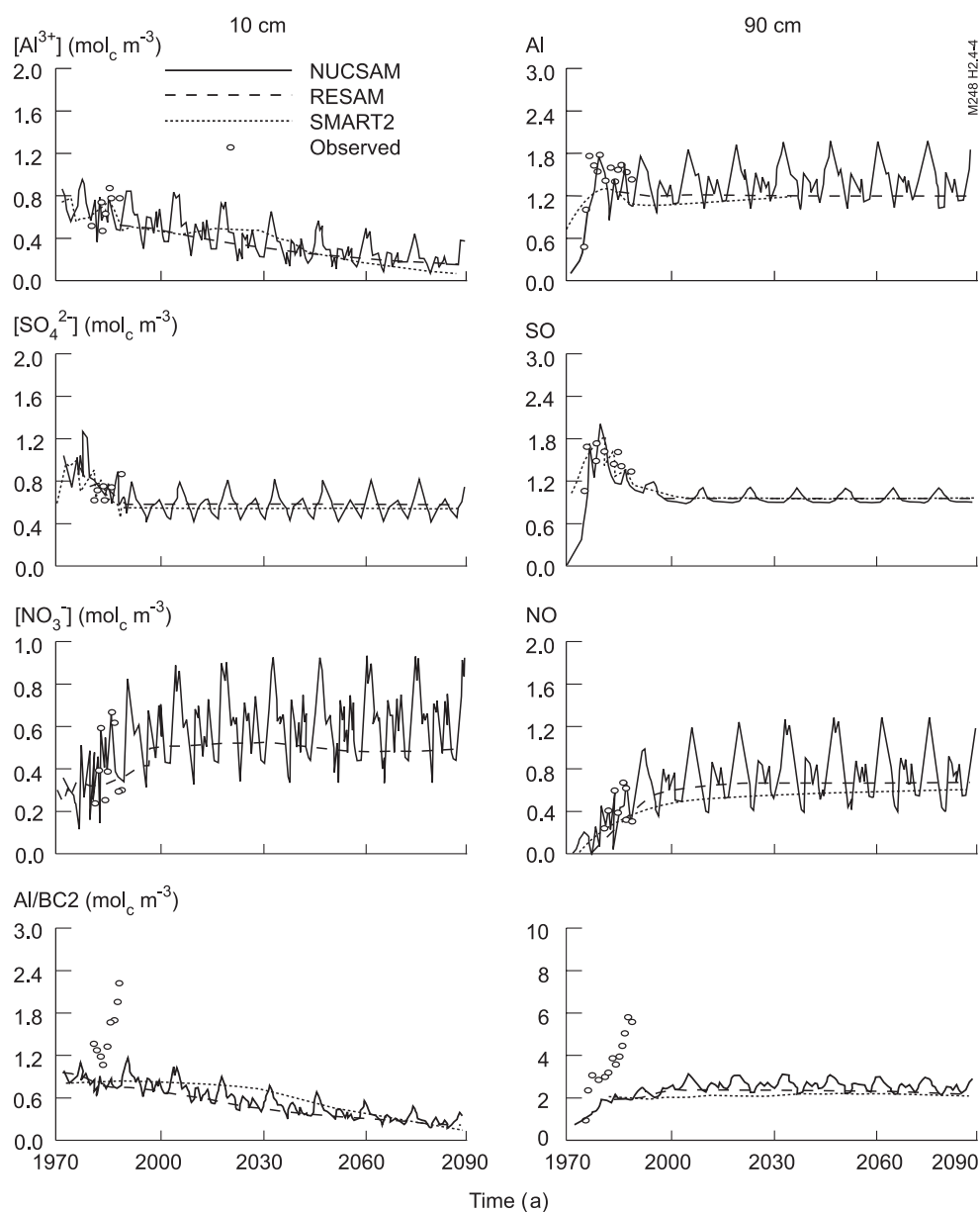
Figure 4 Flux-weighted annual averaged concentrations simulated with NUCSAM, RESAM and SMART2 of the concentrations of SO₄, NO₃, Al and the Al/BC2 ratio at 10 cm (left-hand side) and 90 cm (right-hand side) depth, under the *Business as Usual* scenario. The observed flux-weighted annual averaged concentrations are also given

135
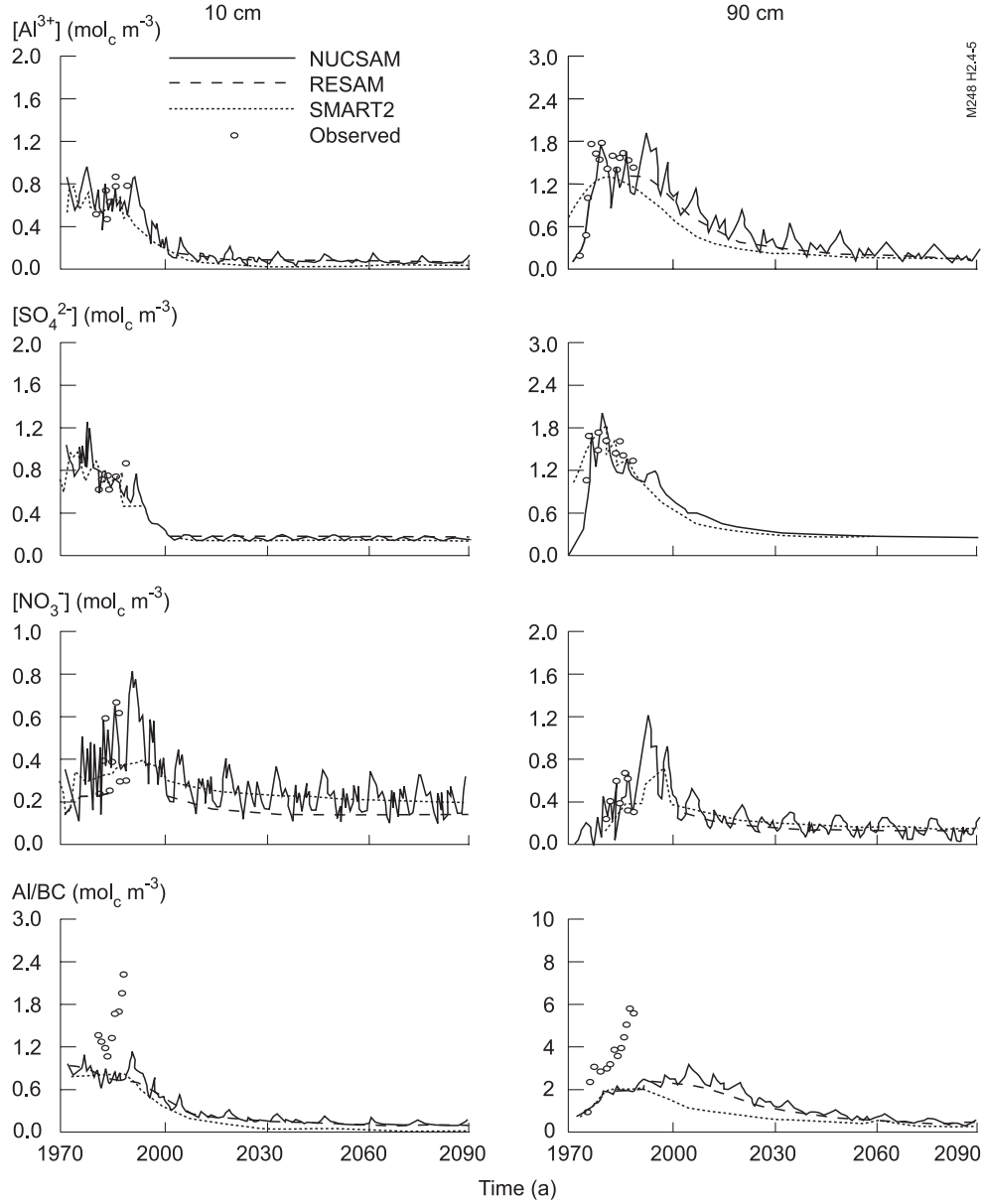
Figure 5 Flux-weighted annual averaged concentrations simulated with NUCSAM, RESAM and SMART2 of the concentrations of SO₄, NO₃, Al, and Al/BC2 ratio at 10 cm (left-hand side) and 90 cm (right-hand side) depth, under the *Improved Environment* scenario. The observed flux-weighted annual averaged concentrations are also given.

Comparing the NUCSAM results for the two scenarios in general, it was striking that seasonal variability under the *IE* scenario was much smaller than under the *BU* scenario. This especially holds for the SO₄ concentration in the subsoil, where

eventually all seasonal variability ceased. To a lesser extent this also happened for the SO_4 concentration in the topsoil and the Al concentration and the Al/BC2 ratio in both considered soil layers. This was caused by the relative increase in importance of SO_4 sorption and cation exchange at lower concentration levels, resulting in a stronger buffering of concentrations. This also explained that the seasonal variability of NO_3 was the same for both scenarios, which is difficult to see in Figure 4 and Figure 5. However, this was checked by normalising the NUCSAM concentrations by dividing them by the concentrations calculated with RESAM, which showed clearly that the seasonal variability under both scenarios was comparable.

The long-term trends show that the models produce very similar trends for both scenarios. For most model outputs the NUCSAM results fluctuating around the SMART2 and RESAM results. A notable exception is the Al/BC2 ratio in the subsoil under the *IE* scenario. The SMART2 simulated a much quicker response of the Al/BC2 ratio to the deposition reduction than the models RESAM and NUCSAM. To a lesser extend this is also true for the SO_4 and Al concentration. Again, this difference in time-delay is due to the difference in considered soil layers. Figure 5 clearly shows that the differences vanished several decades after the deposition reached a new constant level, i.e. the year 2000 (see Section *Deposition data and scenarios*).

Cumulative leaching fluxes

Cumulative leaching fluxes of Al, SO_4, NO_3 and NH_4 over a period of 120 years predicted by SMART2, RESAM and NUCSAM are presented in Figure 6 and Figure 7. All modes gave similar leaching fluxes for SO_4. Although, the SMART2 flux in the subsoil for the *BU* scenario was slightly higher and in the topsoil for the *IE* scenario slightly lower. The Al and NO_3 leaching fluxes predicted by SMART2 and RESAM were invariably lower than the NUCSAM fluxes, for both scenarios and both depths. The low Al and NO_3 fluxes were mainly due to ignoring seasonal variability. Although ignoring seasonality created additional model uncertainty, the identified differences are acceptable when making long-term predictions.

This study showed that time resolution has only a rather small effect on the uncertainty in long-term (> 100 year) soil acidification. On a shorter time scale (10-50 years), during strong changes in deposition, the effect is more significant, especially for the Al/BC2 ratio.
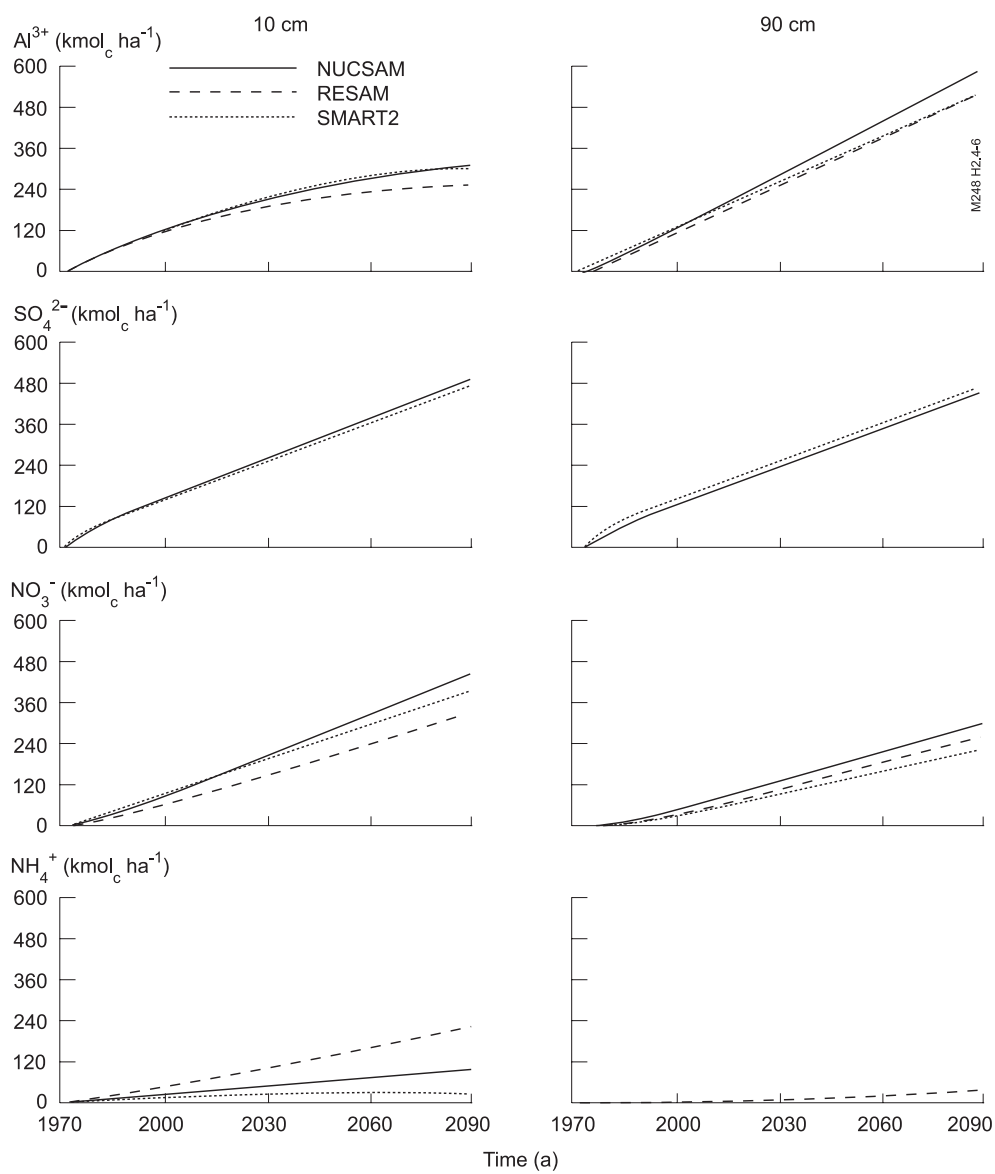
Figure 6 Cumulative leaching fluxes of SO_4, NO_3, Al, and NH_4 at 10 cm (left-hand side) and 90 cm (right-hand side) depth as simulated with NUCSAM, RESAM and SMART2, using the *Business as Usual* scenario
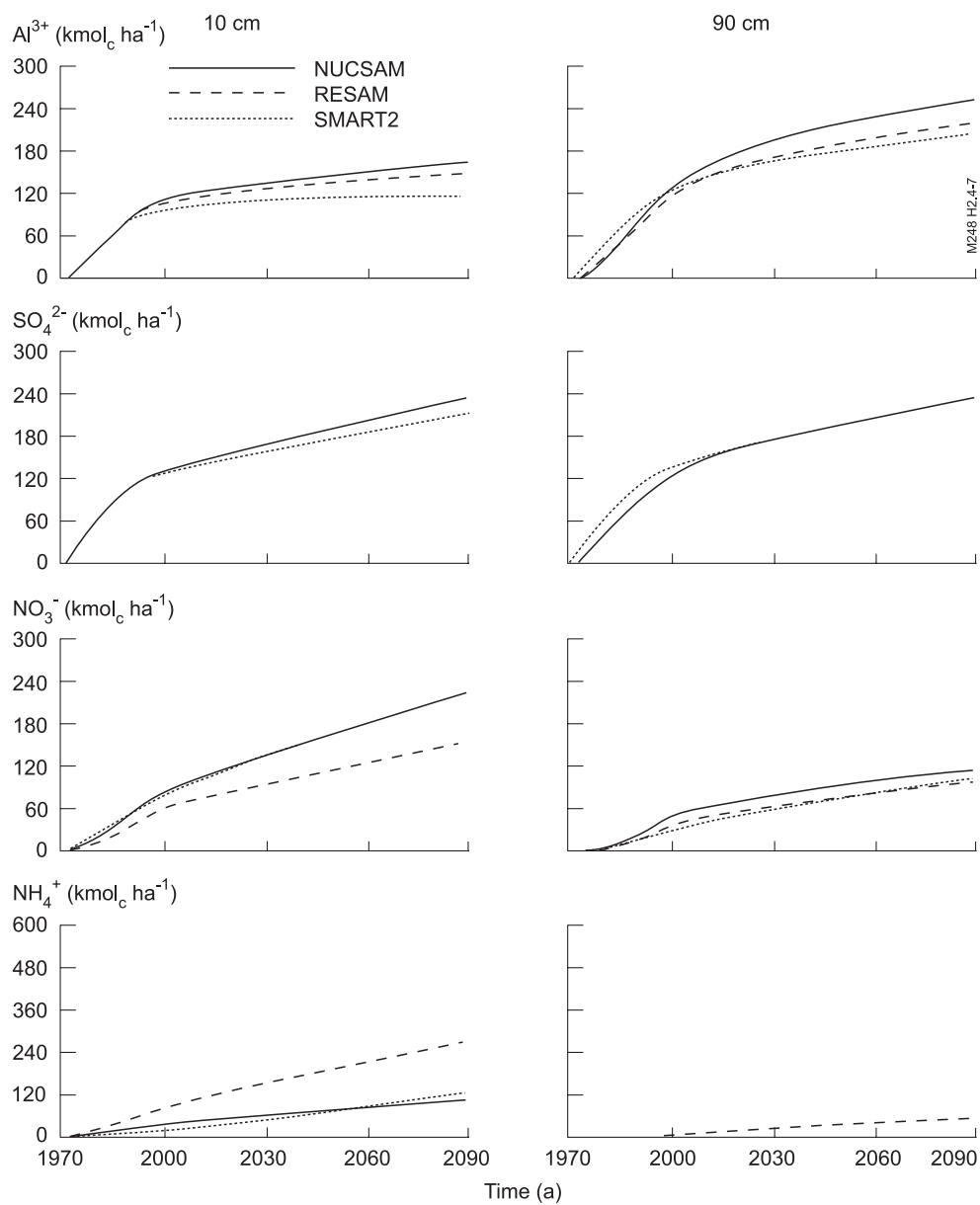
Figure 7 Cumulative leaching fluxes of SO$_4$, NO$_3$, Al and NH$_4$ at 10 cm (left-hand side) and 90 cm (right-hand side) depth as simulated with NUCSAM, RESAM and SMART2 using the *Improved Environment* scenario

2.4.4 Conclusions

Testing and Validation

The validation of NUCSAM, RESAM and SMART2 at the Solling site, shows that the models reproduce the main features of the concentration variations over time for most concentrations. In particular:

- trends and dynamics of the concentrations of NO_3, SO_4 and Al are reproduced well;
- simulated NH_4 concentrations in the topsoil is reproduced fairly by SMART2, but overestimated by NUCSAM and RESAM;
- simulated Al/BC2 ratios in the subsoil are too low. This is of concern because the Al/BC2 ratio is an important criterium in critical acid loads.

Despite differences in their process descriptions, SMART2, RESAM and NUCSAM simulate most of the solute concentrations reasonably well. Whether the dissolution of Al-hydroxides was modelled by a rate-limited reaction (NUCSAM, RESAM) or by an equilibrium equation (SMART2) hardly affected modelled Al concentrations. The differences in N cycling processes also hardly affect the quality of the modelled NO_3 and NH_4 concentrations.

The influence of vertical resolution of the models was clearly shown by the simulated concentration of SO_4 and base cations in the subsoil. All models mimicked the observed a rise in SO_4 concentration between 1975 and 1980, due to a decrease in sulphate adsorption. However, the one-layer model, SMART2, overestimated the initial rise in dissolved SO_4, due to a large dispersion of the sulphur front in a one-layer system. On the other hand for the simulation period as a whole SMART2 showed the best performance for SO_4 in the subsoil.

We expected a strong influence of temporal resolution in the simulation of NO_3 by NUCSAM compared to RESAM and SMART2. In the topsoil, NO_3 concentrations simulated by these models were in the same range as the measurements. Subsoil NO_3 concentrations were slightly underestimated by RESAM and SMART2, as these models simulated a higher N uptake than NUCSAM. Albeit, NUCSAM slightly overestimated the subsoil NO_3 concentrations, and the temporal fluctuations were poorly simulated. The same is true for the NH_4 concentrations. The *NMAE* values for the NO_3 concentrations in the top- and the subsoil were higher for NUCSAM than for RESAM. In the topsoil the higher *NMAE* values resulted from the fact that simulated fluctuation were sometimes out of phase with the measured fluctuations. The NH_4 concentration in topsoil was best modelled by SMART2, the two other models seriously modelled too high NH_4 concentration in the topsoil. All three models underestimated the NH_4 concentrations in the subsoil, but the observed NH_4 concentration in subsoil are already very low.

In general it can be concluded that the performance of the regional scale model SMART2 is as good as the performance of the more complex models RESAM and NUCSAM. A model such as NUCSAM proved to be a valuable link between relatively short data records and long-term predictions generated with RESAM and SMART2.

Long-term predictions

RESAM, which does not include seasonal variation, simulated the observed flux-weighted annual averaged concentrations (and ratios) comparable or even better than NUCSAM. Because the uncertainties in long-term predictions of soil and soil solution response induced by ignoring seasonal variability are rather small, it can be concluded that RESAM, which neglects seasonal variability, is acceptable for making long-term annual average predictions.

SMART2, which does not take into account seasonal variation and vertical heterogeneity, yields in most cases results that are as good as the model NUCSAM and RESAM. However, during abrupt changes in inputs the concentrations and fluxes of adsorbing compounds, such as SO_4 and Al, some deviations may occur. Bearing this in mind, it can be concluded that the use of the simplified model SMART2, that neglects seasonal variation and vertical heterogeneity, is in most aspects acceptable for the evaluation of long-term trends in soil and soil solution chemistry.

II Evaluation on a site scale

III   Evaluation on a regional scale

3.1   Modelling of soil acidity and nitrogen availability in natural soil ecosystems in response to changes in acid deposition and hydrology
A revised version of:
-   SMART2: Modelling of soil acidity and nitrogen availability in natural soil ecosystems in response to changes in acid deposition and hydrology
By: J. Kros, J.P. Mol-Dijkstra, W. de Vries and G.J. Reinds
Submitted to Ecological Modelling

3.2   Uncertainty assessment in modelling soil acidification at the European scale a case study
A slightly revised version of:
-   Uncertainty assessment in modelling soil acidification at the European scale a case study
By: J. Kros, E.J. Pebesma, G.J. Reinds and P.A. Finke, 1999
Published in: Journal of Environmental Quality 28/2:366-377

3.3   Assessment of the Prediction Error in a Large-Scale Application of a Dynamic Soil Acidification Model
A slightly revised version of:
-   Assessment of the Prediction Error in a Large-Scale Application of a Dynamic Soil Acidification Model
By: J. Kros, J.P. Mol-Dijkstra and E.J. Pebesma
Accepted for publication in:
Stochastic Environmental Research and Risk Assessment

3.4   Quantification of nitrate leaching from forest soils on a national scale
A slightly revised version of:
-   Quantification of nitrate leaching from forest soils on a national scale
by: J. Kros, A. Tietema, J.P. Mol-Dijkstra and W. de Vries
Submitted to: Environmental Research & Risk Assessment

III Evaluation on a regional scale

3.1 Modelling of soil acidity and nitrogen availability in natural soil ecosystems in response to changes in acid deposition and hydrology

Abstract

SMART2 has been developed to provide a simple, nationally applicable model to gain insight into the effects of hydrology, atmospheric deposition and nutrient cycling on soil and soil water quality. SMART2 was derived from a dynamic soil acidification model SMART (Simulation Model for Acidification's Regional Trends), aimed at the evaluation of the effectiveness of emission control strategies for SO_2, NO_x and NH_3 at the European scale. SMART is a one-compartment model which only includes geochemical buffer processes (e.g. weathering and cation exchange). SMART2 furthermore, includes nutrient cycling and solute input through upward seepage. The SMART2 model is linked to the Multiple stress mOdel for VEgetation (MOVE), that predicts the probability of occurrence of individual plant species as a function of the acid, nutrient and moisture status of the soil.

In this paper we evaluate SMART2 for various acidification and seepage scenarios (1990-2050) in the Netherlands. The results are focused on pH and nitrogen availability. We considered combinations of five vegetation structure types (three forest types, heather and grass) on seven soil types (three sandy soils, two clay soils, peat and loess soils) and five water-table classes, using a 250×250 km^2 grid. Effects of changes in pH, as calculated with SMART2, on the forest understorey in a nutrient poor deciduous forest were evaluated with MOVE.

Model simulations indicate that reductions in acid atmospheric deposition lead to a relatively fast increase in pH and base saturation and a decrease in N availability. As a result of deposition reductions the predicted number of species in the forest understorey in a nutrient poor deciduous forest increases from 40 to 80% in 1990 to 60 to 100% in 2050.

3.1.1 Introduction

Changes in vegetation are often caused by changes in site factors, such as pH and nitrogen availability (cf. Huston, 1979; Grime, 1979; Tamm, 1991). Abiotic site factors are affected by changes in atmospheric deposition (Galloway, 1995), water-tables (Van Wirdum, 1986), changes in management. and land use and internal processes such as vegetation succession. Changes in abiotic site factors may affect the structure and functioning of semi-natural ecosystems, and thus to biodiversity (cf. Bobbink *et al.*, 1998). Often, ecosystems are affected by various threats simultaneously (multiple stress effect). Environmental effects on ecosystems are usually studied for one stress factor at a time.

Started in the second half of the 20th century, Dutch ecosystems received increasingly inputs of NH_4 and SO_4. These affected soil solution concentrations, pH and nitrogen availability (Van Breemen *et al.*, 1982). Two groups of effects of enhanced atmospheric deposition of sulphur and nitrogen can be distinguished: (i) (soil) acidification, leading to enhanced leaching of base cations, and increased dissolution of potentially toxic aluminium, and (ii) eutrophication by nitrogen only. In

wet ecosystems eutrophication is also due to input of polluted ground- and surface water. A thorough review of the impacts of N inputs on semi-natural ecosystems, i.e. bogs and wetlands, species-rich grasslands, heathlands and forest, related to vegetation changes, is given in Bobbink *et al.* (1998).

Research on forests indicated that increased nitrogen inputs cause high concentrations of NH_4 and NO_3 in the soil solution (Roelofs *et al.*, 1985; Kleijn *et al.*, 1989), associated with a shift towards nitrophilous grass-species in the forest understorey (Hommel *et al.*, 1990). pH decrease may affect the original ground vegetation (Bobbink *et al.*, 1998). Besides vegetation changes, increased nitrogen input and acidification may lead to: (i) nutrient imbalances, resulting from an increase in biomass, causing an increased demand of base cations (Ca, Mg, K) and the counteracting effect of reduced uptake of these cations due to increased NH_4 concentrations (Boxman and Van Dijk, 1988) and (ii) increased susceptibility to secondary stress factors such as frost (Aronsson, 1980) and fungi (Roelofs *et al.*, 1985).

In heathlands high inputs of atmospheric nitrogen are a significant factor in the transition of heathland to grassland (Heil and Diemont, 1983). Apart from the changes in competitive interactions between heather and grasses under the influence of nitrogen accumulation in the soil, heather beetle plagues are important factors in vegetation changes in heathlands (Berdowski and Zeilinga, 1987; Berendse *et al.*, 1987). Generally, the species that contribute most to biodiversity tend to grow on soils with a relative high pH, low nitrogen content, and low Al/Ca ratio (Bobbink *et al.*, 1998).

Also in semi-natural species-rich grassland, increased nitrogen availability that gives more highly productive grassland depresses botanical diversity (Bobbink *et al.*, 1998). Wetland ecosystems showed also a significant decrease in diversity at elevated nitrogen inputs (Vermeer and Berendse, 1983).

In the Netherlands many vegetation types used to depend on shallow water-table. In the last decades, these vegetation types have suffered severely from lowering of the water-table, by intensive drainage and groundwater abstraction (Van Amstel *et al.*, 1989). In addition, Hendriks (1994) showed that 29% of the Dutch forests suffers from drought. Decrease upward seepage water quality has also affected species diversity in many wetland ecosystems (Van Wirdum, 1991).

To evaluate effects of eutrophication, acidification and drought on species diversity, a conceptual, species-centred, Multiple stress mOdel for VEgetation (MOVE) has been developed (Latour and Reiling, 1991). MOVE calculates the probability of occurrence of plant species as a function of soil pH, soil nitrogen availability and depth of the groundwater-table in spring. Because combined samples of vegetation and these site factors are rare, the indication values of plant species by Ellenberg *et al.* (1991) are used to assess the site factors. The Ellenberg's indication values were calibrated with samples of vegetation relevés combined with measured site factors (Wiertz *et al.*, 1992).

To evaluate the soil pH and nitrogen availability in response to acidification, drought and eutrophication scenarios the SMART model (De Vries *et al.*, 1989) was extended to serve as soil module for the MOVE model. The dynamic soil acidification model SMART was developed to evaluate the effectiveness of emission control

strategies for SO_2, NO_x and NH_3 on a European scale. SMART is a simple one-compartment model which mainly includes geochemical buffer processes such as weathering and cation exchange. To model abiotic site factors in both dry and wet natural ecosystems SMART was extended with nutrient cycling and improved hydrology (including upward seepage transport). The extended model is called SMART2.

With the combination of the SMART2 model and the MOVE model (see Figure 1) it is possible to evaluate the response of site factors of terrestrial ecosystems to deposition and upward seepage scenarios to (i) assess the effectiveness of the combination of emission-deposition reductions and reduction in groundwater abstractions on a national scale, and (ii) identify areas with a large probability of occurrence of specific plant species. shows the general concept of the integrated SMART2-MOVE model.
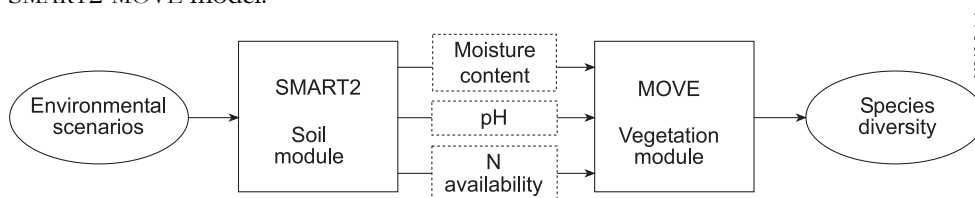
Figure 1 Schematic presentation of the integrated SMART2-MOVE model

The major objectives of this Chapter are (i) to present a simple, nationally applicable model to gain insight into the effects of upward seepage, atmospheric deposition and nutrient cycling on terrestrial ecosystems, (ii) the validation and evaluation on a national scale using regionally available data, and (iii) an application of the model on a national scale using various deposition and hydrology scenarios. A complete description of the model SMART2 is given in Chapter 2.3. This Chapter provides an evaluation and validation of SMART2 on a national scale using a nation-wide inventory and the background on geographical information and data used for a national application of SMART2, as well as an indicative application of the combined SMART2-MOVE using two deposition scenarios.

3.1.2 The SMART2 Model

SMART2 (Kros *et al.*, 1995a) predicts changes in H, Al, divalent base cation (BC2), NO_3 and SO_4 concentrations in the soil solution, as well as solid phase characteristics depicting the acidification status, i.e. carbonate content, base saturation and amorphous Al precipitates. The SMART2 model consists of a set of mass balance equations, describing the soil input-output relationships, and a set of equations describing the rate-limited and equilibrium soil processes (Table 1).

Table 1 Processes and process descriptions included in SMART2

Process	Element	Process description
Input		
Total deposition	SO$_4$, NO$_3$, NH$_4$, BC2 [1], Na, K	Inputs: deposition fluxes are multiplied by an element- and vegetation-dependent filtering factor[2]
Upward seepage	SO$_4$, NO$_3$, NH$_4$, BC2 [1], Na, K	Inputs
Water Balance	-	Inputs: precipitation, upward seepage, evapotranspiration
Rate-limited reactions:		
Foliar uptake	NH$_4$	Linear function of total deposition
Foliar exudation	BC2 [1], K	Equals foliar uptake
Litterfall	BC2 [1], K, NH$_4$, NO$_3$	Logistic growth
Root decay	BC2 [1], K, NH$_4$, NO$_3$	linear function of litterfall
Mineralisation	BC2 [1], K,	first-order reaction and as a function of pH, Mean Spring Water table (*MSW*) and C/N ratio of the litter
	NH$_4$, NO$_3$	
N immobilisation	NH$_4$, NO$_3$	Proportional to N deposition and as a function of the C/N ratio soil organic matter
Growth uptake	BC2 [1], K, NH$_4$, NO$_3$	Logistic growth
Nitrification	NH$_4$, NO$_3$	Proportional to net NH$_4$ input and as a function of pH, Mean Spring Water table (*MSW*) and C/N ratio
Denitrification	NO$_3$	Proportional to net NO$_3$ input and as a function of pH, Mean Spring Water table (*MSW*) and C/N ratio
Silicate weathering	Al, BC2, Na, K	Zero order reaction
Equilibrium reactions:		
Dissociation/association	HCO$_3$	CO$_2$ equilibrium equation
Carbonate weathering	BC2	Carbonate equilibrium equation
Al hydroxide weathering	Al	Gibbsite equilibrium equation
Cation exchange	H [3], Al, BC2	Gaines-Thomas equations
Sulphate sorption	H, SO$_4$	Langmuir equation

[1] BC2 stands for divalent base cations (Ca, Mg)
[2] The vegetation-dependent filtering factor takes into account the roughness length of the canopy
[3] Implicitly, H is affected by all processes. This is accounted for by the charge balance

The soil solution chemistry in SMART2 depends on the net element input from the atmosphere (the product of deposition and filtering factor, i.e. a correction factor for the roughness length of the canopy) and groundwater (upward seepage), canopy interactions (foliar uptake, foliar exudation), geochemical interactions in the soil (CO$_2$ equilibria, weathering of carbonates, silicates and/or Al hydroxides, SO$_4$ sorption and cation exchange), and a complete nutrient cycle (litterfall, mineralisation, root uptake, nitrification and denitrification). The growth of the vegetation and litterfall are

modelled by a logistic growth function, which acts as a forcing function. Nutrient uptake only stops when the soil solution concentration of the corresponding nutrient becomes zero. Soil interactions are either described by simple, rate-limited (zero-order) reactions (e.g. uptake and silicate weathering) or by equilibrium reactions (e.g. carbonate and Al-hydroxide weathering and cation exchange). The influence of environmental factors, e.g. pH and temperature, on weathering and exchange reactions is ignored. Solute transport is described by assuming complete mixing of the element input within one homogeneous soil compartment with a constant density and a fixed depth (generally the root zone), so SMART2 only predicts the solutes leaving the root zone. The annual water flux percolating from this layer equals the annual precipitation excess, which must be specified as a model input. The time step of the model is one year, so seasonal variations are not considered.

3.1.3   The vegetation effect module MOVE

We used the model MOVE (Latour and Reiling, 1993) to evaluate the effects of a changes in soil pH and N availability, as calculated by SMART2, on species diversity for plant species of nutrient-poor deciduous forests. MOVE predicts the probability of occurrence of plant species as a function of three abiotic soil factors: soil acidity, nutrient availability and soil moisture. With regression statistics the probability of occurrence of a species can be calculated for each combination of soil factors or for each environmental variable separately resulting in species-response curves. Species-response curves of about 900 plant species have been determined for soil moisture, nutrient availability and soil acidity (Wiertz et al., 1992) using Gaussian logistic regression models. Although, it is known that species diversity is affected by several nutrients (cf. Olde Venterink, 2000), MOVE only take N into account.

Regression was based on an extensive database developed for a revision of the Dutch classification of plant communities (Schaminée et al., 1989). This database consists of 30 000 vegetation relevés. However, no information on abiotic site factors of these vegetation relevés was available. Hence, abiotic site factors were assessed in retrospect based on Ellenberg indication values (Ellenberg et al., 1991), using the method of Ter Braak and Gremmen (1987). Ellenberg indication values indicate the relationship between the occurrence of a plant species and nutrient availability, acidity, soil moisture, salt dependency, and temperature. These values have been assigned to most plant species of western and central Europe, and the Netherlands (Wiertz et al., 1992). The abiotic site factors of each vegetation relevé are assessed by averaging the indication values of all the observed species. Calculated averages of the Ellenberg indication values are used as a semi-quantitative assessment of the abiotic soil factors. Next, the frequency of probability of occurrence of each species is derived as a function of the average Ellenberg indication values of the vegetation relevés, using Gaussian logistic regression models (Jongman et al., 1987). Because this analysis used only floristic information to assess the abiotic site factors, any (historical) vegetation relevé can be included in the analysis. Moreover, such an analysis excludes potential bias caused by high temporal and spatial variation in the actual measurements of

abiotic site factors. Species occurrence has been described as being significant for 95% of the species using unimodal and linear regression models. Most of the significant models were unimodal. Linear models were found for nutrients (4%) and salt (20%).

Ellenberg indication values were calibrated with quantitative values for the abiotic soil factors using combined samples of vegetation and environmental variables. This calibration connects SMART2 with MOVE. For this purpose a database has been compiled with combined samples for pH (N = 3988), mean spring water table (*MSW*) (N = 13) and N availability (N = 266). For pH, MSW, biomass production and N availability satisfying relations with Ellenberg values were found, explained variances of respectively 0.58, 0.54, 0.59 and 0.58 (Alkemade *et al.*, 1996).

MOVE input consist of a yearly average pH and N availability in the root zone and the (*MSW*). The pH and N availability were calculated by SMART2, whereas the *MSW* was provided by the hydrological scenario derived by the national groundwater model (LGM, Pastoors, 1993; cf. Section *Hydrology scenario*). The pH in SMART2 refers to a 'real' pH of the soil solution, which must not be mixed up with regular soil analysis parameters like pH(KCl) and pH(H_2O). In this study the N availability is defined as the sum of the N throughfall flux and the mineralisation flux. This can be regarded as a gross N availability, which is available for root uptake, immobilisation and denitrification. The remainder will be leached from the root zone.

Characteristic species for nutrient-poor deciduous forest *Quercion Robori-Petraeae* and *Fago-Quercetum* were inferred from Loopstra and Van der Maarel (1984). Ecological response curves of 13 plant species were inferred from Wiertz *et al.* (1992). These species are: *Convallaria majalis, Ceratocapnos claviculata, Deschampsia flexuosa, Hieracium laevigatum, Hieracium umbellatum, Holcus mollis, Luzula pilosa, Luzula sylvatica, Melampyrum pratense, Polypodium vulgare, Pteridium aquilinum, Solidago virgauria*, and *Teucrium scorodonia*.

For each species the 10 and 90 percentiles of the species-response curves were calculated. The 10 percentile corresponds with a reduced probability of occurrence due to 'shortage or limitation', the 90 percentile to reduced occurrence due to 'excess or intoxication'. Next, the probability of occurrence was plotted for each grid cell. A species was considered to have a probable occurrence when both the predicted pH and N availability in a grid cell were between the 10 percentile and the 90 percentile value of the ecological response curve. The probability of occurrence for each grid cell was calculated from the number of the mentioned 13 plant species which are probable to occur.

3.1.4   Model parameterisation, calibration and validation

Data acquisition strategy

Data needed to apply SMART2 on a national scale, include system inputs (driving variables), the initial state of model variables and model parameters. System inputs refer to a specific deposition scenario and upward seepage scenario for each grid cell.

Model variables and parameters refer to particular combinations of generic soil types and generic vegetation structure types.

In predicting the long-term impact of atmospheric deposition scenarios on site factors on a national scale, we distinguished:

- geo-referenced information on system inputs, for each grid cell i.e. (i) soil type, vegetation structure type, and water table class, (ii) the deposition of SO_4, NO_3, NH_4, base cations and Cl (iii) precipitation and (iv) upward seepage fluxes;
- generic information, i.e. average values for initial values of model variables and model parameters for each combination of vegetation structure type and soil type.

Soil type, vegetation structure type and water table class were derived form national maps, which were generalised en gridded toward a $250 \times 250 m^2$ grid. Hydrological information was derived from the National Groundwater Model (LGM; Pastoors, 1993), with a resolution of 250×250 m². Deposition values of SO_2, NO_x and NH_3 for 1980, 1990 and 1997 were available on a 1×1 km² grid (Eerens and Van Dam, 2000, see section *Deposition Scenarios*) and deposition values of base cations and Cl (derived from a 10×10 km² grid database; De Vries *et al.*, 1994c). The grid-related information was stored in database tables, whereas the vegetation and soil related parameter were stored in ascii-files (cf. Mol-Dijkstra *et al.*, 2001). The model output was stored as grid - and time related data in database tables or grid-ascii-files.

Validation data

To gain insight into the reliability of the model predictions, we compared model results of the soil and solution chemistry for forest with soil and soil solution measurements at 60-100 cm depth. Validation data were based on an inventory of about 200 forested stands throughout the Netherlands. For acid sandy soils, measurements from 150 forest stands were used, which were sampled once during the period March to May in 1990 (De Vries *et al.*, 1995b). For clay, loess and peat soils measurements from 100 forest stands were used, which were sampled once during the period March to May in 1994 (Klap *et al.*, 1999).

It is important to realise that there exists some crucial differences between the modelled and observed samples (see also De Vries *et al.*, 1994a):

- the number of the observed soil/vegetation combinations differed from those that were simulated and most observations concerning forest on poor sandy soils;
- the soil depth of the observations was always 60-100 cm, whereas the soil depth used for the simulations varied from 20-100 cm (cf. Table 9);

SMART2 simulated flux weighted annual average concentrations, whereas the field data were single observations in early spring.

Areal distribution of soil-vegetation combinations

We considered seven soil types and five water-table classes, which were derived from the 1 : 50 000 soil map of the Netherlands. Soil types were generalisation based on soil

chemical criteria: parent material, presence of calcite, base saturation and texture (Table 2).

Table 2 Distinguished soil types

Code	Soil class	Common soil types (FAO, 1988)
SP	Sand Poor	Carbic Podzols, Arenosols
SR	Sand Rich	Gleyic Podzols, Gleysols
SC	Sand Calcareous	Arenosols
CN	Clay Non-calcareous	Fluvisols
CC	Clay Calcareous	Fluvisols
PN	Peat Non-calcareous	Histosols
LN	Loess Non-calcareous	Luvisols

The relation between the 1 : 50 000 soil map codes and the seven soil types used is given in Kros *et al.* (1995a). The five water-table classes were the same as used by De Waal (1992) (Table 3). The corresponding Mean Highest Water-table (*MHW*) and Mean Lowest Water-table (*MLW*) were derived (weighted averaged) from Van der Sluijs (1990).

Table 3 Used water-table classes and their corresponding water-table classes from the 1 : 50 000 soil map of the Netherlands and the corresponding averaged *MHW*, *MLW*, *MSW*

Water-table Class used in this study	Water-table Class from the 1 : 50 000 soil map	*MHW*[1] (m)	*MLW* (m)	*MSW* (m)
1	I	-0.05	0.38	0.08
2	II	0.07	0.66	0.24
3	II*, III, III*, V, V*	0.24	1.18	0.48
4	IV, VI	0.60	1.43	0.82
5	VII, VII*	1.29	2.21	1.51

[1] Averaged *MHW* (Mean Highest Water-table), *MLW* (Mean Lowest Water-table) *and MSW* (Mean Spring Water-table)as given by or calculated from Van der Sluijs (1990)

We attributed the existing vegetation to five classes of 'functional types' of vegetation (Table 4), based on difference in canopy characteristics, litter production, growth and vegetation management.

The areal distribution of the vegetation structure types over the soil types (Table 5) and the water-table classes (Table 6) was obtained by an overlay of 250 × 250 m² grid maps, i.e. (i) generalised soil map (including water-table information), (ii) the Dutch forest inventory (Nederlandse, 1985), (iii) 'nature conservation value map' (Natuurbeleidsplan, 1989) and a detailed vegetation map based on satellite observations (LGN; Thunnissen *et al.*, 1992). Because of the inaccuracy of the various vegetation maps, more than one vegetation class could be assigned to a 250 × 250 m² grid cell. For these cases the following allocation sequence was used: (i) first grassland and heather from the satellite observation map first assigned to the 250 × 250 m² grid cells; (ii) second forest (DEC, SPR, PIN) was assigned only when no grassland and no heather was assigned during the previous step. This sequence was used because the

LGN data (dated from 1990) was more recent than the forest inventory data (dated from 1985).

Table 4 Distinguished vegetation classes

Code	Vegetation Class	Common species Characteristics
DEC	Deciduous forest	Oak, beech, Japanese larch Needle or leaf-shedding trees with: low forest filtering, growth rate and transpiration rate
PIN	Pine forest	Scots pine and black pine Evergreen trees with: moderate forest filtering, growth rate and transpiration rate
SPR	Spruce forest	Douglas fir, Norway spruce Evergreen trees with: high forest filtering, growth rate and transpiration rate
HEA	Heather	Calluna, Erica
GRP	Grassland (nutrient-poor)	Common grass species no fertilisation or grazing

Table 5 Area of the vegetation/soil combinations considered in the model application as a percentage of the total vegetation-covered area in the Netherlands[1] (326 614 ha)[2]

Soil type	Area (%)					
	Pine forest	Spruce Forest	Deciduous forest	Heather	Grass (nutrient-) Poor	Total
Sand Poor	35.54	5.97	18.73	3.70	3.19	67.14
Sand Rich	4.97	3.11	10.19	0.18	0.29	18.74
Sand Calcareous	0.29	0.12	1.28	0.00	2.94	4.63
Clay Non-calcareous	0.27	0.30	2.57	0.00	0.27	3.42
Clay Calcareous	0.02	0.03	2.21	0.00	0.29	2.54
Peat Non-calcareous	0.22	0.39	1.62	0.12	0.44	2.79
Loess Non-calcareous	0.14	0.05	0.52	0.02	0.02	0.74
Total	41.45	9.97	37.12	4.02	7.44	100.00

[1] Information on the areal distribution of tree species and soil types in each grid cell was derived by overlaying a 250 × 250 m² grid with vegetation coverage information and a soil database with soil type information in a 250 x 250 m² grid. The latter database was derived by transforming the digitised 1 : 50 000 soil polygon map of the Netherlands (De Vries and Denneboom, 1992).

[2] This value excludes the vegetation coverage in the southern part of the Province of Limburg and the southern part of the Province of Flevoland.

Table 6 Area of the vegetation/water-table class combinations considered in the model application as a percentage of the total vegetation covered area in the Netherlands (326 614 ha)

Water-table Class	Area (%)					
	Pine forest	Spruce Forest	Deciduous forest	Heather	Grass (nutrient-) Poor	Total
1	0.03	0.01	0.28	0.01	0.50	0.82
2	0.21	0.13	1.25	0.01	0.99	2.59
3	5.66	3.41	11.75	0.61	1.21	22.64
4	5.77	2.72	8.81	0.22	1.08	18.60
5	29.76	3.71	15.02	3.18	3.67	55.35
Total	41.43	9.98	37.11	4.03	7.45	100.00

Data related to vegetation structure types

Data used for the five vegetation structure types are presented in Table 7. The vegetation age (age_{vg}) was set to 40 years old for forest and 10 years old for short vegetation. This refers to a semi mature forest which will double in biomass during the next 50 years. The stand age (age_{st}) for forest (PIN, SPR, DEC) was derived by assuming that most of the actual forest in the Netherlands was planted at the beginning of the 20th century. For heather (HEA) and grassland (GRP) is was assumed that they were sod cutted or ploughed 10 years ago.

Most data on canopy interactions (filtering factors, dry deposition factors, interception fractions, foliar uptake fractions and foliar exudation fractions), nutrient cycling (reallocation fractions and nutrient contents in leaves) and growth uptake (nutrient contents in stems) in forests were directly taken from De Vries *et al.* (1994c). Values for pine, spruce and deciduous trees related to Scots pine, Douglas fir and Oak respectively. The amounts of litterfall for these forests were the product of the average values for leaf biomass and litterfall rate constant given by De Vries *et al.* (1994a). Nutrient cycling factors (*ncf*), the fraction of roots in the litter layer (*fr*$_{rt \, ll}$) and mineralisation constants for forest were taken from a literature survey by De Vries *et al.* (1990).

Filtering factors for heathlands and grasslands were assumed to be 1.0. Dry deposition factors, foliar uptake fractions and foliar exudation fractions for heather and grassland were derived from Bobbink and Heil (1993) and Bobbink *et al.* (1990), respectively. Interception fractions for both vegetation structure types were derived from De Visser and De Vries (1989).

As with forests, the amounts of litterfall in heathlands and grasslands were calculated as the product of average values of above ground biomass and litterfall rate constants, using data from Berendse (1988) for *Erica* (wet heathland) and *Molinia* (grass). Reallocation factors, nutrient cycling factors, nutrient contents in above ground biomass and mineralisation constants were derived from the same source. The fraction of roots in the humus layer in heathlands was based on Tinhout and Werger (1988). Actually, these authors found that about 75% of the fine root biomass (cf.

Table 7) was in the top 5 cm of the soil. We assumed this amount to occur in the litter layer. The same assumption was made for the organic top-layer in grassland. Concentrations of monovalent base cations (K) in above-ground biomass in heathlands and grasslands were based on Heil and Diemont (1983) and Bobbink *et al.* (1990), respectively. Values for divalent base cations (Ca, Mg) were derived from Pruyt (1984). Mineralisation constants for heather and grassland were based on Berendse (1988) assuming that they relate to well-drained soils (no reduction for groundwater level).

Table 7 Values used for the canopy interactions, nutrient cycling, growth uptake and mineralisation parameters for the five vegetation structure types

Parameter [1]	Unit	PIN	SPR	DEC	HEA	GRP
age_{tg}	a	40	40	40	10	10
age_{lt}	a	80	80	80	10	10
Canopy Interaction						
$ffSO_2$	-	1.4	1.6	1.15	1.0	1.0
$ffNH_3$	-	1.3	1.5	1.1	1.0	1.0
$ffNO_x$	-	0.85	1.0	0.7	1.0	1.0
f_{dd}	-	2.5	3.0	2.0	1.5	1.5
fr_{int}	-	0.3	0.4	0.2	0.1	0.05
$frNH_{4\,fu}$	-	0.3	0.3	0.3	0.4	0.3
frH_{fu}	-	0.3	0.3	0.3	0.4	0.3
frK_{fe}	-	0.63	0.63	0.66	0.65	0.5
Nutrient Cycling						
Am_{lf}	kg m^{-2} a^{-1}	0.41	0.30	0.33	0.24	0.30
ncf	-	0.5	0.5	0.5	3	3
ru_{exp}	-	2	2	2	2	2
fr_{re}	-	0.36	0.36	0.36	0.10	0.50
$fr_{rt\,lt}$	-	0.25	0.25	0.25	0.75	0.75
$ctBC2_{lv}$	%	0.31	0.54	0.64	0.75	0.75
ctK_{lv}	%	0.60	0.61	0.92	0.25	0.70
$ctN_{lv\,mn}$	%	1.5	1.5	2.5	0.9	1.6
$ctN_{lv\,mx}$	%	2.5	2.5	3.5	0.9	1.6
Growth Uptake						
ctN_{st}	%	0.12	0.11	0.17	0	0
$ctBC2_{st}$	%	0.11	0.08	0.06	0	0
ctK_{st}	%	0.05	0.04	0.12	0	0
Mineralisation						
$fr_{mi\,mx}$	-	0.8	0.8	0.8	0.4	0.8
$k_{mi\,mx}$	a^{-1}	0.05	0.05	0.05	0.3	0.3

[1] See Annex 1 for explanation of the used symbols, and Chapter 2.3 for the equations in which the parameters are used.

Data related to soil types

Data used for the soil parameters of the seven soil types are presented in Table 8. Data on bulk density, soil moisture content, carbonates, *CEC*, base saturation, organic matter content, total nitrogen content and secondary Al compounds were derived from an extensive field survey of 150 non-calcareous sandy soils (SP and SR; De Vries

et al., 1995b), about 50 calcareous sandy soils (Alterra, W. de Vries, pers. comm.), 30 clay soils (CN, CC), 40 loess soils (LN) and 30 peat soils (PN; Klap *et al.*, 1999). Note that all sampling sites were forest site. Exchange constants and the Al equilibrium constant were calculated, using the measured adsorbed and dissolved concentrations of H, Al and BC2 averaged of the considered soil depth. Here we present the median values related to the root zone for forest, which was set equal for all forest types. Similarly KAl_{ox} derived from averaged soil solution concentrations of Al and H for sites with a pH below 4.5. The pH criterion was also used for the calculation of the exchange constant and was introduced to prevent use of unrealistic values.

Maximum denitrification fractions ($fr_{de,mx}$) and the parameters relating denitrification to water-table ($rf_{de,MSW,mn}$ and z_{de}) were derived from Breeuwsma *et al.* (1991). Nitrification fractions were calculated as a function of the water-table class, using data on deposition and leachate concentrations of NH_4 (cNH_4) and NO_3 (cNO_3) in the mentioned 300 forest stands on sandy, clay, loess and peat soils, assuming that the NH_4 to NO_3 ratio at the bottom of the root zone can be described as:

$$\frac{cNH_4}{cNO_3} = \frac{(1 - fr_{ni}) \cdot NH_{4,td}}{NO_{3,td} + (1 + fr_{ni}) \cdot NH_{4,td}}$$ (1)

or:

$$fr_{ni} = \frac{\dfrac{NH_{4,td}}{NO_{3,td}} - \dfrac{cNH_4}{cNO_3}}{\dfrac{NH_{4,td}}{NO_{3,td}} \cdot \left(1 + \dfrac{cNH_4}{cNO_3}\right)}$$ (2)

When deposition data for NH_4 and NO_3 were not available, a ratio of 2 was assumed between the total deposition of NH_3 ($NH_{4,td}$) and the total deposition of NO_x ($NO_{3,td}$). The results for the various sandy soils were lumped, because differences appeared to be small. Using these data, a linear relationship between the nitrification fraction and *MSW* was assumed (see Chapter 2.1).

The SO_4 sorption capacity was set at 2% of the secondary Al compounds content (Johnson and Todd, 1983). The partial CO_2 pressure was derived from Koorevaar *et al.* (1983). Weathering rates of base cations for the non-calcareous sandy soils were taken from De Vries (1994), who derived weathering rates on the basis of one-year batch experiments that were scaled to field observations. Weathering rates for calcareous soils were derived from De Vries *et al.* (1994a). For peat and loess soils weathering rates were derived from Van Breemen *et al.* (1984) and Weterings (1989) respectively. Note, however, that these weathering rates refer to silicate weathering. The weathering in calcareous soils is fully dominated by carbonate weathering, cf. Eq. (69) in Chapter 2.3.

Table 8 Values used for the soil parameters for the seven soil types, related to the depth of the root zone for forest

Parameter [1]	Unit	SP	SR	SC	CN/CC	LN	PN
Depth	m	0.7	0.6	0.8	1.0	1.0	0.5
Soil physical properties							
fr_{pp}	-	0.1	0.2	0.2	0.0	0.2	0.0
ϱ_{rz}	g cm^{-3}	1.45	1.26	1.62	1.16	1.52	0.17
ϱ_{lt}	g cm^{-3}	0.13	0.13	0.13	0.13	0.13	0.13
θ	m^3 m^{-3}	0.13	0.18	0.061	0.27	0.41	0.84
Organic matter							
OM	kg kg^{-1}	0.02	0.06	0.01	0.07	0.03	0.90
CN_{mn}	kg kg^{-1}	15	15	15	15	15	15
CN_{cr}	kg kg^{-1}	40	40	20	40	40	40
CN_{om}	kg kg^{-1}	21	26	10	10	21	35
CN_{mo}	kg kg^{-1}	15	15	15	15.	15.	15.
DA_{mo}	kg kg^{-1}	1.5	1.5	1.5	1.5	1.5	1.5
(De)nitrification							
$fr_{ni\,mx}$	-	1.0	1.0	1.0	1.0	1.0	1.0
$rf_{ni\,MSW\,mn}$	-	0.3	0.3	0.3	0.5	0.5	0.3
z_{ni1}	m	0.1	0.1	0.1	0.0	0.2	0.5
z_{ni2}	m	0.5	0.5	0.5	0.5	0.85	0.85
$fr_{de\,mx}$	-	0.9	0.9	0.9	1.0	0.9	1.0
$rf_{de\,MSW\,mn}$	-	0.25	0.25	0.25	0.7	0.7	0.85
z_{de}	m	1.3	1.3	1.3	2.5	1	1.5
Soil Chemical Parameters							
CEC	mmol$_c$ kg^{-1}	11	41	8	319	54	414
$frBC2_{ac}$	-	0.07	0.06	0.83	0.89	0.16	0.58
KAl_{ex}	log (mol l^{-1})	0.79	0.16	-1.2	-3.4	0.6	-2.1
KH_{ex}	log (mol l^{-1})	4.0	3.8	5.0	6.7	4.2	3.5
KAl_{ox}	log (mol l^{-1})	8.1	7.9	8.1	9.4	8.3	6.5
$ctCa_{cb}$	mmol$_c$ kg^{-1}	0.0	0.0	182.4	0.(109.)[1]	0.0	0.0
$ctAl_{ox}$	mmol$_c$ kg^{-1}	85	109	9	196	155	101
SSC	mmol$_c$ kg^{-1}	1.7	2.2	0.18	3.9	3.1	3.1
C	mol$_c$ m^{-3}	1.0	1.0	1.0	1.0	1.0	1.0
pCO2	hPa	0.1	0.1	0.1	0.2	0.1	0.5
$BC2_{we}$	mol$_c$ m^{-3} a^{-1}	0.009	0.025	0.008	0.030	0.015	0.010
K_{we}, Na_{we}	mol$_c$ m^{-3} a^{-1}	0.011	0.020	0.010	0.040	0.020	0.020

[1] See Annex 1 for explanation of the used symbols, and Chapter 2.3 for the equations in which the parameters are used.

[2] Value in bracket was used for calcareous clays soils (CC)

Data related to soil-vegetation combinations

Model parameters that depend on both soil and vegetation refer to the depth of the root zone, transpiration rate and growth parameters. Values used for each combination of soil and vegetation are given in Table 9.

Table 9 Values used for the soil and vegetation-dependent parameters for all soil vegetation combinations

Vegetation	Soil	T_{rz} (m)	Tr (m a^{-1})	k_{gl} (a^{-1})	$t_{1/2}$ (a)	$Am_{st\,mx}$ (kg m^{-2})
PIN	SP	0.7	0.276	0.067	40	22.2
	SR	0.6	0.292	0.066	39	28.3
	SC	0.8	0.298	0.085	34	10.5
	CN, CC	1.0	0.378	0.085	34	10.5
	LN	1.0	0.282	0.066	39	28.3
	PN	0.5	0.378	0.085	34	10.5
SPR	SP	0.7	0.296	0.072	38	25.0
	SR	0.6	0.304	0.077	37	41.1
	SC	0.8	0.329	0.072	38	25.0
	CN, CC	1.0	0.417	0.072	38	25.0
	PN	0.5	0.417	0.072	38	25.0
	LN	1.0	0.306	0.077	37	41.1
DEC	SP	0.7	0.326	0.088	50	28.8
	SR	0.6	0.328	0.088	48	76.9
	SC	0.8	0.34	0.088	48	76.9
	CN	1.0	0.397	0.090	49	49.9
	CC	1.0	0.397	0.088	48	76.9
	LN	1.0	0.326	0.088	48	76.9
	PN	0.5	0.397	0.090	49	49.9
HEA[2]	SP, SC	0.2	0.335	0.15	10	1.4
	SR	0.2	0.37	0.15	10	1.4
	SC	0.2	0.335	0.15	10	1.4
	PN	0.2	0.41	0.15	10	1.4
GRP	SP, SC	0.2	0.40	0.15	5	0.5
	SR, LN	0.2	0.44	0.15	5	0.5
	SC	0.2	0.40	0.15	5	0.5
	CN, CC, PN	0.2	0.48	0.15	5	0.5

[1] See Annex 1 for explanation of the used symbols, and Chapter 2.3 for the equations in which the parameters are used.

[2] Heather on loess and clay soils do not occur

The thickness of the root zone and actual evapotranspiration rates for forest were taken from De Vries *et al.* (1994c), who derived transpiration fluxes from model calculations (SWATRE, Belmans *et al.*, 1983) for various forest types on sandy soils, while using expert judgement for forests on peat, loess and clay soils. Actual evapotranspiration rates for short vegetation on sandy soils were derived from De Visser and De Vries (1989). Values for loess soils were taken from Van der Salm (1999). Values for clay and peat soils were set equal to potential evapotranspiration rates as given in De Visser and De Vries (1989). For sandy soils and loess soils actual transpiration rates were corrected when the precipitation deviates form 780 mm a^{-1}, i.e. the value used for the water balance calculations (cf. Hootsmans and Van Uffelen (1991). Growth rate parameters for forest were based on a literature survey by De Vries *et al.* (1990). Growth rates for short vegetation refer to shoot growth only (i.e. increase in litterfall), and were derived from Berendse (1988). The increase of non shoot material was assumed to be negligible. This was mimicked in the model by setting the nutrient contents in stems to zero (cf. Table 7).

Deposition and hydrology scenarios

The temporal trends of chemical soil parameters predicted by SMART2 are driven by scenarios for atmospheric deposition and hydrology. Deposition scenario is related to changes in the atmospheric deposition fluxes of NH_x, NO_x and SO_x. The deposition of base cations and of Cl was kept constant. The hydrology scenario is related to the changes in the quantity of the upward seepage flux and related changes in phreatic water level. The solute concentrations of the upward seepage flux was kept constant. For both deposition and hydrology a *Business as Usual* (*BU*) and an *Improved Environment* (*IE*) scenario was evaluated and their mutual combinations (Table 10). The scenarios were generated for the period 1990-2050.

Table 10 Considered scenarios with respect to deposition and hydrology

Hydrology	Deposition	
	Business as Usual	Improved Environment
Business as Usual	*BB*	*IB*
Improved Environment	*BI*	*II*

[1] Refers to precipitation
[2] Refers to SO_x, NO_x and NH_3. Atmospheric deposition of base cations and chloride was assumed to be constant

Deposition scenarios

The two deposition scenarios consists of: (i) a continuation of the deposition in the year 1997, *BU* and (ii) a reducing deposition scenario, reflecting the planned emission reductions in the Netherlands for the next 20 years, *IE*.

Simulations started in 1980 to initialise the model, using deposition estimates for the year 1980, 1990 and 1997 (Eerens and Van Dam, 2000). These estimates are based on calculations with an empirical model (DEADM; Erisman, 1991) of the wet and dry deposition of these elements on a national scale for a 5×5 km^2 grid, using the concentrations of NH_x, NO_x and SO_x that were measured at several weather stations of the National Air Quality Monitoring Network.

For the *BU* scenario values for the year 1997 were maintained until 2050. For the *IE* deposition anticipated deposition values for the years 2010 and 2030 were taken from the National Environmental Plan (cf. Beck *et al.*, 2001). The *Improved Environment* scenario values for the 2010 deposition were related to the National Emission Ceiling (NEC) for the Netherlands and the Gothenburg protocol for the rest of Europe. Deposition values for 2030 correspond with deposition values for which 90% of the semi-natural areas has a deposition below the critical load (cf. Beck *et al.*, 2001). For 2050 the same values were used as for 2030.

For all deposition inputs in each 250×250 m^2 grid values from the corresponding 5×5 km^2 grid were used. For each grid cell values for in between years were derived by linear interpolation.

Table 11 National averaged deposition and emission values used for NH_x, NO_x and SO_x deposition within the scenarios

Year	Average deposition[1] $(mol_c\ ha^{-1}\ a^{-1})$			Total emissions[2] $(kton\ a^{-1})$		
	NH_x	NO_x	SO_x	NH_3	NO_2	SO_2
1980	1832	834	1478	234	585	481
1990	1823	811	719	231	575	202
1997	1499	642	394	187	453	118
2010	880	361	177	104	238	50
2030	239	105	77	50	80	40
2050	239	105	77	50	80	40

[1] Deposition values refer to the beginning year of the period

[2] National emissions

Values used for the deposition of base cations and Cl were taken from De Vries (1991), who performed an interpolation from 22 monitoring-stations for the period 1978-1985 (Anonymous, 1985) to a $10 \times 10\ km^2$ grid. For each $1 \times 1\ km^2$ grid values from the corresponding $10 \times 10\ km^2$ grid were used. Base cation and Cl deposition fluxes were kept constant throughout the simulation period.

Precipitation data were derived from weather stations from the Royal Netherlands Meteorological Institute (KNMI). Selected records of precipitation normals from 280 stations over the period 1950-1980 were interpolated to a $10 \times 10\ km^2$ grid. As with the base cation deposition, values for each $1 \times 1\ km^2$ cell were taken from the corresponding $10 \times 10\ km^2$ grid and were assumed constant during the simulation period. Details on the interpolation procedure have been given in Hootsmans and Van Uffelen (1991). Most values ranged between 700 and 900 mm a^{-1}.

Upward seepage scenarios

Scenarios for the quantity on upward seepage were generated with the National Groundwater Model for the Netherlands (LGM, Pastoors, 1993). The effects of upward seepage on the site factors were evaluated for two scenarios: (i) a constant upward seepage flux, using the values for the year 1988 (Pastoors, 1993), *Bussiness as Usual*, and (ii) 25% reduction of groundwater extractions for public drinking water, resulting in increased upward seepage fluxes for the year 2010 (Pastoors, 1992), *Improved Environment*. For the *Improved Environment* scenario, values between 1988 and 2010 were linearly interpolated. It must be emphasised that the surface area that showed an increase in upward seepage flux is restricted to about 12% of the model area, on 9% of the surface area of the Netherlands (cf. Pastoors, 1992). Calculated changes in phreatic water level were converted to absolute values by adding them to the initial phreatic water level (Kros *et al.*, 1995a). These actual values of phreatic water level were used as input for both SMART2 and MOVE.

Information on upward seepage water chemistry was based on the National Survey on landscape ecology (LKN; Bolsius *et al.*, 1994). For each 1 km^2 grid cell, the LKN groundwater quality database provides a quality class. To assign a chemical composition to the quality classes, the chemical composition of reference water types

from Van Wirdum (1991) were used. Using solute concentrations of the reference samples from Van Wirdum (1991), ionic concentrations were derived for the considered *seepage types* (Table 12, cf. Kros *et al.*, 1995a).

Table 12 Groundwater concentrations (mol_c m^{-3}) used for the seepage type

Seepage type	SO_4	NO_3	NH_4	BC2 [1]	K	Na	Cl
No seepage	0.20	0.06	0.05	3.23	0.03	0.30	0.20
Mixed water	0.20	0.06	0.05	3.23	0.03	0.30	0.20
Groundwater	0.27	0.02	0.04	6.42	0.05	0.52	0.31
Brackish water	5.74	0.02	0.12	19.5	1.05	46.0	54.1
Sea water	55.0	0.02	0.78	137.7	10.0	456.0	538.0
Surface water	1.67	0.27	0.05	4.93	0.18	4.17	5.01

[1] BC2 = Ca + Mg

3.1.5 Results

We present results from a validation and an application of the model SMART2 on a national scale. Results concerning model outputs required for applications of MOVE, i.e. pH and N availability. N availability is defined as the sum of the N throughfall flux and the total N mineralisation flux (see Chapter 2.3, Eq. 28). Base saturation as such is not an input for the MOVE model, but is also presented because of its (hydro)ecological implication. For the validation some other model outputs are presented as well.

Validation

Soil solution concentrations

To gain insight into the reliability of the model predictions, we compared model results on soil and solution chemistry for forests with soil and soil solution measurements at 60-100 cm depth (cf. Table 13).

Table 13 Median values of important soil and soil solution parameters as observed at 60-100 cm depth (Obs.) and predicted for 1990 (Mod.) by SMART2 for deciduous forest

Soil type	N [1]		pH		Al (mol_c m^{-3})		NH_4 (mol_c m^{-3})		NO_3 (mol_c m^{-3})	
	Obs.	Mod.	Obs.	Mod.	Obs.	Mod.	Obs.	Mod.	Obs.	Mod.
Sand poor	27	44093	4.0	3.8	0.42	1.08	0.08	0.00	0.25	0.58
Sand rich	28	10051	3.8	3.9	0.49	0.52	0.08	0.00	0.33	0.23
Peat	30	6363	3.8	3.8	0.04	0.04	0.24	0.01	0.02	0.01
Loess	40	926	4.3	4.1	0.18	0.37	0.04	0.19	0.72	0.47
Clay	13	6386	6.3	5.9	0.01	0.00	0.00	0.07	0.11	0.22
Clay calc.	17	3884	7.4	6.8	0.00	0.00	0.00	0.00	0.06	0.08

[1] N represents the number observed and simulated soil/vegetation combinations.

The agreement between the observed and simulated pH was generally good. The agreement for the Al concentration appeared to be reasonable. Alternatively, the Al in concentration in poor sandy soils was overestimated. The agreement for NH_4 and NO_3 was generally moderate (deviations larger than 50%). NH_4 concentrations were clearly underestimated in peat soils. Given that NO_3 concentrations were slightly underestimated too, N mineralisation might be underestimated or denitrification overestimated. For the poor sandy soils and the clay soils the NO_3 was clearly overestimated, whereas for rich sandy soils and loess soils it was underestimated. These deviations indicate that the nitrogen dynamics in SMART2 are parameterised inadequately. It is likely that the mineralisation and or (de)nitrification parameters need some improvements. Moreover, in SMART2 the N mineralisation flux, which strongly influences the concentrations of dissolved N, depends largely on the age of the vegetation and the N content in the foliage (cf. Chapter 2.3) However, nation wide data on the age of the vegetation and the N content in the foliage is lacking. Finally, our validation is mainly limited to deciduous forest on non-calcareous soils. For other vegetation structure types, additional data gathering on soil and soil solution would be required.

Nitrogen mineralisation fluxes

We also compared the calculated N mineralisation fluxes with observations, as they are a substantial part of the N availability. N mineralisation fluxes depend on: (i) the age of the vegetation, (ii) vegetation management (mowing, grazing or forest harvesting) and (iii) the N flux in atmospheric deposition. The N mineralisation fluxes calculated by SMART2 for the year 1990 refer to: (i) relatively mature terrestrial ecosystems (heathlands/grasslands are assumed to be 10 years old; forests are assumed to be 40 years old), (ii) from which no biomass is removed during the simulation period and (iii) with a high atmospheric N input.

Validation should thus focus on data for similar systems. Mineralisation data are comparatively scarce, except in steady-state situations when mineralisation equals litterfall which has been measured more frequently. Table 14 summarised N mineralisation data. When available, the age of the ecosystem is presented as well.

For heathlands and grasslands, data given by Gorree and Runhaar (1992) for a steady-state situation (mineralisation equals litterfall) are 2 - 2.5 $kmol_c$ ha^{-1} a^{-1}. These, however, do not include root turnover, which is generally 75% of the total N turnover in these ecosystems (cf. Berendse, 1988). Consequently, the total N mineralisation flux would be increased by 8 to 10 $kmol_c$ ha^{-1} a^{-1} at a steady-state. Note that data on heathlands and grasslands used in SMART2 are based on Berendse (1988), i.e. Erica and Molinia respectively. Validation should thus focus on mineralisation data by Berendse (1988).

Table 14 Observed N mineralisation rates

Type of ecosystem	Age (a)	N mineralisation flux ($kmol_c$ ha^{-1} a^{-1})	Source
Pine Forest			
Gerritsfles	ca. 60	5.1	Van Dobben *et al.* (1992)[1]
Tongbersven	ca. 80	5.7	Van Dobben *et al.* (1992)[1]
Deciduous Forest			
Oak+mixed; Beech	50-100	7 - 8	Tietema (1992)
Oak+mixed; Birch	ca. 45	7 - 8	Van Breemen *et al.* (1988)[1]
Deciduous forest	varying	3 - 10	Melillo (1981)
Heathland			
Calluna	varying	0.8 - 4.2	Berendse (1990)
Erica	10	0.5 - 3.0	Berendse (1988, 1990)
Erica	30	3.5 - 7.0	Berendse (1988, 1990)
Erica	50	8.2 - 9.1	Berendse (1988, 1990)
Grassland			
chalk grassland	unknown	3.5	Van Dam (1990)
Molinia	10	2 - 3	Berendse (1988)
Molinia	30	6 - 7	Berendse (1988)
Molinia	50	7.6 - 9.3	Berendse (1988)

[1] These data refers to litterfall fluxes

N mineralisation fluxes as calculated by SMART2, using the *BU* scenarios both for deposition and seepage, are summarised in Table 15. In Table 15 the N mineralisation fluxes in 1990 for forest (Spruce, Pine, Deciduous) refer to a forest of 40 years old and for short vegetation (Heather, Grass) to a site of 10 years old, whereas the values in 2050 can be regarded as a mature ecosystem were litterfall equals mineralisation.

Table 15 Calculated N mineralisation fluxes, under the *BU* scenario

Vegetation	N mineralisation flux ($kmol_c$ ha^{-1} a^{-1})	
	1990	2050
Spruce	2.8	3.2
Pine	3.5	4.2
Deciduous	4.6	5.3
Heather	2.7	3.1
Grass	4.3	4.6

In general, therefore, comparisons are problematic and should be regarded as indicative. Model results from Table 15 generally compared reasonable with observed N mineralisation fluxes. The modelled mineralisation fluxes for short vegetation in 2050 (i.e. 70 years old) were comparable with the appropriate ranges in Table 14, whereas the modelled fluxes in 1990 (i.e. 10 years old) are slightly higher than the observed values. Modelled mineralisation fluxes for forest were always lower than the observed fluxes. This might be an indication that the N litterfall fluxes for forest we used in this SMART2 application were underestimated. Data used in SMART2 for the N

litterfall flux are a multiplication of average litterfall fluxes with a varying N content depending on the N deposition level. Multiplication of observed ranges in litterfall fluxes and N contents in foliage (Table 16) provides an indication of N mineralisation rates at steady-state.

Table 16 N litterfall fluxes

Tree species	Litterfall[1] (Mkg ha^{-1} a^{-1})	N contents[2] (%)	N litterfall flux (kmol$_c$ ha^{-1} a^{-1})
(Scots) Pine	0.5 – 8.5[1]	1.6 - 3.0	0.4 - 12
(Norway) Spruce	1.5 – 7.5[1]	1.1 - 2.3	0.8 - 8
(Oak) Deciduous	1.6 – 5.6[3]	2.2 - 3.2	1.6 - 8

[1] Data based on a literature compilation for Northern Europe (Reurslag and Berg, 1993)

[2] Data for 45 pine stands, 15 spruce stands and 30 oak stands in the Netherlands (Hendriks *et al.*, 1994). Contents refers to contents of the foliage, for the calculation of the litterfall flux a reallocation factor of 0.36 was assumed (cf. Table 7)

[3] Data based on a review by De Vries *et al.* (1990); Duvigneaud *et al.* (1971) gives ranges of 4.7-7.5 Mkg ha^{-1} a^{-1}

Considering the average maximum litterfall fluxes used in SMART2, i.e. ca. 3 Mkg ha^{-1} a^{-1} for the various tree species (Table 7), indicates that for forest the litterfall fluxes are underestimated, which in turn result in too low mineralisation fluxes in forest.

Geographical distribution of pH and nitrogen availability

Maps of the median pH and nitrogen availability per 1×1 km^2 grid cell for all vegetation structure types in the year 1990 and 2050 for *IE* deposition scenario (i.e. reducing deposition) combined with the *IE* seepage scenario (increasing upward seepage) are presented in Figure 2 and Figure 3.

Spatial variability in pH was high, which mainly corresponds with the variability in soil types. Calcareous sandy soils and clay soils along the coast-line, clay soils in along the rivers are well buffered soils, with relatively high pH values. Non-calcareous sandy soils in the central part and the southern part of the country have a lower buffer capacity, resulting in relatively low pH. Figure 2 show that deposition reductions and increase in upward seepage result in an increase in pH values, especially for the non-calcareous soils.

N availability will have decreased in 2050 compared to 1990. N availability also showed a highly spatial variability, mainly due to the spatial variability in atmospheric N deposition. N availabilities appeared to be high in the central part and the southern part of the country, were atmospheric deposition of N is high. In the northern part of the country the atmospheric deposition of N is low, resulting in lower N availabilities.
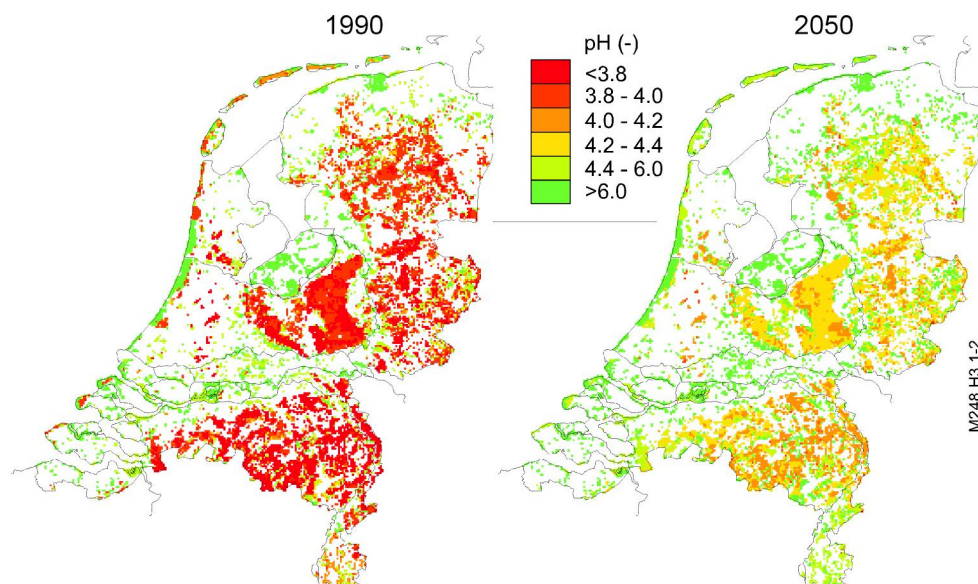
Figure 2 Geographical distribution of dominant values for the pH in the root zone of semi-natural terrestrial ecosystems in 1990 (left) and 2050 (right), for the *IE* deposition scenario combined with the *IE* seepage scenario

Figure 3 Geographical distribution of dominant values for the N availability (kmol$_c$ ha^{-1} a^{-1}) in the root zone of semi-natural terrestrial ecosystems in 1990 (left) and 2050 (right), for the *IE* deposition scenario combined with the *IE* seepage scenario
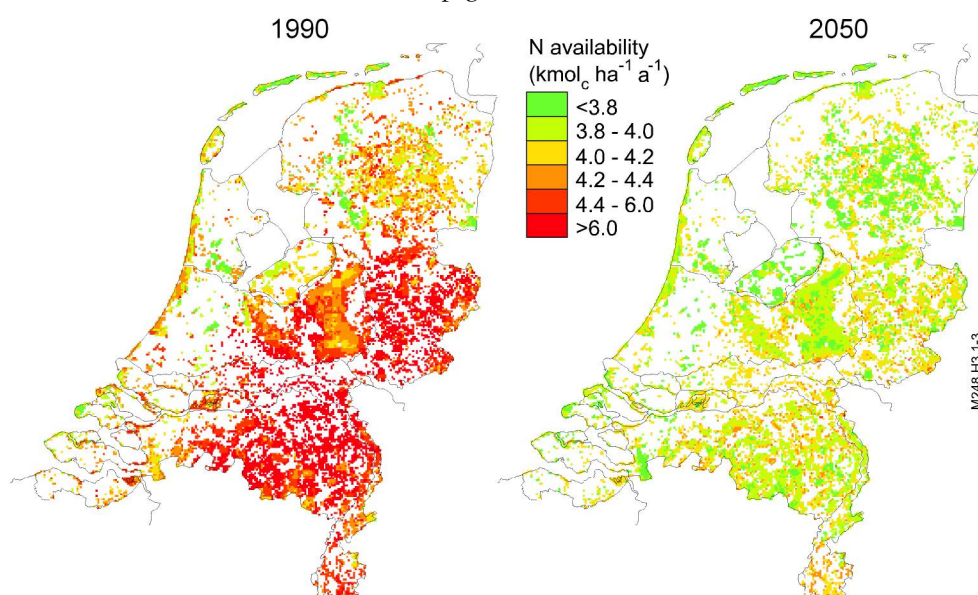
Effects of vegetation and soil on abiotic site factors

Changes in soil pH, N availability and base saturation under different vegetation structure types are summarised in Table 17. Vegetation structure types influence the soil chemistry by differences in nutrient cycle, filtering of dry deposition and transpiration.

Reduced atmospheric deposition and increased upward seepage, is expected to increase the soil pH and base saturation, and to decrease N availability. The pH and base saturation increase was rather limited, except in grassland soils. Grassland soils also showed higher pH and base saturation throughout the simulation period. However, the relatively high soil pH and base saturation for grassland were biased by the fact that about 45% of the considered sites are located on calcareous sandy soils or clay soils. For other vegetation structure types the differences in pH and base saturation were generally small. Deciduous forest, though, show a slightly higher pH and a higher base saturation, which was mainly an effect of soil type and water-table class. Compared to coniferous forest, deciduous forest are generally located on richer soils with a higher water-table (i.e. wetter circumstances). The higher base saturation for spruce forest was most likely due to a higher filtering of dry deposition, resulting to an higher input of base cations.

Table 17 Effects of vegetation on the predicted median pH, N availability and base saturation (BS) in the root zone for all soil types in 1990, 2010 and 2050 in response to the *IE* deposition scenario combined with the *IE* seepage scenario

Vegetation	$N^{1)}$	pH			N availability ($kmol_c$ ha^{-1} a^{-1})			BS (%)		
		1990	2010	2050	1990	2010	2050	1990	2010	2050
Spruce	3961	3.7	3.9	4.1	6.6	4.8	3.5	2	3	10
Pine	24435	3.8	4.0	4.2	7.3	5.7	4.6	1	2	8
Deciduous	18046	4.0	4.2	4.5	7.6	6.4	5.8	6	9	27
Heather	6556	3.8	3.9	4.3	5.8	4.3	3.3	1	2	7
Grass	23362	4.1	4.5	6.0	6.5	5.8	5.1	51	63	84

[1)] N represents the number of grid cells evaluated

For all vegetation structure types the N availability was clearly lower in 2010 and 2050 than in 1990. N availability decrease most for heather (43%), spruce (36%) and pine forest (47%). For grassland (21%) and deciduous forest (24%) reductions were lower. That the N availability reduced less than the atmospheric deposition, (which was more than 80%; see Table 11), is due to increased N mineralisation, at higher pH. In addition, in the beginning of the simulation period N accumulated in soils, whereas in 2050 there was more or less a steady-state between litterfall and mineralisation. Furthermore, the litterfall flux also increased slightly during the simulation period, because in 1990 the maximum amount of litterfall was not yet achieved. Between 1990-2050, N mineralisation increased from 2.8 to 3.2 $kmol_c$ ha^{-1} a^{-1} for spruce forest, from 2.7 to 3.1 $kmol_c$ ha^{-1} a^{-1} for pine forest and from 4.3 to 4.6 $kmol_c$ ha^{-1} a^{-1} for deciduous forest.

Soil type (Table 18) influences the soil chemistry by differences in weathering rates and cation exchange capacity. The effect of soil type was much more pronounced than the effect of vegetation. Of course, a clear distinction exists between calcareous and non-calcareous soils.

Calcareous soils have a high pH and base saturation due to the presence of calcite. There was no effect of the combined scenario on the pH of calcareous soils. Which was kept at about pH, irrespective of deposition level and seepage input. The non-calcareous sandy soils have the lowest pH and very low base saturation, indicating that these soil are strongly acidified. Deposition reductions and increase in upward seepage caused an increase in pH and base saturation in the non-calcareous soils. The increase was most pronounced for loess soils, indicating that soil acidification is reversible for these soils. For peat soils the remarkable combination of a pH around 3.9 and a base saturation around 50% is in agreement with field observations (Klap *et al.*, 1999).

Table 18 Effects of soil type on the predicted median pH, N availability and base saturation (BS) in the root zone below deciduous forest in 1990, 2010 and 2050 in response to the *IE* deposition scenario combined with the *IE* seepage scenario

Soil type	$N^{1)}$	pH			N availability ($kmol_c$ ha^{-1} a^{-1})			BS (%)		
		1990	2010	2050	1990	2010	2050	1990	2010	2050
Sand poor	44093	3.8	3.9	4.2	7.1	5.7	4.6	1	2	8
Sand rich	10051	3.9	4.1	4.3	7.5	6.2	5.2	3	4	10
Sand calc.	4657	7.0	7.1	7.1	5.9	5.3	4.9	100	100	100
Clay	6386	5.9	6.0	6.1	7.6	6.3	5.1	87	87	87
Clay calc.	3884	6.8	6.9	6.9	5.5	4.8	4.2	100	100	100
Loess	926	4.1	4.3	5.1	7.4	6.6	6.3	7	9	26
Peat	6363	3.8	4.1	4.2	4.4	3.7	3.0	51	52	52

[1] *N* represents the number of grid cells evaluated

The calculated changes in pH and base saturation were relatively small compared to those derived in another evaluation of a similar deposition scenario (cf. De Vries *et al.*, 1994a). This study refers to the one box model SMART2, whereas De Vries *et al.* (1994a) presented results for the top 30 cm using the multi-layer model RESAM, i.e. the layer where the major changes in pH and base saturation occur. In the one layer compartment (up to 1 m) considered here, changes in pH and base saturation averaged out. The results on N availability, by contrast, were not influenced by the thickness of the soil compartment, because this output refers to a flux for the root zone (including the litter layer) as whole.

The N availability of calcareous and peat soils was relatively low, because they are generally located in areas with relatively low atmospheric input of N. For peat soils, the low N availability was also due to low mineralisation fluxes. The median N mineralisation flux for peat soil in 2050 was 1.9 $kmol_c$ ha^{-1} a^{-1}, whereas the average mineralisation flux for all soil was 3.5 $kmol_c$ ha^{-1} a^{-1}. The low relatively low mineralisation flux for peat soils is mainly due to the correlation with wet

circumstances. Under (man-induced) dry circumstances the N mineralisation in peat soil can be very high, up to 100 $kmol_c$ ha^{-1} a^{-1} (cf. De Vries *et al.*, 2001).

Effects of deposition and seepage scenarios on abiotic site factors

Deposition reductions alone (Table 19; compare the columns *BB* vs. *IB*), increased in median values of pH and base saturation and decrease N availability. Although, the average pH increase for a specific vegetation structure type was rather small, 0.1 - 0.4 pH, large regional differences occurred (see Figure 2). The largest increase in pH were found under pine forest and grassland. Compared to the reduction in N deposition, the reduction in N availability were rather small.

Increase in upward seepage (Table 19; compare the columns *IB* vs. *II*), had only a slight effect on the median values of pH, N availability and base saturation. The results for the *IE* seepage scenario, as presented in Table 19 should be handled with care. The surface area affected by *IE* seepage scenario is relatively small, whereas deposition scenario affects all systems. Increase in upward seepage is restricted to sites with water-table class 1, 2 and 3 (cf. Table 3) in the surroundings of groundwater extraction wells, viz only in 3088 grid cells (i.e. 9% of the surface area of the Netherlands). In addition, the average increase in upward seepage flux for these cell was only 50 mm a^{-1}.

Table 19 Effects of combinations of the various scenarios[1] on the predicted median pH, N availability and base saturation (BS) in the root zone of all soil types for the different vegetation structure types in the year 2050

Vegetation	N[2]	pH			N availability ($kmol_c$ ha^{-1} a^{-1})			BS (%)		
		BB	IB	II	BB	IB	II	BB	IB	II
		3.8	4.1	4.1	6.3	3.5	3.4	2	10	10
Pine	24435	3.8	4.2	4.2	7.2	4.6	4.5	2	8	9
Deciduous	18046	4.1	4.2	4.4	7.7	5.8	5.6	12	27	27
Heather	6556	3.9	4.3	4.3	5.0	3.3	3.3	1	7	7
Grass	23362	5.7	6.0	6.0	6.5	5.1	5.1	81	84	84

[1] The first character refers to the deposition scenario, the second character refers to the seepage scenario, e.g. *IB* refers to *IE* deposition scenario and to the *BU* seepage scenario

[2] N represents the number of grid cells evaluated

Effects on plant species in for nutrient-poor deciduous forest

The effects of calculated changes in the output variable soil pH on species diversity were predicted for plant species of nutrient-poor deciduous forests (i.e. the forest on non-calcareous sandy soils) for 1990 and 2050 using the vegetation model MOVE (Latour and Reiling, 1993; see section 3.1.3)

For all soil types the median N availability remained above the optimum value of 3 $kmol_c$ ha^{-1} a^{-1} (Latour *et al.*, 1993). For the pH Latour *et al.* (1993) reported an optimum value of 4.2 for nutrient-poor deciduous forest. Results showed for all soils,

except the non-calcareous sandy soils and peat soils, a median pH above 4.2 at the end of the simulation period.

Figure 4 presents the probability of occurrence of species of nutrient-poor deciduous forests on rich an poor sandy soils for 1990, 2010 and 2050. In 1990 the predicted number of species varies on average between 40 and 80% of the considered 13 species. In 2010 this increases to 40 to 100% and in 2050 the occurrence increased in general to 60 to 100% of the species. In some specific areas the predicted percentage of species remained below 20%. In these areas the soil pH is higher than 5.8, i.e. the upper limit for the considered species in nutrient-poor deciduous forests (see section 3.1.3).
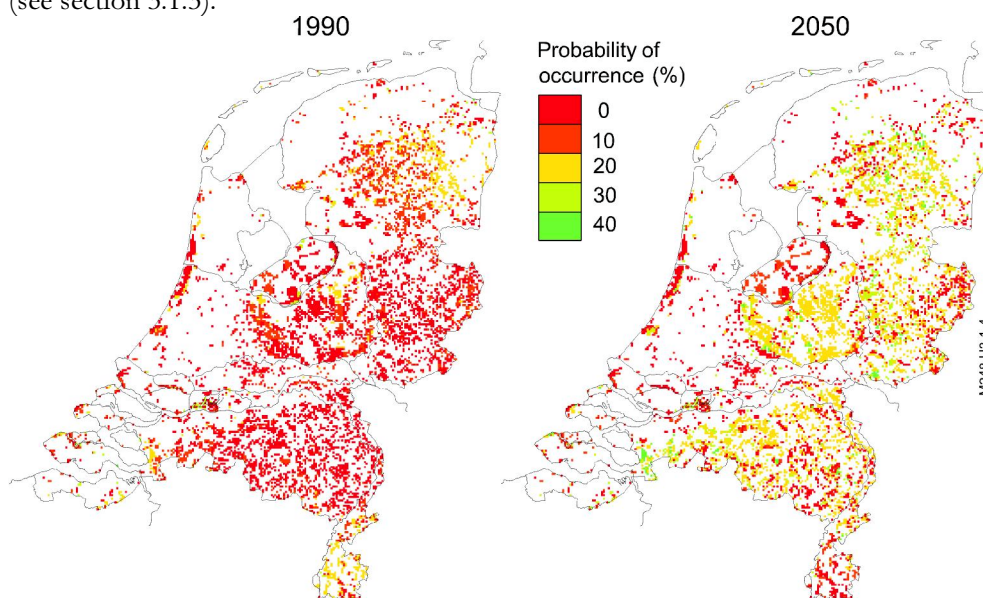

Figure 4 Predicted geographical distribution of the probability of occurrence of plant species typical for nutrient poor deciduous forest (see section 3.1.3) for 1990 (a) and 2050 (b), in response to the *IE* deposition scenario combined with the *IE* seepage scenario

3.1.6 Discussion and conclusion

Discussion

Uncertainties

The assessment of the uncertainty in model predictions caused by input data due to the uncertainty and spatial variability in those data will be addressed in Chapter 3.2 and Chapter 3.3. Here we restrict ourselves to a qualitative discussion of the consequences of crucial assumptions made in this model application.

Uncertainties caused by model structure are due to model assumptions and simplifications. Assumptions and simplifications are made because of insufficient knowledge, to limit data requirements and for operational reasons (e.g. application on a scale, that requires model simplification). The lack of knowledge with respect to acidification and nutrient cycling models mainly concerns the dynamics of organic matter, N and Al (De Vries, 1994; Kros *et al.*, 1993). Especially the uncertainties in Al and N dynamics may seriously contribute to the uncertainty in the results of pH and N availability.

E.g. SMART2 assumes that there is always equilibrium with secondary Al compounds (cf. section 3.1.2). In reality equilibrium is approached only in the subsoil, while under-saturation prevails in the topsoil. This equilibrium assumption will accelerate the depletion of secondary Al compounds and will lead to higher pH and Al concentrations in the top soil. Yet, improvement on the speciation of Al in relation to organic anions and the dissolution of amorphous Al precipitates have been incorporated (cf. Posch *et al.*, in prep.)

The N availability highly depend on the N mineralisation flux, which in turn depend on the age of the vegetation, vegetation management (e.g. sod cutting, mowing, grazing and tree harvesting), litterfall and N uptake. These aspects have not yet been adequately incorporated in the model for all vegetation structure types. In addition, the effect of pH and MSW (cf. Chapter 2.3) on modelled N mineralisation and N transformation processes have an inadequate experimental basis. Therefore, we recommend to improve and extend the N transformations processes, especially related to pH and water-table.

Management aspects, like sod cutting, mowing, grazing and tree harvesting should be included to properly calculate N availability, which highly depend on the age of the vegetation and the removal of biomass. Our assumption that each vegetation structure type has a particular age, strongly influences the model results. Furthermore, we assumed that the net production was nil. This was based on the assumption that biomass return to the soil equals biomass production. This shortcoming has in the mean time been captured by linking the SMART2 to the succession model SUMO (cf. Wamelink *et al.*, 2000).

Validation

Validation on solute chemistry yield satisfactory results, however, the validation part of this study was limited to soil solution concentrations under forests. The validation on N availability gave good indicative results, but was hindered by a lack of a regional dataset on mineralisation rates. A more comprehensive validation of SMART2 for all soil and vegetation structure types especially for the model output on N availability, is desirable. Obviously, there is a need for additional measurement campaigns aimed at improving the model descriptions and reducing the uncertainty in the model results.

Spatial and temporal resolution

In this study calculations are performed for the root zone as a whole (compartments up to 1 m), whereas most of changes in soil and soil solution occur in the top 30 cm, where also most of the fine roots occur. Since the thickness highly influence the pH, it is recommended to reconsider the choice of the calculations for shallower depth, e.g. 30 cm. This is especially relevant with respect to the linkage SMART2-MOVE.

The thickness of the soil compartment seriously influenced the model results. Here we considered the root zone as one homogeneous compartment. This assumption implies that the calculated concentrations refer to the bottom of the root zone. Generally there is a strong gradient in soil solution chemistry and fine root distribution with depth. pH and Al concentrations generally decrease with depth, as most of the fine roots occur in the top soil. Furthermore, most of the changes in time in soil and soil solution chemistry occur in the top 30 cm. Consequently, the assumption of one homogeneous relatively large compartment (up to 1 m) cancelled out changes with depth. To investigate the effect of soil depth within the root zone in more detail, both SMART and SMART2, have been extended to multi-layer models with variable depth of the soil layers. The annual time-scale may affect the long-term predictions, but this effect is likely to be small (cf. Chapter 2.4 and Kros *et al.*, 1994b).

The use of a 250×250 m^2 grid as a reference grid places various restrictions on geographical resolution. This resolution is far too coarse to model ecosystems which forms the topo-sequence within brook-valleys, with potentially high nature conservation value. Geographical resolution needs to be improved for an adequate modelling of site factors in wetlands and brook-valleys. Various studies with SMART2 on a more detailed spatial scale have been performed, e.g. in the Drentsche Aa area (cf. Kros *et al.*, in prep) and in the Beerze Reusel (cf. Van Dobben *et al.*, 2001). These studies show that greater spatial resolution, especially with respect to hydrology, clearly improved the output. Applying such detail at the national scale, however, would tremendously increase the logistic problems already encountered in the local application (see Chapter 2.1). In conclusion, modelling at that spatial resolution on a National scale is one step too far for logistic reasons and lack of data.

Conclusions

SMART2 appeared to be a flexible and quick tool to evaluate effects of deposition and upward seepage scenarios on soil solution chemistry.

Model predictions on pH and Al concentration for deciduous forest showed a reasonable to good agreement with observations. Alternatively, the Al in concentration in poor sandy soils was overestimated. Model predictions for the NO_3 and NH_4 concentrations showed moderate relationship with the observations. A preliminary validation on N mineralisation fluxes, showed a reasonable agreement between calculated fluxes and measured fluxes available from literature. N mineralisation fluxes in forests are likely to be underestimated.

Reductions in N and S deposition lead to an improvement of the abiotic site factors, i.e. a moderate increase in pH and base saturation in non-calcareous soil and a clear decrease in N availability for all soils with forest. The spatial variability in all

investigated model outputs, i.e. pH, base saturation and N availability was large. The spatial variability in pH and base saturation is linked with the spatial variability in soil type, whereas the spatial variability in N availability is linked with the spatial variability in N deposition. N availability strongly depends on the age of the vegetation. Litterfall increase followed by mineralisation increase, subsequently resulted in an increase in N availability that may abolish the reductions in N deposition. Consequently, reductions in N deposition not necessarily lead to a reduction in N availability.

The effects of *IE* seepage scenario on the inspected site factors were negligibly small, which is a result that only a very small parts of the Netherlands is affected by the reduction in groundwater extractions. The probability of occurrence of typical plant species in nutrient-poor deciduous forests increased with 20% in 2050, due to the evaluated *IE* deposition scenario combined with the *IE* seepage scenario.

3.2 Uncertainty assessment in modelling soil acidification on the European scale: a case study

Abstract

When modelling soil acidification on the European scale, it is inevitably that both model and data have varying degrees of associated uncertainty. The present study attempted to quantify the uncertainty in long-term forecasts of soil solution concentrations of Al and NO_3 resulting from the uncertainty in low resolution European-scale maps (1:1000 000) and input data. We used the Netherlands as a case study. Large-scale forecasts were made with a relatively simple dynamic process-oriented model, SMART2. Model outputs were considered as block median concentrations and the block areal fractions in which concentrations exceeded a critical level. As sources of uncertainty we considered (i) the soil and vegetation maps (categorical data), and (ii) the soil and vegetation-related parameters (continuous data). The uncertainty in categorical data was quantified by comparing European soil and vegetation maps, and the more detailed maps of the Netherlands. The uncertainty in continuous data was derived from various European databases and literature. The uncertainty in model outputs was quantified by an efficient two-step Monte Carlo simulation approach, which takes spatial correlation into account. The uncertainty in the input data on the European scale led to major uncertainties in the predicted Al concentration. Uncertainties in the areas where the Al concentration exceeded the maximum allowable concentration were much smaller. The uncertainties in soil-related parameters contributed most to the uncertainty in the Al concentration, whereas the uncertainty contributed by the soil and vegetation maps was negligible. For the NO_3 concentration, however, the soil and vegetation maps were important sources of uncertainty. Evaluation of the different error sources is of great practical significance, as it identifies which sources need further improvement. The present study shows that the uncertainty contribution of the different error sources depends greatly on the model output considered.

3.2.1 Introduction

Elevated NO_3 and Al concentrations, in soil water and groundwater in semi-natural ecosystems are primarily caused by elevated atmospheric deposition. This is a major European-scale environmental problem. Atmospheric deposition of acidifying substances (S and N) increase the dissolution and leaching of Al, especially in acidic sandy soils. The resulting elevated Al concentration in groundwater is a threat to its use as drinking water both for people and animals, especially from shallow wells. In the Netherlands, e.g. elevated levels of Al in shallow aquifers below forests are related to acid atmospheric deposition (e.g. Mulder *et al.*, 1990). Arable land is usually limed to a soil pH above 5, where the Al concentration is negligible. Consequently, only groundwater below semi-natural ecosystems is at risk of contamination with Al. As regards NO_3, however, a most serious impact originates from agricultural soils. According to RIVM (1991), atmospheric deposition of N compounds in the European Union (EU) accounts for 10% of the total N supply, including both deposition and direct application of manure and fertiliser. As a result, the threat of

NO$_3$ leaching from semi-natural ecosystems is less serious than in agricultural soils. In areas with large atmospheric N deposition, e.g. in north-western Europe, however, the groundwater quality below semi-natural ecosystems is under threat (De Vries, 1994). Eutrophication via atmospheric deposition is still a serious problem in the whole of Europe (De Vries, 1994). An assessment of the threat to groundwater in Europe by Al resulting from acid deposition has been made by Kämäri *et al.* (1990) and RIVM (1991). Both studies have produced maps of the sensitivity of groundwater to acidification in Europe.

At present, various models are available for large-scale prediction of ecosystem acidification, e.g. MAGIC (Cosby *et al.*, 1985), SAFE (Sverdrup *et al.*, 1995), and SMART (De Vries *et al.*, 1989). SMART has been specially developed for the European scale, to evaluate various deposition scenarios (De Vries *et al.*, 1994b). Models for regional scale assessments should be used with caution as both models and data have varying levels of associated uncertainty (Loague *et al.*, 1998). Consequently, it is imperative that these uncertainties are quantified. Until now, quantification of uncertainties has mostly been limited to a specific generic soil vegetation combination (Chapter 2.2; Kros *et al.*, 1993) or to one mapping unit in a region (Finke *et al.*, 1996).

In regional scale assessments, model input data are usually derived from generally available data, e.g. soil and landcover maps, using (pedo)transfer functions (Bouma *et al.*, 1986; Tiktak *et al.*, 1998). Finke *et al.* (1996) quantified the output uncertainty resulting from both spatial variability and the uncertainty in pedotransfer functions by a Monte Carlo approach and analysed the contribution of these sources to the total variance. Finke *et al.* (1996) considered only one soil mapping unit, representative for only a part of the Netherlands for which a detailed network of soil profile descriptions was available. Furthermore, they ignored the spatial correlation of the model input data. By including spatial correlation of model input data in a Monte Carlo analysis made it possible to quantify both the spatial variability of the point concentration within a block (i.e. the spatial variation in values occurring within single blocks of a single Monte Carlo run) and the uncertainty of block-aggregated values (i.e. the statistical variation in block-aggregated values among the entire ensemble of Monte Carlo runs) can be evaluated.

The present study was intended to quantify uncertainties associated with European-scale forecasts of Al and NO$_3$ concentrations in soil water, leaching from the root zone of semi-natural ecosystems towards the phreatic groundwater. We used the dynamic and process-oriented model, SMART2 (Kros *et al.*, 1995a), an extended version of the SMART model (De Vries *et al.*, 1989). To minimise input data requirements, SMART2 uses rather simple process formulations and is confined to a single layer. Its model input consists of the annual average atmospheric deposition flux. Parameter values were assigned by using data relating to either soil type or vegetation, irrespective of the location. Aggregated soil and vegetation maps were used to link parameter values to a specific location, using (pedo)transfer functions.

The objective of the present paper was to quantify the uncertainty in long-term forecasts of soil solution concentrations of Al and NO$_3$ resulting from of the uncertainty in maps and model parameters available on the European scale. We focused on the 15 member states of the European Union (EU). Compared to Europe

as a whole, this means that we could use more detailed information, such as the 1:1 000 000 soil map of the EU (EC, 1985). Furthermore, we limited ourselves to a case study, using the Netherlands as an example. The sources of uncertainty investigated included: (i) soil and vegetation maps (categorical data), and (ii) soil-related and vegetation-related parameters (continuous data). Apart from quantifying uncertainties in model outputs, the most important aim was to quantify the relative contributions of the various sources of uncertainty investigated. The uncertainty associated with the model structure itself was not taken into account.

Uncertainties in model outputs are presented as prediction intervals (i.e. the 90% confidence interval). Prediction intervals were obtained by a Monte Carlo analysis using Latin Hypercube Sampling of spatially correlated fields. Relative contributions of individual sources of uncertainty to the output uncertainty were investigated by an analysis of variance of the Monte Carlo sample of the model outputs.

3.2.2   Methods and materials

Model application

The SMART2 model

SMART2 (Chapter 2.3, Kros *et al.*, 1995a) predicts changes in H, Al, base cation (BC), NO_3 and SO_4 concentrations in the soil solution, as well as solid phase characteristics depicting the acidification status, i.e. carbonate content, base saturation and readily available Al content. The SMART2 model consists of a set of mass balance equations, describing the soil input-output relationships, and a set of equations describing the rate-limited and equilibrium soil processes (See Chapter 2.3).

The soil solution chemistry in SMART2 depends on the net element input from the atmosphere (the product of deposition and filtering factor, i.e. a correction factor for the roughness length of the canopy) and groundwater (seepage), canopy interactions (foliar uptake, foliar exudation), geochemical interactions in the soil (CO_2 equilibria, weathering of carbonates, silicates and/or Al hydroxides, SO_4 sorption and cation exchange), and nutrient cycling (litterfall, mineralisation, root uptake, nitrification and denitrification). The growth of the vegetation and litterfall are modelled by a logistic growth function, which acts as a forcing function. Nutrient uptake only stops when the soil solution concentration of the corresponding nutrient becomes zero. Soil interactions are either described by simple, rate-limited (zero-order) reactions (e.g. uptake and silicate weathering) or by equilibrium reactions (e.g. carbonate and Al-hydroxide weathering and cation exchange). The influence of environmental factors, e.g. pH and temperature, on weathering and exchange reactions is ignored. Solute transport is described by assuming complete mixing of the element input within one homogeneous soil compartment with a constant density and a fixed depth (generally the root zone). Because SMART2 neglects vertical heterogeneity, it predicts the concentration of the soil water leaving the root zone.

The annual water flux percolating from this layer equals the annual precipitation excess, which must be specified as a model input. The time step of the model is one year, so seasonal variations are not considered.

Model inputs and outputs

Input data for the SMART2 application include system inputs and initial values of variables and parameters. Input data refer to (i) a specific deposition scenario for each grid cell, (ii) model variables and parameters which are either related to a soil type or a vegetation or to a combination of both, and (iii) soil and vegetation maps. System inputs are the atmospheric deposition, hydrology and vegetation development. All input data were derived as a functions of location (grid cell), soil type or vegetation, or a combination of vegetation and soil type.

For the European-scale application, the soil and vegetation maps were aggregated and rasterised towards a 1×1 km^2 grid, using the dominant soil type and vegetation respectively (Kleeschulte, 1997). Seven soil classes were distinguished: poor sand (SP), rich sand (SR), calcareous sand (SC), non-calcareous clay (CN), calcareous clay (CC), loess soils (LN) and peat soils (PN). We used four vegetation structure types: coniferous forest (CON), deciduous forest (DEC), heather (HEA) and non-fertilised grassland (GRP) (Tables 2 and 3). The aggregation of soil types was based mainly on soil chemistry criteria, i.e. presence of calcite, texture, and base saturation. Moisture condition was not taken into account as a separate criterion, because this information was not available on the European scale. The range of vegetation structure types chosen, was mainly determined by the data availability on the European scale. Ideally, coniferous forest should be split up into spruce forest (i.e. forests with large forest filtering, growth rate and transpiration rate) and pine forest (i.e. forest with moderate forest filtering, growth rate and transpiration rate), but this was not feasible on the European scale.

Table 1 Soil categories considered

Code	Soil Class	Common soil types		Characteristics
		FAO (FAO, 1981)	USDA-SCS	
SP	Sand Poor	Humic and Orthic Podzols (1)[1]	Entic Haplortod	Coarse texture, low CEC, low weathering rate
SR	Sand Rich	Gleyic Podzols (1)	Typic Haplaquod	Finer texture, slightly larger CEC and weathering rate as SP
SC	Sand Calcareous	Gleyo-calcaric Fluvisol (1)	Hydraquent	All calcareous sandy soils
CN	Clay Non-calcareous	Fluvisols (2,3,4)	Hydraquent	Large weathering rate, large CEC
CC	Clay Calcareous	Calcaric Fluvisols (2,3,4)	Hydraquent	Calcareous, large weathering rate, large CEC
PN	Peat Non-calcareous	Histosols (NA)	Medihemist	CEC
LN	Loess Non-calcareous	Orthic Luvisols[2] (3)	Typic Hapludalf	Moderately large weathering rate and CEC

[1] Figures in brackets refer to texture classes: 1: coarse: clay content less than 18%, 2 = medium: clay content between 18 and 35% and 3 = fine: clay content greater than 35%. NA: not applicable

[2] For geographical reasons, luvisols outside the loess area were included in the CN class

Table 2 Vegetation categories considered

Code	Vegetation Class	Forest type, from EU Landcover data base	Characteristics
DEC	Deciduous forest	Broad-leaved forest Mixed forest	Needle or leave shedding trees with low forest filtering, growth rate, and transpiration rate
CON	Coniferous forest	Coniferous forest	Evergreen trees with moderate forest filtering, growth rate, and transpiration rate
GRP	(Nutrient-poor) Grassland	Natural grassland	moderate growth rate, low filtering
HEA	Heathland	Moors and heathland	low growth rate, low filtering

Although SMART2 is intended to be used on a regional scale, it still operates at the point support. In order to assess soil-water quality on a regional or European scale (e.g. for 5×5 km² or larger blocks), the model was applied to many point locations within each block. Subsequently, model results at these point locations were aggregated to yield a single block value. An important reason for not applying the model directly at the block scale (i.e. 'upscaling' the model by feeding it with block-aggregated inputs) was that it is extremely difficult to define the right form of input aggregation. Because SMART2 is a non-linear model, simply averaging the inputs prior to running it will usually not yield the block-averaged model output (Heuvelink and Pebesma, 1999).

The model output investigated was mainly limited to the annually averaged Al concentration at a depth of 1 m (i.e. below the root zone for all ecosystems considered). Model outputs were generated for point locations on a 1×1 km² grid located in semi-natural ecosystems. For the Netherlands, which was used as a case study, this resulted in 7 435 1×1 km² point locations for which calculations were performed. Model outputs for these point values were aggregated to block values for 5×5 km² blocks, by taking (i) the median concentration value from the points within each block and (ii) the percentage of the area in which the individual concentration values exceeded a specific environmental standard.

Within the European Union, the threshold values for the Al concentration in drinking water are as follows (EU Council Directive 80/778/EEC). The guide value is 0.05 mg l^{-1} (0.006 mol$_c$ m^{-3}), while the maximum allowable concentration (MAC) is 0.2 mg l^{-1} (0.02 mol$_c$ m^{-3}). In the present study, we focused on the MAC value. The MAC value for drinking water, however, is less relevant when phreatic groundwater is concerned, as was the case in our study. For the protection of the deeper groundwater used in the preparation of drinking water, the Al concentration at the bottom of the root zone could be allowed to exceed the MAC, because considerable immobilisation of Al may occur between phreatic groundwater and the level of drinking water wells. Therefore, we used a less stringent threshold, which is related to forest vitality, i.e. 0.2 mol$_c$ m^{-3} (De Vries, 1994), although the scientific support for this threshold is rather weak. For NO$_3$, we used only the MAC as the threshold value, i.e. 50 mg l^{-1} (0.8 mol$_c$ m^{-3}).

Uncertainty analysis

General Approach

A Monte Carlo approach a large number of equally probable realisations of the model input data are generated, followed by running the model for each set of realisations. At a sufficiently large number of runs, the uncertainty in the model output can be derived from the variability of the output of all Monte Carlo runs. The reasons for using Monte Carlo analysis were that (i) no assumptions have to be made about the model, and (ii) it can easy handle the spatial application, i.e. the inclusion of spatial correlations. In order to limit the computation load, we used Latin Hypercube Sampling (cf. Chapter 2.2).

For a given 5×5 km² grid cell, a single Monte Carlo run resulted in a distribution of model results for each point in a 1×1 km² grid. The entire Monte Carlo sample yielded an ensemble of distributions. Each Monte Carlo sample allowed us to estimate the median concentration for each block or the areal fraction of each block exceeding a threshold. Using sample order statistics, we constructed 90% prediction intervals for the block median concentration and for the block areal fraction exceeding a threshold.

Two Monte Carlo experiments were used, one to quantify the output uncertainty and one to quantify the uncertainty contributions of the categorical maps, continuous soil parameters, and continuous vegetation parameters. In order to obtain the prediction intervals for block-aggregated model outputs resulting from the uncertainty in all inputs considered, a nested Monte Carlo experiment was carried out simulating 25 realisations of the categorical map, and 25 realisations of continuous maps attached to the categorical maps. This led to a total of 625 Monte Carlo simulations with SMART2 for each 1×1 km². This was done because the continuous maps (with the continuous soil-related and vegetation-related parameters) depend on the categorical maps (i.e. combined EU soil/vegetation).

The relative contributions of the three individual sources of uncertainty were quantified using an ANOVA experiment (Jansen *et al.*, 1994), which was also nested. For each of the 25 realisations of the combined soil/vegetation map, five realisations of the soil-related parameters were crossed with five realisations of the vegetation-related parameters. This also resulted in 625 ($25 \times 5 \times 5$) Monte Carlo simulations. The stability of the calculated variances was checked visually by comparing the differences between two executions of the experiment. Using analysis of variance for each 5×5 km² block, the total variance of the results was split into contributions from (i) categorical maps, (ii) soil-related parameters, (iii) vegetation-related parameters, and (iv) interaction. Latin Hypercube Sampling was not used for this experiment, because the sample size (five) would disturb the spatial correlation too much.

Uncertainty in categorical data

The uncertainty in the categorical data, i.e. the aggregated soil and vegetation maps, was quantified by comparison national maps and EU maps, assuming that the national maps represent the 'ground truth' (i.e. the real world). Obviously, European scale maps having a smaller resolution compared to national maps. For an application on the European scale, however, European maps are often essential. Data from national sources either require substantial edge matching at national borders, or might be based on data collection using different basic assumptions. The second approach leads to data sets which are difficult to compare (cf. Kleeschulte, 1997). The maps of the Netherlands we used included a aggregated version of the 1:50 000 digital soil map (De Vries and Denneboom, 1992) and a 25×25 m² pixel satellite image for the vegetation (Noordman *et al.*, 1997). The EU maps comprised the 1:1 000 000 soil map of the EU (EC, 1985) and the EU landcover database (Corine land cover database, scale 1:1 000 000; EC, 1993). The soil map of the Netherlands (NL-map) and the EU soil map (EU-map) were aggregated to seven soil types, while both vegetation maps were aggregated to four vegetation types. The EU-maps were rasterised to a 1×1 km² grid, whereas the NL-maps remained at their original resolution. An example for the soil map is shown in Figure 1. Figure 1 illustrates the error introduced by using the EU soil map instead of the soil map of the Netherlands.

Because it is likely that soil type and vegetation type are dependent, the different categories were combined to unique categorical variables. The derived error variances, nugget variances and sill variances were stored in error matrices, as described in Finke *et al.* (1999). Variograms were only fitted for matrix elements belonging to an EU-stratum in which the summed NL-classes were larger than 1 500 ha or occupied more than 2.5% of the EU-stratum, this yielded 89 matrix elements. Using the indicator variables, exponential variograms with a nugget were fitted, using the geostatistical program GSTAT (Pebesma and Wesseling, 1997). The remaining matrix elements were modelled as spatial white noise, i.e. no spatial correlation. Using sequential multiple indicator simulation of categorical variables, equally probable realisations of the 'true' maps were generated.

The assumption that the maps of the Netherlands represent 'reality' causes an underestimation of the uncertainty in the EU-maps, because (i) the detailed NL-maps are, of course subject to uncertainty too and (ii) the EU maps and the maps of the Netherlands maps are not derived from independent sources. The uncertainty thus derived reflected the uncertainty due to the use of European databases instead of more detailed national data, as was aimed in this study. The uncertainty in the maps of the Netherlands is known to some extent. The fraction of the area occupied by a land cover type which actually corresponds to its classification (i.e. the map accuracy) is near 90% for natural vegetation (Noordman *et al.*, 1997). The target accuracy of the 1:50 000 soil map of the Netherlands is 70% (Steur and Heijink, 1991).
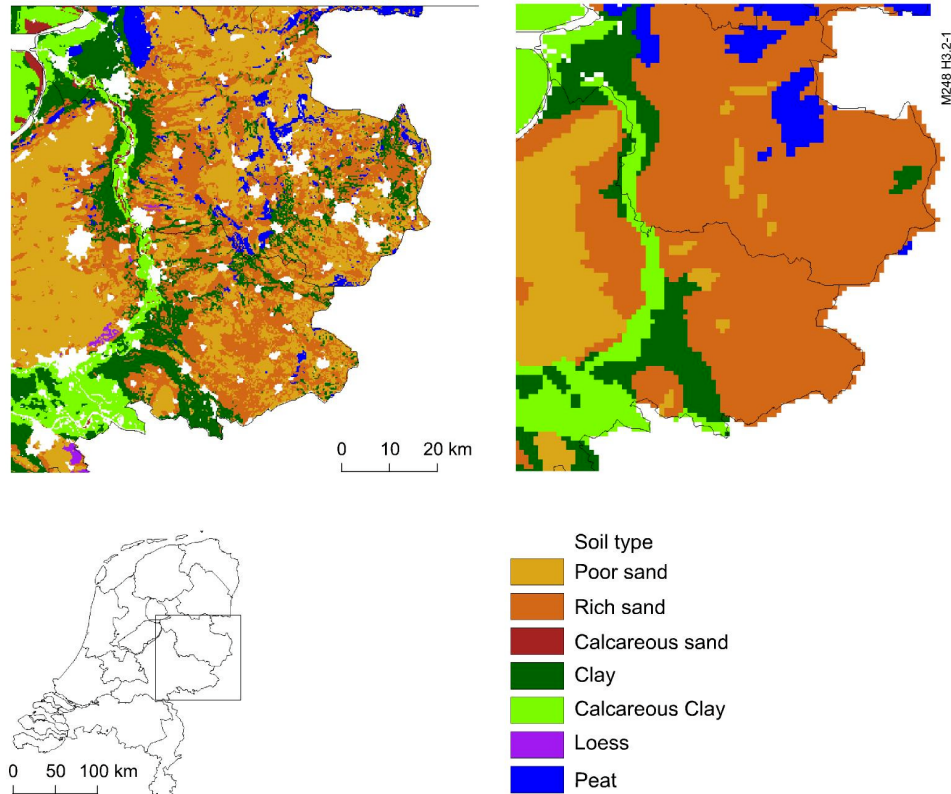
Figure 1 Fragments of the 1:50 000 soil map of the Netherlands and the 1:1 000 000 soil map of the EU

Uncertainty in continuous data

The selection of continuous parameters to be included in the uncertainty analysis was based on the results of a sensitivity analysis and on process knowledge. Parameters that were *a priori* considered to be either rather certain, e.g. carbonate equilibrium or insensitive, e.g. sulphate sorption constants were omitted from the analyses. In addition, litterfall parameters were not included, because they mainly affect the soil solution concentration in the topsoil and not at the bottom of the root zone (cf. Kros *et al.*, 1993). As a result, eight vegetation-related parameters and eleven soil-related parameters were included in the uncertainty analysis (Table 3). Each vegetation-related parameter was specified for four vegetation classes, while each soil-related parameter was specified for seven soil classes, by means of class transfer functions. Each class transfer function (i.e. $11 \times 7 + 8 \times 4 = 109$ class/parameter combinations) consisted of an average value, a minimum value, a maximum value, a variogram and cross correlations (correlations between variables) with other parameters in the same class.

Table 3 Characterisation of parameters inspected

Codes	Description	Affect[3]	Distr. Type[4]	Cross Correlation[5]	Spatial Correlation[6]	Derived from
Vegetation-related parameters						
$ffSO_2$	Forest filtering SO_2	Al	N	+	-	literature[7]
$ffNH_3$	Forest filtering NH_3	NO_3	N	+	-	literature
$ffNO_x$	Forest filtering NO_x	NO_3	N	+	-	literature
f_{dd}	Dry deposition factor	Al	N	+	-	literature
Tr [1]	Transpiration	Al, NO_3	N		*	literature/ calibration
Am_{stmx}	Amount of stems	NO_3	N		*	Literature
ctN_{sh}	N content in shoot/stem	NO_3	N		*	Literature
k_{mimx}	Mineralisation rate constant	Al, NO_3	N		*	Literature
Soil-related parameters						
CN_{om}	C/N ratio of organic matter	Al, NO_3	L	*	+	EFSDF
fr_{nimx}	Nitrification fraction	Al, NO_3	N		*	calibration
fr_{demx}	Denitrification fraction	Al, NO_3	N		*	calibration
KAl_{ox}	Dissolution constant Al_{ox}	Al	N		+	Derived from 250 monitoring sites in the Netherlands
$ctAl_{ox}$ [3]	secondary Al compounds	Al	L		+	EFSDF[8]
Na_{we} [2]	Na weathering rate	Al	N		*	Literature/ EFSDF
$BC2_{we}$ [3]	BC2 weathering rate	Al	N		*	Literature/ EFSDF
CEC [3]	CEC	Al	L	*	+	EFSDF
$frBC2_{ac}$ [3]	Fraction BC2 at CEC	Al	N	*	+	EFSDF
KAl_{ex}	Al-BC2 exchange constant	Al	N		+	Derived from 250 monitoring sites in the Netherlands [9]
KH_{ex}	H-BC2 exchange constant	Al	N		+	Derived from 250 monitoring sites in the Netherlands [9]

[1] Transpiration rate basically depends on both vegetation and soil, but we have only included the dependence on vegetation

[2] K_{we} was set equal to Na_{we}.

[3] Refers to soil solution concentrations of Al and NO_3; other model outputs were not considered in the present study

[4] N = normal; L = lognormal

[5] The symbols '*' and '+' indicate groups of parameters which were cross-correlated, no symbol means no cross-correlation assumed

[6] '-': no spatial correlation, simulated as white noise; '*': spatial correlation was estimated, based on process knowledge; '+': spatial correlation was derived from fitting experimental variograms, using data from 250 monitoring sites (Leeters *et al.*, 1994; Klap *et al.*, 1999)

[7] 'literature' refers to Kros *et al.* (1993), Kros *et al.* (1995a), and references therein

[8] European Forest Soil Data Base (Reinds, 1994)

[9] See Leeters *et al.* (1994) and Klap *et al.* (1999)

Cross correlations across classes were not taken into account. Parameter distributions types were assumed to be either normal or lognormal. The uncertainty in continuous data was based on the literature, on a database covering about 250 extensively monitored forest sites in the Netherlands (NLFSDB, Leeters *et al.*, 1994; Klap *et al.*, 1999), and on a European Forest Soil Database (EFSDB, Reinds, 1994). For those model parameters for which it was not possible to derive statistical properties from existing data sets, the minimum and maximum values were estimated. These parameters included forest filtering, nitrification and denitrification fractions, and weathering rates. In these cases, the standard deviation was estimated from the minimum and maximum value by (max - min) / 4 and the distribution type was assumed to be normal. Minimum and maximum values from national sources were decreased by about 10% and increased by about 10% respectively, in order to derive a range for the European scale.

Cross correlations were included between all forest filtering factors (Table 3), based on process knowledge (Kros *et al.*, 1993). Cross correlations were assigned to the C/N ratio of organic matter (CN_{mo}), cation exchange capacity (*CEC)* and the initial base saturation (*fr*$BC2_{ac}$), based on data in the NLFSDB and EFSDB.

As with the categorical data, spatial correlation was also included for the continuous data. Therefore, variogram models were fitted with exponential variograms using the available data (i.e. NLFSDB). When no data was available for the derivation of spatial correlation, spatial correlation was taken into account by assuming a spatial correlation over a distance of 5 km. Spatial correlation was omitted only for those parameters that obviously lacked spatial dependence. These parameters were simulated as spatial white noise, i.e. no spatial correlation (Table 3).

The distribution attributes and the variogram parameters for each generated combined soil/vegetation map (i.e. categorical data) were used to generate equally probable realisations of maps, using non-conditional, stratified, sequential, multivariable Gaussian simulation (Pebesma and Wesseling, 1997).

The following uncertainties in model input data were excluded from the uncertainty analysis: (i) deposition scenario (variable in space and in time) and (ii) soil or vegetation-related parameters. Because the product of the filtering factors (*ff*SO_2, *ff*NH_3, *ff*NO_3) and the deposition yields the site specific deposition flux, all of the uncertainty in the spatial pattern of the deposition was loaded on the forest filtering factors. Uncertainties in the temporal evolution of the deposition scenario were excluded because these are mainly the result of political and technical factors (e.g. the feasibility of emission reduction measures).

The uncertainty analysis was performed using an existing national deposition scenario, because no detailed scenarios were available on the European scale. We believe that existing acidification scenarios (Alcamo *et al.*, 1990) are too rough for our purpose. Consequently, we used an official deposition scenario from the Netherlands Environmental Outlook (RIVM, 1997). This scenario includes predictions of SO_2, NO_x, and NH_3 deposition for the years 1995, 2000, 2010, and 2020, for each 1×1 km^2 grid cell. Annual averaged values are presented in Table 4. In order to mimic European data, the deposition scenario was aggregated to a 20×20 km^2 grid, because

it is likely that European-scale scenarios with this level of detail will become available in the near future.

Table 4 Average values of N deposition and potential acid deposition for the deposition scenario[1] used

Year	N deposition	Potential acid
	$(mol_c\ ha^{-1}\ a^{-1})$	
1995	2 119	3 193
2000	1 858	2 653
2010	1 661	2 281
2020	1 642	2 301

[1] The Netherlands Environmental Outlook presents three scenarios for atmospheric deposition. For this study we used the 'middle-of-the-road' scenario, called the European Co-ordination (EC) scenario

Although annual precipitation values are available for Europe, we also used precipitation data from the Netherlands. We used data representing the long-term annual averaged precipitation on a $10 \times 10\ km^2$ grid data (cf. De Vries *et al.*, 1994c). As with the deposition data, the $10 \times 10\ km^2$ grid data was aggregated to $20 \times 20\ km^2$ grid mean values.

3.2.3   Results and discussion

Uncertainty in Model Predictions

Uncertainties in model forecasts are presented as 90% prediction intervals for $5 \times 5\ km^2$ block-aggregated values in 1995 and 2020 as: (i) the block median Al concentration (Figure 2), (ii) the block areal percentage where the Al concentration exceeds the MAC value (0.02 $mol_c\ m^{-3}$; Figure 3), and (iii) the block areal percentage where the Al concentration exceeds the forest vitality criterion (0.2 $mol_c\ m^{-3}$; Figure 4).

It is clear that the uncertainty in the predicted Al concentration was large (Figure 2). For a substantial part of the country, the block median concentration exceeded 0.2 $mol_c\ m^{-3}$, i.e. the critical value for forest vitality, both in 1995 and 2020. This is also illustrated by Table 5, which presents the median values of all $5 \times 5\ km^2$ blocks (i.e. the entire map) for different statistical parameters. Despite the high levels of uncertainties, the spatial differentiation was large. The largest concentrations occurred in the central and southern parts of the country. These are the areas with large atmospheric deposition and poor sandy soils (SP). Low concentrations occurred along the western coastline, where calcareous sandy soils (SC) dominate, and in the centre of the country, i.e. newly re-claimed land with calcareous clay soils (CN). Because the spatial variation in pH and the related Al concentration are mainly determined by the soil-related parameters (Kros *et al.*, 1995a), Table 6 summarises the median values, for all $5 \times 5\ km^2$ blocks (i.e. the entire map), of various statistical parameters per soil type. The uncertainty was found to be smaller (90% prediction interval about [0, 1] in 1995, cf. Table 6) for the low concentration areas (mainly SC

and CN) than for the areas with large concentrations (mainly SP) (90% prediction interval about [0.1, 2.8] in 1995, Table 6). In terms of the coefficient of variation (CV), however, the opposite was found: a large CV for SP and CC soils and a low CV for SP soils. The reducing deposition scenario clearly resulted in a decrease in the spread of the prediction interval, and a clear shift towards smaller values: both the lower side (P05, i.e. the 5-percentile) and the upper side (P95, i.e. the 95-percentile) of the prediction interval decreased. As for the median values for the map as a whole (Table 5), the lower side (P05) decreased from 0.02 to 0.01, while the upper side (P95) decreased from 2.1 to 1.3. The deposition scenario clearly affected the various soil types in the same way, i.e. smaller mean and median values and a narrower 90% prediction interval, although the CV hardly changed.
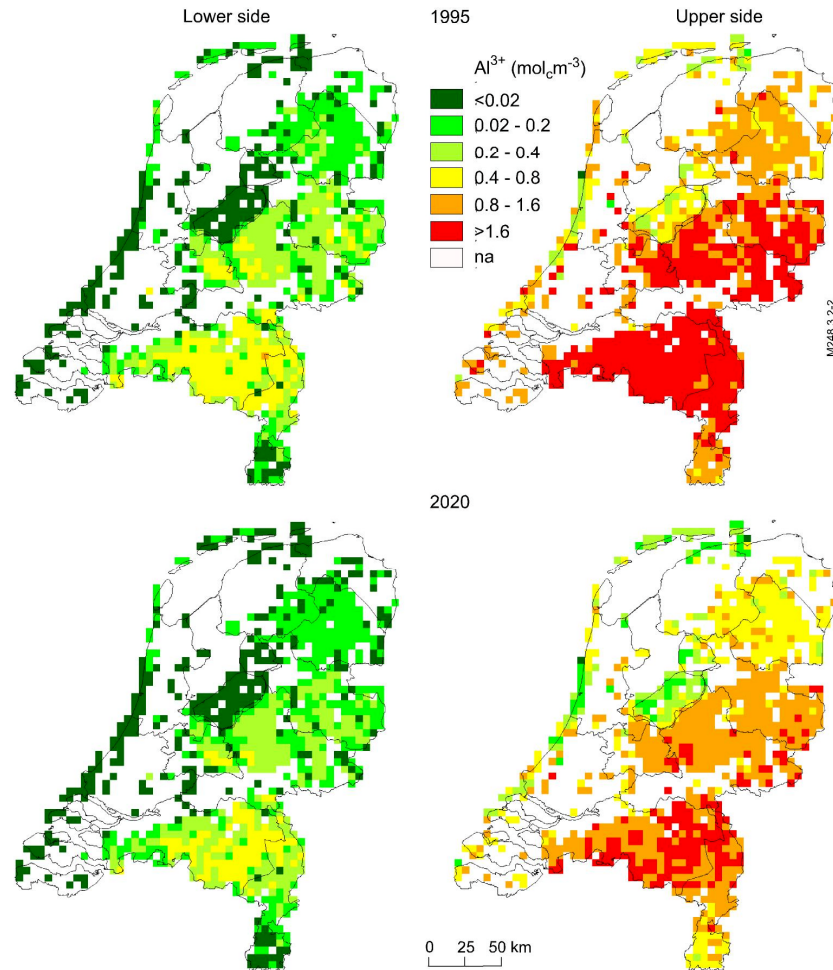

Figure 2 The 90% prediction interval (left: lower side; right: upper side) of the block median Al concentration for 5 x 5 km^2 blocks, for 1995 (top) and 2020 (bottom)
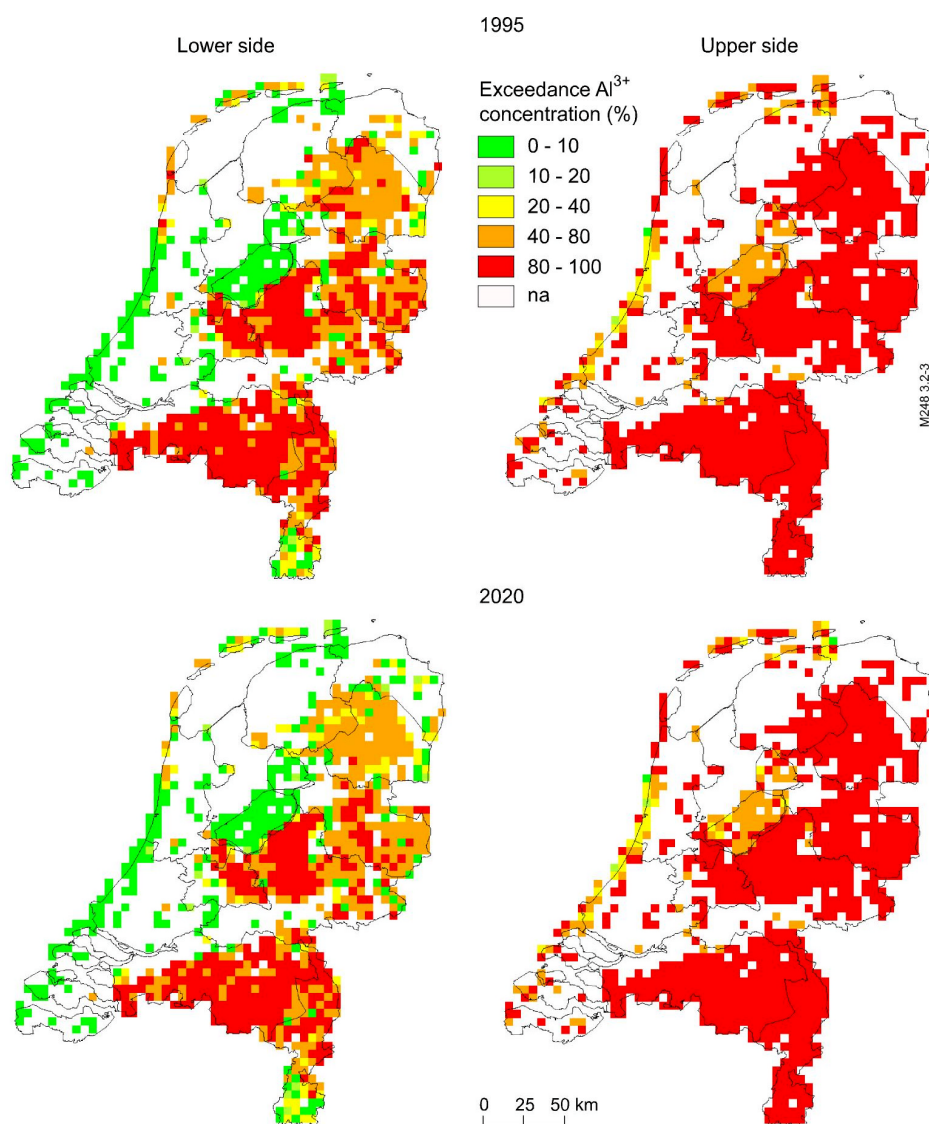
Figure 3 The 90% prediction interval (left: lower side; right: upper side) of the block areal percentage where the Al concentration exceeds the MAC value for Al (0.02 mol$_c$ m^{-3}) for 5 x 5 km^2 blocks, for 1995 (top) and 2020 (bottom)

Table 5 Median values over the entire map of 5×5 km^2 blocks of the 90% prediction intervals (P05 = lower side; P95 = upper side), the median, the mean, and the coefficient of variation (CV) of the Al concentration (Al), areal exceedances for the Maximum Allowable Concentration (Al$_{ex\ 0.02}$), and the forest vitality criterion (Al$_{ex\ 0.2}$), for 1995 and 2020

Output	Year	P05	P95	median	mean	CV
Al	1995	0.02	2.09	0.40	0.66	0.99
(mol$_c$ m^{-3})	2020	0.01	1.33	0.28	0.42	0.99
Al$_{ex\ 0.02}$	1995	71	100	100	93	0.12
(%)	2020	63	100	95	89	0.15
Al$_{ex\ 0.2}$	1995	25	100	71	67	0.35
(%)	2020	14	100	60	60	0.43

The uncertainty in the percentage of the block area where the Al concentration exceeding the MAC value (Figure 3) was small, especially in the areas with large concentrations. This was obviously, due to large predicted Al concentrations (median value about 0.4 mol$_c$ m^{-3}) in comparison with the MAC criterion (0.02 mol$_c$ m^{-3}). Exceptions were the calcareous soils, along the western coastline (i.e. sandy soils) and the newly re-claimed land in the centre (i.e. clay soils), in which the predicted Al concentrations were much smaller (90% prediction interval about [0, 67]). Using the less stringent forest vitality criterion (0.2 mol$_c$ m^{-3}) yielded a much larger uncertainty in the exceedance area, but it was still smaller than the uncertainty in the Al concentration (see also Table 5). Furthermore, unlike the exceedance area of the MAC value, that for the forest vitality criterion showed a decrease in exceedance as a result of the decreasing deposition scenario. Although this decrease was restricted to the areas with relatively low Al concentrations.

1995

Lower side

Upper side

Exceedance Al³⁺
concentration (%)

0 - 10

10 - 20
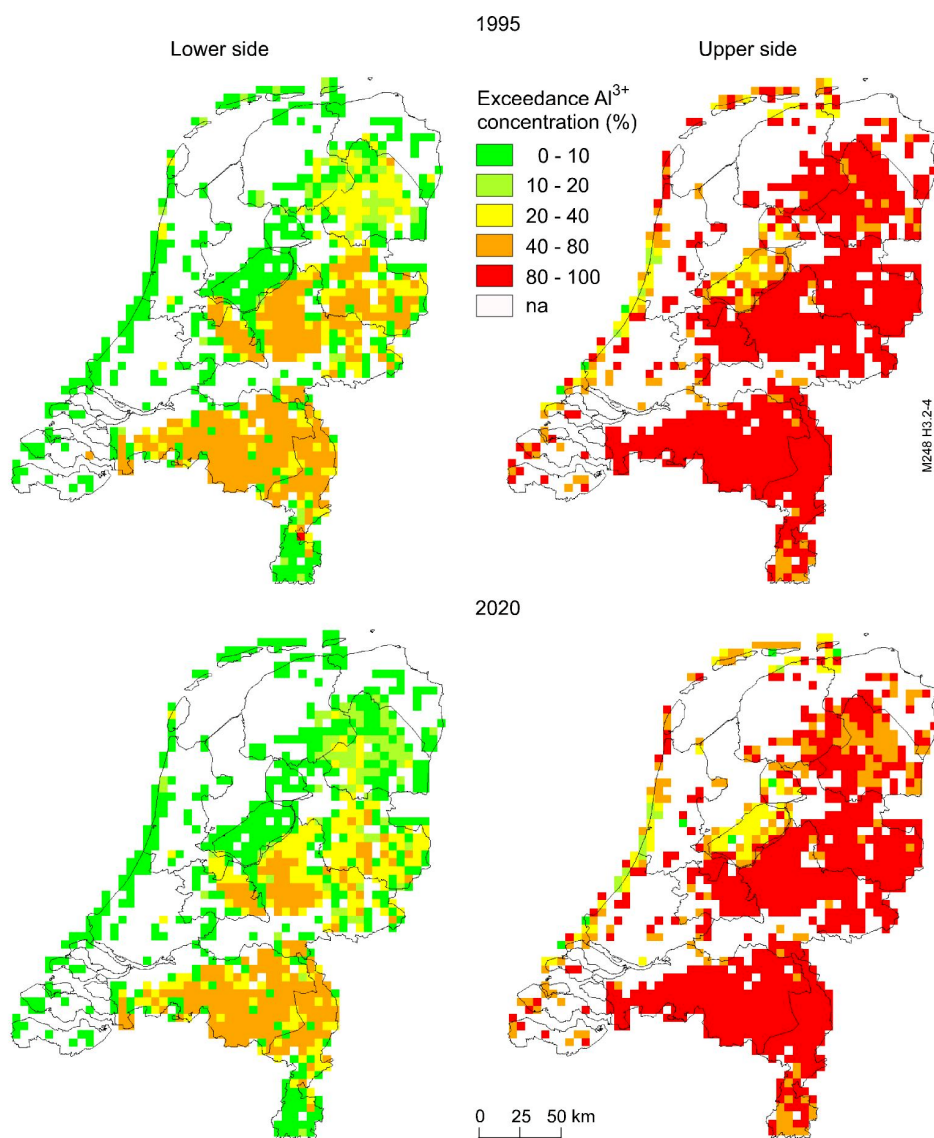
20 - 40

40 - 80

80 - 100

na

2020

0   25   50 km

Figure 4 The 90% prediction interval (left: lower side; right: upper side) of the block areal percentage where the Al concentration exceeds the forest vitality criterion for Al (0.2 mol$_c$ m^{-3}) for 5 x 5 km² blocks, for 1995 (top) and 2020 (bottom)

187

Table 6. Median values over the entire map of 5 × 5 km² blocks of the 90% prediction intervals (P05 = lower side; P95 = upper side), the median, the mean, and the coefficient of variation (CV) of the Al concentration (mol$_c$ m³) in 1995 and 2020 for various soil types[1]

Soil type	Year	P05	P95	median	mean	CV
SP	1995	0.09	2.80	0.82	1.10	0.80
	2020	0.07	1.90	0.66	0.78	0.74
SR	1995	0.03	2.43	0.60	0.85	0.91
	2020	0.02	1.61	0.44	0.58	0.88
SC	1995	0.00	0.73	0.00	0.09	3.85
	2020	0.00	0.45	0.00	0.06	3.84
CC	1995	0.00	1.08	0.00	0.15	2.54
	2020	0.00	0.59	0.00	0.09	2.76
CN	1995	0.01	2.07	0.28	0.56	1.15
	2020	0.00	1.22	0.16	0.33	1.15
PN	1995	0.00	1.36	0.19	0.37	1.25
	2020	0.00	0.80	0.10	0.21	1.32
LN	1995	0.00	1.47	0.09	0.30	1.61
	2020	0.00	0.85	0.05	0.17	1.62

[1] Dominant soil type within a 5 × 5 km² grid cell according the EU soil map

Relative Uncertainty Contribution

The relative contributions of the three uncertainty sources (i.e. the combined soil/vegetation map, continuous soil-related, and continuous vegetation-related parameters), are presented as (i) the corresponding variances for the median Al concentration for the 5 × 5 km² blocks (Figure 5) and (ii) summarised in a figure presenting the average variances for the maps of 5 × 5 km² block aggregated values for the Al and NO$_3$ concentrations and the exceedances (Figure 6).

The results show that the variance in soil parameters accounted for more than 50% of the total variance for almost all grid cells, whereas the vegetation parameters accounted for less than 10% of the total variance for almost all grid cells (Figure 5). The contribution of the categorical maps to the total uncertainty was clearly larger than that of the vegetation parameters. Remarkably, the uncertainty contribution of the categorical data was large mainly for soils with low Al concentrations (i.e. mainly calcareous soils). This was probably due to mis-classification of calcareous soils in the EU map. A calcareous soil results in a negligible Al concentration, whereas under the same circumstances a non-calcareous poor sandy soil may result in a considerable Al concentration. Note, however, that Figure 5 only presents the main effects of the three sources of uncertainty, scaled to the sum of the three main effects.
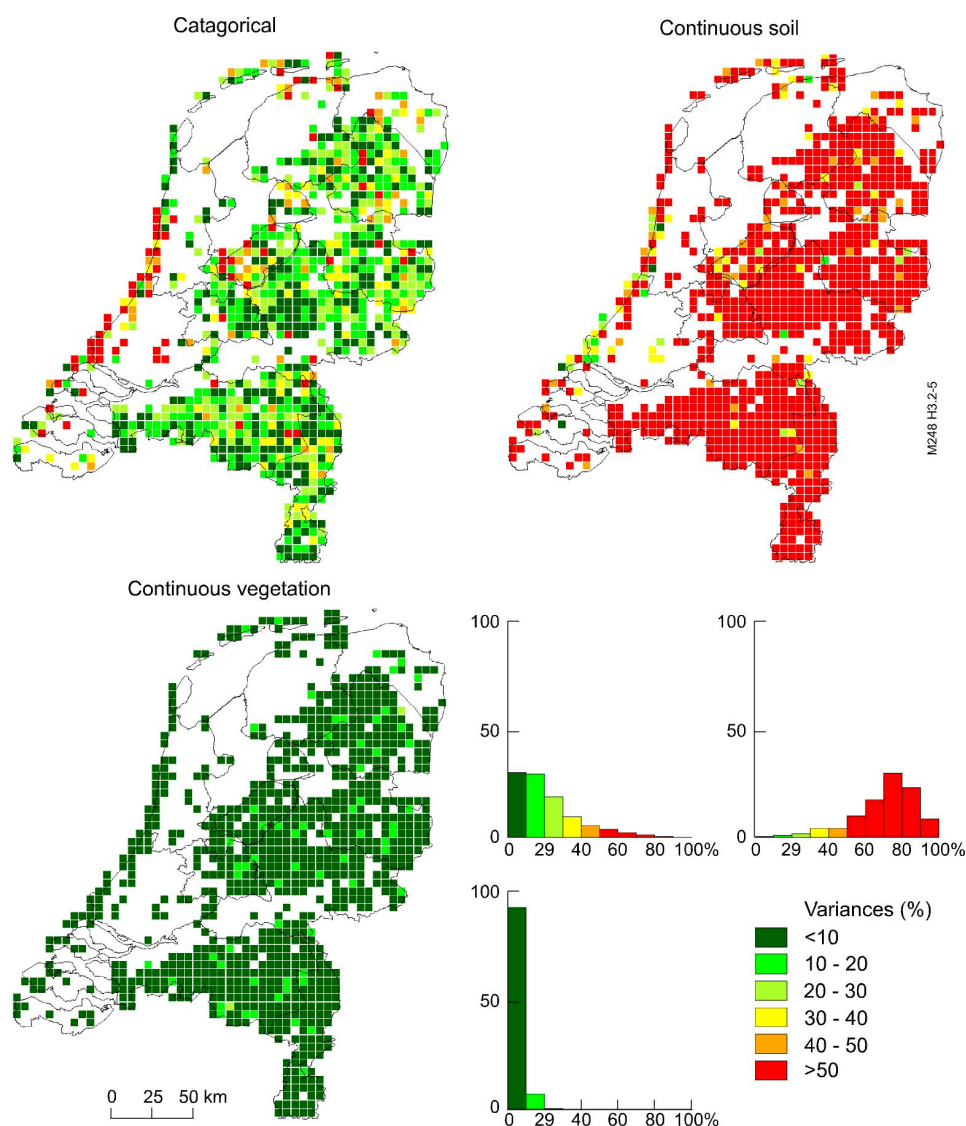
Figure 5 Relative variance (percentage of the sum of the three main variance components) of the soil and vegetation maps (Categorical), continuous soil-related parameters (Continuous Soil) and continuous vegetation-related parameters (Continuous Vegetation) for the median Al concentration for 5×5 km^2 blocks, for 1995

Relative uncertainty contributions were summarised by calculating the average contributions of the variances of the three uncertainty sources to the total variance of the inspected model outputs for the whole map with 5×5 km^2 blocks (Figure 6). Contrary to Figure 5, the main effects were not scaled to the sum of the main effects,

189

so the figure presents an interaction term. It is clear that the uncertainty in the continuous soil parameters contributed most to the uncertainty in the Al concentration, as well as to the uncertainties in areal exceedances. This was confirmed by an uncertainty analysis performed with comparable models (see Chapter 2.2; Kros *et al.*, 1993), which concluded that the uncertainty in the Al concentration at the bottom of the root zone, as well as the associated pH, is mainly determined by typically soil-related parameters, e.g. KAl_{ox} and $ctAl_{ox}$. It should be stressed, however, that the situation in the top soil may differ, because the Al concentration and the associated pH in the top soil are strongly affected by the nutrient cycle (see Chapter 2.2; Kros *et al.*, 1993) through vegetation-related parameters such as ctN_{sh} and k_{mimx}. This is, however, not relevant for leaching towards the phreatic groundwater.
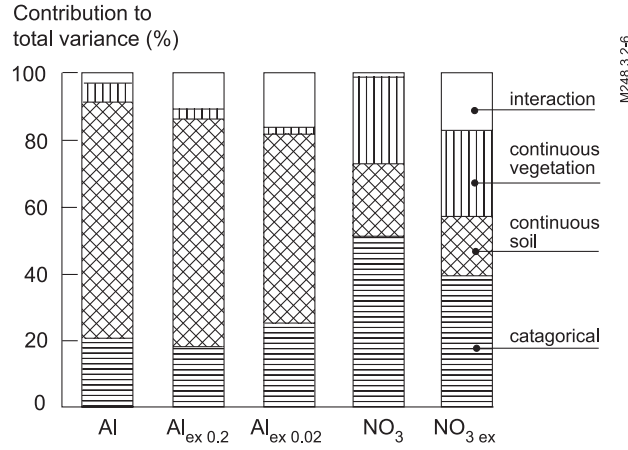

Figure 6 Average variances over the entire map of 5×5 km^2 blocks of the three main components and the interaction component explaining the total variance in various model outputs for 1995

Results for NO$_3$, however, were markedly different. For both the NO$_3$ concentration and the exceedance, the largest uncertainty contribution originated from the categorical data, followed by the continuous vegetation-related parameters, whereas the smallest contribution stemmed from the continuous soil-related parameters. Unlike Al, the NO$_3$ concentration and exceedance at the bottom of the root zone were generally determined to a larger extent by vegetation processes, e.g. ctN_{sh}, $ffNH_3$, $ffNO_3$, making the uncertainty contribution of the vegetation parameters more important than that of the soil parameters. Remarkably, the three exceedance parameters showed a larger interaction term than the two concentrations. This might be due to the fact that the exceedance parameters range from 0 to 1, whereas the concentration ranges from 0 to infinity. A 0 to 1 scale usually leads to skewed distributions, which may lead to large interaction terms. The skewness of the distributions is illustrated by the differences between the mean and median values in Table 6.

Regarding the uncertainty thus quantified, it is important to stress that the size of the grid cell considered (i.e. the size used for presenting the results) is critical, because aggregation to larger blocks leads to more accurate results (narrower prediction intervals) at the cost of the spatial resolution of the results. The number of categories used for soil type and vegetation (seven soil classes and four vegetation classes) may also affect the results. If more categories had been distinguished, the uncertainty in the continuous data could have become smaller, whereas the uncertainty in the categorical data could have become larger. For instance, the uncertainty in *CEC* might become smaller if the poor sandy soils are split into soils with high organic matter contents and those with low organic matter content. At the same time, the uncertainty in the two new soil classes would become larger. Thus, there is a trade-off in the uncertainty contribution between the categorical data and the continuous data, depending on the extent of aggregation. For the application of SMART2 on the European scale, splitting soil types or vegetation any further than was done here makes little sense, unless additional data necessary to estimate the newly introduced class transfer functions become available.

3.2.4 Conclusions

It is showed that the width of the prediction interval largely depends on whether block median concentrations or block areal exceedances are considered. The Al concentration showed wide 90% prediction intervals both for areas with low Al concentrations (i.e. SC and CC soils) and for areas with high concentrations (mainly SP soils). The implications of these wide intervals are probably most important for the calcareous soils (SC and CC). It is for these soils that the environmental thresholds (both 0.2 and 0.02) were within in the 90% prediction interval (0 to 1.1 mol$_c$ m^{-3}) in 1995, whereas for the SP soils the 90% prediction interval in 1995 ranged from 0.09 to 2.8 mol$_c$ m^{-3}. In conclusion, it is highly certain that the environmental threshold is exceeded in areas with high concentrations, but not in those with low concentrations. This effect was clearly illustrated by the 90% prediction intervals for the block areal exceedance of the MAC threshold, which showed a narrow prediction interval for the large concentration areas (SP soils) (95 to 100% in 1995 and 92 to 100% in 2020) and a wide interval for the low concentration area (SC and CC soils) (0 to 67%, both in 1995 and 2020). For the less stringent forest vitality criterion, however, this contrast was less pronounced.

For the scenarios evaluated, the model was able to predict a considerable decrease in Al concentration, despite the large prediction intervals due to uncertainty in the model input data. This effect was, however, less profound for the exceedances, which was especially true for the block areal exceedances of the MAC threshold.

The relative uncertainty contribution largely depended on the model output considered. For the Al concentration and the exceedances of the two Al thresholds, the soil-related parameters contributed most to the output uncertainty, whereas the uncertainty contribution of the vegetation-related parameters was negligible. By contrast, the results for NO$_3$ showed that the average uncertainty contribution mainly

191

stemmed from the categorical parameters, followed by the continuous vegetation-related parameters, whereas the continuous soil-related parameters contributed least. The larger contribution of the vegetation-related parameters to the uncertainty of the NO_3 concentration is due to the fact that N processes are dominated by the vegetation-related processes rather than by soil-related processes.

Given the large costs associated with measures to prevent increased Al and NO_3 concentrations, it is important to assess whether the collection of more data would result in a reduction of the prediction interval. From the present study useful information can be derived to support decisions on different alternatives for reducing uncertainties associated with long-term model predictions. Possible alternatives are either improving of the EU soil and vegetation maps (categorical parameters) or collecting additional input data in order to reduce the uncertainty in parameters (continuous parameters). Our study showed, however, that this largely depends on the model output considered.

Finally, it is important to notice that the present study only assessed the uncertainty in model output resulting from uncertainty in model inputs. We ignored sources of uncertainties related to the parameters not considered as uncertain, or those related to the model structure. Therefore, the presented prediction intervals should be considered with caution. If all input uncertainties were modelled correctly, the prediction intervals of the model output would at the best underestimate the true uncertainty. Further insight into the extent of underestimation would require a comparison of model results with measured values.

3.3 Assessment of the prediction error in a large-scale application of a dynamic soil acidification model

Abstract

The prediction error of a relatively simple soil acidification model (SMART2) was assessed before and after calibration, for the Al and NO₃ concentrations on a block scale. Although SMART2 was especially developed for application on a national to European scale, it still runs at a point support. A 5 × 5 km² grid was used for application on the European scale. Block characteristic values were obtained simply by taking the median value of the point support values within the corresponding grid cell. In order to increase confidence in model predictions on larger spatial scales, the model was calibrated and validated for the Netherlands, using a resolution that is feasible for Europe as a whole. Because observations are available only at the point support, it was necessary to transfer them to the block support of the model results. For this purpose, about 250 point observations of soil solution concentrations in forest soils were upscaled to a 5 × 5 km² grid map, using multiple linear regression analysis combined with block kriging. The resulting map with upscaled observations was used for both validation and calibration. A comparison of the map with model predictions using nominal parameter values and the map with the upscaled observations showed that the model overestimated the predicted Al and NO₃ concentrations. The nominal model results were still in the 95% confidence interval of the upscaled observations, but calibration improved the model predictions and strongly reduced the model error. However, the model error after calibration remains rather large.

3.3.1 Introduction

SMART2 is a model developed for the assessment of soil acidification and eutrophication on a large spatial scale (Kros *et al.*, 1995a). It is a relatively simple dynamic one-layer model that predicts soil and soil solution concentrations of major ions in non-agricultural soils in response to atmospheric deposition.

The reliability of large-scale forecasts with SMART2 is seriously hampered by uncertainties in the input data. In Chapter 3.2 (see also Kros *et al.*, 1999; Pebesma *et al.*, 2000) the prediction uncertainties in Al and NO_3 concentrations on a European scale due to uncertainty in input data have been quantified. These studies indicated that model predictions were very uncertain, mainly because of the uncertainty in model parameters related to crucial soil processes. To reduce these uncertainties and increase confidence in model predictions for large spatial scales, the model results need to be compared with observations. Although in most cases, model inputs and variables can be directly derived from the available literature or measurements, certain model parameters can only be derived in an indirect way. Consequently, there is a general shortage of knowledge about the precise values to be used, which seriously affects the credibility of the model results.

Reduction of uncertainty in simulated soil solution concentrations on a large spatial scale, may be achieved by a calibration in order to deduce more reliable values

for these parameters. Therefore, in the present study we calibrated the model SMART2 by using soil chemistry data for the Netherlands, assuming that the adaptation of model parameters would lead to more accurate model predictions at large spatial scales. In this paper, the term calibration is used for model parameter adjustment in view of observations of corresponding model output variables. The benefits of the model calibration procedure can be assessed by quantifying the model error for both the non-calibrated, using nominal parameter values, and the calibrated model. The only way to quantify the model error is through a model validation, achieved by comparing model results with independent observations, cf. Heuvelink and Pebesma (1999). Usually, observations originate from conventional soil sampling, resulting in a data set containing multiple values in some cells and no values in others. Furthermore, the scale of the observations for calibration and validation usually does not correspond with the scale of the model application. One of the expected effects is that variability caused by natural variability and outliers decreases as a result of the conversion from point support to block support (Heuvelink and Pebesma, 1999). Therefore, a procedure was developed to convert point scale data from about 250 forest stands in the Netherlands to a block scale data set.

In addition to model calibration, the upscaled monitoring data were also used to quantify the prediction error of the model. According to Heuvelink and Pebesma (1999), the only way to quantify the model error is through model validation. Like calibration, model must also be validated at a block support. The model error itself can be divided into a structural part and a part that originates from input uncertainty. The latter, the model input error, has been quantified previously (Kros *et al.*, 1999).

The present paper illustrates the benefits and feasibility of calibration on a large spatial scale (i.e. the Netherlands), in which point observations on soil solution chemistry were upscaled to the same support as the model results. Furthermore, we illustrate how to subdivide the model error into a model structure error and a model input error. The aim of this study was to reduce the level of uncertainty, and increase confidence in the quantification of the effects of soil acidification on the European scale. This was done by (i) searching for parameter sets that give an acceptable difference between model outputs and measurements, (ii) obtaining smaller ranges of model parameter values, i.e. reducing parameter uncertainty, and (iii) quantifying the model error for both nominal and calibrated model results. The results of the present study may in turn guide the gathering of additional information for further parameter calibration and model improvement.

3.3.2 Model and data

Model

SMART2 (Kros *et al.*, 1995a, see Chapter 2.3) predicts changes in pH, aluminium (Al), base cation (BC), nitrate (NO_3) and sulphate (SO_4) concentrations in the soil solution, and solid phase characteristics depicting the acidification status, i.e. carbonate content,

base saturation and readily available Al content. SMART2 extends the dynamic soil acidification model SMART (De Vries *et al.*, 1989), by including nutrient cycling and improved hydrology. The SMART2 model consists of a set of mass balance equations describing the soil input-output relationships and a set of equations describing the rate-limiting and equilibrium soil processes.

In the present study we considered only the modelled annual averaged Al and NO_3 concentrations at a depth of 1 m (i.e. below the root zone) below coniferous and deciduous forest. Model outputs were first generated on a 'point scale' using a 1×1 km^2 grid, and including only those cells that contained (semi)-natural vegetation. Model output for these point values was aggregated to block values for 5×5 km^2 blocks, by (i) taking the block median concentration value from the points within the block and (ii) taking the areal fraction where the individual concentration values exceeded an environmental standard.

Input data and model parameters to be calibrated

Input data for the SMART2 application can be divided into system inputs and initial values of variables and parameters. System inputs are atmospheric deposition, hydrology and vegetation development. All input data are derived as a function of location (grid cell) or soil type or vegetation type or the combination of vegetation type and soil type. Input data refer to (i) a specific deposition scenario for each grid cell, (ii) model variables and parameters which are either related to a soil type or a vegetation type or to a combination of both and (iii) a soil map and vegetation map. For the application on a European scale, the gridded soil map and vegetation map, representing the dominant soil type and vegetation type for a 1×1 km^2 grid, respectively, were generalised. Seven soil classes were distinguished and four vegetation types. Model simulations were performed for the period 1985 to 1995, using deposition values for the corresponding years. Although the original national deposition values were available for a 1×1 km^2 grid, the original values were aggregated to a 20×20 km^2, because this is the resolution for which Europe-wide scenarios may become available.

The number of parameters to be calibrated had to be restricted in order to (i) restrict the computational load and (ii) avoid identification problems. We based our selection of parameters to be calibrated on a sensitivity and an uncertainty analysis (cf. Chapter 3.2 and Kros *et al.*, 1999), using only the most sensitive and uncertain model parameters. First parameters to which the model output was insensitive were fixed. We then excluded those parameters which we considered relatively well-known (e.g. growth and litter fall parameters). We also excluded those parameters which were impossible to identify with this data set, because the calibration criterion was not sensitive to changes in their values. Finally, we ended up with five vegetation-dependent parameters and five soil-dependent parameters for calibration (Table 1). The parameters not included in the calibration were set at their nominal value. The nominal values were taken from Kros *et al.* (1995a).

Table 1 Parameters calibrated

Code	Description	Affects[1]	Unit	Dependent on	derived from
$ffSO_2$	Forest filtering SO_2	Al	-	Vegetation	literature
$ffNH_3$	Forest filtering NH_3	NO_3	-	Vegetation	literature
$ffNO_x$	Forest filtering NO_x	NO_3	-	Vegetation	literature
f_{dd}	Dry deposition factor	Al	-	Vegetation	literature
k_{mi}	Mineralisation fraction	Al, NO_3	a^{-1}	Vegetation	literature
fr_{ni}	Nitrification fraction	Al, NO_3	-	Soil	global calibration[2]
fr_{de}	Denitrification fraction	Al, NO_3	-	Soil	global calibration[2]
KAl_{ox}	Al_{ox} dissolution constant	Al	$\log(mol^{-2}\ l^{-2})$	Soil	Derived from ca. 250 plots in NL
KAl_{ex}	Al/BC2 exchange constant	Al	$\log(mol\ l^{-1})$	Soil	Derived from ca. 250 plots in NL
KH_{ex}	H/BC2 exchange constant	Al	$\log(mol^{-1}\ l)$	Soil	Derived from ca. 250 plots in NL

[1] Refers to soil solution concentrations of Al and NO_3; other model output was not considered in the present study

[2] i.e. manual calibration, only focussing on the average concentrations

Calibration and validation data

Soil solution concentrations were sampled at 241 forest stands, including 147 non-calcareous sandy soils, sampled during the spring of 1990 (De Vries *et al.*, 1995b), 38 loess soils, sampled during the spring of 1992, 30 peat soils, sampled during the spring of 1993 and 26 clay soils, sampled during the spring of 1993 (Klap *et al.*, 1999). The soil solution was sampled during the period from February to May. Composite samples, consisting of 20 subsamples, were taken from the mineral topsoil (0 to 30 cm) and the mineral subsoil (60 to 100 cm) in early spring. At this time of the year, the composition of the soil solution corresponds reasonably well with the flux-weighted average annual soil solution concentration. Soil solution was extracted by centrifugation of soil samples. The locations were restricted to non-calcareous soils throughout the country, because sampling was performed in the context of acidification research (cf. De Vries *et al.*, 1995b). The forest types included were Scots pine, black pine, Douglas fir, Norway spruce, Japanese larch, oak and beech.

The observation sites were lumped into the same forest type classes and soil type classes that were used for the model simulations. The tree species were lumped into two forest type classes:
- Coniferous stands (Douglas fir, Norway spruce, Scots pine and black pine), i.e. evergreen trees with moderate to high forest filtering capacity, growth rate and transpiration rate (CON);
- Deciduous stands (Japanese larch, oak and beech), i.e. needle- or leaf-shedding trees with low forest filtering capacity, growth rate and transpiration rate (DEC).

The soil types were lumped into five classes (Table 2), based on parent material (texture, mineralogical composition, organic matter). Moisture condition was not taken into account as a separate criterion, since this information is not available on a European scale. Note, however, that previous applications of SMART2 (cf. Kros *et al.*, 1999) also included calcareous sandy soils (SC), calcareous clay soils, non-fertilised

grassland (GRA) and heathland (HEA). Since no observation data were available for these soil and vegetation types, these categories were not included in the calibration and validation.

Table 2 Overview of the soil type classes distinguished

Code	Soil class	Common soil types (FAO, 1988)
SP	Sand Poor	Carbic Podzols, Arenosols
SR	Sand Rich	Gleyic Podzols, Gleysols
CN	Clay Non-calcareous	Fluvisols
PN	Peat Non-calcareous	Histosols
LN	Loess Non-calcareous	Luvisols

SMART2 simulates averaged annual values, whereas the data set represents the concentration of ions in early spring (February to May). Although average concentrations in April may be used as an estimate of the flux-weighted annual average concentration (De Vries *et al.*, 1995b), our data set was sampled only once. This influences the quality of the calibration because of extreme values due to specific, temporary circumstances, such as weather conditions and deposition. Since upscaling smoothes such extreme values, this is another important motivation for performing an upscaling operation. The upscaling procedure use average information on e.g. annual deposition in combination with a multiple regression equation, yielding a smoothing of extreme values and outliers.

3.3.3   Methodology

Upscaling of observation data

In order to calibrate and validate the model it was necessary to bring observations and model results to the same support. Several techniques are available to perform spatial upscaling, including regression analysis (cf. Leeters *et al.*, 1994), generalised additive modelling (cf. Tiktak *et al.*, 1998), ordinary block kriging (Journel and Huijbregts, 1978), stratified block kriging (Pebesma and De Kwaadsteniet, 1997) and a nonparametric distance-weighting procedure (Han *et al.*, 1993). Two disadvantages of kriging are that (i) it spreads out sharp boundaries which do exist in reality, and (ii) it assumes similar mean and variogram for all soil units (Brus *et al.*, 1996). Rarely are natural processes explained with an estimate of variability. Therefore, as stated by, e.g. Heuvelink and Bierkens (1992), it is advisable to use all relevant additional information, such as the relation between atmospheric deposition and soil solution concentrations (Leeters *et al.*, 1994). It remains unlikely that this information alone can fully explain the object variable, because (i) crucial additional information may not be available and (ii) soil parameters are often spatially correlated. The structure in spatial data can usually be divided into a systematic part and a stochastic part (Han *et al.*, 1993). Therefore, we decided to use a hybrid of a systematic and a stochastic method. However, the division between the systematic part and the stochastic part is rather arbitrary. Multiple linear regression was used for the systematic behaviour, whereas

ordinary block kriging was used for the stochastic behaviour. Here we derived nation wide upscaled monitoring data from about 250 forest stands in the Netherlands (Mol-Dijkstra and Kros, 1999).

Model results at a block support for 5×5 km² blocks were obtained by taking the block median value from the corresponding point support model runs (see section 2.1). To use the observation data for a model calibration at a block support for 5×5 km² blocks, the observations must be aggregated to the same support. Therefore, a map was generated with the major soil solution concentrations (Al, NO_3, SO_4, Ca+Mg, Cl and pH) for a 5×5 km² grid (cf. Mol-Dijkstra and Kros, 1999). To account for both systematic and stochastic behaviour, the block values were derived in three steps, according to the scheme in Figure 1:

1. multiple regression analyses for a 250×250 m² grid, in order to estimate values at unsampled locations by including all available additional information which may explain the systematic effect;
2. aggregation of the 250×250 m² values to a 5×5 km² grid;
3. adjusting the 5×5 km² grid values by adding that part of the residual that can be predicted from spatial correlated observations. This procedure was performed using residual kriging on log-transformed data.
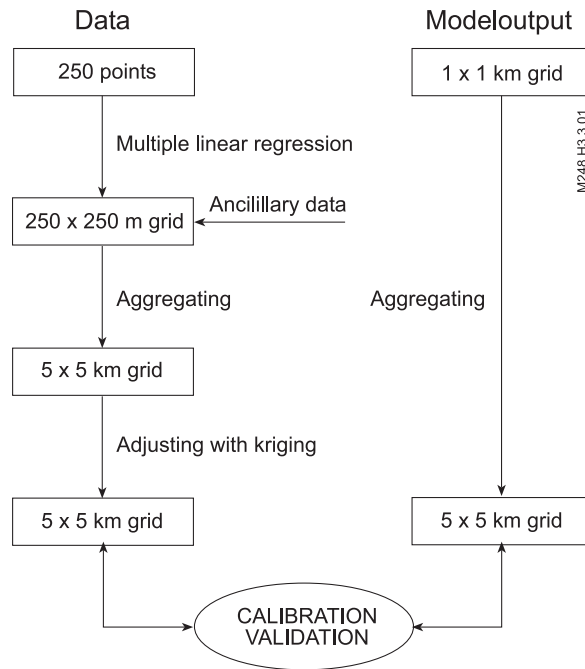

Figure 1 Upscaling procedure for available point observations and model results

Regression analysis and aggregation

Candidate predictor variables for the regression analysis were: land use, soil type, tree species, total deposition of N and S, canopy closure, tree height, total area covered by

the forest, nearest distance to the forest edge and principal land use at the nearest forest edge (Mol-Dijkstra and Kros, 1999). These variables were used because they are available on a national scale at a resolution of 250×250 m² and we assumed that they might have a significant effect on soil solution concentrations. The use of national data made it possible to split up the category of coniferous forest (CON), which was used for the model calibration, into pine forest (PIN) and spruce forest (SPR). Multiple linear regression was used to fit the soil solution concentrations to the candidate predictor variables, using the GENSTAT statistical package (Genstat 5, 1987). Since the predictor variables are either quantitative (e.g. deposition) or qualitative (e.g. soil type), the regression equations include both quantitative and qualitative variables. The best regression models were obtained by means of the following procedure: (i) find the best model with the SELECT option in GENSTAT, (ii) investigate whether non-linearities lead to improvements, using the SPLINE option in GENSTAT and (iii) investigate whether the inclusion of interactions leads to a better model. To meet the assumption of normally distributed regression residuals, the soil solution concentrations (response variables) were log-transformed (using the $\log_e$). For the presentation, results were transformed back to the original scale.

The 'point maps' thus derived at a resolution of 250×250 m² were aggregated to 5×5 km² 'block maps', being the spatial scale of the model predictions, by taking the median value within each of the 5×5 km² blocks.

Residual kriging

The non-explained part of the regression model (i.e. the residual) consists of an unstructured part, which originates from measurement errors, but also of a structural part, which could be explained by known predictor variables, causing a spatially correlated residual. The systematically explained part was described using predictor variables, while the residuals are random and were treated stochastically. For this stochastic part, we used ordinary block kriging. The stochastic part was included by analysing the log-transformed residuals, based on the 250×250 m² map, for spatial relationships. Residuals were estimated by:

$$\hat{e}_{p,r}(k) = y_{p,r}(k) - \hat{y}_{p,r}^{R}(k) \tag{1}$$

where $\hat{e}_{p,r}(k)$ denotes the residual at a point support (denoted by the subscript $_p$) for the log-transformed observed concentration of constituent r, at location k ($y_{p,r}(k)$) and the estimated log-transformed concentration r for the 250×250 m² grid cell in which location k is located ($\hat{y}_{p,r}^{R}(k)$). These values are still treated as points. Experimental semivariograms for $\hat{e}_{p,r}$ were fitted using an exponential model. Where necessary, the nugget variance was adjusted manually. Subsequently, ordinary block kriging for 5×5 km² blocks was applied to the spatially correlated residuals. Finally, the upscaled concentrations at the 5×5 km² block support ($\hat{y}_{B,r}(l)$) were calculated as:

$$\hat{y}_{B,r}(l) = \hat{y}_{B,r}^{R}(l) + \hat{e}_{B,r}(l) \tag{2}$$

where $\hat{y}_{B,r}^{R}(l)$ denotes the upscaled concentration r for 5×5 km² blocks (denoted by the subscript B) on a log-scale derived by multiple regression only and $\hat{e}_{B,r}(l)$ the part of the residual that was predicted by considering spatial correlation on a 5×5 km² block scale.

Assuming independence of both terms in Eq. (2), the predicted variances of the upscaled observations thus derived for all 5×5 km² block support values were estimated as:

$$\hat{\sigma}_{B,r}^{2}(l) = \hat{\sigma}_{R,r}^{2}(l) + \hat{\sigma}_{K,r}^{2}(l) \tag{3}$$

with $\hat{\sigma}_{R,r}^{2}(l)$ being the block median regression variance for the upscaled observation r and $\hat{\sigma}_{K,r}^{2}(l)$ being the kriging variance of the predicted residuals ($\hat{e}_{B,r}(l)$), both for 5×5 km² blocks l and on the log-scale.

Model calibration

Calibration approach

The calibration was performed on a grid-to-grid basis using a 5×5 km² grid, which was considered representative of application on the European scale. Because observations were only available for forest, the calibration included only those 5×5 km² grid cells that contained at least 20% of nature conservation area, of which at least 50% consisted of forest. This means that the upscaled 'observations' for a 5×5 km² block, i.e. the block median values, originated from at least 40 cells (=$20^2 \times 0.2 \times 0.5$) from the 250×250 m² subgrid, whereas the upscaled model results originated from at least 3 ($\approx 5^2 \times 0.2 \times 0.5$) subgrids of 1×1 km². As a result, 153 of the original 918 blocks were used for the calibration.

In general, two calibration methods are available for solute transport models, a Monte Carlo based method (cf. Hornberger *et al.*, 1986) and a mathematically based method, the Bayesian approach (cf. Klepper and Hendrix, 1994). If several (say more than 5) independent parameters have to be calibrated, the Monte Carlo method seems to be rather inaccurate (cf. Scott, 1992). Therefore, we used the mathematically based method.

Calibration steps

Because several model parameters do have the same overall effect on the soil solution concentration, it was necessary to perform the calibration in sequential steps as outlined in Table 3. Furthermore, where applicable, the calibration criterion was also adapted per calibration step, as outlined below.

Table 3 Overview of the consecutive calibration steps

Calibration step	Parameters	Criterion	Plots included	Process
Nitrogen parameters				
1	k_{mi}	NO_3+NH_4 [1]	Only dry sandy soils	Mineralisation (internal N input)
2	$ffNH_3$ $ffNO_x$ [2]	NO_3+NH_4 [1]	Only dry sandy soils	Forest filtering of NH_3 and NO_x (external N input)
3	fr_{ni}	$NO_3+pH+Al$	All grid cells	Nitrification
4	fr_{de}	$NO_3+pH+Al$	All grid cells	Denitrification
Aluminium parameters				
5	$ffSO_4$	SO_4	All grid cells	Forest filtering of SO_2 (external S input)
6	f_{dd}	BC2	All grid cells	Forest filtering of BC (external BC input)
7	KAl_{ox}	$Al+pH$	All grid cells	Dissolution of secondary Al precipitates
8	KAl_{ex} KH_{ex}	$Al+pH+NO_3$	All grid cells	Cation exchange

[1] Since no upscaled NH_4 concentrations were available, we used the average NH_4 concentration from the individual plots, i.e. 0.1 mol_c m^{-3}

[2] Since the simultaneous calibration of both filtering factors resulted in identification problems, the filtering factors were first calibrated individually. The resulting optimal values were then used as the initial values for the simultaneous calibration of both filtering factors.

We first considered only the parameters affecting the N input, i.e. the forest filtering factors for NO_x and SO_x ($ffNO_x$, $ffSO_x$) and the mineralisation rate constant (k_{mi}). These parameters were calibrated using the total N concentration ($NO_3 + NH_4$) at the bottom of the root zone of forest locations on dry sandy soils only, which excludes the possibility of substantial N loss by denitrification. Apart from the growth parameters and N contents in the various biomass compartments, which determine the loss of N by uptake, and denitrification from this calibration step, no other parameters affect the N leaching flux. Next, the nitrification parameter (f_{ni}) and the denitrification parameter (f_{de}) were calibrated using the entire data set. Because nitrification leads to the formation and denitrification to the consumption of NO_3 and H, which in turn results in dissolution or precipitation of Al, we used NO_3, pH and Al as criteria.

From the parameters that indirectly influence the Al budget (viz through the charge balance), those that directly influence the base cation concentrations (i.e. the dry deposition factor, f_{dd} and the weathering rates, $BC2_{we}$) were calibrated first, followed by the forest filtering factor for SO_x ($ffSO_2$). This ensured that the base cation and sulphur budgets were optimally simulated before the parameters that directly influence the Al concentration (KAl_{ox}, KAl_{ex}) were adjusted.

Calibration criterion and optimisation algorithm

The model parameters considered were calibrated simultaneously for each calibration step. The squared difference between the model outputs considered and the corresponding (upscaled) observations for all 5×5 km² grid cells was minimised.

Candidate parameter values were selected from *a priori* specified uncertainty ranges. Unlike the regression analysis and kriging, the calibration was performed with the original data. The calibration criterion was based on the non-weighted summed square of the differences.

The model to be calibrated can be written as:

$$\hat{y}^{o}_{M,r}(l) = f(l, \boldsymbol{\theta}) \tag{4}$$

where $\hat{y}^{o}_{M}$ is the original (non log-transformed) model output for concentration constituent r ($r = 1, \dots, I$) for a 5×5 km^2 block l ($l=1, \dots, J$) and θ denotes the p-dimensional parameter vector reflecting the parameter constraints specified in Table 1. The model parameters depend on either the vegetation type or the soil type. The summed squared difference between model and data over all concentration constituents for grid cell l was expressed as:

$$C(l; \boldsymbol{\theta}) = \sum_{r=1}^{M} \left(e_r(l; \boldsymbol{\theta}) \right)^2 \tag{5}$$

where

$$e_r(l; \boldsymbol{\theta}) = \hat{y}^{o}_{B,r}(l) - \hat{y}^{o}_{M,r}(l; \boldsymbol{\theta}) \tag{6}$$

is the difference between the back-transformed upscaled observation of component r at block l, $\hat{y}^{o}_{B,r}(l)$ and the associated upscaled model prediction $\hat{y}^{o}_{M,r}(l;\theta)$ for the original scale. Eventually, the various misfits per grid cell $C(l;\theta)$ were combined into one overall criterion by summing over N blocks:

$$C(\boldsymbol{\theta}) = \sum_{l=1}^{N} C(l; \boldsymbol{\theta}) \tag{7}$$

For each calibration step (cf. Table 3) an optimal parameter vector θ was determined by minimising the overall misfit function:

$$\min_{\theta} \left[C(\boldsymbol{\theta}) \right] \tag{8}$$

The optimisation was carried out with a constraint minimisation function using the Gauss-Levenberg-Marquardt algorithm. Physical boundaries were used for the constraints. The optimisation was carried by using a model-independent parameter optimiser PEST (Doherty *et al.*, 1994). The optimisation delivered the „best linear unbiased' estimator of the set of true model parameters. Therefore, also the 95% confidence limits of the optimised parameters was calculated from the covariance matrix (cf. Doherty *et al.*, 1994).

Model error quantification

The benefits of the model calibration procedure were assessed by quantifying the model error for both the nominal and the calibrated model run. According to Heuvelink and Pebesma (1999), the only way to quantify the model error is through a model validation, achieved by comparing model results with independent observations. Currently, however, no independent data set on a national scale is available. Therefore, it was decided to 'validate' the model by quantifying the model error before and after calibration. As with calibration, the model validation was performed at a block support, taking into account the uncertainty due to the upscaling of the observations. We used a procedure that takes this into account (see Heuvelink and Pebesma (1999).

Consider the difference between the model prediction at the block support $\hat{y}_{M,r}$ and the observation data (i.e. the validation data at the block support on the log-scale), $\hat{y}_{B,r}$:

$$\hat{y}_{B,r} = \hat{y}_{M,r} - \hat{y}_{B,r} \tag{9}$$

This difference does not yield the real model error, because it also includes the estimation error in $\hat{y}_{B,r}$:

$$\hat{y}_{B,r} - y_{B,r} \tag{10}$$

where $y_{B,r}$ denotes the true block support value. The squared difference of Eq. (10) can be simply derived from the model outputs and observation data at the block support (cf. Eq. 9). It can be decomposed as follows:

$$\begin{aligned}(\hat{y}_{M,r} - \hat{y}_{B,r})^2 &= ((y_{B,r} - \hat{y}_{M,r}) - (y_{B,r} - \hat{y}_{B,r}))^2 \\ &= (y_{B,r} - \hat{y}_{M,r})^2 + (y_{B,r} - \hat{y}_{B,r})^2 - 2(y_{B,r} - \hat{y}_{M,r})(y_{B,r} - \hat{y}_{B,r})\end{aligned} \tag{11}$$

In Eq. (11) $(y_{B,r} - \hat{y}_{M,r})^2$ represents the true but unknown model error at a block support and $(y_{B,r} - \hat{y}_{B,r})^2$ represents the estimation error of the upscaled observations, both on the log-scale.

Heuvelink and Pebesma (1999) describe the situation in which the cross-product in Eq. (11) is zero. In such a situation it can be seen from Eq. (11) that evaluating the model error as $(\hat{y}_{M,r}-\hat{y}_{B,r})$ results in an overestimation. In fact, the model error should be judged by the term $(\hat{y}_{M,r}-y_{B,r})$, which of course gives smaller values. In our situation, however, the cross-product in Eq. (11) was not zero. The upscaled observations were based on multiple regression relations using ancillary information such as vegetation type, soil type and deposition (see section 3.3.3), whereas the model input data for the SMART2 application was partly based on the same ancillary information (see section 2.1). This means that the errors in the ancillary information yielded artificial similarities between the aggregated validation data and the model

results, so the cross-product in Eq. (11) between $(y_{B,r} - \hat{y}_{M,r})$ and $(y_{B,r} - \hat{y}_{B,r})$ is not zero but positive. Consequently, we have to evaluate Eq. (11) with a non-zero cross-term.

The estimation error of the upscaled observations was estimated by Eq. (3), and consisted of the block median estimation variance of the multiple linear regression model and the kriging variance. Since the squared observable differences, $(\hat{y}_{M,r} - \hat{y}_{B,r})^2$, were only available in an average sense (we only had one value per block), it was impossible to estimate the model error for individual blocks. However, the model error could be estimated as an average from the mean square error of prediction ($MSEP$) for component r:

$$MSEP(r) = \frac{1}{N} \sum_{l}^{N} [\hat{y}_{M,r}(l) - \hat{y}_{B,r}(l)]^2 \tag{12}$$

where l is the grid cell indicator and N the total number of grid cells. Using Eq. (3) and (12), and averaging over all 5×5 km^2 blocks, Eq. (11) can be written as:

$$MSEP(r) = \overline{\sigma}_{M,r}^2 + \overline{\sigma}_{B,r}^2 - 2\rho_{MD}\overline{\sigma}_{M,r}\overline{\sigma}_{B,r} \tag{13}$$

with $\overline{\sigma}_{M,r}^2$ being the average model error for output r, $\overline{\sigma}_{B,r}^2$ the estimation error of the upscaled observations averaged over all grid cells and ρ_{MD} the correlation coefficient between the model error at the block support $(\hat{y}_{B,r} - \hat{y}_{M,r})$ and the estimation error at the block support based on observation data $(\hat{y}_{B,r} - \hat{y}_{B,r})$.

Because it is not easy to estimate the correlation coefficient, three extremes were evaluated, viz, –1, 0 and 1 Although it was obvious (see above) that the correlation coefficient was positive, we also included –1, for the sake of completeness. We assumed that ρ_{MD} was independent of the model output considered. Given a known correlation coefficient, the only sensible solution to Eq. (13) is:

$$\overline{\sigma}_{M,r} = \frac{2\rho_{MD}\overline{\sigma}_{B,r} + \sqrt{4\rho_{MD}^2\overline{\sigma}_{B,r}^2 - 4(\overline{\sigma}_{B,r}^2 - MSEP(r))}}{2} \tag{14}$$

The average model error ($\overline{\sigma}_{M,r}^2$) can be divided into a structural part ($\overline{\sigma}_{MES,r}^2$) and a part that originates from input uncertainty ($\overline{\sigma}_{MEI,r}^2$):

$$\overline{\sigma}_{M,r}^2 = \overline{\sigma}_{MES,r}^2 + \overline{\sigma}_{MEI,r}^2 \tag{15}$$

Given the model error due to input error, which has been quantified by Kros *et al.* (1999), and the model error derived from Eq. (14), the structural part of the model error can be quantified by:

$$\overline{\sigma}^2_{MES,r} = \overline{\sigma}^2_{ME,r} - \overline{\sigma}^2_{ME,r} \qquad (16)$$

Note, however, that $\overline{\sigma}^2_{MES,r}$ is only defined for values ≥ 0. The contribution of the input error was quantified by performing Monte Carlo simulations. The sources of uncertainty considered were (i) uncertainty/impurity in soil maps and vegetation maps (categorical data) and (ii) uncertainty in soil and vegetation related parameters (continuous data). The uncertainty in categorical data was quantified by a comparison between the cruder European Union soil and vegetation maps and the more detailed maps from the Netherlands. The uncertainty in the continuous data was derived from various European databases and the literature. The resulting uncertainty was expressed as variances of the block median Al and NO_3 concentrations for 5×5 km^2 blocks in the year 1995, i.e. the year for which the model error was quantified (cf. Kros *et al.*, 1999). Since the input error was quantified for the non-calibrated model, we were only able to quantify the model structure error for the nominal model run.

3.3.4 Results and discussion

Upscaled observed soil solution concentrations

Regression models

Stepwise selection process showed that significant predictive variables for the $\log_e$ NO_3 concentration included (i) soil type (i.e. SP, SR, LN, PN, CN), (ii) tree species (i.e. SPR, PIN, DEC), (iii) deposition of NH_x ($NH_{x \, dep}$), (iv) mean spring water table depth (*MSW*), (v) area of contiguous forest (*area*) and (vi) tree height. The inclusion of non-linear relationships (for *MSW* and *area*) resulted in a loss of significance for tree height. No significant interactions were discovered. Finally, the following multiple regression equation was derived for the NO_3 concentration at depths of 60-100 cm (cf. Mol-Dijkstra and Kros, 1999):

$$\ln NO_3 = soil(i) + veg(j) + 0.33NH_{x \cdot dep} - 5.5 \cdot 0.025^{MSW} - 1.24\,area^{0.24} - 0.1 \qquad (17)$$

where NO_3 is the NO_3 concentration in mol$_c$ m^{-3}, *soil(i)* and *veg(j)* are constants that differ per soil type i and vegetation type j, $NH_{x \, dep}$ is the ammonium deposition in kmol$_c$ ha^{-1} a^{-1}, *MSW* is the mean spring water table depth in m below the soil surface and *area* is the area of connected forest in ha. The percentage of variance accounted for was 48%. There was a positive relation between $NH_{x \, dep}$ and the NO_3 concentration. $NH_{x \, dep}$ affects the NO_3 concentration through nitrification, which is generally complete in (dry) forest soils (cf. Tietema, 1992). Remarkably, there was no significant contribution of the NO_x deposition to the NO_3 concentration. This was most probably caused by the fact that NO_x deposition in the Netherlands is considerably lower than NH_x deposition, with average values of about 750 and 2000

mol$_c$ ha^{-1} a^{-1}, respectively, for the period 1990-1995 (Bleeker and Erisman, 1996). The relationship with *MSW* originated from a lower denitrification flux at deeper water table depths. *MSW* < 1 m yields higher negative values for the whole term, whereas *MSW* > 1 m yields lower negative values. The negative relation with *area* of contiguous forest was a result of the lower rate of forest filtering of atmospheric deposition in larger contiguous forest areas. A larger contiguous forest area means shorter forest edges, resulting in a smaller roughness length, which in turn yields a lower rate of forest filtering (cf. Draayers *et al.*, 1988). The estimated constants for *soil(i)* ranged from –1.2 for loess soils to 0.8 for rich sandy soils (SR). The constants for *veg(j)* ranged from 0 for deciduous to 1.4 for spruce forest.

The significant main effects for the Al concentration at depths of 60-100 cm were found to be soil type, tree species and mean spring water table (*MSW*). Although deposition was not significant as a main effect, the interaction between soil type and NH$_x$ deposition was significant. Since some soil types showed a negative relationship with deposition, which could not be explained, the relationship with NH$_x$ deposition was not included in the regression equation. Finally, the following multiple regression equation was derived for Al (cf. Mol-Dijkstra and Kros, 1999):

$$\ln Al^{3+} = soil(i) + veg(j) - 2.0 \cdot 0.1^{MSW} - 1.3 \tag{18}$$

where *soil(i)* and *veg(j)* are constants that differ per soil type *i* and vegetation type *j* and *MSW* is the mean spring water table. The percentage of variance accounted for was 50%. The estimated constants for *soil(i)* ranged from –2.6 for clay soils to 0.2 for rich sandy soils (SR). The constants for *veg(j)* ranged from 0 for deciduous to 1.5 for spruce forest. The Al concentration was best explained by soil type and vegetation type, and decreased with soil type in the following order: SP > SR > LN > PN > CN, which coincides with an increase in weathering rate. Furthermore, the Al concentration increased with the vegetation structure type, in the following order: SPR > PIN > DEC, which coincides with a decrease in the input of (acid) atmospheric deposition. The negative relation with the *MSW* stemmed from higher pH and base cation concentrations under wet circumstances, which means low Al concentrations due to a lower solubility. It was remarkable that no significant contribution of the atmospheric deposition was found. However, this effect was partly included in the vegetation type, since pine and spruce trees have higher filtering capacities, resulting in a higher input (throughfall) flux. Furthermore, it is understandable that the effect of deposition was overruled by the effect of soil type. The soil types included ranged from clay soil (CN), with negligible Al concentrations, to poor sandy soils (SP) with extremely high Al concentrations.

Observation-based Maps

The regression equations 17 and 18 were used to calculate Al and NO$_3$ concentrations for 250 × 250 m^2 grid cells followed by aggregation to 5 × 5 km^2 blocks (Figure 2). Figure 2 also shows the map that was adjusted with ordinary block-kriged residuals for

5×5 km² blocks. Only those cells are presented that included more than 20% of (semi) natural vegetation, of which more than 50% consisted of forest. The map of NO_3 concentrations clearly shows higher concentrations in the southern and to a lesser extent in the central and eastern part of the country, which were the areas with high nitrogen deposition rates. Lower concentrations were found in the northern and central parts. The Al concentrations, however, were more evenly spread over the country. This was caused by the absence of the deposition variable from the regression equation (cf. Eq. 18). The addition of the kriged residuals yielded a much more dynamic image. This effect was strongest in the northern part of the country.

Since the effect of kriging cannot be quantified in terms of the percentage of variance accounted for, the consequences of the addition of the block-kriged residuals is illustrated by the Normalised Mean Squared Error of Prediction (*NMSEP*) for all grid cells (Table 4):

$$NMSEP(r) = \frac{\frac{1}{N}\sum_{l=1}^{N}[y_{p,r}(l) - \hat{y}_{u,r}(l)]^2}{\bar{y}_{p,r}} \qquad (19)$$

where $\hat{y}_{u,r}(l)$ are the intermediate upscaled observation for either a 250×250 m² or 5×5 km² block l determined either with regression analysis or with regression analysis combined with kriging. $y_{p,r}(l)$ represents the observed point-concentration of component r within block l, N the number of available observations and $\bar{y}_{p,r}$ the mean of observations r on a point scale. Normalisation of the *MSEP* by the mean of the observations yields a dimensionless measure, which makes it possible to compare it across different model outputs.

The resulting *NMSEP* value was calculated for four situations (Table 4):
1. the original regression for a 250×250 m² grid using the complete data set of 241 point observations (cf. section 3.1) (Regression 250×250 m² with data);
2. the original regression for a 250×250 m² grid using only those 250×250 m² cells that were situated within 5×5 km² blocks with more than 20% (semi) natural vegetation, of which more than 50% consisted of forest. This subset included about 8000 grid cells sized 250×250 m²;
3. upscaled regression results for 5×5 km² blocks containing more than 20% (semi) natural vegetation, of which more than 50% consisted of forest, and the observation points situated within these blocks (Regression 5×5 km²);
4. like (iii) but with the addition of the block-kriged residuals (Regression + kriging 5×5 km²).

Regression

Regression + Kriging

Al (mol$_c$.m^{-3})

<0.02

0.02 - 0.4

0.4 - 0.8

>0.8

M248 H3.3 02abcd

NO$_3$ (mol$_c$.m^{-3})

<0.02

0.02 - 0.4

0.4 - 0.8

>0.8
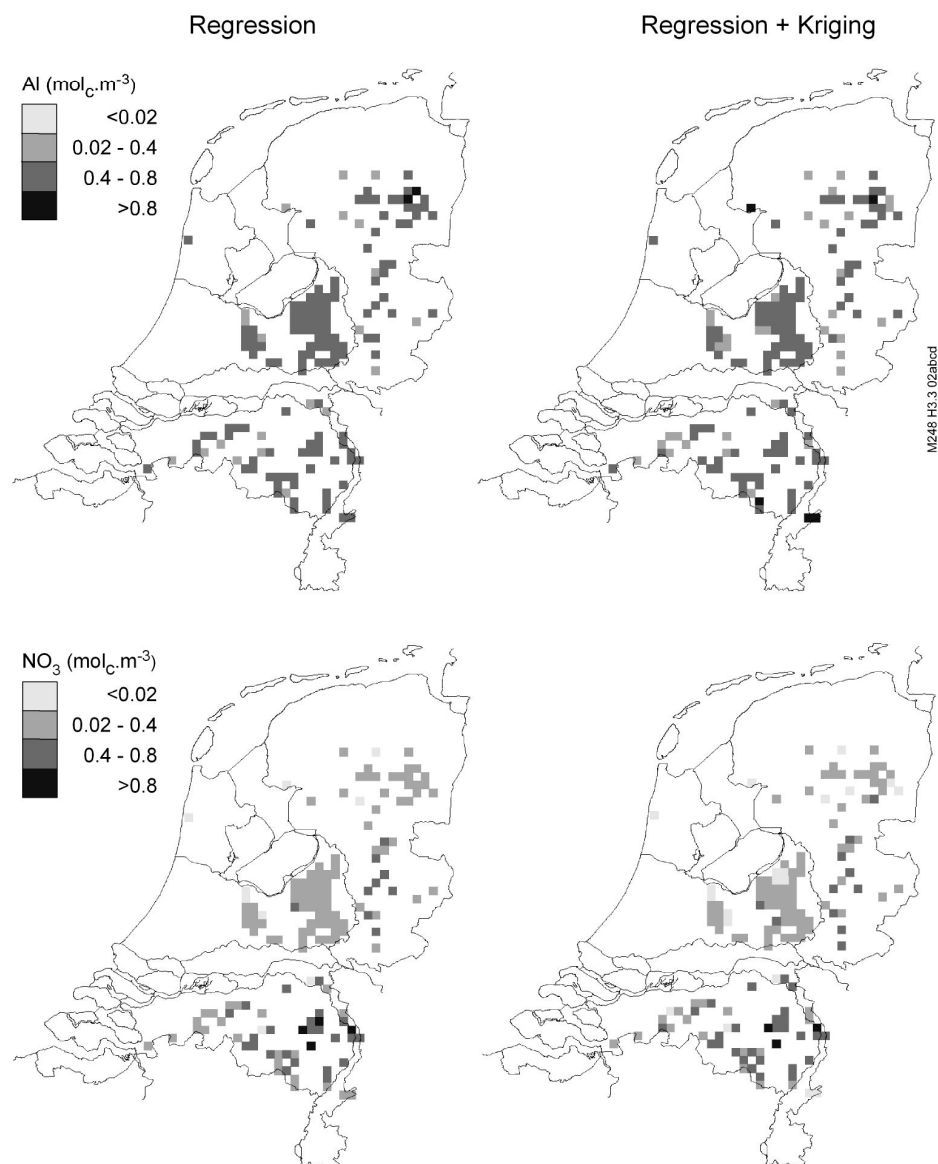
Figure 2 Maps of estimated upscaled observations of soil solution concentrations of Al (top) and NO₃ (bottom) in the subsoil (60-100 cm) for 5 × 5 km² block median values, based on regression analysis alone (left) and regression analysis combined with block-kriged residuals (right)

Table 4 *NMSEP* values for all 5×5 km^2 grid cells for the Al and NO$_3$ concentrations predicted by regression analysis and regression analysis combined with block-kriging. The *NMSEP* at a 250×250 m^2 point support is also given

Level of upscaling	N	Al				NO$_3$			
		Median[1] Regr.	Median[1] Obs.	*NMSEP*	R^2_{adj}	Median[1] Regr.	Median[1] Obs.	*NMSEP*	R^2_{adj}
		(mol$_c$ m^{-3})			(df=7)[2]	(mol$_c$ m^{-3})			(df=9)[2]
Regression (only cells with obs.) 250 × 250 m², point support	241	0.20	0.20	10.11	0.50	0.24	0.24	7.13	0.48
Regression (all cells) 250 × 250m², point support	7996	0.48				0.27			
Regression (only cells with obs.) 5 × 5km², block support	85	0.51	0.31	10.22	-	0.40	0.28	7.74	-
Regression+Kriging (only cells with obs.) 5 × 5km², block support	85	0.43	0.31	7.35	-	0.40	0.28	5.63	-

[1] Back-transformed average of the log$_e$-transformed mean

[2] Degrees of freedom of the regression, i.e. number of predictive variables. Note, however, that *soil(I)* and *veg(j)* in Eqs. 17 and 18 refer to categorical variables consisting of 5 and 2 categories respectively (cf. section 4.1)

Inspection of the *NMSEP* (Table 4) showed that the 'regression + kriging' map was a better estimate than the map based on regression analysis alone, with the *NMSEP* decreasing *by* 28% for both Al and NO$_3$. It might be concluded from the *NMSEP* that the estimation of the NO$_3$ concentration was better than that of the Al concentration. This was, however, not reflected in the percentage of variance accounted for (R^2_{adj}). The R^2_{adj} values were almost equal for Al and NO$_3$: 50% and 48% respectively (see section 4.1). This was because (i) the NO$_3$ regression equations include more degrees of freedom (i.e. the number of predictive variables + 1) and (ii) the variances of the Al observations were larger. Both aspects yielded a reduced R^2_{adj}. If we limit ourselves to those grid cells that contain more than 20% (semi) natural vegetation, of which more than 50% consists of forest, we find higher concentrations for both Al and NO$_3$.

The maps derived by a combination of regression analysis and block-kriging of the residuals were regarded as the maps with upscaled observations that can be used for either model calibration or model validation.

The effect of upscaling on the width of the distribution is illustrated by cumulative distribution functions (CDF, Figure 3). Upscaling from point values to block median values clearly results in a narrower distribution. The first step of the upscaling process, i.e. from the original observation points to values for all 250×250 m^2 cells containing (semi) natural vegetation, considerably narrows the distribution. The reason was that the regression analysis was performed with averaged ancillary information (i.e. on soil, land cover and deposition, cf. section 3.1) instead of site-specific information. Averaged information was used, since we wanted to make predictions on a national scale, and no site-specific information was available for the country as a whole. Yet the resolution of the available ancillary information was still wide. The resolution was lowest for atmospheric deposition: 1×1 km^2, whereas that for soil types was 125×125 m^2 (scale 1:50 000). The use of averaged information

combined with a multiple regression equation resulted in a smoothing of extreme values or outliers due to e.g. measurement errors or location-specific circumstances, such as a farm being situated nearby, preferential water transport or upward seepage. The second step of the upscaling process, from 250×250 m^2 to 5×5 km^2, further narrowed the distribution, though the reduction was less than the first step. The narrowing was simply caused by averaging out the differences. Note that the CDF value thus derived for NO$_3$ is much smoother than the CDF for Al. This was due to the fact that the regression equation for Al (Eq. 18) was explained purely by class predictor variables, viz soil type and vegetation type, and the continuous predictor variable *MSW*, for which only 5 values were used, whereas NO$_3$ (Eq. 17) was also explained by the continuous predictor variables NH$_3$ deposition and *area*. The final step, i.e. the addition of the kriged residuals, resulted in a smoother curve and more variability among predicted values, an effect which was most pronounced for Al.
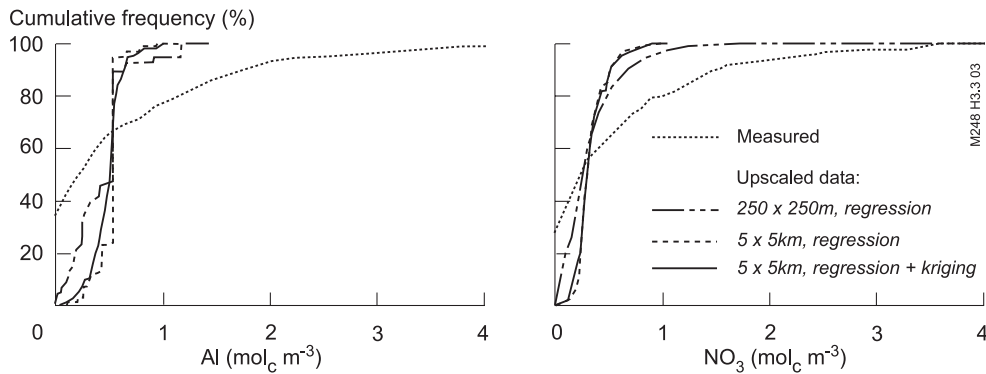

Figure 3 Cumulative frequency distribution of Al concentration (left) and NO$_3$ concentration (right) for upscaled values for 5×5 km^2 blocks with kriging, upscaled values for 5×5 km^2 blocks without kriging, regression results for 250×250 m^2 grid points and *c* 250 point measurements in forest stands

Model calibration

Effect of model calibration on predicted NO$_3$ and Al concentrations

Both the nominal and the calibrated parameter values were used for the simulation of maps with SMART2 (Figure 4). A comparison between the nominal and calibrated maps showed that the simulated concentrations for both NO$_3$ and Al were considerably lower when using calibrated model parameters. Model simulations with the nominal parameter values clearly overestimate the observed Al and NO$_3$ concentrations (compare Figure 2 and Figure 4).
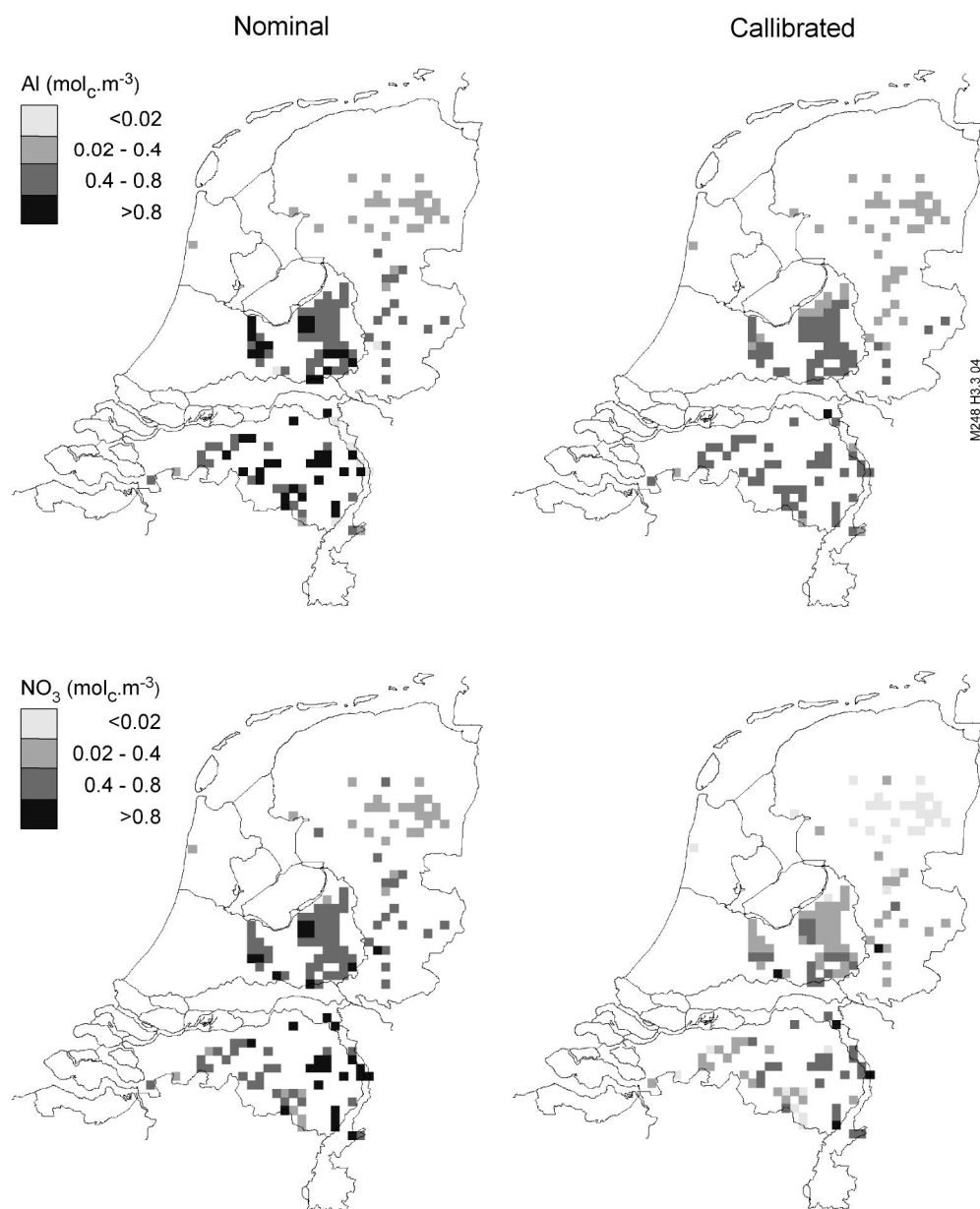
Nominal

Callibrated

Figure 4 Maps of simulated soil solution concentrations of Al (top) and NO₃ (bottom) in the subsoil (60-100 cm) for 5 × 5 km² block median values, based on SMART2 simulations using nominal parameter values (left) and calibrated parameters (right)

To evaluate the benefits of the calibration for the map as a whole, calibration results were also compared with the upscaled observations using cumulative distribution functions (CDF) (Figure 5). The upscaled observations were presented as a 95% prediction interval. Assuming that the log-transformed observations were normally distributed, approximate 95% prediction intervals were calculated by:

$$[\hat{y}_{B,r}(l) - 2\hat{\sigma}_{B,r}(l), \hat{y}_{B,r}(l) + 2\hat{\sigma}_{B,r}(l)] \tag{20}$$

where $\hat{y}_{B,r}$ denotes the upscaled log-transformed concentration r for 5×5 km² block l (Eq. 2) and $\hat{\sigma}_{B,r}(l)$ the standard error of the upscaled concentrations for 5×5 km² block l (i.e. the standard error due to regression and kriging of the residuals, cf. Eq. 3).
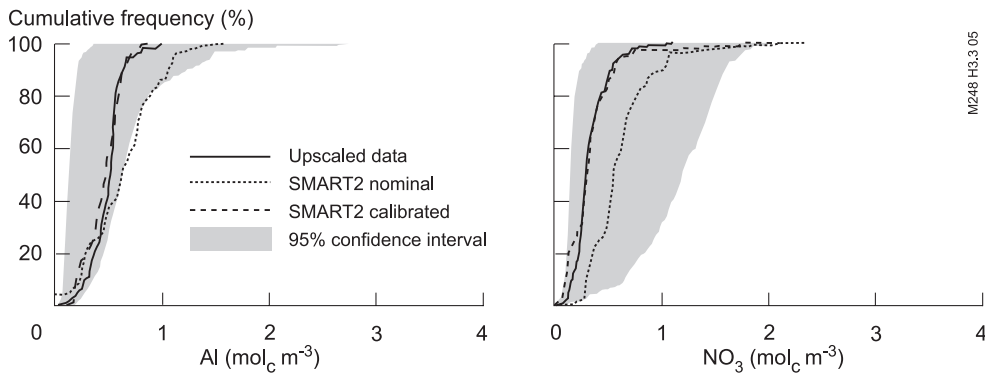

Figure 5 Cumulative frequency distribution of Al concentration (left) and NO₃ concentration (right) for the upscaled observations; SMART2 results with nominal parameters and calibrated parameters for 5×5 km² block median values, together with 95% confidence intervals

The resulting prediction intervals appeared to be wide for both model outputs (Figure 5), although the interval for NO₃ was much wider than that for Al.

The benefits of the calibration were clearly illustrated by the shift in the CDF of the nominal model run towards the CDF of the calibrated model run. Note, however, that a comparison on the basis of CDFs may result in too optimistic a judgement, because it means that the relation with geographical location was abandoned. The CDF of the model results corresponded quite well with the CDF of the upscaled observations for both model outputs, whereas the nominal model results were clearly underestimated for both outputs. It was remarkable, however, that the nominal model results for both Al and NO₃ were almost completely covered by the 95% confidence interval of the upscaled observations.

Effect of calibration steps

The effect of the consecutive calibration steps was inspected by calculating the mean square error of prediction (*MSEP*) (Table 5). The nominal *MSEP* for all three inspected

model outputs appeared to be comparable, though it must be noted that the values were not normalised by the mean, which makes comparisons between the three inspected model outputs precarious. The first calibration step of the mineralisation rate constant (k_{mi}), considerably improved of the NO_3 performance, decreasing the *MSEP* by 50%. The calibrated median values for k_{mi} were clearly lower than the nominal values (Table 6), which resulted in lower mineralisation fluxes. The calibration also profoundly narrowed the confidence interval for k_{mi}. The calibration of the filtering factors (*ff*NH_3 *ff*NO_x) improved the *MSEP* only slightly (Table 5). The slight improvement of step 2 also resulted in a minor adaptation of the median parameter values (Table 6). Only the calibrated median value for deciduous forest ended up somewhat below the nominal values. Yet the 95% confidence interval for *ff*NH_3 (CON) was clearly compressed, while the confidence intervals for deciduous forest were expanded. This last result was most likely due to a smaller number of 5 × 5 km^2 blocks with deciduous forest (24) than with coniferous forest (129). Although the Al concentration was not considered during the first two calibration steps, its performance clearly improved. This was due to an overestimation of both Al and NO_3 during the nominal run (cf. Figure 2 and Figure 4) and the positive relationship between NO_3 and Al. Higher inputs of NO_3 (either by mineralisation or by throughfall) yield a higher acid load and hence higher Al concentrations. At the same time the performance of the model for the pH slightly deteriorated.

Table 5 Overview of the performance of the consecutive calibration steps

Calibration Step	Parameter	Mean squared error of prediction[1]			Criterion
		Al	NO_3	pH	
0	Nominal	0.17	0.18	0.16	
1	k_{mi}	0.13	0.09	0.17	NO_3 + NH_4
2	*ff*NH_3 *ff*NO_x	0.12	0.08	0.17	NO_3 + NH_4
3	fr_{ni}	0.08	0.06	0.19	Al, NO_3, pH
4	fr_{de}	0.08	0.06	0.19	Al, NO_3, pH
5	*ff*SO_4	0.07	0.06	0.18	SO_4
6	f_{dd}	0.07	0.06	0.18	BC_2
7	KAl_{ox}	0.07	0.06	0.17	Al, pH
8	KAl_{ex} KH_{ex}	0.05	0.08	0.02	Al, NO_3, pH

[1] Based on concentrations expressed in mol_c m^{-3}

The calibration of the nitrification fraction fr_{ni} profoundly improved the prediction of both Al (33% reduction of the *MSEP*) and NO_3 (25% reduction of the *MSEP*), whereas that of the pH deteriorated further. The calibration of fr_{ni} gave lower median values of fr_{ni} for sandy soils (SP and SR) and clay soils (CN) (Table 7). Those for peat (PN) and loess (LN) did not changed, because the lack of data on these soil types caused identification problems. Only 9 blocks of size 5 × 5 km^2 included PN and LN, whereas there were 144 blocks for SP and SR. This also explains why the confidence interval, was narrowed only for SP and SR. Although fr_{ni} directly influences the NO_3 concentration, its effect on the Al concentration (in terms of *MSEP* values) was much large than on the NO_3 concentration, which appeared to be negligible.

The calibration of the denitrification fraction had no effect. This was also due to identification problems, caused by a lack of information on the moisture condition. Adjusting the filtering factor for SO_2 ($ffSO_2$) improved both the Al concentration and the pH. Remarkably, the calibration of $ffSO_2$ resulted in a median value for deciduous forest (DEC) that was considerably higher than for coniferous forest (CON) (Table 6). This was a rather unexpected result, because the filtering capacity of spruce forest is higher than that of deciduous forest (De Vries *et al.*, 1995b). The anomaly was most probably induced by the fact that the number of blocks with deciduous forest was much smaller than the number of blocks with coniferous forest.

Table 6 Nominal (Nom.) and calibrated (Cal.) 95% confidence intervals and median values of the vegetation-related parameters

Tree species	95% conf. interval	k_{mi} [a^{-1}]		$ffNH_3$ [-]		$ffNOx$ [-]		$ffSO_2$ [-]		f_{dd} [-]	
		Nom.	Cal.	Nom.	Cal.	Nom.	Cal.	Nom.	Cal.	Nom.	Cal.
CON	P02.5[1]	0.02	0.02	1.0	1.0	0.6	0.6	1.0	1.4	1.5	2.9
	Median	0.05	0.03	1.3	1.3	0.9	1.0	1.5	1.5	2.8	3.5
	P97.5[2]	0.10	0.03	1.8	1.6	1.2	1.3	1.8	1.6	3.5	4.1
DEC	P02.5	0.02	0.01	0.8	0.9	0.5	-0.5	0.8	1.7	1.5	2.0
	Median	0.05	0.04	1.1	1.0	0.7	0.6	1.2	2.0	2.0	3.4
	P97.5	0.10	0.06	1.4	1.9	1.0	1.8	1.4	2.4	2.5	4.7

[1] P02.5 = 2.5 percentile, i.e. lower side of the 95% confidence interval
[2] P97.5 = 97.5 percentile, i.e. upper side of the 95% confidence interval

The use of the dry deposition factor (f_{dd}) did not improve the performance of Al, NO_3 and pH, although its calibration yielded higher median parameter values for both DEC and CON (Table 6). This step resulted in increased BC2 and BC concentrations, which were obviously underestimated by the nominal values. As with the other filtering factors, the confidence interval was only narrowed for coniferous forest.

The calibration of the dissolution constant of secondary Al precipitates (KAl_{ox}) resulted in a slight improvement of the pH performance. The median values for SP, SR and LN were reduced, whereas the values for CN and PN remained unchanged (Table 7). Finally, the calibration of the exchange constants (KAl_{ex} and KH_{ex}) resulted in a considerable performance improvement of the pH and to a lesser extent of the Al concentration, whereas the performance of the NO_3 concentration worsened. The latter must be attributed to feedbacks between pH and the N transformation processes. The calibration was able to reduce the width of the confidence interval of KAl_{ox} considerably for all soil types, except for LN. Furthermore, slight improvements were found for the exchange constants KAl_{ex} and KH_{ex} for the soil types SR, CN and PN.

In conclusion, the calibration clearly improved of the model performance and reduced uncertainty in the model input data. The model performance for the Al and NO_3 concentrations was improved mostly by the calibration of the 'N related' process parameters, i.e. mineralisation (k_{mi}) and the nitrification (f_{ni}). The improvement due to the calibration of the 'Al related' parameters was clearly less successful. Of the 'Al-

related' process parameters, it were especially the exchange constants which improved the model performance.

Table 7 Nominal (Nom.) and calibrated (Cal.) 95% confidence intervals and median values of the soil-related parameters

Soil type	95% conf. interval	f_{ni} [-] Nom.	f_{ni} Cal.	f_{de} [-] Nom.	f_{de} Cal.	KAl_{ox} [log(mol^{-2} l^2)] Nom.	KAl_{ox} Cal.	KAl_{ex} [log(mol l^{-1})] Nom.	KAl_{ex} Cal.	KH_{ex} [log(mol^{-1} l)] Nom.	KH_{ex} Cal.
SP	P02.5[1]	0.8	0.6	0.0	n.o.[3]	7.6	7.6	-0.3	-1.7	3.6	-5.7
	Median	1.0	0.7	0.9	0.9	8.2	7.8	0.8	-0.1	3.9	3.7
	P97.5[2]	1.0	0.8	1.0	n.o.	8.7	8.1	1.7	1.5	4.5	13.2
SR	P02.5	0.8	0.6	0.0	n.o.	6.8	7.8	0.2	-0.2	3.7	-0.1
	Median	1.0	0.7	0.9	0.9	8.2	8.0	0.3	0.1	3.9	1.7
	P97.5	1.0	0.8	1.0	n.o.	8.0	8.3	1.0	0.3	4.3	3.5
CN	P02.5	0.6	0.6	0.5	n.o.	8.5	8.7	-4.3	-4.9	3.8	2.2
	Median	1.0	0.8	1.0	1.0	9.4	9.4	-3.4	-3.4	6.7	2.4
	P97.5	1.0	1.1	1.0	n.o.	10.2	10.1	-2.9	-3.0	9.1	2.8
LN	P02.5	0.7	-2.0	0.6	n.o.	7.1	5.8	-1.7	-4.6	2.8	-9.6
	Median	1.0	1.0	0.9	0.9	8.3	7.5	0.6	-0.4	4.2	3.8
	P97.5	1.0	4.0	1.0	n.o.	9.0	9.2	1.5	3.9	7.1	17.2
PN	P02.5	0.5	$-\infty$	0.0	n.o.	4.9	5.6	-4.0	-2.6	2.1	3.1
	Median	1.0	1.0	1.0	1.0	6.5	6.5	-2.1	-2.1	3.5	3.5
	P97.5	1.0	∞	1.0	n.o.	9.2	7.1	-1.0	-1.7	5.7	3.9

[1] P02.5 = 2.5 percentile, i.e. lower side of the 95% confidence interval
[2] P97.5 = 2.5 percentile, i.e. upper side of the 95% confidence interval
[3] n.o. = not optimised, due to identification problems

Of the vegetation-related parameters, narrowed confidence intervals and the resulting reduction in the uncertainty level of the model input were found especially for k_{mi} and the filtering factors in coniferous forests, except for ffNOx. For deciduous forest, however, it was only feasible to reduce the level of input uncertainty for k_{mi} and ffSO$_2$.

The calibration resulted in a reduction of the uncertainty of most soil-related input data. This reduction was, however, limited to the SP and SR soil types. As was the case for the vegetation-related parameters, the uncertainty in soil-related parameters for CN, LN and PN was hardly improved, due to data limitations. Finally, our data set did not allow us to reduce the uncertainty of the denitrification fraction (f_{de}).

Model error quantification

Using the methodology described in section 3.3, the model was 'validated' on a block scale for 5 × 5 km^2 blocks. This was done by quantifying the model error for both the nominal model results and the results of the calibrated model. Because the input error

was only quantified for the nominal model (cf. section 3.3; Kros *et al.*, 1999), the partitioning of the model error into a structural part (σ^2_{MES}) and an input part (σ^2_{MEI}) was only possible for the nominal model run. The model errors thus quantified for Al and NO_3 are presented in Table 8.

Table 8 Model error (σ^2_{ME}) and relative contribution of the model structure error (MS) to the model error for three correlation coefficients of the cross-terms (cf. Eq. 13) for the block median Al and NO_3 concentration for 5×5 km^2 blocks for different categories of vegetation and soil types

		Nominal				Calibrated	
		$\rho = 0$		$\rho = 1$		$\rho = 0$	$\rho = 1$
Constituent	Category	σ^2_{ME}[1]	MS (%)	σ^2_{ME}[1]	MS (%)	σ^2_{ME}[1]	σ^2_{ME}[1]
Al	CON	0.7 (1.0)	<0[2]	3.4 (5.4)	49	0.02 (0.14)	2.1 (2.7)
	DEC	0.6 (0.9)	<0[2]	3.0 (4.3)	44	0.13 (037)	2.2 (2.8)
	SP	0.2 (0.5)	<0[2]	2.5 (3.3)	41	-[3]	1.6 (2.0)
	SR	1.1 (1.4)	<0[2]	4.0 (7.3)	53	0.2 (0.51)	2.5 (3.3)
	CN	-[3]	-	2.0 (2.6)	19	-	2.0 (2.5)
	LN	0.3 (0.6)	<0[2]	2.7 (3.7)	15	0.04 (0.19)	2.2 (2.9)
	PN	-[3]	-	-	-	-	-
	Over all	0.7 (1.0)	<0[2]	3.3 (5.1)	48	0.04 (0.20)	2.1 (2.7)
NO_3	CON	2.3 (3.0)	<0[2]	5.4 (14.4)	45	-[23]	1.3 (1.6)
	DEC	2.9 (4.1)	<0[2]	5.9 (19.1)	52	-	1.6 (2.0)
	SP	3.3 (5.1)	24	6.6 (27.1)	63	-	1.5 (1.9)
	SR	1.9 (2.4)	<0[2]	4.7 (10.4)	30	-	1.2 (1.5)
	CN	1.2 (1.5)	<0[2]	3.8 (6.6)	32	0.05 (0.23)	1.9 (2.4)
	LN	3.0 (4.4)	43	6.4 (24.5)	73	-	1.0 (1.3)
	PN	-[3]	-	-	-	-	-
	Over all	2.4 (3.2)	<0[2]	5.4 (14.8)	46	-	1.4 (1.7)

[1] Values in brackets denote the coefficients of variation (CV) of the back-transformed data derived from the variance of the log-transformed data by: $CV = \sqrt{e^{\sigma^2} - 1}$. Concentration are given in mol$_c$ m^{-3} on the original scale.

[2] <0 means input error (σ^2_{MEI}) > model error (σ^2_{ME}), resulting in a negative value for the model structure error (cf. Eq. 16)

[3] means no real solution for Eq. 14, discriminant < 0

It is obvious that the correlation coefficient in Eq. (13) must be positive. This means that a realistic estimate of the average model error lies between the results for $\varrho = 0$ and $\varrho = 1$ (cf. section 3.3). Thus, the average model error for Al for the nominal model run lies between 0.7 and 3.3, whereas for NO_3 the average model error was considerably higher, between 2.4 and 5.4. The larger average model error for NO_3 is supported by Figure 5, where the CDF of the nominal SMART2 run deviates more from the CDF for upscaled data than was the case for Al. Model calibration obviously lowered the model error for both Al and NO_3 concentrations.

Inspection of the model error per soil and vegetation category showed that the greatest model error for Al occurred for rich sandy soils (SR), whereas the greatest model error for NO_3 was found for poor sandy soils (SP). It was for these categories that the calibration produced the greatest gain, confirming the findings reported in

section 4.2. Again, this was caused by the fact that more data were available for SP and SR soils.

The differences in model error between the two forest types were small for both compounds, although Al showed a slightly smaller error for DEC, whereas NO_3 showed a slightly smaller error for CON. The differences for the five soil types, however, were larger. The model error was relatively small for CN (both for Al and NO_3) and for LN (for Al). Relatively large model errors were found for SR (Al), LN and SP (NO_3).

The subdivision of the model error into an input error part and a structural error part should ideally provide useful information on weak and strong aspects of the model. A small structural part means that a large part of the model error is absorbed by the input error or vice versa. A large structural error means that efforts should concentrate on improving the process formulation of the model, whereas a large input error indicates that the emphasis should be on both better and additional data gathering.

Inspection of the relative contributions of the input error and the model structure error to the total model error shows that there are no major differences between Al and NO_3. In the case of $\varrho = 1$, the model error for both outputs is equally distributed over both terms. However, these results depend greatly on the value of ϱ. As the correlation coefficient decreases, the relative contribution of the model structure error increases, because the model error decreases while the input error remains constant. At a certain point, the model error even exceeds the input error, yielding a negative model structure error. This indicates an unrealistic value of either the correlation coefficient or the input error.

The present study has shown that the relative contribution of the model structure error was remarkably small for the Al concentrations in CN and LN. For these soil types, additional data gathering might be the most beneficial approach. To a lesser extent, this was also true for the NO_3 concentrations in SR and CN.

3.3.5   Conclusions

Upscaling model outputs

The present study assessed the calibration and validation of a relatively simple soil acidification model on a block scale. Although SMART2 was developed especially for application on a national to European scale, it still runs on a point support. Heuvelink and Pebesma (1999) showed that the most appropriate way to obtain results at a block support is to run the model on a point scale for multiple point locations within the block, followed by aggregation of the model output. This avoids application of the model on a larger scale, which is essential because application on a larger scale requires block-averaged parameters, and it is hardly possible to aggregate point support inputs in such a way that they yield the correct block-averaged model output (cf. Wen and Gómez-Hernández, 1996). Furthermore, this procedure has several additional advantages since point support output is available, any linear or non-linear aggregation

may be used (e.g. block mean, block median, areal fractions exceeding a threshold) and any block size or shape may be chosen (cf. Heuvelink and Pebesma, 1999).

Upscaling monitoring data

To obtain calibration and validation data on a block scale, c 250 point observations have been extrapolated to points in a 250 $\times$ 250 m² grid, using multiple regression analysis. The regression analysis was able to explain 48% of the variance in the NO_3 concentration, whereas the percentage of Al variance accounted for was 50%. The NO_3 concentration was best explained by soil type, vegetation type, NH_x deposition, mean spring water table and area of contiguous forest. The Al concentration could be fully explained by soil type, vegetation type and mean spring water table. The subsequent extrapolations of these point values to 5 $\times$ 5 km² blocks substantially narrowed the distributions. The final step towards the upscaled observation, i.e. the addition of the kriged residuals at 5 $\times$ 5 km² blocks, clearly improved the predictions, reducing the *MSEP* by c 15% for both compounds. We conclude that the procedure used is well suited for the upscaling of observed soil solution concentrations of NO_3 and Al from a point support to a block support.

Calibration

The SMART2 model was calibrated at a 5 $\times$ 5 km² block support using the upscaled monitoring data. The used calibration procedure appeared to be a useful tool for finding optimal parameter ranges, and for reducing input uncertainties. Although the effects of reduced input uncertainty on the uncertainty in the model outputs remained unquantified, our study provided useful results. The calibration appeared to be very successful in correcting the overestimation of Al and NO_3 concentrations resulting from the nominal parameter set. It seems likely that these overestimations were mainly due to an overestimation of the mineralisation rate and the nitrification rate parameters, although this result is biased by the sequence of the calibration steps. When calibrating the forest filtering factors (ffNH₃, ffNO$_x$) prior to the mineralisation rate, results would definitely have been different. However, it was assumed that the filtering factors were more certain than the mineralisation rate, since the filtering factors were derived from various individual throughfall measurements throughout the country, whereas the mineralisation rates were roughly derived from various literature sources (Kros *et al.*, 1995a). The calibration of the Al-related parameters only resulted in a slight improvement of the model performance, with the exception of the exchange constants, although this was only true for the Al concentration and pH. The improvement in modelled pH was remarkable.

As already mentioned, it is most likely that calibration results generally depend on the order of the calibration steps. However, in our case identification problems made it absolutely necessary to perform a stepwise procedure, and we had good reasons for the order of the consecutive calibration steps we used (cf. section 3.2). Another important aspect is that data used for calibration, i.e. the upscaled monitoring data, introduce an additional uncertainty caused by upscaling (cf. section 3.3). Because

this error was not included in the calibration procedure, the calibration may seem to provide a level of accuracy that is not really substantiated. Analysis of this error shows that the nominal run is already within the 95% confidence interval of the data. Nevertheless, it can be concluded that calibration leads to an obvious improvement of the model performance and a reduction of the uncertainty in the model input data.

Model error

It has been shown that it is possible to perform a model validation at a block support using point support validation measurements. Quantification of the model error showed that it was relatively large for the nominal run, whereas calibration greatly reduced the model error when focussing on the block median results.

Splitting the model error into an input error part and a structural error part should ideally provide useful information on weak and strong aspects of the model. In the present study, however, the model validation was impeded by a correlation between the upscaled observations and the upscaled model results. Therefore, it was not feasible to unambiguously split the model errors into a part originating from the uncertainty in the model input data and the uncertainty due to the model structure. Nevertheless, it can be concluded that the relative contribution of the model structure error was remarkably small for the Al concentration in clay (CN) and loess (LN) soils. For these soil types, therefore, additional data gathering might be beneficial. To a lesser extent, this is also true for the NO_3 concentration in rich sandy soils (SR) and clay soils (CN).

Final remarks

We do believe there is a value in fitting parameters to data to be simulated, especially when it is not a goal in itself but rather done in conjunction to comparing a non-calibrated model simulation to these data (our nominal model simulation). Also, we do not use validation in the sense of proving that the model is capable of producing the results it was intended for. First of all no standards were defined ahead of the validation procedure, second the data available were insufficient (small numbers, large variations) to allow such a decision to be well-founded.

In plain terms, the most important result is that soil acidification modelling on a regional scale is, despite all efforts, still prone to large uncertainties. To circumvent these problems, more data would be required both in time and space. Lack of such data can regarded as the principal bottleneck towards further improvement of the model. Just as stated by Janssen and Heuberger (1995), model validation is not a 'once-and-for-all' activity leading to an absolute and definite judgement on the model's adequacy. This is especially true for this research since the remaining model error after model calibration is still considerably high for both Al and NO_3.

Acknowledgement

3.4 Quantification of nitrate leaching from forest soils on a national scale

Abstract

To evaluate the effects of N emission policies it is necessary to have a reliable information of nitrate concentrations and leaching fluxes from forest ecosystems. It is specially desirable to have insight into the regional variability of nitrate concentrations, to support local policy on emission abatement strategies.. In this paper, three methods for calculation of a spatial distribution on soil nitrate concentrations in Dutch forest ecosystems are compared. We considered (i) a regression model based on observed nitrate concentrations and additional data on explanatory variables (ii) a semi-empirical dynamic model WANDA, and (iii) a process-oriented model SMART2. The two dynamic models are frequently used for the evaluation of effects of reductions in nitrogen deposition at a scale ranging from region to a country as a whole. We considered the results of the regression model as a reference to evaluate the performance of the two dynamic models. Furthermore, the results of the three methods are also compared with a steady-state approach that is currently used for the derivation of critical loads on N.

Results show that both dynamic models give similar results on a national scale, when inspected in the form of cumulative distribution functions. The regional variability is predicted differently by both models. Discrepancies are mainly caused by a difference in handling forest filtering. All three methods show that, despite the high N inputs, Dutch forest still accumulate more N than they release. This implies that presently acceptable N deposition in view of groundwater quality are higher than the (long-term) critical loads. However, in areas with high atmospheric N input all three methods predict that the EU standard for nitrate in groundwater for (50 mg l^{-1}) is exceeded.

3.4.1 Introduction

In large parts of western Europe, in particular the Netherlands, N input through atmospheric deposition to forest ecosystems exceeds the long-term capacity of the ecosystem to retain N (De Vries *et al.*, 1995b; Dise *et al*, 1998; Gundersen, 1995). This may have several adverse effects: (i) decrease in botanical diversity (cf. Bobbink *et al.*, 1998), (ii) eutrophication of ground - and surface waters (cf. De Vries, 1994), (iii) acidification (cf. Van Breemen *et al.*, 1982) and (iv) decreased tree vitality (cf. Boxman and Van Dijk, 1988). For decades, governmental authorities have been busy with policy and measurements aimed at reducing of N inputs in semi-natural ecosystems. Notable examples are the NO$_x$ protocol (Sophia protocol, UN/ECE) and the multi-pollutant-multi-effect protocol (Gothenburg protocol, UN/ECE). For the evaluation of N emission policy it is desirable to have a reliable map at an appropriate spatial scale, ranging from regional to national or even European scale, of the NO$_3$ concentration in drainage water and N leaching fluxes from semi-natural ecosystems.

Various methodologies are available for the quantification of the extend and geographical distribution of N leaching. They range from statistical methods based directly on measurements, such as multiple regression (cf. Leeters *et al.*, 1994), generalised additive modelling (cf. Tiktak *et al.*, 1998, though this refers to cadmium

leaching), stratified block-kriging (Pebesma and De Kwaadsteniet, 1997) and process-oriented models ranging from simple (cf. De Vries *et al.*, 1989, 1995a) to complex models (cf. Boers *et al.*, 1995, used for agricultural soils). For large-scale analyses, complex models are generally not appropriate, because of the huge data demand. At large spatial scales these large amounts of data are not available or are at least associated with large uncertainties. Therefore, the use of simpler models with a smaller data demand is justified on a large spatial scale (cf. Chapter 2.4; De Vries *et al.*, 1998). Statistical methods have the disadvantage that they are generally not able to generate future predictions, however, they have proven to be suitable for the generation of the actual geographical distribution. Process-oriented dynamic models, however, have been developed mainly to analyse temporal trends, either for a point application or an application in a spatial context. They do suffer a high dependency on (usually) scarce observations.

In this research results from two simple dynamic models, which differ in degree of complexity, are compared with NO_3 concentrations based on statistically scaled-up monitoring data in Dutch forest soils. In this way, we gave an indication of the reliability of national scale assessment of NO_3 concentrations below the root zone. We also discuss the implications of the results with respect to critical N loads.

3.4.2 Methodology

General

We compared three methods for the quantification of NO_3 concentrations below forest ecosystems in the Netherlands: (i) regression analysis based on observations and additional data on explanatory variables (cf. Mol-Dijkstra and Kros, 1999), (ii) a semi-empirical model WANDA (Tietema *et al.*, in prep.), and (iii) a simple process oriented model SMART2 (Kros *et al.*, 1995a). The results of the regression analysis were used as a reference, to quantify the performance of the two dynamic models, assuming that those results are the best estimate of the actual geographical distribution of the NO_3 concentration.

We investigated the yearly average NO_3 concentration at 1 m depth (i.e. below the root zone). A common feature of the three methods is that they are based on point information, i.e. either model-input data or observed concentrations. In order to derive a map with NO_3 concentrations, the available point information (point support) must be transformed towards a plane (block support). We aggregated 'point values' to block values by taking the block median values of the underlying point values (see Figure 1). All basic (point) calculations, were performed at a 250×250 m^2 grid. These 'point' calculations where aggregated to 1×1 km^2 blocks by taken the block median value. A 1×1 km^2 grid was chosen as a reference, because deposition estimates were available at that scale.
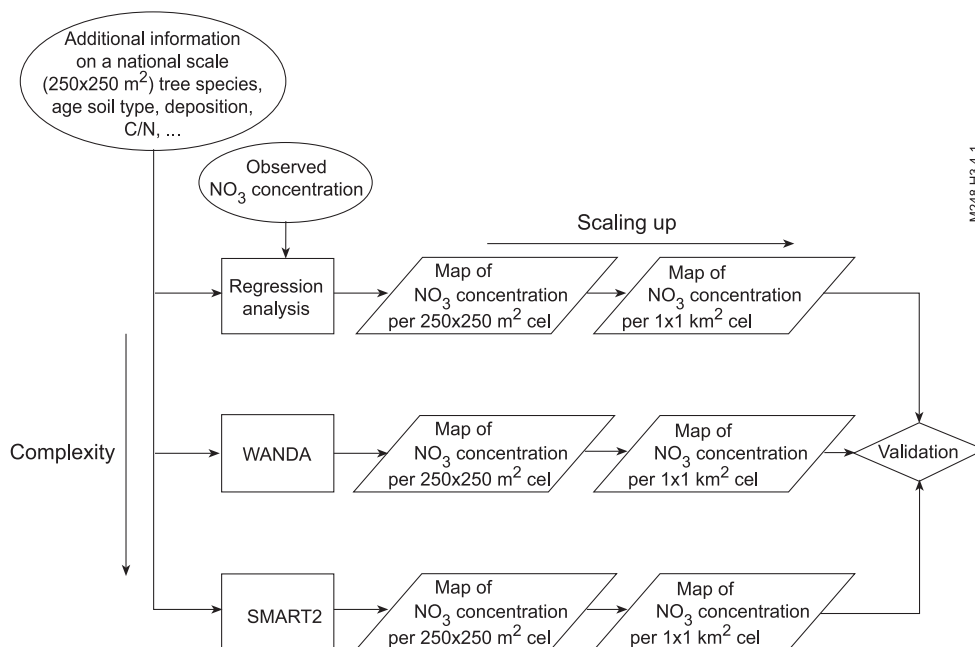
Figure 1 Diagram showing the procedure of model validation and up-scaling

Up-scaling point observations by regression analysis

Regression analysis was applied to generate a map with soil solution concentrations of NO_3 for a 1×1 km^2 grid (cf. Mol-Dijkstra and Kros, 1999). First a multiple regression analyses at a 250×250 m^2 grid was used to estimate values at unsampled locations by including all relevant additional information which may accounted for systematic effects. Secondly, the 250×250 m^2 values were aggregated towards a 1×1 km^2 grid.

Regression analysis was based on a data set of about 150 measurements on soil solution concentrations in forest stands on non calcareous sandy soils throughout the Netherlands (De Vries *et al.*, 1995b). The soil solution was sampled between February to May 1990. Composite samples, consisting of 20 sub samples were taken from the mineral top soil (0 to 30 cm) and the mineral subsoil (60 to 100 cm) in early spring. During this period the composition of the soil solution reasonably corresponds with the flux weighted annual average soil solution concentration (De Vries *et al.*, 1995b). Soil solution was extracted by centrifugation. The locations were restricted to non-calcareous soils throughout the country. The tree species included were Scotch pine, black pine, Douglas fir, Norway spruce, Norway spruce, Japanese larch, oak and beech.

The observations sites were lumped into forest type classes, watertable classes and soil type classes that were also used for the model simulations. The tree species were lumped into tree forest type classes:

- Coniferous stands (Scotch pine), i.e. evergreen trees with moderate forest filtering capacity, growth rate and transpiration rate;
- Spruce stand (Douglas fir, Norway spruce and black pine), i.e. evergreen trees with high forest filtering capacity, growth rate and transpiration rate
- Deciduous stands (Japanese larch, oak and beech), i.e. needle or leaf sheddy trees with low forest filtering capacity, growth rate and transpiration rate.

All soil types were lumped into one class, i.e. non-calcareous sandy soils. A distinction was made into five water table class (cf. Kros *et al.*, 1995a).

For the regression analysis candidate predictor variables were derived from available national databases and maps at a resolution of 250×250 m² (cf. Mol-Dijkstra and Kros, 1999). These variables include: land-use, soil type, tree species, total deposition of N and S, canopy closure, tree height, total area of the forest, nearest distance to the forest edge and the principal land-use at the nearest forest edge. We selected these variables because they were available it was known from previous research that they potentially have a significant effect on the soil solution concentration and are available on a national scale (Leeters *et al.*, 1994). With multiple linear regression the soil solution concentrations were fitted to the candidate predictor variables, using the statistical package GENSTAT (Genstat 5, 1987). Since the predictor variables are either quantitative (e.g. deposition) or qualitative (e.g. tree type) the regression equations includes both types of variables. The models with the best fit were derived by the following procedure: (i) find the best model with the SELECT option from GENSTAT, (ii) investigate whether non-linearity's leads to improvements, by using the SPLINE option from GENSTAT, (iii) investigate whether the inclusions of interactions leads to a better model. In order to meet the prerequisite of a normal distribution, the explaining variables were log-transformed using the natural logarithm. For the presentation, results were back-transformed towards the linear scale.

The WANDA Model

WANDA (regional model With Aggregated Nitrogen DynAmics) is a semi-empirical process oriented model (Tietema, 1999). The basis of the model is the predictive importance of the C/N ratio for NO_3 leaching. A negative correlation between both parameters has been found in various large data sets (McNulty *et al.*, 1991; Tietema and Beier, 1995; Gundersen, 1995; Gundersen *et al.*, 1998). WANDA consist of three organic nitrogen pools: trees, labile organic matter (LOM) and refractory organic matter (ROM) and two inorganic nitrogen pools: NH_4 and NO_3. The sources of inorganic nitrogen are atmospheric deposition and mineralisation of ROM. The sinks are plant uptake, microbial immobilisation in LOM and NO_3 leaching. Net plant uptake and ROM mineralisation are negative linear functions of tree age. Beyond a certain tree age there is no plant uptake nor ROM mineralisation. Microbial immobilisation is a function of C/N ratio of the organic layer. Below a certain critical C/N ratio no inorganic nitrogen is being immobilised, beyond a maximal feasible C/N ratio all available inorganic nitrogen is immobilised. Between these two values, the fraction taken up varies in a linear fashion with C/N.

The net uptake of NH_4 and NO_3 in the various pools is calculated in a certain order. NH_4 is taken up preferentially over NO_3 by both plants and microbes, and the trees take up all required nitrogen before it becomes available for microbial uptake. The NH_4 and NO_3 available in excess of the demand leaves as NO_3, assuming a complete nitrification and no denitrification. This assumption limits the use of WANDA to well-drained soils.

There are only five unknown parameters in this relatively simple model. These parameters are the four threshold C/N ratios for microbial immobilisation in LOM (upper and lower limit for NH_4 and NO_3 immobilisation) and the maximum rate of ROM mineralisation at a theoretical tree age of zero. All other parameters could be derived from available forestry information. The five unknown parameters were identified by parameter optimalisation using the relationship between C/N ratio in the organic layer and NO_3 leaching found by Gundersen (1995) in the ECOFEE data set (Figure 1; Table 1). WANDA directly calculates NO_3 leaching. In order to calculate NO_3 concentrations in drainage water, the drainage water flux is calculated as a function of tree species and tree age.

The SMART2 Model

SMART2 (Kros *et al.*, 1995a) is a simple one-compartment soil acidification and nutrient cycling model that includes the major hydrological and biogeochemical processes in the vegetation, litter and mineral soil. Apart from nitrate (NO_3) and ammonium (NH_4) concentrations the model also predicts changes in aluminium (Al), base cation (BC), and sulphate (SO_4) concentrations and the pH, in the soil solution and solid phase characteristics depicting the acidification status, i.e. carbonate content, base saturation and readily available Al content. The SMART2 model is an extension of the dynamic soil acidification model SMART (De Vries *et al.*, 1989). The major extensions in SMART2 are the inclusion of a nutrient cycle and an improved modelling of hydrology. The SMART2 model consists of a set of mass balance equations, describing the soil input-output relationships, and a set of equations describing the rate-limited and equilibrium soil processes.

The soil solution chemistry in SMART2 depends solely on the net element input from the atmosphere (the product of deposition and filtering factor) and groundwater (seepage), canopy interactions (foliar uptake, foliar exudation), geochemical interactions in the soil (CO_2 equilibria, weathering of carbonates, silicates and/or Al-hydroxides, SO_4 sorption and cation exchange) and a complete nutrient cycle (litterfall, mineralisation, root uptake, nitrification and denitrification). Nitrogen The adsorption of NH_4 is not taken into account.

Growth of the vegetation and litterfall are modelled by a logistic growth function, which acts as a forcing function. Nutrient uptake is only limited when there is a shortage in the soil solution. Litterfall and root decay is the input to an organic pool containing N, BC2 and K. Mineralisation of above-ground organic matter (litter, including dead roots in the litter layer) a distinction is made between a rapidly decomposing pool of fresh litter (less than one year old) and a slowly decomposing

pool of old litter (more than one year). Nitrification and denitrification for the complete soil layer are described in as a fraction of the net input. The mineralisation, nitrification and denitrification rate constant are influenced by the mean water-table and pH.

Soil-solute transfers are described by simple rate-limiting (zero-order) reactions (e.g. uptake and silicate weathering) or by equilibrium reactions (e.g. carbonate and Al-hydroxide weathering and cation exchange). Influence of environmental factors such as pH on rate-limiting reactions and rate-limitation of weathering and exchange reactions are ignored. Solute transport is described by assuming complete mixing of the element input within one homogeneous soil compartment with a constant density and a fixed depth (at least the root zone). Since SMART2 is a single layer soil model neglecting vertical heterogeneity, it predicts the concentration of the soil water leaving the root zone. The annual water flux percolating from this layer is taken equal to the annual precipitation minus the annual evapotranspiration for the considered soil depth. Both terms must be specified as model input. The time step of the model is one year, so seasonal variations are not considered.

National scale application and model comparison

Input data for the national scale application of WANDA and SMART2 can be divided in system inputs and initial values of variables and parameters. System inputs for both models are the atmospheric deposition, hydrology and vegetation development or tree age. Input data included (i) a specific deposition scenario for each grid cell, (ii) model variables and parameters which were either related to a soil type or a vegetation type or to a combination of both and (iii) a soil map and vegetation map relating variables and parameters to grid cells. For the national scale application, a gridded soil map and vegetation map, representing the distinguished dominant soil types and vegetation types for a 250×250 km^2 grid respectively was made. In this map seven soil classes were distinguished and four vegetation types. This study was confined to forest on sandy soils, which means that only one soil type (non-calcareous sandy soils) and three vegetation types (DEC, SPR and CON) were used.

An essential system input for WANDA is the C/N ratio of the organic layer. This ratio was calculated for each grid by using a multiple regression relation based on measured C/N ratios in forest floor and additional data. For this relation the same dataset (i.e. De Vries *et al.*, 1995b) was used as for the derivation of the NO$_3$ concentration map, which also includes solid phase analyses. The derived multiple regression relation ($R^2=0.44$) contained as significant predictor variables, in decreasing order of importance: tree-species, soil type, age of the trees.

The thus derived maps at a resolution of 250×250 m^2 still have a point support, since they are based on point observations of soil solution concentrations. In order to derive values at a block support, the 250×250 m^2 'point maps' were aggregated to a 1×1 km^2 'block map', by taking the block median value.

An important aspect to notice is that WANDA and SMART2 simulate yearly averaged values, whereas the data set represents the concentration of ions in early spring (February to May). This influences the quality of the validation.

3.4.3   Results and discussion

Comparison of maps

The upscaled spatial distribution as calculated with the three methods is given in Figure 2A-C. The three methods show seriously different results. Compared to the regression, SMART2 calculates rather high NO_3 concentrations for the Veluwe area, i.e. a forested area in the centre of the country, whereas WANDA simulates rather low concentrations for this area. This difference was mainly caused by the way in which both models incorporates forest filtering induced by differences in roughness length. Both the regression model and WANDA explicitly account for the total area of the forest, assuming that a larger continuous area of dense forests results in lower forest filtering and thus a lower input of atmospheric deposition (cf. Draayers and Erisman, 1993). The SMART2 model, however, only includes forest filtering factors that depends on forest type, independent of the forested area. These factors were large for spruce forest and small deciduous forest. Taking into account that the Veluwe is a densely forested with spruce, it is obviously that WANDA and the regression model calculates lower NO_3 concentration for this area. Another remarkable difference between SMART2 and WANDA, is that WANDA calculates clearly higher NO_3 concentrations under wet circumstances. This can be recognised in Figure 2C by the lowlands (Gelderse Valley) in the middle of the country and the brook valleys in the southern part of the country, where WANDA also calculates higher NO_3 concentrations than the regression model. In fact this is an artefact of WANDA, which does not include denitrification. Therefore, this model is only applicable for dry ecosystems.

When inspecting the spatial distribution for each method separately and disregarding the above-mentioned omissions, the spatial images appeared to be rather consistent, i.e. high NO_3 concentration in areas with high deposition and vice versa.

Comparison of cumulative distribution functions

When comparing the results as cumulative distribution functions (CDF), the differences between the three methods seem to be much smaller (Figure 3A). Figure 3A shows the corresponding results of the maps shown in Figure 2, i.e. a CDF of all 1×1 km^2 grid cell values. From this figure it is obvious that at high concentrations (> 0.5 mol$_c$ m^{-3}) both WANDA and SMART2 under-estimated the NO_3 concentrations. At lower concentrations (< 0.4 mol$_c$ m^{-3}) SMART2 over-estimated the NO_3 concentrations., while WANDA over-estimated at low concentrations (< 0.3 mol$_c$ m^{-3}). The latter was connected to wet soils, which were not taken into account within WANDA.

A. Regression

B. SMART2

NO$_3$ (mg l^{-1})

☐ < 5
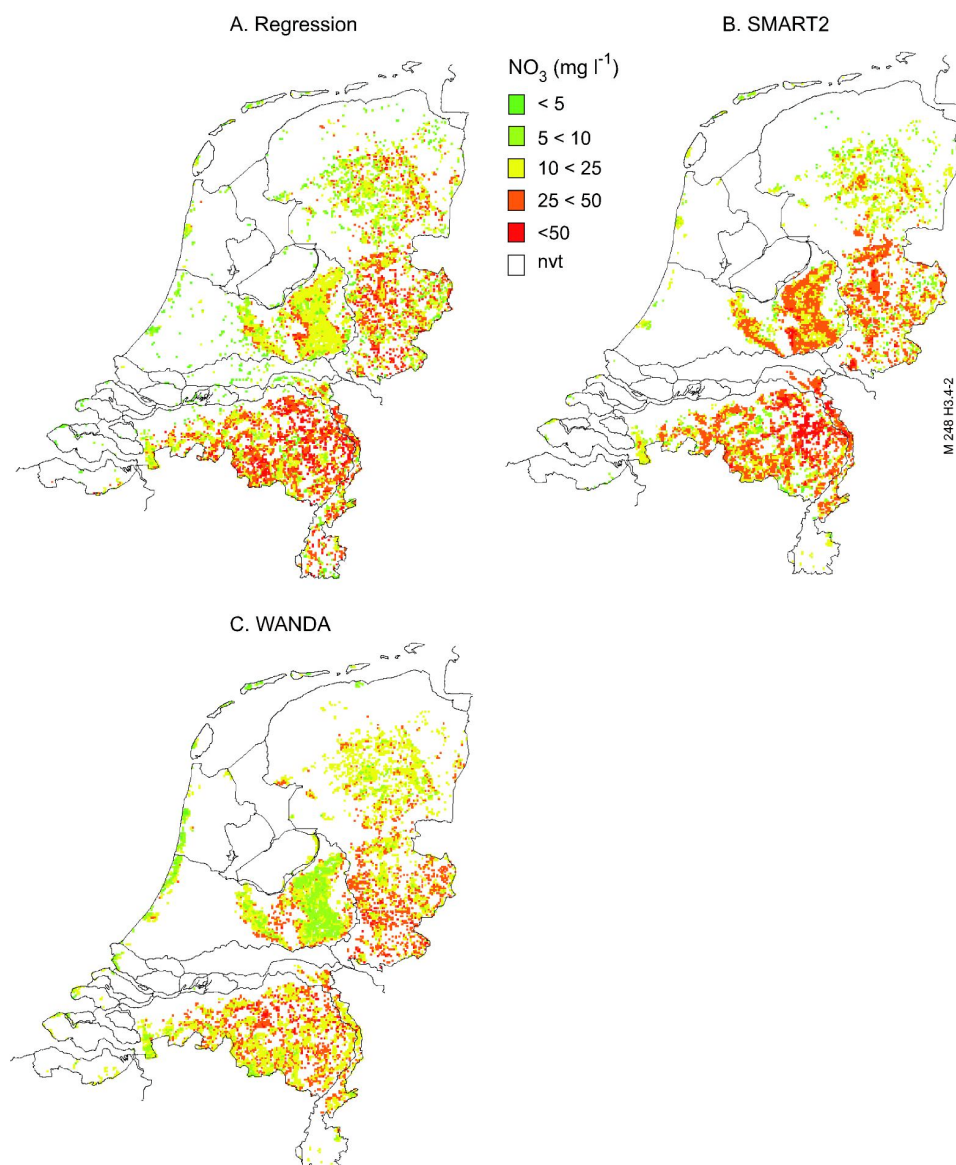☐ 5 < 10
☐ 10 < 25
☐ 25 < 50
☐ <50
☐ nvt

C. WANDA

Figure 2 Maps of the upscaled NO$_3$ concentration as estimated with the regression model (A) and via the dynamic models SMART2 (B) en WANDA (C)

To investigate the role of spatial scale in the performance of the two models, both model results as well as the regression data were also aggregated towards a larger grid size, i.e. 5, 10, 15, 20 and 25 km². From Figure 3B and C it is clear that the models perform best at a 5 km² grid, while the performance seems be worse at a 25 km² grid. This effect is only partly confirmed in terms of the calculated mean squared

error of prediction (*MSEP*) (Table 1). When inspecting the *MSEP* a larger grid size yields a better performance for both models. Although, the performance in terms of the *MSEP* is increasing, the spatial resolution of course decrease. Consequently, there is a gain in reliability at the cost of spatial variability. This trade-off between spatial resolution and reliability is, in fact, a well-known phenomenon. An important consequence of the loss of detail, i.e. averaging out of extremes, is a decreasing capability to identify areas where a concentration standard is exceeded. It is, however, precarious to draw conclusions on spatially explicit model results only based on CDFs. Because large regional differences exist, also at a rather small distance (0.5-1 km).
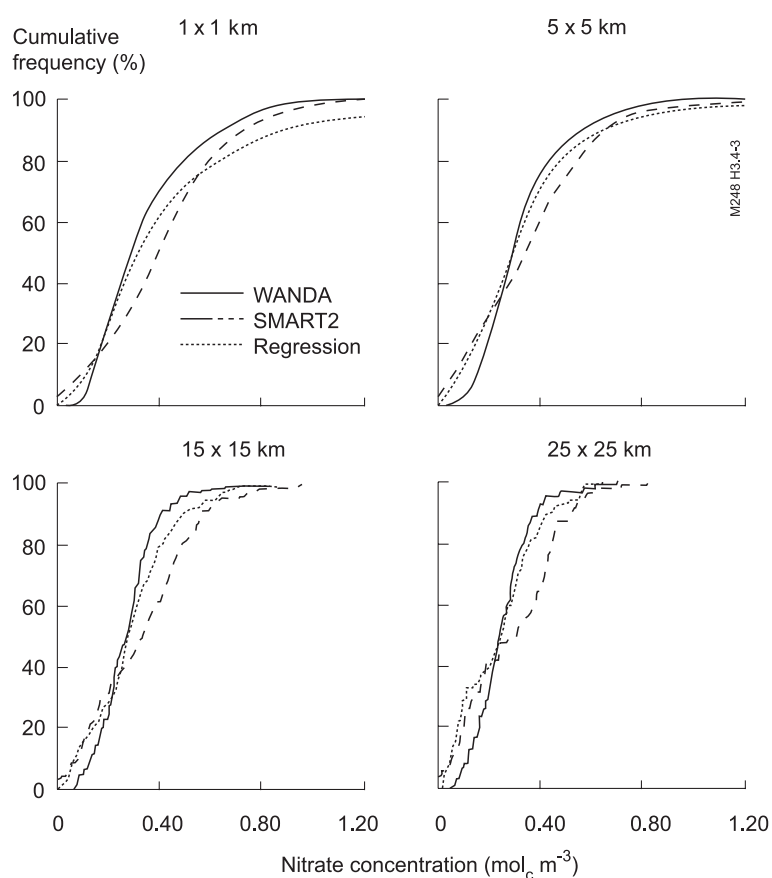

Figure 3 Cumulative distribution functions for a 1×1 km², 5×5 km², 15×15 km² and a 25×25 km² grid of the calculated NO₃ concentration by regression, SMART2 and WANDA

Table 1 Mean squared error of prediction (*MSEP*)[1] between WANDA results and the regression data and SMART2 results and regression data for five grid sizes

Model	1×1 km²	5×5 km²	10×10 km²	15×15 km²	20×20 km²	25×25 km²
SMART2	0.43	0.24	0.20	0.15	0.15	0.14
WANDA	0.49	0.30	0.25	0.18	0.18	0.19

[1]
$$MSEP = \frac{1}{N}\sum_{i}^{N}\left(P_i^{(1)} - P_i^{(2)}\right)^2$$

Impacts of used method on the exceedance of groundwater standards for nitrate

A comparison with the EU groundwater standard for phreatic groundwater value for NO_3 of 50 mg l^{-1} (0.8 mol_c m[-3]), shows that all three methods indicate substantial areas where this standard has been exceeded. This area is ranging from 10 to 20% of the considered area depending on the used method (see Figure 3A). These areas are mainly located in the south-eastern part of the country, which corresponds with areas with high NH_3 emission and deposition. In addition, all three methods show large areas, ranging from 40 to 80% of the total area considered, where the guidance concentration, i.e. 25 mg l^{-1} (0.4 mol_c m[-3]) has been exceeded Note that this range is much wider than where the groundwater standard is exceeded. This is caused by the fact that 25 mg l^{-1} lies around the median values, i.e. in the middle of the distribution, whereas 50 mg l^{-1} lies in the tail of the distribution. In other words the uncertainty in exceedance area is larger for the guidance concentration than for the EU standard.

Note also that the exceedance area highly depends on the used grid size. The larger the grid size, the smaller the exceedance area. It must be noted, however, that the method used here, is not a proper way to derive the exceedance area. A correct way is to start at the point scale data for a 250 × 250 m² grid and count the number of 250 × 250 m² cells within a 1 km² with a concentration higher than the standard concentration (cf. Kros *et al.*, 1999).

Relation with critical loads

Results of a spatial distribution of NO_3 concentrations below the root zone of semi-natural ecosystem are of special interest with respect to the exceedance of critical concentrations. Because critical loads are calculated with a steady-state method, they do take into account N (im)mobilisation from the soil and litter layer. In reality, however, dynamic processes play an important role also within the context of critical loads (Tietema *et al.*, in prep.), especially, when inspecting the short-term (<50 year).

Posch and Hettelingh (2001) also address the relation between dynamics and critical load (see Figure 4). During *Stage 1* the deposition is above the critical load, but the chemical variable is still below the critical value. Therefore, in this stage violation of the criterion do not occur despite the exceedance of the critical load (*Damage Delay Time = $t_2 - t_1$*). During *Stage 4* the deposition is below the critical load, but the criterion is still violated (*Recovery Delay Time = $t_4 - t_3$*).
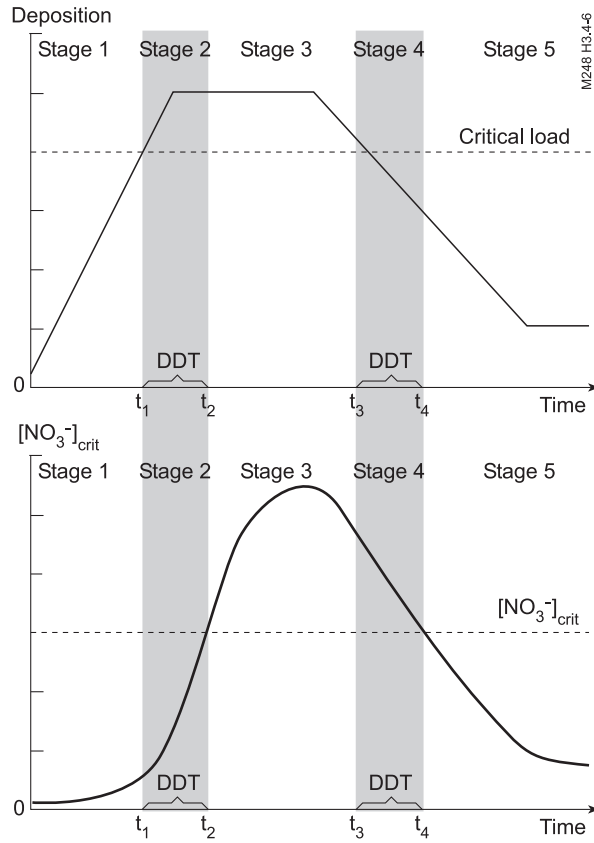
Figure 4 A typical temporal evolution of the deposition (top) and a soil chemical variable (e.g. NO_3 concentration) (bottom). The delay between the (non-) exceedance of the critical load and the (non-)violation of the critical chemical criterion: *Damage Delay Time* (DDT) and *Recovery Delay Time* (RDT) (After: Posch and Hettelingh, 2001)

To quantify the difference between the NO_3 concentration calculated with the dynamic models SMART2 and WANDA at one hand and a steady state method at the other hand, we also calculated the potential NO_3 concentration while neglecting all dynamic aspects. The steady state NO_3 concentration (in mol_c m^{-3}) was calculated as:

$$[NO_3] = \frac{N_{de} - N_{up} - N_{de}}{PE} \qquad (1)$$

where: N_{de} is the N deposition (mol_c m^{-3} a^{-1}), N_{up} is net long-term N uptake (mol_c m^{-3} a^{-1}), N_{de} the denitrification (mol_c m^{-2} a^{-1}), and PE the precipitation excess (m a^{-3}).
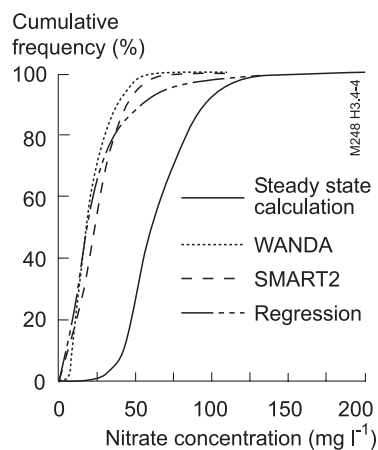
Figure 5 Cumulative distribution functions of the calculated NO$_3$ concentration as calculated with a steady state methods with de deposition for 1990 and the NO$_3$ concentration as calculated with the three methods at a 1×1 km^2 grid

Figure 5 shows that the steady-state NO$_3$ concentration is usually much higher than the actual concentration, indicating that still a lot of N is being immobilised in forest ecosystems in the Netherlands. All three methods provide a consistent result. Although some differences exists, esp. at high concentrations.

To get an impression about the short term and long-term effects in terms of deposition, we compared our data with the recently published updated critical loads for the Netherlands (De Vries *et al.*, 2000). For that purpose, we selected from the model results those sites where the NO$_3$ concentration was between 25 ± 0.56 mg l^{-1} and 50 ± 0.56 mg l^{-1}. The window of ± 0.56 mg l^{-1} (± 0.04 mol$_c$ m^{-3}) was determined empirically, such that the window size does not disturb the distribution. At a wider window the shape of the CDFs changes, whereas at a smaller window the CDFs became less smooth. These results together with the derived critical N load related to a critical NO$_3$ concentration of 25 and 50 mg l^{-1} are given in Figure 6. As already noticed from Figure 5, Figure 6 also shows that the actual situation is far from steady state. For all tree methods and both criteria, the forest soils can accept higher nitrogen deposition loads than the long-term critical loads without violating the critical concentrations. This means that many semi-natural terrestrial ecosystems in the Netherlands are immobilising N under the current circumstances. Also in this situation all three methods provide quite comparable results. However, when most systems will reach steady-state with respect to nitrogen saturation, the situation will be rather serious (see Figure 5). Steady-state seems to have been reached in ca. 10 % of area according to results of the up-scaled monitoring data (regression) for the 50 mg l^{-1} criterion. That the models WANDA and SMART2 do not simulate this, indicates that the two models overestimate the capability to store N in the ecosystem in particular cases.

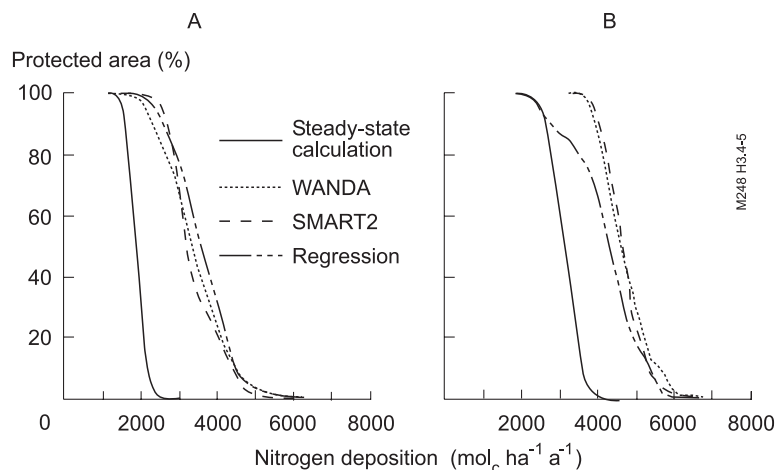A   B

Protected area (%)

Figure 6 Percentage protected area as a function of the total N deposition according to a steady-state calculation and the three inspected methods at the target value on NO$_3$ of 25 mg l^{-1} (A) and the EU standard on NO$_3$ of 50 mg l^{-1} (B)

3.4.4   Conclusions

The NO$_3$ maps as calculated by the three methods provided clearly different results. Yet, the spatial distributions in the form of a cumulative distribution function provided comparable results, especially at 5 × 5 km^2 grid. This gridcell increase, however, cost spatial resolution, and decrease the benefit for determining exceedance areas.

The differences between the three approaches are mainly caused by the differences in handling forest filtering and denitrification. To improve predictions for densely forested areas, the SMART2 model must be extended with a spatial dependent filtering factor, i.e. nearest distance to the forest edge. The incorporation of this effect into the model is rather simple. The predictions of WANDA under wet circumstances, can be improved by the incorporation of denitrification.

All results point to the fact that most forests in the Netherlands are still accumulating N. The actual situation is still a long way from steady state. However, at high atmospheric N input, all three methods indicate that the EU standard for phreatic groundwater for NO$_3$ (50 mg l^{-1}) is exceeded. So, dynamic models are useful for quantifying the gap between the actual state of NO$_3$ leaching and the potential NO$_3$ leaching in case of a steady state. For this goal the models provide a rather consistent result.

IV General discussion and conclusions

Compared to the real world, the structure and processes of the considered biogeochemical system is simplified in any biogeochemical model. Modelling implies necessarily a reduction of complexity. The question is, however, to find the 'optimal' extent of simplification. In this final chapter the main results and conclusions are discussed in view of the research hypotheses:

- Adequate simulation of temporal responses in soil solution chemistry on a daily basis at various depths requires a detailed multi-layer biogeochemical model;
- Annual average responses in soil solution chemistry at the bottom of the root zone can be adequately simulated with a simple, one-layer biogeochemical model;
- Simulation of soil solution chemistry on a regional scale requires a simplified model;
- Adequate simulation of soil solution chemistry on a regional scale requires parameterisation, calibration, validation and uncertainty analysis on that scale.

The hypotheses were tested by the evaluation of various terrestrial biogeochemical models through: (i) validation by comparing model results with measurements, (ii) assessment of model uncertainties and (iii) comparison of different models. Here the validity of the hypotheses are discussed while answering the research questions raised in Chapter 1. Section 4.1 concerns the applicability on a local scale, whereas section 4.2 addresses the regional scale applicability. Finally, the adequacy of a simple biogeochemical model as a policy tool is addressed in Section 4.3.

4.1 Model application on a site scale

Adequacy of detailed soil solution chemistry modelling

Experience with a model such as NUCSAM showed that the model help to summarise and integrate results from individual disciplines and provides a multidisciplinary perspectives of complex systems.

The detailed nutrient cycling and soil acidification model NUCSAM was built to simulate effects of atmospheric deposition on soil solution chemistry on a site scale on a daily basis at different depths. At the intensively monitored site Speuld the agreement between observed and simulated changes in soil solution chemistry was reasonably good. NUCSAM reproduced the magnitude and trends of measured quantities, such as soil water contents and soil solution chemistry. Also the seasonal trends and trends with soil depth could be reproduced rather well. However, there are some exceptions. The pH was slightly overestimated in the topsoil and underestimated in the subsoil. This indicated that the pH and Al behaviour was not described adequately by rate-limited dissolution of Al-hydroxides. Most probably this description can be improved by the inclusion of Al complexation with dissolved organic matter (cf. Wesselink and Mulder, 1995).

Applications of NUCSAM to the intensively monitored sites like Speuld was, however, hampered by large spatial variability in throughfall, soil solution chemistry and stand structure. Either the number of sampling replicates was too small to obtain representative stand averages (soil chemistry), or it was impossible to select more or less homogeneous subplots (hydrology and biomass inventory). It is important to realise that in the Netherlands the Speuld experimental forest had provided one of the most complete datasets available. This implies that the lack of good quality data is a crucial limiting factor for further validation and model improvement.

Despite its complexity, a model such as NUCSAM can be rather useful to evaluate of pre-defined temporal deposition scenarios. Such analysis is, however, only valid for a specific site and cannot be (quantitatively) applied at a larger spatial scale. There is little hope to obtain a reasonable coverage for the Netherlands as a whole, by applying a model as NUCSAM at a sufficient number of intensively monitored sites because of high costs involves and limited flexibility of the model (application time, calculation time and processing time). Accordingly, for regional applications, model simplification is inevitable.

Role of uncertainty analyses in simplifying a detailed terrestrial biogeochemical model

This thesis showed that uncertainty analysis help to decide how to simplify biogeochemical models can contribute to model simplification. The relative contribution of processes to the model outputs appeared to vary with time, model input, depth and model output. The results of the uncertainty analysis indicated that nutrient cycling processes and kinetics of Al dissolution need to be known properly to simulate solute fluxes and concentrations in the topsoil, while in the subsoil they are unimportant. In addition, the need to describe a particular processes also depends on the constituent considered. E.g. pH is mainly influenced by the Al dissolution processes, whereas concentrations of NO_3 and NH_4 are mainly influenced by nutrient uptake and (de)nitrification. Accordingly, a simplified model able to model all major solutes in and below the root zone, must include almost all processes that are included in the detailed model. Subsequently, results from an uncertainty analysis alone are not enough for the guidance of model simplification. Just as with the implementation of a new model, common sense and expert judgement are indispensable for model simplification. Model simplification, that is only based on statistical and/or mathematical techniques would be delicate, because those do not take into account all available information. This type of simplified models are only based within the constraints of the model that is meant to be simplified (cf. section 4.3).

Adequacy of a simple one-layer terrestrial biogeochemical model to simulate soil solution chemistry

A relatively simple biogeochemical model such as SMART2 proved to be a reliable tool for the simulation of changes observed in a whole-ecosystem experiment, where deposition was decreased and temperature increased, viz the Risdalsheia catchment. In

contrast to the observations at Speuld, observations at the Risdalsheia catchments are 'real' annual average concentrations from the runoff of the whole catchment. This means that model and observations have the same temporal and spatial resolution. The observed time-series in runoff chemistry in response to deposition reduction and temperature rise were well reproduced by SMART2. The observed increase in N-runoff was reproduced well by the model, just like the observed increase in mineralisation and nitrification. These results, as referring to a relatively long observation period (more than 10 years), give confidence in applications of SMART2 on a regional scale for the simulation of annual average concentrations.

Change in model performance due to model simplification

To study the influence of model simplifications the models where validated by comparing simulated concentrations and leaching fluxes with measured values at the Solling site during the period 1973-1989. Although differences in process description exist between SMART2, RESAM and NUCSAM, all models were able to simulate most of the concentrations reasonably well during the study period. Differences in the description of e.g. the dissolution of Al-hydroxides and N cycling did not affect modelled long-term annual average Al and N concentrations. The capability of SMART2 to simulate the observed flux-weighted annual averaged concentrations (and ratios) is, in fact, comparable or even better than that of NUCSAM.

Ignoring seasonal variations in weather conditions and nutrient dynamics does not greatly affect the modelled long-term response of flux-weighted annual average soil solution chemistry to acid deposition. The multi-layer models RESAM and NUCSAM nicely reproduced the observed rise in SO_4 concentration, between 1975 and 1980. However, the one-layer model SMART2 tended to overestimate the initial rise in SO_4 concentration, due to a larger dispersion of the SO_4 front. This artefact of a one layer model should be born in mined when simulating leaching fluxes of adsorbing solutes.

When considering annual average concentrations at a certain soil depth, this research showed that the uncertainties in long-term predictions of soil solution response induced by neglecting seasonal and vertical spatial variability and by simplifying process description were rather small. So the simplified model SMART2 proved to be an adequate tool to evaluate long-term effects of environmental abatement strategies.

4.2 Model application on a regional scale

Applicability of a simplified model on a regional scale in view of data availability

SMART2 appeared to be a fairly good model for simulating soil solution chemistry on national scale. Results for the nitrogen availability (here defined as N mineralisation + N deposition) were encouraging, but could not be validated adequately due to a lack

of sufficient data. Nevertheless, SMART2 appeared to be a rather flexible and quick tool to evaluate deposition and seepage scenarios.

Model predictions of the un-calibrated model of pH and Al concentration for deciduous forest on poor sandy soils show a reasonable to good agreement with observations. The modelled concentrations of NO_3 and NH_4 compare moderately well with the observations. An indicative validation of N mineralisation fluxes, shows generally a reasonable agreement between calculated and measured fluxes available from literature. N mineralisation fluxes in forest were most likely underestimated. The Al concentrations in poor sandy soils, however, were clearly overestimated.

Scenarios with reduced deposition of N and S deposition improved the abiotic site factors, such as pH and base saturation (in non-calcareous soils) and N availability in forest soils. Spatial variability in all investigated model outputs, i.e. pH, base saturation and N availability appeared to be large. The spatial variability in pH and base saturation is linked with the spatial variability in soil type, whereas the spatial variability in N availability is linked with the spatial variability in N deposition and vegetation/land-use. Therefore, it is clear that a support tool for decision-making must be spatially explicit.

Impacts of the uncertainty in geographical data and model parameters on regional scale predictions

Given the use of regional models such as SMART2 in decision-making, it is clear that the reliability of spatial information and the consequences for the model predictions must be quantified. Uncertainty at large spatial scales not only originated from parameter uncertainty but also from the used maps. The relative uncertainty contribution largely depended on the model output. For the Al concentration and the exceedances of Al concentration thresholds, soil-related parameters contributed most to the output uncertainty. For NO_3, the uncertainty mainly stemmed from geographical data.

Within the context of policy-making, two questions are crucial: (i) What is the uncertainty in the (areal) exceedance of a critical indicator for a particular region? and (ii) Is the model able to predict (statistically) significant changes in exceedance areas in response to a particular environmental scenario? Concerning these questions, it can be concluded that the width of the prediction interval largely depend on whether block median concentrations or block areal exceedances are considered. Furthermore, despite the large prediction intervals due to uncertainty in model input data, changes in the Al and NO_3 concentrations or exceedance areas could be predicted with confidence.

Given the large costs associated with measures to prevent increased Al and NO_3 concentrations, it is important to assess whether collection of more data would reduce of the prediction interval. From the present study useful information can be derived to decide on different alternatives for reducing uncertainties associated with long-term model predictions. In general it is concluded that most emphasis must put on improvement the soil and vegetation related parameters and less on the improvement of the soil and vegetation maps.

Gain in model performance on a regional scale through a regional calibration

The SMART2 model was calibrated at a 5×5 km² block support using the up-scaled monitoring data. The applied calibration procedure appeared to be a useful for finding optimal parameter ranges, and for reducing input uncertainties. Even though the effects of reduced input uncertainty on the uncertainty in the model outputs remained un-quantified. The calibration appeared to be very successful in correcting the overestimation of Al and NO_3 concentrations resulting from parameter values based on site applications. These overestimates were mainly due to an overestimation of the mineralisation and nitrification.

As with the site scale application, it must be stressed that the regional data-set on about 200 forested sites, mainly on sandy soils, is the only available set for this type of calibration studies in the Netherlands. This set, that was collected in view of the modelling needs, proved to be very useful for model calibration and the assessment of the model error. However, this set, collected in the early nineties remains the only useful set and for progress in regional scale modelling further sets are badly needed.

This thesis also showed that model performance strongly depends on the grid-size used. Usually, increase in grid-size increases performance. This grid-cell increase, however, costs spatial resolution, and decreases the benefit for determining exceedance areas. Given large regional differences, even at a rather small distance, high resolution data on actual soil solution concentration in semi-natural terrestrial ecosystem are crucial to support of regional policy activities such as the regional NH_3 abatement plan in the Netherlands.

In conclusion, application of the SMART2 model to the whole of the Netherlands, while only parameterised and calibrated on a small number of intensive monitored sites yields inadequate results. It is showed that model performance seriously improved and the prediction uncertainties strongly decreased by model calibration at the scale required for the ultimate output.

4.3 Adequacy of simple biogeochemical models as a tool for policy makers

This research showed that a detailed biogeochemical model, such as NUCSAM, can not be applied adequately at a large spatial scale. Even for the application at a single research site the lack of good quality data appeared a serious constraint. This clearly illustrates that models must be simplified for application at larger spatial and temporal scales. Modelling with a complex model on a large regional scale which lacks data for model parameterisation, calibration and validation would be pointless. Especially, from the viewpoint of the considered policy questions optimal or smart adaptation of the model to the available data is crucial. This also means that derivation of a meta-model from a complex non-calibrated and validated model by statistical techniques (Mol-Dijkstra *et al.*, 1999) is bound to fail. This approach may lead to models that can be ran more easily, but less reliable. Models for larger spatial and temporal scale must be simplified as much as possible, while retaining a degree of process description so

that model evaluation through calibration, validation and uncertainty analysis is feasible.

Models such as SMART2 fit to the *policy scale* (see Chapter 1), but in some cases are still too complex. For the sake of applicability and of adaptation to the *policy scale*, even more simplified models, e.g. steady state models, are needed. This is especially true in integrated approaches such as NITROGENIUS (Erisman *et al.*, 2002), a spatial decision support systems on the nitrogen problem for the whole of the Netherlands. NITROGENIUS contains an agronomy/soil module (INITIATOR, De Vries *et al.*, 2002) that is less complex than SMART2, but still process-oriented.

Summary

Evaluation of anthropogenic effects on the environment at local, regional and global scales has become a key activity in environmental research. It forms the basis for emission reduction measures needed to achieve policy leading to a sustainable society. Computer models play an increasing role in the evaluation of those environmental effects. In the Netherlands, at the Environmental Policy Assessment Office (MilieuPlanBureau: MPB) and Nature Policy Assessment Office (NatuurPlanBureau: NPB) a large set of integrated predictive models are used to evaluate the effects of policy scenarios on a wide range of environmental problems. These include eutrophication, acidification, climate change and biodiversity decrease. Within these themes, mechanistic dynamical models, which simulate biogeochemical processes in ecosystems, play a crucial role.

Aims and hypotheses

In this thesis different nutrient cycling and soil acidification models, developed for use at different scales, are presented and evaluated. The models considered are NUCSAM (NUtrient Cycling and Soil Acidification Model), RESAM (REgional Soil Acidification Model) and SMART2 (an extended version of Simulation Model for Acidification's Regional Trends). These are mechanistic dynamic models, which simulate biogeochemical processes in semi-natural terrestrial ecosystems at a variety of scales. The research tool NUCSAM, which is specifically developed for application on a local scale, includes simulation of the daily variability in biogeochemical processes in various soil layers. RESAM and SMART2, tools to support policy makers, were specifically developed to evaluate long-term soil responses to deposition scenarios on a regional scale (national to continental, respectively). For that reason, the models RESAM and SMART2 are relative simple models and operate on a yearly time-scale. These models were developed in view of following research hypotheses:

1. Adequate simulation of temporal responses in soil solution chemistry on a daily basis at various depth requires a detailed multi-layer biogeochemical model (NUCSAM);
2. Annual average responses in soil solution chemistry at the bottom of the root zone can be adequately simulated with a simple, one-layer biogeochemical model (SMART2);
3. Simulation of soil solution chemistry on a regional scale requires a simplified model;
4. Adequate simulation of soil solution chemistry on a regional scale requires parameterisation, calibration, validation and uncertainty analysis on that scale.

Therefore, this thesis primarily aims at testing these hypotheses by (i) validation and calibration, (ii) uncertainty analysis, and (iii) model comparison. More specifically, the models NUCSAM (site scale), RESAM (site scale/regional scale) and SMART2 (regional scale) will be evaluated with respect to the optimal balance between model complexity, data availability and model aim.

Overview of the models

NUCSAM, RESAM and SMART2 are all based on the principle of ionic charge balance and on a simplified solute transport description. All models assume that: (i) a soil layer is a homogeneous compartment of constant density and (ii) the element input mixes completely in a soil layer. NUCSAM is a detailed nutrient cycling and soil acidification model for semi-natural ecosystems, especially developed for site scale applications. Consisting of multi-layers and having a daily temporal resolution. NUCSAM integrates the hydrological- and nutrient cycle and soil chemical processes, while including all relevant processes in the forest canopy, organic surface layer, mineral soil and soil solution. The hydrological cycle is modelled by a separate Darcy-law-based hydrological model. Nutrient cycling, involves nutrient uptake, litterfall, root turnover and mineralisation. Forest growth is described by a logistic growth function. Equilibrium and rate limiting chemical reactions are explicitly modelled in a chemical module. Chemical reactions rates depend on temperature, whereas biochemical processes depend on temperature, moisture content and pH.

Going into the direction NUCSAM, RESAM, SMART2, process aggregation is achieved by (i) confining to annual averages, (ii) confining to one soil layer, (iii) simpler descriptions of processes, (iv) ignoring or lumping elements, and (v) ignoring several processes.. In RESAM and SMART2 the annual water flux percolating through a soil layer is constant and equals the infiltration minus the transpiration, whereas NUCSAM contains a separate hydrological model with a daily timestep. SMART2 is confined to one layer, whereas RESAM and NUCSAM are multi-layer models. Biological processes are all described by rate-limited reactions, usually first-order reactions. In SMART2, geochemical reactions are described by equilibrium equations, except silicate weathering, which is described by a zero-order reaction. So, unlike SMART2, NUCSAM and RESAM account for the effect of mineral depletion on the weathering rate. In NUCSAM and RESAM the geochemical reactions are either described by equilibrium equations or first-order reactions.

Adequacy of simulation on a plot scale

Detailed modelling responses in soil solution chemistry

The detailed NUCSAM model was applied to the Speulderbos Douglas fir stand, and validated using measured data on soil and soil solution chemistry. Applications of the NUCSAM model to the intensively monitored site Speuld site was hampered by the large spatial variability of throughfall, soil solution chemistry and stand structure. This was mainly because separated 'disciplinary' subplots for hydrology, soil chemistry and forest growth were used for monitoring. Either the number of sampling replicates was too small to calculate stand averages (soil chemistry), or it was impossible to select more or less homogeneous subplots (hydrology and biomass inventory). Nevertheless, the agreement between observed and simulated changes in soil solution chemistry was reasonably good. NUCSAM reproduced the magnitude and trends of measured quantities, such as soil water contents and soil solution chemistry. Also the seasonal trends and trends with soil depth could be reproduced rather well

Scenario analyses, that were carried out for Douglas fir on a Cambic podzol and Scots pine on an Haplic Arenosol showed that the model is a suitable instrument for scenario analyses on a local scale. Model results showed that deposition reduction led to: (i) a fast improvement of the SO_4 and Al concentrations after a decrease in SO_x deposition, (ii) time-delay for the NO_3 concentration following a decrease in nitrogen deposition, and (iii) higher soil solution concentrations of all solutes in the soil below Douglas fir. Despite its complexity, a model such as NUCSAM can be rather useful to evaluate of pre-defined temporal deposition scenarios. Such analysis is, however, only valid for a specific site and cannot be (quantitatively) applied at a larger spatial scale. There is little hope to obtain a reasonable coverage for the Netherlands as a whole, by applying a model as NUCSAM at a sufficient number of intensively monitored sites, because of high costs involves and limited flexibility of the model (application time, calculation time and processing time). Accordingly, for regional applications, model simplification is inevitable.

Uncertainties in soil solution chemistry on a site scale

Besides the inevitable role of an uncertainty analysis with in the context of ecological modelling, uncertainty analyses may also be helpful in finding guidelines for model simplification. An uncertainty analyses on a site scale was performed with RESAM, an already simplified version of NUCSAM. Results showed that the uncertainty strongly depends on the considered model output, soil layer and time. The same is true for the contribution of the uncertainty of various parameters to the uncertainty of the considered output variables. The results of the uncertainty analysis indicated that nutrient cycling processes and kinetics of Al dissolution need to be known properly to simulate solute fluxes and concentrations in the topsoil, while in the subsoil they are unimportant. In addition, the need to describe a particular processes also depends on the constituent considered. E.g. pH is mainly influenced by the Al dissolution processes, whereas concentrations of NO_3 and NH_4 are mainly influenced by nutrient uptake and (de)nitrification. Accordingly, a simplified model able to model all major solutes in and below the root zone, must include almost all processes that are included in the detailed model. Subsequently, results from an uncertainty analysis alone are not enough for the guidance of model simplification.

Annual average responses in soil solution chemistry with a simple one-layer biogeochemical model

The simplified model SMART2 meant for application at larger spatial and temporal scales was evaluated at the Risdalsheia catchment. On boreal forest ecosystems at Risdalsheia (southern Norway), catchment-scale experiments of the RAIN and CLIMEX projects were conducted during a period of 15 years. These unique series of experiments at the ecosystem scale provides information on the effects and interactions of N deposition and increased temperature and CO_2 on C and N cycling and especially the runoff chemistry. The observations at the Risdalsheia catchments are annual average concentrations from the runoff of the whole catchment, which means that the time and space resolutions of measurements and modelling are similar.

The inclusion of the climate change effect in SMART2 was restricted to the temperature effect on mineralisation of old litter, (de)nitrification, weathering and Al oxide dissolution constant.

The observed time-series in runoff chemistry in response to deposition reduction and temperature rise were well reproduced. Although, SMART2 tended to underestimate the concentrations of SO_4, NO_3, NH_4 and BC2. The observed increase in N-runoff was reproduced well by the model, just like the observed increase in mineralisation and nitrification. Still, there is a need to pay attention to the N-cycling in SMART2, considering the adaptation of the pH influence on mineralisation in this application. The temperature dependency of mineralisation was simulated adequately, but the temperature effect on nitrification was slightly overestimated. This application, with quite a long observation period, contributes to an increase in confidence in using SMART2 on the regional scale, especially to evaluate deposition scenarios.

Model comparison on a local scale

The site applications of both NUCSAM and SMART2 gave hopeful results. However, before accepting SMART2 as suitable tool for regional applications, it is necessary to analyse the influence of model simplifications, in terms of process detail, number of soil layers and temporal variability, on the modelled of soil solution concentrations and leaching fluxes. To that aim, all three models (NUCSAM, RESAM and SMART2) where first validated by comparing simulated concentrations and leaching fluxes with measured values at the Solling site during the period 1973-1989. Next, long-term soil and soil solution response simulated with three models were compared using two deposition scenarios for the period 1990-2090. Input parameters were derived from measured data at the Solling site. Outputs from the one-layer model SMART2 were compared with measured soil solution concentration averaged over depth.

Despite differences in their process descriptions, SMART2, RESAM and NUCSAM simulate most of the solute concentrations reasonably well. Whether the dissolution of Al-hydroxides was modelled by a rate-limited reaction (NUCSAM, RESAM) or by an equilibrium equation (SMART2) hardly affected modelled Al concentrations. The differences in N cycling processes also hardly affect the quality of the modelled NO_3 and NH_4 concentrations. All models mimicked the observed a rise in SO_4 concentration between 1975 and 1980, due to a decrease in sulphate adsorption. However, the one-layer model, SMART2, overestimated the initial rise in dissolved SO_4, due to a large dispersion of the sulphur front in a one-layer system. On the other hand for the simulation period as a whole SMART2 showed the best performance for SO_4 in the subsoil.

In the topsoil, NO_3 concentrations simulated by these models were in the same range as the measurements. Subsoil NO_3 concentrations were slightly underestimated by RESAM and SMART2, whereas these were slightly overestimated by NUCSAM. The NH_4 concentration in topsoil was best modelled by SMART2, the two other models seriously modelled too high NH_4 concentration in the topsoil. All three models underestimated the NH_4 concentrations in the subsoil, but the observed NH_4 concentration in subsoil are already very low.

This implies that ignoring seasonal variations of weather conditions, ignoring of different soil layers and simplifying process description simplification does not need to greatly affect the modelled long-term response of flux-weighted annual average soil solution chemistry to acid deposition. Consequently, it is concluded that the level of aggregation/simplification as used in the model SMART2 is acceptable for making long-term predictions on a regional scale.

Adequacy of simulation on a regional scale

Annual average responses on soil solution chemistry on a regional scale

The model SMART2 has been incorporated in a framework to support national scale applications using a 250×250 m^2 grid. However, adequate simulation of annual average response at a particular soil depth on a plot scale does not necessarily imply that the results are also acceptable on a regional scale. This requires testing and validation on a regional scale. Therefore, SMART2 has been applied and validated for the Netherlands as a whole using regionally available data. Furthermore, the model was used to analyse the effects of upward seepage, atmospheric deposition and nutrient cycling on changes in semi-natural terrestrial ecosystems. The model SMART2 was also linked with a vegetation effect model MOVE to quantify the effects on floristic diversity.

SMART2 appeared to be a rather flexible and quick tool to evaluate deposition and seepage scenarios. Model predictions for the NO_3 and NH_4 concentrations showed a moderate relationship with the observations. Model predictions of pH and Al concentration show a reasonable to good agreement with observations, but the Al in concentration in poor sandy soils was overestimated. The (spatial) variability in all investigated model outputs, i.e. pH, base saturation and N availability is large. The spatial variability in pH and base saturation is linked with the spatial variability in soil type, whereas the spatial variability in N availability is linked with the spatial variability in N deposition. N availability highly depends on the age of the vegetation. Consequently, it is inevitable that spatially explicit modelling is needed.

Uncertainties in soil solution chemistry on a regional scale

When modelling soil solution chemistry on a regional scale, it is inevitably that both model and data have varying degrees of associated uncertainty. Therefore, SMART2 was subjected to an uncertainty analysis in a spatial context. Given the large costs associated with measures to prevent increased Al and NO_3 concentrations, it is important to assess whether the collection of more data would result in a reduction of the prediction interval. From the present study useful information can be derived to support decisions on different alternatives for reducing uncertainties associated with long-term model predictions. Possible alternatives are either improving the soil and vegetation maps or collecting additional input data in order to reduce the uncertainty in parameters.

The analyses was focussed on the uncertainty in long-term large-scale predictions of soil solution concentrations of Al and NO_3 resulting from the

uncertainty in low resolution European-scale maps (1:1000 000) and other input data. Model outputs were considered as block median concentrations (for 5×5 km² grid cells) and the block areal fractions (for 5×5 km² grid cells) in which concentrations exceeded a critical level. As sources of uncertainty we considered (i) the soil and vegetation maps (categorical data), and (ii) the soil and vegetation-related parameters (continuous data). The uncertainty in categorical data was quantified by comparing European soil and vegetation maps, and the more detailed maps of the Netherlands. The uncertainty in continuous data was derived from various European databases and literature. The uncertainty in model outputs was quantified by an efficient two-step Monte Carlo simulation approach, which takes spatial correlation into account.

It is showed that the width of the prediction interval largely depends on whether block median concentrations or block areal exceedances are considered. The Al concentration showed wide 90% prediction intervals both for areas with low Al concentrations (i.e. calcareous and clay soils) and for areas with high concentrations (mainly poor sandy soils). For the scenarios evaluated, the model was able to predict a considerable decrease in Al concentration, despite the large prediction intervals due to uncertainty in the model input data.

The relative uncertainty contribution largely depended on the model output considered. For the Al concentration the soil-related parameters contributed most to the output uncertainty, whereas the uncertainty contribution of the vegetation-related parameters was negligible. By contrast, the results for the NO_3 concentration showed that the average uncertainty contribution mainly stemmed from the soil and vegetation maps, directly followed by the continuous vegetation-related parameters, whereas the continuous soil-related parameters contributed least. In general it is concluded that most emphasis must put on improvement the soil and vegetation related parameters and less on the improvement of the soil and vegetation maps.

Reducing the uncertainty in regional model prediction by model calibration

To quantify of the beneficial effect of model calibration at a large spatial scale, the prediction error of SMART2 was assessed before and after calibration, for the median Al and NO_3 concentrations in a 5×5 km² grid cell. Because observations are available only as point values, it was necessary to transfer them to representative values for a 5×5 km² grid. For this purpose, about 250 point observations of soil solution concentrations in forest soils were upscaled to a 5×5 km² grid map, using multiple linear regression analysis combined with block kriging. The resulting map with upscaled observations was used for both validation and calibration. A comparison of the map with model predictions using nominal parameter showed that the model overestimated the predicted Al and NO_3 concentrations. The nominal model results were still in the 95% confidence interval of the upscaled observations, but calibration improved the model predictions and strongly reduced the model error.

The used calibration procedure appeared to be a useful tool for finding optimal parameter ranges, and for reducing input uncertainties. The calibration appeared to be very successful in correcting the overestimation of Al and NO_3 concentrations

246

resulting from the nominal parameter set. However, the model error after calibration remains rather large, but further improvement through calibration is hampered from the lack of good quality data.

Model comparison on a regional scale

A reliable spatial distribution of NO_3 concentrations below the root zone of semi-natural ecosystem are of special interest with respect to the exceedance of critical concentrations.

To gain additional insight into the uncertainty due to the model structure of SMART2, the simulated spatial distribution on solute concentrations on NO_3 in Dutch forest ecosystems were compared with: (i) a regression model based on observed NO_3 concentrations and additional data on explanatory variables and (ii) a semi-empirical dynamic model WANDA. The comparison was performed for the Netherlands as whole, using a 250×250 km² grid. The NO_3 maps as calculated by the three methods provided clearly different results. However, the spatial distributions in the form of a cumulative distribution function provided comparable results, especially at 5×5 km² grid. This grid-cell increase, however, cost spatial resolution, and decrease the benefit for determining exceedance areas.

Main findings

The detailed model NUCSAM reproduced the magnitude and trends of measured quantities, such as soil water contents and soil solution chemistry. However, the application on a site scale hampers from the lack of good quality data. Results showed that it is inevitable that a model, such as NUCSAM, can not be applied at a large spatial scale because of the lack of data availability. This makes it clear that the model must be simplified for application at larger spatial and temporal scale. Results of the uncertainty analysis indicated that a simplified model able to model all major solutes in and below the root zone, must include almost all processes that are included in the detailed model.

The capability of the simplified model SMART2 to simulate the observed flux-weighted annual averaged concentrations is comparable or even better than NUCSAM. This implies that ignoring seasonal variations of weather conditions, ignoring of different soil layers and simplifying process description simplification does not need to greatly affect the modelled long-term response of flux-weighted annual average soil solution chemistry to acid deposition. Accordingly, is concluded that a simplified model, such as SMART2, is an acceptable tool for making long-term evaluation of environmental abatement strategies.

Application of a regional model, such as SMART2, to the whole of the Netherlands, while only parameterised and calibrated on a small number of intensive monitored sites yields inadequate results. Model performance is seriously improved and the prediction uncertainties strongly decreased by model calibration at the scale required for the ultimate output. However, the model error after calibration remains rather large, but further improvement through calibration is hampered from the lack of good quality data on a national scale. It is concluded that most emphasis must put

on improvement the soil and vegetation related parameters and less on the improvement of the soil and vegetation maps.

Models for larger spatial and temporal scale must be simplified as much as possible, while retaining a degree of process description so that model evaluation through calibration, validation and uncertainty analysis is feasible.

Samenvatting

Zowel op de locale als regionale schaal staat het evalueren van effecten van het menselijk handelen op het milieu erg in de belangstelling binnen het milieuonderzoek. Dit type onderzoek vormt de basis voor het beleid ten aanzien van emissiebeperkende maatregelen ten behoeve van een duurzame samenleving. Bij het evalueren van milieueffecten zijn computermodellen een steeds grotere rol gaan spelen. Zo wordt binnen het Nederlandse Milieu- en Natuurplanbureau gebruik gemaakt van diverse geïntegreerde modellen, welke ingezet worden voor het evalueren van beleidsscenario's ten aanzien van een brede range van milieuproblemen, zoals: eutrofiëring, verzuring, klimaatverandering en afname van biodiversiteit. Binnen al deze thema's spelen procesgeoriënteerde dynamische modellen voor het simuleren biogeochemische processen in ecosystemen, een belangrijke rol.

Doel en hypothesen

In dit proefschrift worden diverse nutriëntenkringloop- en bodemverzuringsmodellen, die ontwikkeld zijn voor toepassing op verschillende schaalniveaus beschreven en geëvalueerd. Het gaat hierbij om de modellen NUCSAM (NUtrient Cycling and Soil Acidification Model), RESAM (REgional Soil Acidification Model) en SMART2 (een uitgebreide versie van het model Simulation Model for Acidification's Regional Trends). Dit zijn allen mechanistische dynamische modellen voor het simuleren van biogeochemische processen in half-natuurlijke terrestrische ecosystemen. Het onderzoeksmodel NUCSAM is speciaal ontwikkeld is voor toepassing op de locale schaal. Daarom zijn in dit model onder andere de biogeochemische processen op dagbasis gemodelleerd en wordt er ook onderscheid gemaakt in diverse bodemlagen. De modellen RESAM en SMART2 zijn speciaal ontwikkeld als beleidsondersteunende modellen. In het bijzonder voor de evaluatie van lange-termijn veranderingen in de bodem op regionale schaal (variërend van nationaal tot continentaal) ten gevolge van atmosferische depositie- en hydrologische- scenario's. Daarom zijn de modellen RESAM en SMART2 relatief eenvoudige modellen die op jaarbasis rekenen. Deze modellen zijn ontwikkeld uitgaande van de volgende onderzoekshypothesen:

1. het op dagbasis adequaat simuleren van temporele veranderingen in bodemvochtchemie vereist een gedetailleerd meerlagig biogeochemisch model (NUCSAM);
2. jaargemiddelde veranderingen in bodemvochtchemie aan de onderkant van de wortelzone zijn adequaat te modelleren met een eenvoudig eenlagig biogeochemisch model (SMART2);
3. het simuleren van de bodemvochtchemie op een regionale schaal vereist een eenvoudig model;
4. het adequaat simuleren van de bodemvochtchemie op een regionale schaal vereist parameterisatie, calibratie, validatie en een onzekerheidsanalyse op datzelfde schaalniveau.

Dit proefschrift heeft met name tot doel om deze hypothesen te toetsen middels: (i) validatie en calibratie, (ii) onzekerheidsanalyse en (iii) modelvergelijking. Meer specifiek houdt dit in dat de modellen NUCSAM (plotschaal), RESAM (plotschaal/regionale schaal) en SMART2 (regionale schaal) geëvalueerd zullen worden met het oog op een optimale balans tussen modelcomplexiteit, databeschikbaarheid en doel van het model.

Overzicht van de modellen

NUCSAM, RESAM en SMART2 zijn allen gebaseerd op het ladingsbalansprincipe en een eenvoudige beschrijving voor het transport van bodemvocht. Alle modellen veronderstellen dat: (i) een bodemlaag homogeen is en een constante dichtheid heeft, en (ii) de stoffen in een bodemlaag volledig gemengd worden. NUCSAM betreft een gedetailleerd nutriëntenkringloop- en bodemverzuringsmodel voor half-natuurlijke terrestrische ecosystemen, special bedoeld voor toepassing op een plotschaal. Het model bevat meerdere bodemlagen en rekent met tijdresolutie van een dag. In NUCSAM worden hydrologische -, nutriëntenkringloop - en bodemchemische processen geïntegreerd. Hierbij zijn alle relevante processen in het kronendak, de strooisellaag, de minerale bodem en het bodemvocht meegenomen. De hydrologische kringloop is gemodelleerd middels een apart hydrologisch-model gebaseerd op de wet van Darcy. De gemodelleerde nutriëntenkringloop omvat nutriëntopname, bladval, wortelsterfte en mineralisatie. Bosgroei is beschreven met een logistische groeicurve. Chemische-evenwichten en snelheidsprocessen worden in een aparte chemische-evenwichtsmodule gemodelleerd. Chemische-reacties zijn binnen het model afhankelijk van de temperatuur, terwijl de biochemische-processen naast de temperatuur ook afhankelijk zijn van het bodemvochtgehalte en de pH.

Gaande in de richting van NUCSAM, RESAM, SMART2, is er sprake van vereenvoudiging en aggregatie door (i) het rekenen met jaarlijks gemiddelde waarden, (ii) het beperken tot een bodemcompartiment, (iii) het eenvoudige beschrijven van processen, (iv) het negeren of lumpen van element, en (v) het negeren van diverse processen. Zo wordt in RESAM en SMART2 de jaarlijkse waterflux door een bodemlaag bepaald door de opgelegde jaarlijkse waterbalans: infiltratie minus transpiratie, terwijl de hydrologie in NUCSAM door een apart hydrologisch-model met een dagelijkse tijdstap wordt berekend. SMART2 is bestaat uit slechts een bodemlaag, terwijl RESAM en NUCSAM meerdere bodemlagen bevatten. Biologische-processen zijn als snelheidsprocessen gemodelleerd, meestal als eerste-orde processen. In SMART2 zijn de meeste geochemische processen beschreven als evenwichten. De verwering van silicaten is opgenomen als een 0^e-orde proces. In tegenstelling tot SMART2, houden NUCSAM en RESAM rekening met het effect van uitloging van mineralen gehalten op de verweringssnelheid. In NUCSAM en RESAM zijn de geochemische-reacties of middels evenwichtsvergelijkingen of middels 1^e-orde reacties beschreven.

Het adequaat simuleren op plotschaal

Gedetailleerd modelleren van veranderingen in bodemvochtchemie

Het gedetailleerde NUCSAM model is toegepast op een intensief doorgemeten onderzoekslocatie in het Speulderbos bestaande uit douglassparren. Het model is gevalideerd aan de hand van bodem- en bodemvochtmetingen. De toepassing van NUCSAM op de douglassparrenopstand in het Speulderbos werd echter belemmerd door een grote ruimtelijke variabiliteit van doorval, bodemvochtchemie en de structuur van de opstand. Dit was met name problematisch omdat de metingen plaatsvonden in afzonderlijke discipline-georiënteerde subplots: één voor de hydrologie, één voor de bodemchemie en een voor de bosgroei. Met als gevolg dat of het aantal replica's te klein was om een opstandsgemiddelde grootheden te bepalen (in het geval van de bodemchemieplot), of het onmogelijk was om een voldoende homogene subplot te vinden (in het geval van de hydrologie - en bosgroeiplot). Desondanks, was er sprake van een goede overeenkomst tussen de gemeten en de gesimuleerde veranderingen in de bodemvochtchemie. NUCSAM bleek in staat om zowel de mate als de trend van de gemeten grootheden, zoals vochtgehalten en bodemvochtconcentraties, goed te reproduceren. Ook de seizoenstrend en de trend met de diepte werden goed gesimuleerd

Scenario-analysen, die zijn uitgevoerd voor generieke combinaties van een douglassparrenopstand op een holtpodzolgrond en een grove-dennenopstand op een duinvaaggrond, laten zien dat het model een hanteerbaar en geschikt instrument is voor het uitvoeren van scenario-analyses op de locale schaal. Modelresultaten laten zien dat depositie-reductie leidt tot (i) een snelle afname van de SO_4- en Al-concentraties als gevolg reducties in de SO_x-depositie, (ii) een naijlling in de afname van de NO_3-concentraties als gevolg van de afname in de N-depositie, en (iii) hogere bodemvochtconcentraties in de douglassparrenopstand dan in de grove-dennenopstand. Ondanks de hoge mate van complexiteit, is een model zoals NUCSAM bijzonder geschikt voor het evalueren van te voren vastgestelde tijdsafhankelijke depositie-scenario's. Een dergelijke analyse kan echter niet gerbuikt worden uitspraken op regionale - of nationale schaal, omdat de resultaten van een specifieke plottoepassing niet (kwantitatief) vertaald kunnen worden naar grotere ruimtelijke schaal. Er is echter weinig hoop op het verkrijgen van een acceptabele dekkingsgraad met NUCSAM-toepassingen voor geheel Nederland. Als gevolg van de hoge kosten die daarmee gemoeid zijn, is er een gebrek aan intensief doorgemeten locaties en is een model als NUCSAM niet flexibel genoeg voor toepassing op een grotere ruimtelijke schaal (hoge tijdsinvestering voor het uitvoeren van veel toepassingen en lange rekentijden). Daarom is het voor regionale – of nationale toepassingen noodzakelijk om het model te vereenvoudigen.

Onzekerheid in bodemvochtchemie op locale schaal

Naast de reguliere rol die een onzekerheidsanalyse speelt bij het modelleren van biogeochemische processen, kan een onzekerheidsanalyse ook een bijdrage leveren bij het vinden van richtlijnen die kunnen leiden tot modelvereenvoudigingen. Een

onzekerheidsanalyse op de locale schaal is uitgevoerd met het model RESAM, een al reeds vereenvoudigde versie van NUCSAM. De resultaten laten zien dat de onzekerheid sterk afhankelijk is van de beschouwde modeluitgang, bodemlaag en tijd. Datzelfde geldt ook voor de onzekerheidsbijdrage van de modelparameters aan de onzekerheid van de beschouwde modeluitgangen. De onzekerheidsanalyse geeft aan dat de nutriëntenkringloopprocessen en de kinetiek van het oplossen van Al-precipitaten in belangrijke mate bepalend zijn voor het adequaat simuleren van bodemvochtfluxen en – concentraties in de bovengrond, terwijl deze processen voor de ondergrond relatief onbelangrijk zijn. Daarnaast hangt de noodzaak om een proces wel of niet mee te nemen ook af van het beschouwde modeluitgang. Zo wordt de pH met name beïnvloed door het oplossen van Al-precipitaten, terwijl de NO_3- en NH_4-concentraties met name beïnvloedt worden door nutriëntopname en (de)nitrificatie. Een vereenvoudigd model dat in staat moet zijn om alle belangrijke bodemvochtcomponenten te modelleren, zowel in als aan de onderrand van de wortelzone, dient daarom vrijwel alle processen in zich te hebben die ook in het complexe model zitten. Het gevolg hiervan is dat een onzekerheidsanalyse maar een beperkte bijdrage kan leveren bij het verstrekken van richtlijnen voor het vereenvoudigen van modellen.

Jaargemiddelde veranderingen in bodemvochtchemie gemodelleerd met een eenvoudig eenlagig biogeochemisch model

Het vereenvoudigde model, SMART2, dat ontwikkeld is voor lange-termijn toepassingen op regionale schaal is eerst toegepast op een experimenteel vanggebied in Risdalsheia, zuidelijk Noorwegen. In een vanggebied nabij Risdalsheia begroeid met een boreaal bos zijn gedurende 15 jaar experimenten uitgevoerd op het schaalniveau een vanggebied. Deze experimenten zijn uitgevoerd in het kader van de EU-onderzoeksprojecten RAIN (manipulatie-experimenten met depositie) en CLIMEX (manipulatie-experimenten met klimaat). Het betreft een unieke serie van experimenten op ecosysteemschaal, dat informatie verschaft over de effecten van de interactie tussen N depositie en toename in temperatuur en CO_2 op C- en N-kringloop en bovenal op de concentraties in het afstromende water. De metingen in het Risdalsheia-vanggebied zijn eenvoudig te herleiden tot jaargemiddelde concentraties in het afstromende water. Dit betekent dat de ruimtelijke - en temporele schaalniveaus van metingen en model goed overeenkomen. Voor deze toepassing is SMART2 voorzien van klimaatsveranderingsprocessen te weten, temperatuureffect op mineralisatie van oud strooisel, (de)nitrificatie en de verwering van Al-precipitaten.

De gemeten tijdreeks van concentraties in het afstromende water, dat gemanipuleerd werd door depostie-reductie en temperatuur toename, werd door het model goed gereproduceerd. De door SMART2 gemodelleerde concentraties van SO_4, NO_3, NH_4 en BC2, werden echter enigszins onderschat. De gemeten toename in N-afvoerflux werd door het model goed gereproduceerd, evenals de waargenomen toename in mineralisatie en nitrificatie. Desondanks is er aanleiding om de N-kringloop processen in het model te verbeteren. Het gaat hierbij met name om het ingebouwde effect van de pH op de mineralisatie. De gemodelleerde temperatuur

afhankelijkheid van de mineralisatie leverde goede resultaten op, maar het temperatuur effect op de nitrificatie werd enigszins overschat. De bevredigende resultaten van deze validatiestudie op basis van een relatief lange dataset, laten zien dat het model SMART2 een adequaat model is om in te zetten bij regionale - en nationale toepassingen. In het bijzonder wanneer het gaat om de evaluatie van depositie-scenario's.

Model vergelijking op locale schaal

Plotschaal toepassingen van zowel NUCSAM als SMART2 hebben hoopvolle resultaten opgeleverd. Maar voordat we een model als SMART2 kunnen accepteren als een geschikt model voor regionale – en nationale toepassingen, is het noodzakelijk om de effecten van modelvereenvoudigingen in meer detail te analyseren. Het gaat hierbij om de effecten van vereenvoudigingen in procesbeschrijvingen, reductie in het aantal bodemlagen en reductie in de temporele variabiliteit op de gemodelleerde bodemvochtconcentraties en uitspoelingsfluxen. Hiertoe zijn de drie modellen (NUCSAM, RESAM en SMART2) eerst gevalideerd middels een vergelijking tussen de gemeten en gemodelleerde concentraties en uitspoelingsfluxen. Hierbij is gebruik gemaakt van gegevens van de onderzoekslocatie Solling (midden Duitsland), die gedurende de periode 1973-1989 zijn verzameld. Vervolgens zijn de resultaten van lange-termijn (1990-2090) simulaties, uitgevoerd met de drie modellen, onderling vergeleken 1990-2090. De uitvoer van het eenlaagmodel SMART2 werd vergeleken met de laagdikte gewogen gemiddelde van de gemeten bodemvochtconcentraties in de corresponderende lagen.

Ondanks de verschillen in procesbeschrijvingen, worden de meeste bodemvochtconcentraties door de modellen SMART2, RESAM en NUCSAM redelijk goed gesimuleerd. Of het oplossen van Al-precipitaten nu gemodelleerd wordt met een snelheidsreactie (NUCSAM, RESAM) of met een evenwichtsvergelijking (SMART2), beïnvloedt de gemodelleerde Al-concentraties niet of nauwelijks. De verschillen in N-kringloopprocessen beïnvloedt ook nauwelijks de gemodelleerde NO_3- en NH_4-concentraties. Alle modellen simuleren ook de waargenomen toename in SO_4-concentratie in de periode tussen 1975 en 1980, als gevolg van een afname in sulfaatadsorptie, hoewel het eenlagige SMART2 de initiële toename in opgelost SO_4 overschat. Dit laatste als gevolg van de grote mate van dispersie van het sulfaatfront in een eenlagigsysteem. Desondanks laat SMART2 over de gehele simulatieperiode de beste performance zien voor de SO_4-concentratie in de ondergrond.

In de bovengrond vallen de gesimuleerde NO_3-concentraties van alle modellen binnen de range van de gemeten concentraties. In de ondergrond, werden de NO_3-concentraties enigszins onderschat door RESAM en SMART2, terwijl deze door NUCSAM iets overschat werden. De NH_4-concentraties in de bovengrond werden het best gemodelleerd door SMART2. De twee andere modellen berekende duidelijk te hoge NH_4-concentraties in de bovengrond. Alle drie modellen onderschatten de NH_4-concentraties in de ondergrond, maar het gaat hierbij wel om zeer lage gemeten concentraties.

Uit deze vergelijkende studie volgt dat het negeren van seizoensvariatie in weerscondities en nutriëntendynamiek, het lumpen tot een bodemcompartiment en het vereenvoudigen van procesbeschrijvingen, niet of nauwelijks de kwaliteit van de

gesimuleerde jaarlijksgemiddelde bodemvochtconcentraties – en fluxen beïnvloedt. Het aggregatieniveau en de mate van detaillering van procesbeschrijvingen zoals dat in het model SMART2 is toegepast is dus acceptabel voor het maken van lange-termijn simulaties op regionale schaal.

Het adequaat simuleren op regionale schaal

Jaargemiddelde veranderingen in bodemvochtchemie op regionale schaal

Het model SMART2 is ondergebracht in een raamwerk voor het uitvoeren van landelijke toepassingen op basis van een 250×250 m^2 grid. Omdat het adequaat simuleren van jaargemiddelde bodemvochtconcentraties op een bepaalde diepte voor een specifieke plot nog geen garantie biedt voor adequate simulatie op een regionale schaal, dient het model ook getest en gevalideerd te worden op de regionale schaal. Hiertoe is SMART2 toegepast en gevalideerd voor geheel Nederland met gebruikmaking van een landelijke datasets. Vervolgens is het landelijke model gebruikt om effecten te kwantificeren van veranderingen in de hydrologie (kwelflux), atmosferische depositie en vegetatiesuccessie in half-natuurlijke terrestrische ecosystemen. Het model SMART2 is tevens gekoppeld met het vegetatie-effectmodel MOVE om een uitspraak te kunnen doen omtrent veranderingen in floristische diversiteit.

SMART2 onder gebracht in een landelijk-raamwerk, blijkt een flexibel en snel instrument voor het evalueren van depositie - en hydrologie (kwel) scenario's. Gemodelleerde NO$_3$- en NH$_4$-concentraties komen goed overeen met waarnemingen uit een landelijke dataset. Gemodelleerde pH en Al-concentraties laten ook bevredigende resultaten zien, maar de gemodelleerde Al-concentraties in arme zandgronden bleken te hoog. De resultaten laten ook een grote mate van ruimtelijke variabiliteit zien in de gemodelleerde pH, basenverzadiging en N-beschikbaarheid. De ruimtelijke variabiliteit in pH en basenverzadiging hangt nauw samen met de variatie in bodemtype, terwijl die van de N-beschikbaarheid nauw samenhangt met de ruimtelijke variabiliteit in N-depositie. Daarnaast hangt de N-beschikbaarheid ook in hoge mate af van het successiestadium van de vegetatie. Deze resultaten geven aan dat voor het uitvoeren van landelijke evaluaties ruimtelijk expliciet gemodelleerd dient te worden.

Onzekerheid in bodemvochtchemie op locale schaal

Bij het modelleren van de bodemvochtchemie op regionale schaal dient zowel rekening te worden gehouden met de onzekerheden gerelateerd aan de modelstructuur en aan de onzekerheid in de gebruikte data. Hiertoe is met SMART2 een onzekerheidsanalyse uitgevoerd in een ruimtelijke context. Gegeven de hoge kosten die gemoeid zijn met maatregelen om Al en NO$_3$-concentraties in bodem- en grondwater te reduceren, is het van belang om na te gaan of met aanvullende dataverzameling een reductie in de onzekerheid van de modeluitkomsten is te bewerkstelligen. Een dergelijk onderzoek levert belangrijke informatie op basis

waarvan een besluit kan worden genomen over de te volgen strategie om onzekerheden in lange-termijn modelvoorspelling te reduceren. Mogelijk alternatieven zijn het verbeteren van de betrouwbaarheid van de gebruikte bodem- en vegetatiekaarten of het verzamelen aanvullende gegevens ten behoeve van de modelparameterisatie.

De in dit proefschrift uitgevoerde analyse richt zich op de onzekerheid in lange-termijn voorspellingen van de Al- en NO_3-concentraties in het bodemvocht als gevolg van de onzekerheid in grootschalige bodem- en vegetatie-kaarten (bijv. de EU-bodemkaart van 1:1000 000) en andere niet kaartgebonden gegevens. Gekeken is naar de mediane concentraties per gridcel (5×5 km²) en de areale fractie per gridcel (5×5 km²) waar sprake is van overschrijding van een kritische concentratie. Beschouwde onzekerheidsbronnen zijn (i) de gebruikte bodem- en vegetatiekaarten (categorische data) en (ii) de bodem- en vegetatie-gerelateerde modelparameters (continue data). De onzekerheid in de categorische data is bepaald door het vergelijken van de Europese bodem- en vegetatiekaarten met de gedetailleerde Nederlandse kaarten. De onzekerheid in de continue data is bepaald aan de hand van diverse Europese databases en literatuurgegevens. De onzekerheid in de modeluitgangen is bepaald middels een efficiënte tweetraps Monte-Carlo-simulatie, waarbij rekening is gehouden met ruimtelijke correlatie.

Resultaten laten zien dat de onzekerheid in hoge mate afhangt van de beschouwde modeluitgang, zoals de medianeconcentraties per gridcel en de areale overschrijdingen per gridcel. Voor de Al-concentratie worden brede 90% voorspellingsintervallen berekend, zowel in gebieden met lage Al-concentraties (kalkrijke – en kleigronden) als in gebieden met hoge concentraties (met name arme zandgronden). Ondanks de grote onzekerheid in de modeluitkomsten, was het model in staat om significante reductie in de gemodelleerde Al-concentraties te voorspellen als gevolg van de geëvalueerde depositie-scenario's.

De relatieve onzekerheidsbijdrage hangt eveneens in hoge mate af van de beschouwde modeluitgang. Aan de onzekerheid in de Al-concentratie dragen de bodemgerelateerde parameters het meeste bij, terwijl de onzekerheidsbijdrage van de vegetatie-gerelateerde parameters verwaarloosbaar klein bleek. Voor de NO_3-concentratie daarentegen, leverende gebruikte bodem- en vegetatiekaart de grootste onzekerheidsbijdrage, direct gevolgd door de continue vegetatie-gerelateerde parameters, terwijl de continue bodemgerelateerde parameters het minst bijdroegen. In het algemeen kan geconcludeerd worden dat de meeste nadruk gelegd dient te worden op het verbeteren van de bodem- en vegetatie-gerelateerde parameters en minder nadruk op het verbeteren van de bodem- en vegetatiekaarten.

Reductie van de onzekerheid bij regionale modelstudies middels modelcalibratie

Voor het kwantificeren van het effect van modelcalibratie op nationale schaal is de fout in de modeluitkomsten van SMART2 voor en na calibratie bepaald. Dit is gedaan voor de mediane Al- en NO_3-concentraties in een 5×5 km² gridcel. Omdat er alleen metingen beschikbaar zijn op puntschaal, zijn deze gegeven eerst opgeschaald naar

hetzelfde schaalniveau als waarop de modeluitkomsten worden berekend. Hiertoe zijn ongeveer 250 punt-waarnemingen van gemeten bodemvochtconcentraties in bosbodems opgeschaald naar een 5×5 km^2 gridkaart. Hierbij is gebruik gemaakt van een combinatie van multiple-lineaire-regressieanalyse en blockkriging. De daardoor verkregen opgeschaalde kaarten met waarnemingen zijn zowel gebruikt voor de validatie als de calibratie. Een vergelijking tussen de kaart met modelvoorspellingen op basis van nominale parameter-instellingen met de kaart met opgeschaalde waarnemingen laat zien dat het model zowel de Al- als de NO$_3$-concentraties overschat. De nominale modelresultaten lagen weliswaar binnen het 95% betrouwbaarheidinterval van de opgeschaalde waarnemingen, maar de calibratie levert wel een duidelijke reductie van de modelfout op.

De gebruikte calibratie-procedure blijkt een bruikbare methodiek om op nationale schaal te komen tot optimale parameterranges en voor het reduceren van onzekerheden. De calibratie blijkt tevens succesvol in het corrigeren van de overschattingen van de Al- en NO$_3$-concentraties. Ondanks deze verbeteringen blijft de modelfout na calibratie nog steeds relatief groot. Verdere verbeteringen zijn echter niet mogelijk door het gebrek aan de juiste gegevens.

Modelvergelijking op regionale schaal

Een betrouwbaar ruimtelijk beeld van NO$_3$-concentraties in onder de wortelzone van half-natuurlijke ecosystemen is met name van belang voor het bepalen van de overschrijding van kritische concentraties. Om nader inzicht te krijgen in de onzekerheid ten gevolge van de modelstructuur van SMART2, zijn met SMART2 gesimuleerde kaarten met NO$_3$-concentraties in het bodemvocht van Nederlandse bossen vergeleken met NO$_3$-concentratiekaarten gebaseerd op: (i) een multiple-regressiemodel op basis van gemeten bodemvochtconcentraties en aanvullend data, zoals bodemtype en depositie, als verklarende variabelen en (ii) een half-empirisch dynamisch model WANDA. De vergelijking is uitgevoerd voor geheel Nederland, voor een 250×250 km^2 grid. De met de drie methoden bepaalde NO$_3$-kaarten laten duidelijk verschillende resultaten zien. Wanneer echter alleen maar vergeleken wordt op basis van een cumulatieve frequentieverdeling, zijn de resultaten behoorlijk verglijkbaar, in het bijzonder op het aggregatieniveau van een 5×5 km^2 grid. Een dergelijke opschaling gaat uiteraard ten koste van de ruimtelijke resolutie, en daarmee neemt ook de functionaliteit af om overschrijdingsarealen te bepalen.

Belangrijkste conclusies

Het gedetailleerde model NUCSAM is goed in staat om zowel het niveau als de trend in gemeten groootheden zoals bodemvochtgehaltes en bodemvochtconcentraties te simuleren. De modeltoepassingen worden echter belemmerd door het gebrek aan gegevens van een goede kwaliteit. Resultaten laten zien dat het onmogelijk is om een model zoals NUCSAM toe te passen op regionale schaal, met name als gevolg van het gebrek aan gegevens. Dit maakt het noodzakelijk om het model te vereenvoudigen ten hoeve van de regionale en nationale toepasbaarheid. De onzekerheidsanalyse laat zien dat een vereenvoudigd model vrijwel alle processen inzicht moet hebben als het

gedetailleerde model bevat, om zodoende instaat te zijn om alle belangrijke componenten in en aan de onderkant van de wortelzone te kunnen simuleren.

Het vereenvoudigde model SMART2 is goed in staat om de fluxgewogen jaargemiddelde bodemvochtconcentraties te simuleren. De resultaten zijn vergelijkbaar of zelfs beter dan de resultaten verkregen met het complexe model NUCSAM. Dit houdt in dat het negeren van de seizoensdynamiek, het niet onderscheiden van verschillende bodemlagen en het vereenvoudigen van procesbeschrijvingen niet of nauwelijks van invloed is op de gemodelleerde lange-termijn veranderingen in de jaargemiddelde bodemvochtconcentraties. Een vereenvoudigd model, zoals SMART2, kan dan ook beschouwd worden als een bruikbaar en adequaat instrument voor het maken van lange-termijnvoorspellingen ten behoeve van het beleid ten aanzien van bestrijdingsmaatregelen.

Het toepassen voor geheel Nederland van een regionaal model, zoals SMART2, terwijl het alleen geparameteriseerd en gecalibreerd is op een klein aantal intensief gemonitoorde locaties leidt tot niet adequate resultaten. Middels een calibratie op nationale schaal is de modelperformance te verbeteren en de onzekerheid in de modelresultaten te verkleinen. Na calibratie blijft de uiteindelijke modelfout echter groot. Deze is ook niet verder te reduceren middels aanvullende calibratie-experimenten als gevolg van het gebrek aan de juiste data op nationale schaal. Ten aanzien van aanvullende dataverzameling kan geconcludeerd worden dat de meeste nadruk gelegd dient te worden op het verzamelen van gegevens ten behoeve van de bodem- en vegetatie-gerelateerde parameters en minder op het verbeteren van de gebruikte bodem- en vegetatiekaarten.

Modellen voor toepassing op grotere ruimtelijke schaalniveaus dienen zo eenvoudige mogelijk van opzet te zijn. Hierbij is wel zaak dat ze een bepaald niveau van procesgeörienteerdheid behouden, zodat modelevaluatie middels calibratie, validatie en een onzekerheidsanalyse mogelijk blijft.

References

Addiscott, T., J. Smith and N. Bradburdy, 1995. Critical evaluation of models and their parameters. *J. Environ. Qual.* 24: 803-807.

Ågren, G.I., R.E. McMurtrie, W.J. Parton, J. Pastor, H.H. Shugart, 1991. State-of-the-art of models of production-decomposition linkage in conifers and grassland ecosystems. *Ecol. Appl.* 1, 118-138.

Alcamo, J. and J. Bartnicki, 1987. A framework for error analysis ofa long-range transport model with emphasis on parameter uncertainty. *Atmos. Environ.* 21: 2121-2131.

Alcamo, J., R. Shaw and L. Hordijk, 1990. *The RAINS model of acidification. Science and Strategies in Europe.* Dordrecht, the Netherlands, Kluwer Academic Publishers, 402 pp.

Alkemade, J.R.M., J. Wiertz and J.B. Latour, 1996. *Calibratie van Ellenberg's milieu-indicatie-getallen aan werkelijk gemeten bodemfactoren.* RIVM-rapport 711912016, Bilthoven.

Alkemade, J.R.M., J.J.M. van Grinsven, J. Wiertz and J. Kros, 1998. Towards integrated national modelling with particular reference to the environmental effects of nutrients. *Environ. Pollut.* 102: S1:101-105.

Anonymous, 1985. *Samenstelling van de neerslag over Nederland.* Bilthoven, KNMI/RIVM Jaarrapport 1985, ISSN 0169-1759, Bilthoven, 124 pp.

Aronsson, A., 1980. Frost hardiness in Scots pine. II Hardiness during winter and spring in young trees of different mineral status. *Studia Forest Suecica* 155: 1-27.

Arp, P.A., 1983. Modelling the effects of acid precipitation on soil leachates: a simple approach. *Ecol. Model.* 19: 105-117.

Arp, W. and F. Berendse, 1997. Effects on the dwarf shrub vegetation. In: Jenkins A. (Ed.) *CLIMEX project: Results from the third year of treatment.* Climate Change Research Report 9/1997, Norwegian Institute for Water Research, Oslo.

Beck, M.B. and G. van Straten, 1983. *Uncertainty and forecasting of water quality.* Springer-Verlag, Berlin, Heidelberg.

Beck, J.P., L. van Bree, M.L.P. van Esbroek, J.I. Freyer, A. van Hinsberg, M. Marra, K. van Velze, H.A. and W.A.J. van Pul, 2001. *Evaluatie van de verzuringsdoelstellingen: de emissievarianten.* Rapport 725501002, RIVM, Bilthoven.

Beier, C. and L. Rasmussen, 1997. Tree responses. In: Jenkins, A. (Ed.) *CLIMEX project: Results from the third year of treatment.* Climate Change Research Report 9/1997, Norwegian Institute for Water Research, Oslo.

Belmans, C., J.G. Wesseling and R.A. Feddes, 1983. Simulation model of the water balance of a cropped soil providing different types of boundary conditions SWATRE. *J. Hydrol.* 63: 27-286.

Berdowski, J.J.M. and R. Zeilinga, 1987. Transition from heathland to grassland: damaging effects of the heather beetle. *J. Ecol.* 75: 159-175.

References

Berdowski, J.J.M., C. van Heerden, J.J.M. van Grinsven, J.G. van Minnen and W. de Vries, 1991. *SoilVeg: A model to evaluate effects of acid atmospheric deposition on soil and forest. Volume 1: Model principles and application procedures.* Dutch Priority Programme on Acidification, rep. no. 114.1-02, RIVM, Bilthoven, Netherlands, 93 pp.

Berendse, F., 1988. *De nutriëntenbalans van droge zandgrondvegetaties in verband met de eutrofiëring via de lucht. Deel 1 Een simulatiemodel als hulpmiddel bij het beheer van vochtige heidevelden.* Wageningen, Centrum voor Agrobiologisch Onderzoek, 51 pp.

Berendse, F., 1990. Organic matter accumulation and nitrogen mineralisation during secondary succession in heathland ecosystems. *J. Ecol.* 78: 413-427.

Berendse, F., B. Beltman, B.R. Bobbink, R. Kwant, M.B. Schmitz, 1987. Primary production and nutrient availability in wet heathland ecosystems. *Acta Oec./Oecol. Plant.* 8: 265-276.

Bergström, S., 1975. The Development of a snow routine for the HBV-2 model. *Nordic Hydrol.* 6: 73-92.

Bierkens, M.F.P., P.A. Finke and P. de Willigen, 2000. *Upscaling and downscaling for environmental research.* Kluwer Academic Publishers, 190 pp.

Black, T.A., W.R. Gardner and G.W. Thurtell, 1969. The prediction of evaporation, drainage and soil water storage for a bare soil. *Soil Sci. Soc. Am. Proc.* 33:655-660.

Bleeker, A. and J.W. Erisman, 1996. *Depositie van verzurende elementen in Nedereland in de periode 1980-1995.* RIVM rapport nr. 722108018, Bilthoven.

Bloom, P.R. and D.F. Grigal, 1985. Modelling soil response to acidic deposition in nonsulfate adsorbing soils. *J. Environ. Qual.* 14: 489-495.

Blöschl, G. and M. Sivapalan, 1995. Scale issues in hydrological modelling: a review. *Hydrol. Proces.* 9: 251-290.

Bobbink, R. and G.W. Heil, 1993. Atmospheric deposition of sulphur and nitrogen on heathland ecosystems. In: R. Aerts and G.W. Heil (Eds.) *Heathlands: Patterns and processes in a changing environment*, pp. 25-50.

Bobbink, R., G.W. Heil and M. Scheffers, 1990. *Atmosferische depositie van NO$_x$ in bermvegetaties langs autosnelwegen.* University of Utrecht, Dept. Botanische Oecologie en Evolutiebiologie, Utrecht, 64 pp.

Bobbink, R., M. Hornung and J.G.M. Roelofs, 1998. The effects of air-borne nitrogen pollutants on species diversity in natural and semi-natural European vegetation. *J. Ecol.* 86: 717-738.

Boers, P.C.M., P.A. Finke, J.J.M. van Grinsven and P. Groenendijk, 1995. *Definition and feasibility of a model for the calculation of nutrient emission to groundwater and surface water, a co-operration between three institutes.* RIZA werkdoment 96.081 X. Lelystad, 55 pp. (in Dutch).

Bolsius, E.C.A, J.H.M. Eulderink, C.L.G. Groen, W.B. Harms, A.K. Bregt, M. van der Linden, B.J. Looise, G.J. Maas, E.P. Querner, W.L.M. Tamis, R.W. de Waal, H.P. Wolfert and M. van 't Zelfde, 1994. *Eén digitaal bestand voor de landschapsecologie van Nederland.* LKN rapport 4, VROM, Den Haag.

Bouma, J., H.A.J. van Lanen, A. Breeuwsma, J.M.J. Wösten and M.J. Kooistra, 1986. Soil survey data needs when studying modern land use problems. *Soil Use and Man.* 2(4): 125-130.

Bouma, J., P.A. Finke, M.R. Hoosbeek and A. Breeuwsma, 1998. Soil and water quality at different scales: concepts, challenges, conclusions and recommendations. *Nutr. Cycl. Agroecosyst.* 50: 5-11.

Bouten, W., 1992. *Monitoring and modelling forest hydrological processes in support of acidification research.* PhD Thesis, University of Amsterdam, Amsterdam, Netherlands, pp. 218.

Bouten, W., T.J. Heimovaara and A. Tiktak, 1992. Spatial patterns of throughfall and soil water dynamics in a Douglas fir stand. *Water Res. Res.* 28:3227-3233.

Boxman, A.W. and H.F.G. van Dijk, 1988. *Het effect van landbouw ammonium deposities op bos- en heidevegetaties.* Katholieke Universiteit Nijmegen, 96 pp.

Boxman, A.W., H.F.G. van Dijk, A. Houdijk and J.G.M. Roelofs, 1988. *Critical loads for nitrogen with special emphasis on ammonium, in Critical loads for sulphur and nitrogen.* Background documents for a Nordic IUN-ECE workshop on Critical loads, Skokloster.

Bredemeier, M., 1988. Forest canopy transformation of atmospheric deposition. *Water, Air, Soil Pollut.* 40: 121-138.

Bredemeier, M.A., A. Tiktak and C. van Heerden, 1995. The Solling spruce stand-Background information on the data set. *Ecol. Model.* 83: 7-15.

Breeuwsma, A., J.P. Chardon, J.F. Kragt and W. de Vries, 1991. Pedotransfer functions for denitrification. In ECE 1991, *Soil and Groundwater Research Report II 'Nitrate in Soils',* Commission of the European Community, Luxembourg: 207-215.

Brus, D.J., J.J. de Gruijter, B.A. Marsman, R. Visschers, A.K. Bregt and A. Breeuwsma, 1996. The performance of spatial interpolation methods and chloropleth maps to estimate properties at points: a soil survey case study. *Environmetrics* 7: 1-16.

Chen, C.W., S.A. Gherini, R.J.M. Hudson and J.D. Dean, 1983. *The Integrated Lake-Watershed Acidification Study. Volume 1: Model principles and application procedures.* EPRI EA-3221, Volume 1, Research Project 1109-5, TETRA TECH INC., Lafayette, California, 194 pp.

Christophersen, N., H.M. Seip and R.F. Wright, 1982. A model for streamwater chemistry at Birkenes, Norway. *Wat. Resour. Res.* 18: 977-996.

Christophersen, N., L.H. Dymbe, M. Johanssen and H.M. Seip, 1983. A model for sulphate in streamwater at Storgama, Southern Norway. *Ecol. Model.* 21:35-61.

Cosby, B.J., G.M. Hornberger, J.N. Galloway and R.F. Wright, 1985. Modeling the effects of acid deposition: Assessment of a lumped parameter model of soil water and streamwater chemistry. *Wat. Resour. Res.* 21: 51-63.

Cosby, B.J., R.C. Ferrier, A. Jenkins, B.A. Emmett, R.F. Wright and A. Tietema, 1997. Modelling the ecosystem effects of nitrogen deposition: Model of Ecosystem Retention and Loss of Inorganic Nitrogen (MERLIN). *Hydrol. Earth System Sci.* 1: 137-158.

Dale, V.H., H.I. Jager, R.H. Gardner and A.E. Rosen, 1988. Using sensitivity and uncertainty analyses to improve predictions of a broad-scale forest developement. *Ecol. Model.* 42: 165-178.

References

De Visser, P.H.B. and W. de Vries, 1989. *De gemiddelde jaarlijkse waterbalans van bos-, heide- en graslandvegetaties (The yearly average water balance of forest, heathland and grassland vegetation)*. STIBOKA rapport nr. 2085, Wageningen, Netherlands, 136 pp.

De Vries, W., 1988. Critical deposition levels for nitrogen and sulphur on Dutch forest ecosystems. *Water, Air, Soil Pollut.* 42: 221-239.

De Vries, W., 1991. *Methodologies for the assessment and mapping of critical loads and the impact of abatement strategies on forest soils*. Wageningen, the Netherlands, DLO Winand Staring Centre for Integrated Land, Soil and Water Research, Report 46, Wageingen, 109 pp.

De Vries, W., 1994. *Soil response to acid deposition at different regional scales; Field and laboratory data, critical loads and model predictions*, PhD Thesis Wageningen University, Wageningen, Netherlands, 487 pp.

De Vries, W. and A. Breeuwsma, 1986. Relative importance of natural anthropogenic proton sources in soils in the Netherlands. *Water, Air, Soil Pollut.* 28, 173-184.

De Vries, F. and J. Denneboom, 1992. *De bodemkaart van Nederland digitaal*. Wageningen, the Netherlands, DLO Winand Staring Centre for Integrated Land, Soil and Water Research, Technical Document 1, 48 pp.

De Vries, W. and J. Kros, 1989. The Long-Term Impact of Acid Deposition on the Aluminium Chemistry of an Acid Forest Soil. In: Kämäri, J., Brakke, D.F., Jenkins, A., Norton, S.A. and Wright, R.F. (Eds.) *Regional Acidification Models*, Springer-Verlag, Berlin, Heidelberg, pp. 113-128.

De Vries, W., M.J.P.H. Waltmans, R. van Versendaal and J.J.M. van Grinsven, 1988. *Aanpak, structuur en voorlopige proces beschrijving van een bodemverzuringsmodel voor toepassing op regionale schaal*. Wageningen, Stichting voor Bodemkartering, Rapport nr. 2014, Wageingen.

De Vries, W., M. Posch and J. Kämäri. 1989. Simulation of the long-term soil response to acid deposition in various buffer ranges. *Water, Air, Soil Pollut.* 48: 349-390.

De Vries, W., A. Hol, S. Tjalma and J.C. Voogd, 1990. *Literatuurstudie naar voorraden en verblijftijden van elementen in een bosecosysteem*. DLO- Winand Staring Centrum, Rapport 94, Wageningen, 205 pp.

De Vries, W., J. Kros and C. van der Salm, 1994a. The long-term impact of three emission-deposition scenarios on Dutch forest soils. *Water, Air, Soil Pollut.* 75: 1-35.

De Vries, W., M. Posch, G.J. Reinds and J. Kämäri, 1994b. Simulation of soil response to acidic deposition scenarios in Europe. *Water, Air, Soil Pollut.* 78: 215-246.

De Vries, W., J. Kros and J.C.H. Voogd, 1994c. Assessment of critical loads and their exceedance on Dutch forests using a multi-layer steady state model. *Water, Air, Soil Pollut.* 76: 407-448.

De Vries, W., J. Kros and C. van der Salm, 1995a. Modelling the impact of nutrient cycling and acid deposition on forest soils. *Ecol. Model.* 79: 231-254.

De Vries, W., J.J.M. van Grinsven, N. van Breemen, E.E.J.M. Leeters and P.C. Jansen, 1995b. Impacts of acid deposition on concentrations and fluxes of solutes in acid sandy forest soils in the Netherlands. *Geoderma* 67: 17-43.

De Vries, W., J. Kros, C. van der Salm, J.E. Groenenberg and G.J. Reinds, 1998. The use of upscaling procedures in the application of soil acidification models at different spatial scale. *Nutr. Cycl. Agroecosyst.* 50: 223-236.

De Vries, W., C. van der Salm, A. van Hinsberg and J. Kros, 2000. Gebiedsspecifieke, kritische depositieniveaus voor stikstof en zuur voor terrestrische ecosystemen. *Milieu* 15(3): 144-158.

De Vries, W., J. Kros, O. Oenema and J. de Klein, 2002. Uncertainties in the fate of nitrogen II: A quantitative assessment of the uncertainties in major nitrogen fluxes in the Netherlands. *Nutr. Cycl. Agroecosyst.* in press.

De Waal, R.W., 1992. *Bodem- en grondwatertrappen. Toelichting bij het databestand 'BODEMGT' van het LKN-project.* SC-DLO rapport 132, Wageningen.

Dise, N.B. and A. Jenkins (Eds.), 1995. *The CLIMEX project: Whole catchment manipulation of CO$_2$ and temperature. Climate Change Report 3/95,* Norwegian Institute for Water Research, Oslo, 130 pp

Dise, N.B., E. Matzner and P. Gundersen, 1998. Synthesis of nitrogen pools and fluxes from European forest ecosystems. *Water, Air, Soil Pollut.* 105: 143-154.

Doherty J., L. Brebber and P. Whyte, 1994. *PEST, Model-independent parameter estimation,* Watermark Computing.

Downing, D.J., R.H. Gardner and H.O.F. Hoffman, 1985. An estimation of respons-surface methodologies for uncertainty analysis in assessment models, *Technometrics* 27: 151-163.

Draayers, G.P.J., 1993. *The variability of atmospheric deposition to forests. The effects of canopy structure and forest edges.* Ph.D. Thesis, University of Utrecht, Utrecht, Netherlands, pp. 156.

Draayers, G.P.J. and J.W. Erisman, 1993. Atmospheric sulphur deposition to forest stands throughfall estimates compared to estimates from inference. *Atmospheric Env.* 27A: 43-55.

Draayers G.P.J., W.P.M.F. Ivens and W. Bleuten, 1988. Atmospheric deposition in forest edges measured by monitoring canopy throughfall. *Water, Air, Soil Pollut.* 42: 129-136.

Draper, N.R. and H. Smith, 1981. *Applied Regression Analysis,* John Wiley & Sons, Inc., second edition.

Duvigneaud, P., P. Kestemont and P. Ambroes, 1971. Productivité primaire des forêts tempérées d'essences feuillues caducifoliées en Europe occidentale. In: P. Duvingneaud (Ed.). *Productivity of forest ecosystems,* Proceedings of the Brussels symposium, Ecology and Conservation 4. UNESCO, Paris, pp 259-270.

Eary, L.E., E.A. Jenne, L.W. Vail and D.C. Girvin, 1989. Numerical models for predicting watershed acidification. *Archiv. Environ. Contam. Toxicol.* 18: 29-53.

EC, 1985. *Soil Map of the European Communities, 1:1 000 000.* Commission of the European Communities, Directorate General for Agriculture. Luxembourg.

EC, 1993. *Corine land cover, Technical guide.* Office for Official Publications and Directorate General Environment, Nuclear Safety and Civil Protection of the European Communities, Luxembourg.

Edwards, N.T., 1975. Effects of temperature and moisture on carbon dioxide evolution in a mixed deciduous forest floor. *Soil Sci. Soc. Am. J.* 39: 361-365.

References

Eerens, H.C., and J.D. van Dam (eds), 2000. *Grootschalige luchtverontreiniging en depositie in de nationale milieuverkenning,* RIVM, rapportnr 408129016, Bilthoven.

Ellenberg, H., H.E. Weber, R. Dull, V. Wirth, W. Werner and D. Paulissen, 1991. *Indicator values of plants in Central Europe.* Erich Goltze, Göttingen.

Erisman, J.W., 1991. *Acid deposition in the Netherlands.* National Institute of Public Health and Environmental Protection, Report nr. 723001002, Bilthoven, the Netherlands, 72 pp.

Erisman, J.W., 1993. Acid deposition onto nature areas in the Netherlands. Part I. Methods and results. *Water, Air, Soil pollut.* 71: 51-80.

Erisman, J.W., A. Hensen, W. de Vries, H. Kros, T. van de Wal, W. de Winter, J.E. Wien, M. van Elswijk and M. Maat, 2002. NitroGenius: A nitrogen decision support system in the form of a game to develop the optimal policy to solve the Dutch nitrogen pollution problem. *Ambio,* in press.

Evers, P.W., C.J.M. Konsten and A.W.M. Vermetten, 1987. *Acidification research on Douglas fir forests in the Netherlands (ACIFORN project).* Proc. Symp. Effects of Air Pollution on Terrestrial and Aquatic Ecosystems. Grenoble, pp. 887-909.

Evers, P.W., W.W.P. Jans and E.G. Steingröver, 1991. *Impact of air pollution on ecophysiological relations in two Douglas fir stands in the Netherlands.* De Dorschkamp Research Institute for Forestry and Urban Ecology, Report no. 637, Wageningen, Netherlands, pp. 306.

FAO, 1981. *FAO-UNESCO soil map of the world, 1:5 000 000.* Volume V Europe, Unesco Paris.

FAO, 1988. *Soil map of the World, revised legend.* World soil resources report 60, FAO, Rome, pp. 138.

Ferrier, R.C. and R.C. Helliwell, 2000. DYNAMO: Dynamic models to predict and scale up the impact of environmental change on biogeochemical cycling. In: Sutton, M.A., J.M. Moreno, W.H. van der Putten and S. Struwe (Eds.). *Terrestrial Ecosystem Research in Europe: Successes, Challenges and Policy.* European Commission, Brussels.

Finke, P.A., J.H.M. Wösten and M.J.W. Jansen. 1996. Effects of uncertainty in major input variables on simulated functional soil behaviour. *Hydrol. Process.* 10: 661-669.

Finke, P.A., D. Wladis, J. Kros, E.J. Pebesma and G.J. Reinds, 1999. Quantification and simulation of errors in categorical data for uncertainty analysis of soil acidification modelling. *Geoderma* 93: 177-194.

Galloway, J.N., 1995. Acid deposition: perspectives in time and space. *Water, Air, Soil Pollut.* 85: 15-24.

Gardner, R.H., B. Röjder, and U. Bergström, 1983. *PRISM: A systematic Method for Determining the Effect of Parameter Uncertainties on Model prediction.* Studsvik Energiteknik AB, Report Studsvik/NW-83/555, Nykoping, Sweden.

Gash, J.H.C., 1979. An analytical model of rainfall interception by forests. *Quart. J. R. Met. Soc.* 105: 43-55.

Genstat 5 Committee, 1987. *Reference Manual.* Oxford, Clarendon Press.

Georgakakos, K.P., G.M. Valle-Filho, N.P. Nikolaidis and J.L. Schnoor, 1989. Lake-Acidification studies: the role of input uncertainty in long-term predictions *Water Resour. Res.* 25: 1511-1518.

Gherini, S.A., L. Mok, R.J.M. Hudson, G.F. Davis, C.W. Chen and R.A. Goldstein, 1985. The ILWAS model formulation and application. *Water, Air, Soil Pollut.* 26: 425-459.

Gijsman, A.J., 1990. *Nitrogen nutrition and rhizosphere pH of Douglas-fir.* PhD Thesis, University of Groningen, Groningen, Netherlands, 132 pp.

Gorree, M. and H. Runhaar, 1992. *Haalbaarheidstudie natuurgerichte normstelling nutriënten.* Centre of Environmental Studies Leiden University, CML Report 88, Leiden, 45 pp.

Grant, R.F., 1991. A technique for estimating denitrification rates at different soil temperatures, water contents, and nitrate concentrations. *Soil Sci.* 152: 41-52.

Grier, C.C., K.A. Vogt, M.R. Keyes, and R.L. Edmonds, 1981. Biomass distribution and above- and below-ground production in young and mature *Abies amabilis* zone ecosystems of the Washington Cascades. *Can. J. For. Res.* 11: 155-167.

Grime, J.P., 1979. *Plant strategies and vegetation processes.* Wiley & Sons, Chichester.

Groenenberg, J.E., J. Kros, C. van der Salm and W. de Vries, 1995. Application of the model NUCSAM to the Solling spruce site. *Ecol. Model.* 83: 97-107.

Groenenberg, J.E., W. de Vries, and J. Kros, 1998. Simulation of the long-term carbon and nitrogen dynamics in Dutch forest soils under Scots pine. *Hydrol. Earth System Sci.* 2: 439-449.

Grundmann, G.L., P. Renault, L. Rosso and R. Bardin, 1995. Differential effects of soil water content and temperature on nitrification and aeration. *Soil Sci. Soc. Am. J.* 59: 1342-1349.

Gundersen, P., 1995. Nitrogen deposition and leaching in European forest – preliminary results from a data compilation. *Water, Air, Soil Pollut.* 85: 1179-1184.

Gundersen, P., B.A. Emmet, O.J. Kjønaas, C. Koopmans and A. Tietema, 1998. Impact of nitrogen deposition on nitrogen cycling: a synthesis of NITREX-data. *For. Ecol. Manage.* 101: 37-55.

Han, S., C.E. Goering, M.D. Cahn and J.W. Hummel, 1993. A robust method for estimating soil properties in unsampled cells. *Transactions of the ASEA* 36: 1363-1368.

Hauhs, M., C. Neal, R. Hooper and N. Christophersen, 1996. Summary of a workshop on ecosystem modeling: The end of an era? *Sci. Total Environ.* 183: 1-5.

Heij, G.J. and T. Schneider, 1991. *Acidification research in the Netherlands. Final report of the Dutch Priority Programme on Acidification.* Studies in Environmental Science 46, Elsevier, Amsterdam, 771 pp.

Heil, G.W. and W.M. Diemont, 1983. Raised nutrient levels change heathland into grassland. *Vegetatio* 53: 113-120.

Hendriks, C.M.A., 1994. *De verdrogingstoestand en verdrogingsgevoeligheid van het Nederlandse bos.* Wageningen, SC-DLO rapport 289.

Hendriks, C.M.A., W. de Vries and J. van den Burg, 1994. *Effects of acid deposition on 150 forest stands in the Netherlands. 2. Relationship between forest vitality and the chemical*

composition of the foliage, humus layer and the soil solution. DLO Winand Staring Centre for Integrated Land, Soil and Water Research, Report 69.2, Wageningen, the Netherlands, 55 pp.

Hettelingh, J.P., 1989. *Uncertainty in Modeling Regional Environmental Systems: the Generalisation of a Watershed acidification model for predicting broad scale effects,* PhD Thesis, Free University, Amsterdam, 224 pp.

Heuvelink, G.B.M., 1998a. Uncertainty analysis in environmental modelling under a change of spatial scale. *Nutr. Cycl. Agroecosyst.* 50: 255-264.

Heuvelink, G.B.M., 1998b. *Error propagation in environmental modelling with GIS.* Taylor & Francis, London,. pp. 127.

Heuvelink, G.B.M. and M.F.P. Bierkens, 1992. Combining soil maps with interpolations from point observations to predict quantitative soil properties. *Geoderma* 55: 1-15.

Heuvelink, G.B.M. and E.J. Pebesma. 1999. Spatial aggregation and soil process modelling. *Geoderma* 89: 47-65.

Hommel, P.W.F.M., E.E.J.M. Leeters, P. Mekkink and J.G. Vrielink, 1990. *Vegetation changes in the Speulderbos (the Netherlands) during the period 1958-1988* DLO Winand Staring Centre for Integrated Land, Soil and Water Research, Report 23., Wageningen, the Netherlands.

Hoosbeek, M.R. and R.B. Bryant, 1992. Towards the quantitative modeling of pedogenesis – a review. *Geoderma* 55:183-210.

Hootsmans, R.M. and J.G. van Uffelen, 1991. *Assessment of input data for a simple mass balance model to map critical acid loads for Dutch forest soils.* DLO-Staring Centrum, Interne Mededeling 133, Wageningen, theNetherlands 97 pp.

Hornberger, G.M., B.J. Cosby and J.N. Galloway, 1986. Modeling the effects of acid deposition. Uncertainty and spatial variability in estimation of long-term sulfate dynamics in a region. *Wat. Resour. Res.* 22: 1293-1302.

Houdijk, A.L.M.F., 1993. *Atmospheric ammonium deposition and the nutritional balance of terrestrial ecosystems.* Ph.D Thesis. Catholic University Nijmegen, Nijmegen Netherlands, 127 pp.

Houghton, J.T., G.T. Jenkins and J.J. Ephraums, 1990. *Climate Change: The IPPC Scientific Assessment.* Cambridge University Press.

Huston, M., 1979. A general hypothesis of species diversity. *American Naturalist,* 113: 81-101.

Iman, R.L. and W.J. Conover, 1980. An investigation of uncertainty and sensitivity analyses techniques for computer models. *Commun. Statist.-Theor. Meth.* A9: 1749-1842..

Iman, R.L. and J.C. Helton, 1985. *A Comparison of Uncertainty and Sensitivity Analysis Techniques for Computer Models,* NUREGICR-3904, SAND 84-1461, Snadi National Laboratories, Albuquerque, New Mexico.

Iman, R.L. and J.C. Helton, 1988. An investigation of uncertainty and sensitivity analysis techniques for computer models. *Risk Analysis* 8: 71-90.

Iman, R.J., J.C. Helton, and J.E. Campbell, 1981. An approach to sensitivity analysis of computer models: Part 1 – Introduction, input variable selection and preliminary variable assessement. *Journal of Quality Technology* 13: 174-184.

Ivens, W.P.M.F., G.P.J. Draayers, M.M. Bos, and W. Bleuten, 1988. *Dutch Forests as Air Pollutant Sinks in Agricultural Areas. A Case Study in the Central Part of the Netherlands on the Spatial and Temporal Variability of Atmospheric Deposition to Forest*, Dutch priority programme on Acidification, Report 37-09, Bilthoven.

Jans, W.W.P, G.M. van Roekel, W.H. van Orden and E.G. Steingröver, 1991. *Above ground biomass of adult Douglas fir. A data set collected in Garderen and Kootwijk from 1986 onwards.* IBN Research Report 94/1. Institute for Forestry and Nature Research, Wageningen, Netherlands.

Jansen, M.J.W., W.A.H. Rossing, and R.A. Daamen, 1994. Monte Carlo estimation of uncertainty contributions from several independent multivariate sources. p. 334-343. In: J. Grasman, and G. van Straten (ed.*) Predictability and Nonlinear Modelling in Natural Sciences and Economics*. Kluwer Academic Publishers, Dordrecht, the Netherlands.

Janssen, B.H., 1984. A simple method for calculating decomposition and accumulation of young organic matter. *Plant and Soil* 76: 297-304.

Janssen, P.H.M., 1994. Assessing sensitivities and uncertainties in models: a critical evaluation. In: J. Grasman and G. van Straten (Eds.), *Predictability and nonlinear modeling in natural sciences and economics*, Kluwer, Dordrecht, pp. 542-553.

Jansen, M.J.W., 1998. Prediction error through modelling concepts and uncertainty from basic data. *Nutr. Cycl. Agroecosyst.* 50: 247-253.

Janssen, P.H.M. and P.S.C. Heuberger, 1995. Calibration of process-oriented models. *Ecol. Model.* 83: 55-66.

Janssen, P.H.M., J. Rotmans and W. Slob, 1990. *Gevoeligheidsanalyse en onzekerheidsanalyse: een inventarisatie van ideeën, methodes en technieken*, RIVM rapport 958805001, Bilthoven.

Jenkins, A., J. Kämäri, S.A. Norton, P. Whitehead, B.J. Cosby and D.F.Brakke, 1989. *Models to describe the Geographic Extent and Time Evolution of Acidification and Air Pollution Damage, in Regional Acidification Models*, edited by Kämäri, J., D.F. Brakke, A. Jenkins, S.A. Norton and R.F. Wright, Springer-Verlag, Berlin, Heidelberg, pp. 113-128.

Jenkinson, D.S. and J.H. Rayner, 1977. The turnover of soil organic matter in some of the Rothamsted classical experiments. *Soil Sci.,* 123: 298-305.

Johnson, D.W. and D.E. Todd, 1983. Relationships among iron, aluminum, carbon, and sulfate in a variety of forest soils. *Soil Sci. Soc. Am. J.* 47: 792-800.

Jongman, R.H.G., C.J.F. Ter Braak and O.F.R. van Tongeren, 1987. *Data analysis in community and landscape ecology.* Pudoc, Wageningen, The Netherlands, 299 pp.

Jørgensen, S.E., 1992. *Integration of ecosystem theories.* Kluwer, Dordrecht.

Journel, A.G. and Ch.J. Huijbregts, 1978. *Mining Geostatistics.* Academic Press, London.

Kämäri, J., M. Posch, R.H. Gardner and J.P. Hettelingh, 1986. *A model for analyzing lake water acidification on a regional scale, part 2: regional application*, International Institute for Applied Systems Analysis, Working Paper, WP-86-66, Laxenburg, Austria.

Kämäri, J., J.P. Hettelingh, M. Posch, and M. Holmberg, 1990. Regional freshwater acidification: Sensitivity and Long-term Dynamics. in: J. Alcamo, R. Shaw, and L. Hordijk (Eds.). *The RAINS model of acidification, Science and Strategies in Europe.* Kluwer Academic Publishers, Dordrecht, the Netherlands, pp. 223-260.

References

Kätterer, T., M. Reichstein, O. Andrén and A. Lomander, 1998. Temperature dependence of organic matter decomposition: a critical review using literature data analyzed with different models. *Biol. Fertility Soils* 27: 258-262.

Kauppi, P., J. Kämäri, M. Posch, L. Kauppi and E. Matzner, 1986. Acidification of forest soils: Model developement and application for analyzing impacts of acidic deposition in Europe. *Ecol. Model.* 33: 231-253.

Kauppi, P.E., K. Mielikäinen and K. Kuusela, 1992. Biomass and carbon budget of European forests, 1700 to 1900. *Science* 256: 70-72.

Keizer, V.G., 1994. *Facsimile (June 23 1994) to the Steering Committee.* DGM/LE, The Hague, Netherlands.

Kimmins, J.P., D. Brinkley, L. Chatapaul and L. de Catanzaro, 1985. *Biochemistry of Temperate Forest Ecosystems: Literature on Inventories and Dynamics of Biomass and Nutrients.* Petawawa National Forest Institute. Information Report PI-X-47E/f.

Kirschbaum, M.U.F., 1995. The temperature dependence of soil organic matter decomposition, and the effect of global warming on soil organic C storage. *Soil Biol. Biochem.* 27: 753-760.

Klap, J.M., W. de Vries and E.E.J.M. Leeters, 1999. *Effects of acid atmospheric deposition on the chemical composition of loess, clay and peat soils under forest in the Netherlands.* DLO Winand Staring Centre for Integrated Land, Soil and Water Research, report 97.1., Wageningen, the Netherlands.

Kleeschulte, S., 1997. *Assessment of 'cumulative' uncertainty in Spatial Decision Support Systems.* Proceedings of 3rd EC-GIS Workshop, Leuven, Belgium, 25-27 June 1997.

Kleijn, C.E., G. Zuidema and W. de Vries, 1989. *De indirecte effecten van atmosferische depositie op de vitaliteit van Nederlandse bossen. 2. Depositie, bodemeigenschappen en bodemvochtsamenstelling van acht Douglas opstanden.* Stichting voor Bodemkartering, Rapport 2050, Wageningen, the Netherlands, 96 pp.

Kleijnen, J.P.C., 1987. *Statistical tools for simulation pracitioners*, Dekker, New York.

Klepper O. and E.M.T. Hendrix, 1994. A method for robust calibration of ecological models under different types of uncertainty. *Ecol. Model.* 74: 161-182.

Knowles, R., 1982. Denitrification. *Microbiol. rev.* 46: 43-70.

Konikow, L.F. and J.D. Bredehoeft, 1992. Ground-water models cannot be validated. *Advan. in Water Resour.* 15: 75-83.

Koopmans, C.J. and D. van Dam, 1998. Modelling the impact of lowered atmospheric nitrogen deposition on a nitrogen saturated forest ecosystem, *Water, Air, and Soil Pollut.* 104: 181-203.

Koorevaar, P. G. Menelik and C. Dirksen, 1983. *Elements of soil physics.* Development in Soil Science, 13. Elsevier, Amsterdam, 228 pp.

Kros, J. and P. Warfvinge, 1995. Evaluation of model behaviour with respect to biogeochemistry at the Solling Spruce site. *Ecol. Model.* 83: 255-262.

Kros, J., W. de Vries, P.H.M. Janssen and C.I. Bak, 1993. The uncertainty in forecasting regional trends of forest soil acidification. *Water, Air, Soil Pollut.* 66: 29-58.

Kros, J., P.S.C. Heuberger, P.H.M. Janssen and W. de Vries, 1994a. Regional calibration of a steady-state model to assess critical loads. In: J. Grasman and G. van Straten (eds). *Predictability and Non Linear Modelling in Natural Sciences and Economics*. Kluwer Academic Publ., Dordrecht, the Netherlands, pp. 541-553.

Kros, J., J.E. Groenenberg, W. de Vries and C. van der Salm, 1994b. Uncertainties in long-term predictions of forest soil acidification due to neglecting seasonal variability. *Water, Air, Soil Pollut.* 79: 353-375

Kros, J., G.J. Reinds, W. de Vries, J.B. Latour, and M. Bollen, 1995a. *Modelling of soil acidity and nitrogen availability in natural ecosystems in response to changes in acid deposition and hydrology*. DLO Winand Staring Centre, Report 95, Wageningen, the Netherlands.

Kros, J., G.J. Reinds, W. de Vries, J.B. Latour, and M. Bollen, 1995b, Modelling the response of terrestrial ecosystems to acidification and desiccation scenarios. *Water, Air, Soil Pollut.* 85: 1101-1106.

Kros, J., J.E. Groenenberg, C. van der Salm, W. de Vries and G.J. Reinds, 1996. *Validation and application of soil acidification models at different spatial scales: A compilation of articles on the models NUCSAM, RESAM and SMART*. DLO Winand Staring Centre, Report 98, Wageningen, the Netherlands, 158 pp.

Kros, J., E.J. Pebesma, G.J. Reinds, P.A. Finke, 1999. Uncertainty in modelling soil acidification at the European scale, a case study. *J. of Environ. Qual.* 28/2: 366-377.

Kros, J., G.J. Reinds, D.H. Prins, F.J.E. van der Bolt, R.H. Kemmers, in prep.. *Modelling the response of terrestrial ecosystems to changes in vegetation structure, atmospheric deposition and hydrology*, Alterra report, Alterra, Wageningen, the Netherlands.

Latour, J.B. and R. Reiling, 1991. *On the Move: concept voor een nationaal effecten model voor de vegetatie (MOVE)*. RIVM rapport 711901003, Bilthoven, 23 pp.

Latour, J.B. and R. Reiling, 1993. MOVE: a multiple-stress model for vegetation. *Sci. Tot. Environ. Supplement* 1513-1526.

Latour, J.B., R. Reiling and J. Wiertz, 1993. 'MOVE: a multiple-stress model for vegetation'. In: J.C. Hooghart and C.W.S. Posthumus (Eds.*) The use of hydro-ecological models in the Netherlands. Delft,* Proceedings and Information / TNO Committee on Hydrological Research: no. 47:53-64.

Leeters, E.E.J.M., H. Hartholt, W. de Vries and L.J.M. Boumans, 1994. *Effects of acid deposition on 150 forest stands in the Netherlands. Relationships between deposition level, stand and site characteristics and the chemical composition of needles, mineral soil, soil solution and groundwater.* DLO Winand Staring Centre, Report 69.4, Wageningen, the Netherlands.

Leffelaar, P.A., 1987. *Dynamics of partial anaerobiosis denitrification, and water in soil : experiments and simulation.* Ph. D. dissertation, Wageningen University.

Levine, E.R. and E.J. Ciolkosz, 1988. Computer simulation of soil sensitivity to acid rain. *Soil Sci. Soc. Am. J.* 52: 209-215.

Likens, G.E., F.H. Bormann, R.S. Pierce, J.S. Eaton and N.M. Johnson, 1977. *Biogeochemistry of a forested ecosystem.* Springer Verlag, New York, 146 pp.

Lindsay, W.L., 1979. *Chemical equilibria in soils.* John Wiley and Sons, New York.

References

Loague, K., D.L. Corwin and T.R. Ellsworth., 1998. The challenge of predicting nonpoint source pollution. *Environ. Sci. Technol.* 32: A130-A133.

Loopstra, I.L. and E. van der Maarel, 1984. *Toetsing van de ecologische soortengroepen in de Nederlandse flora aan het systeem van indicatiewaarden volgens Ellenberg,* De Dorschkamp, Report no. 381, Wageningen, the Netherlands, 143 pp.

Lükewille, A. and R.F. Wright, 1997. Experimentally increased soil temperature causes release of nitrogen at a boreal forest catchment in southern Norway. *Global Change Biol.* 3: 13-21.

Makkink, G.F., 1957. Testing the Penman formula by means of lysimeters. *Journ. Inst. of Water Eng.* 11: 277-288.

May, H.M., P.A. Helmke and M.L. Jackson, 1979. Gibbsite solubility and thermodynamic properties of hydroxy-aluminium ions in aqueous solutions at 25° C. *Cheochem. Cosmochim. Acta.* 43: 239.

McKay, M.A., R.J. Beckmann and W.J. Conover, 1979. A comparison of three methods for selecting values of inputs variables in the analysis of output from a computer code, *Technometrics* 21: 239-245.

McNulty, S.G., J.D. Aber and R.D. Boone, 1991. Spatial changes in forest floor and foliar chemistry of spruce-fir forests across New England. *Biogeochemistry* 14: 13-29.

Meiwes, K.J., 1979. Der Schwefelhaushalt eines Buchenwald- und eines Fichtenwaldökosystem im Solling. Göttinger Bodenkundliche Berichte, 60.

Melillo, J.M., 1981. Nitrogen cycling in deciduous forests. In: F.E. Clark and T. Rosswall (Eds.) Terrestrial Nitrogen Cycles. Stockholm, *Ecol. Bull.* 33: 427-442.

Mol-Dijkstra, J.P. and J. Kros, 1999. *Calibration of the model* SMART2 *in the Netherlands, using data available at the European scale.* DLO Winand Staring Centre, report 162, Wageningen, the Netherlands.

Mol-Dijkstra, J.P., J. Kros and C. van der Salm, 1998. Comparison of simulated forest soil response to acid deposition reduction with two models of differing complexity. *Hydrol. Earth System Sci.* 2: 373-483.

Mol-Dijkstra, J.P and J. Kros, 2001. Modelling effects of acid deposition and climate change on soil and runoff chemistry at Risdalsheia, Norway. *Hydrol. Earth System Sci.* 5: 487-498.

Mol-Dijkstra, J.P., W. Akkermans, C.W.J. Roest and M.J.W. Jansen, 1999. Metamodellen voor effecten van N- en P-belasting op de grondwater- en oppervlaktewaterkwaliteit (in Dutch). DLO-Staring Centrum, Technische document 61, Wageningen, the Netherlands.

Mol-Dijkstra, J.P., M.S. Grobben, J. Kros and G.J. Reinds, 2001. *Users guides: SMART_NL & SMS_NL,* Alterra-rapport 229, Alterra, Wageningen, the Netherlands.

Molchanov, A.A., 1960. *The hydrological role of forests.* Academay of Science, USSR, Institute of forestry (translation from Russian by Israel program for science translation).

Mulder, J., C.G.E.M. van Beek and H.A.L. Dierx, 1990. *Acidification of groundwater in forested sandy deposits in the Netherlands due to acid atmospheric deposition.* Report SWE 90.015. KIWA, Nieuwegein, the Netherlands.

Natuurbeleidsplan, 1989. Ministerie van Landbouw, Natuur en Visserij, Den Haag.

Nederlandse Bosstatistiek, De; *Deel 1 De oppervlakte bos van 1980 to 1983*, 1985. Den Haag, Centraal Bureau voor de Statistiek, Staatsdrukkerij, 123 pp.

Nômmik, H. and K. Larsson, 1989. Measurement of denitrification rate in undisturbed soil cores under different temperature and moisture conditions using ^{15}N tracer technique. *Swedish J. Agric. Res.* 19: 35-44.

Noordman, E., H.A.M. Thunnissen, and H. Kramer, 1997. *Vervaardiging en nauwkeurigheid van het LGN2-grondgebruiksbestand (in Dutch).* DLO-Winand Staring Centre, Rapport 515, Wageningen, the Netherlands.

Olde Ventering, H.G.M., 2000. *Nitrogen, phosphorous and potassium flows controlling plant productivity and species richness – Eutrophication and nature management in fens and meadows.* PhD Thesis, University of Utrecht, Utrecht, Netherlands, pp. 151.

Oliver, B.G., E.M. Thurman and R.L. Malcolm, 1983. The contribution of humic substances to acidity of colored nature waters. *Geochem. Cosmochem. Acta.* 47: 2031-2035.

Olsthoorn, A.F.M., 1991. Fine root density and biomass of two Douglas fir stands on sandy soils in the Netherlands. I. Root biomass in early summer. *Neth. J. Agric. Sci.*, 39: 49-60.

Olsthoorn, T.N., J.A. van Jaarsveld, J.M. Knoop, N.D. van Egmond, J.H.C. Mülschlegel and W. van Duijvenbooden, 1990. Integrated modeling in the Netherlands. In: J. Ferhann, G.A. Mackenzie and B. Rasmussen (Eds.), *Environmental models. Emissions and consequences,* pp. 461-479.

Oreskes, N., 2000. Why believe a computer? Models, Measures, and Meaning in the Natural World. In: Schneiderman, J.S. (ed.), *The earth around us,* W.H. Freeman, San Fransisco

Oreskes, N., K. Shrader-Frechette, K. Belitz, 1994. Verification,validation, and confirmation of nemerical models in the earth sciences, *Science* 263: 641-646.

Oterdoom, H.L., A.F. Olsthoorn, R. Postma and W. de Vries, 1991. *De indirecte effecten van atmosferische depositie op de vitaliteit van Nederlandse bossen. 5. Vitaliteitskenmerken, naaldsamenstelling, fijne wortels en groei van acht Douglasopstanden.* De Dorschkamp, Rapport 18.02, Wageningen, the Netherlands.

Parton, W.J., D.S. Schimel, C.V. Cole and D.S. Ojima, 1987. Analysis of factors controlling soil oranic matter levels in Great Plains Grasslands. *Soil Sci. Soc. Am. J.* 51: 1173-1179.

Pastoors, M.J.H., 1992. *Landelijk grondwater model; berekeningsresultaten - Onderzoek effecten grondwaterwinning 12,* RIVM rapport 714305005, Bilthoven, the Netherlands.

Pastoors, M.J.H., 1993. *Landelijk grondwater model; conceptuele modelbeschrijving -- Onderzoek effecten grondwaterwinning 10,* RIVM rapport 714305004, Bilthoven, the Netherlands.

Pebesma E.J. and J.W. de Kwaadsteniet, 1997. Mapping groundwater quality in the Netherlands. J. *Hydrol.* 200: 364-386.

References

Pebesma, E.J., and C.G. Wesseling, 1997. Gstat, a program for geostatistical modelling, prediction and simulation. *Computer and Geosciences* 24: 17-31.

Pebesma E.J., G.B.M. Heuvelink and J. Kros, 2000. Error assessment in a soil acidification modelling study: efficiency issues and change of support. In: G.B.M. Heuvelink and M.J.P.M. Lemmens (Eds.*), Proceedings of Accuracy 2000, the 4th International Symposium on Spatial Accuracy Assessment in Natural Resources and Environmental Science,* Amsterdam, pp. 521-528.

Persson, H., 1983. The distribution and productivity of the fine roots in boreal forest, *Plant and Soil* 71: 87-101.

Posch, M. and J.P Hettelingh, 2001. From critical loads to dynamic modelling. In: Posch, M., P.A.M. de Smet, J.P. Hettelingh and R.J. Dowing (Eds.), *Modelling and mapping of critical thresholds in Europe, Status report 2001 coordination center for effects*, RIVM, Bilthoven, the Netherlands.

Posch, M., G.J. Reinds and W. de Vries, 1993. *SMART Simulation Model for Acidification's Regional Trends. Model Description and User Manual.* Mimeograph Series of the National Board of Waters and the Environment 477, Helsinki, Finland, 43 pp.

Posch, M., G.J. Reinds and W. de Vries, in prep.. *SMART Simulation Model for Acidification's Regional Trends. Model Description and User Manual, Revised version.* Alterra report, Wageningen, the Netherlands.

Price, W.L., 1983. Global optimisation by controlled random search. *Journal of Optimisation Theory and Applications* 55: 333-348.

Pruyt, M.J., 1984. *Vegetatie, waterhuishouding en bodem in twee vochtige duinvalleien in het Noordhollands duinreservaat.* Castricum, PWN-Rapport 1.2-38, 97 pp.

Reinds, G.H., 1994. *A data base for European forest soils. Technical Document 7.* DLO Winand Staring Centre, Wageningen, the Netherlands.

Reurslag, A. and B. Berg, 1993. *Förna och organiskt material i skogsmark.* Vattenfall Research Bioenergi, Vällingby, Sweden, Report U(B) 1993/2.

Reuss, J.O., 1980. Simulation of soil nutrient losses resulting from rainfall acidity. *Ecol. Model.* 11:15-38.

Reuss, J.O. and D.W. Johnson, 1986. Acid deposition and the acidification of soils and waters. *Ecological Studies* 59. Springer-Verlag, Berlin, Germany, 119 pp.

Richardson, C.W. and D.A. Wright, 1984. WGEN: *A model for generating daily weather variables.* U.S. Dept. for Agriculture, Agric. Science, ARS-8, pp. 5-15.

Rijtema, P.E., P. Groenendijk and J.G. Kroes, 1999. *Environmental impact of land use in rural regions. The development, validation and application of model tools for management and policy analysis.* Series on environmental science and management Vol.1, Imperial College Press, London.

RIVM, 1991. *Sustainable use of Groundwater: Problems and threats in the European Communities.* Report no. 600025001. EC Ministers seminar in Den Haag, 26-27 november 1991, RIVM/RIZA, Bilthoven, the Netherlands.

RIVM, 1997. *Nationale Milieuverkenning 1997-2020,* RIVM, Bilthoven, the Netherlands.

Roberts, J., 1983. Forest transpiration: A conservative hydrological process? *J. Hydrol. (Amst.)* 66: 133-141

Roelofs, J.G.M., A.J. Kempers, A.L.F.M. Houdijk and J. Jansen, 1985. The effect of airborne ammonium sulphate on Pinus nigra var. maritima in the Netherlands. *Plant and Soil* 84: 45-56.

Rose, K.A., R.B. Cook, A.L. Brenkert, R.H. Gardner, J.P. Hettelingh, 1991. Systematic comparison of ILWAS, MAGIC and ETD watershed acidification models. 1. Mapping among model inputs and deterministic results. *Water Resour. Res.* 27: 2577-2589.

Rosén, K., 1990. *The critical load of nitrogen to Swedish forest ecosystems.* Swedish University of Agriculture Science, Department of forest soils. Internal Report, Uppsala, Sweden, 15 pp.

Ross, D.J. and Bridger, B.A., 1978. Influence of temperature on biochemical processes in some soils from tussock grassland. 2. Nitrogen mineralisation. *N. Z. J. Sci.,* 21: 591-597.

Rotmans, J., O.J. Vrieze, G.H.J.C. Peek, and W.N.G.M. Veraart, 1988. *Experimenteel ontwerp ten behoeve van metamodellering van een CO_2 simulatie-model,* RIVM rapport 7585471003, Bilthoven, the Netherlands.

Rustad, L.E., J.L. Campbell, G.M. Marion, R.J. Norby, M.J. Mitchell, A.E. Hartley, J.H.C. Cornelissen, J. Gurevitch, 2001. A meta-analysis of the response of soil respiration, net nitrogen mineralisation, and aboveground plant growth to experimental ecosystem warming. *Oecologia* 126: 543-562.

Ryan, M.G., E.R. Hunt jr., R.E. McMurtrie, G.I. Ågren, J.D. Aber, A.D. Friend, E.B. Rastetter, W.M. Pulliam, R.J. Raison and S. Linder, 1996. Comparing models of ecosystem function for temeperate conifer forest. I. Model description and validation. in: A.I. Breymeyer, D.O. Hall, J.M. Melillo and G.I. Ågren (Eds.). *Global change: effects on coniferous forest and grasslands.* John Wiley and Sons, Chichester, UK, pp. 313-362.

Santantonio, D. and R.K. Hermann, 1985. Standing crop, production and turnover of fine roots and dry, moderate and wet sites of nature Douglas fir in western Oregon. *Ann. Sci. For.* 2: 113-142.

Schaminee, J.H.J., V. Westhoff and G. van Wirdum, 1989. Naar een nieuw overzicht van de plantengemeenschappen van Nederland. *De Levende Natuur* 90: 204-209.

Schneider, T. and A.H.M. Bresser, 1988. *Evaluatierapport verzuring, Dutch Priority Programme on Acidification,* Report 00-06, Bilthoven, the Netherlands.

Schnoor, J.L., N.P. Nikolaidis and S.E. Glass, 1986. Lake resources at risk to acidic deposition in the upper midwest. *J. Water Poll. Control Federation* 58: 139-148.

Scott, D.W., 1992. *Multivariate Density Estimation.* Wiley & Sons, New York, 317 pp.

Skeffington, R.A., 1988. Excess nitrogen deposition. *Environ. Pollut.* 54: 159-296.

Stanford, G., Frere, M. and Schwaninger, D.E., 1973. Temperature coefficient of soil nitrogen mineralisation. *Soil Sci.,* 115: 321-323.

Stark, J.M., 1996. Modelling the temperature response of nitrification. *Biochemistry* 35: 33-445.

Steur, G.G.L. and W. Heijink, 1991. *Bodemkaart van Nederland schaal 1:50 000. Algemene begrippen en indelingen, 4e uitgave (in Dutch).* DLO-Winand Staring Centre, Rapport 168, Wageningen, the Netherlands.

Stumm, W. and J.J. Morgan, 1981. *Aquatic Chemistry.* Wiley, New York, 780 pp.

References

Sverdrup, H. and P. Warfvinge, 1993. *The effect of soil acidification on the growth of trees, grass and herbs as expressed by the (Ca+Mg+K)/Al ratio.* Reports in ecology and environmental engeneering, Report 2:1993, Lund University.

Sverdrup, H., P. Warfvinge and B. Nihlgård, 1994. Assessment of soil acidification effects on forest growth in Sweden. *Water, Air, Soil Pollut.* 78: 1-36.

Sverdrup, H., P. Warfvinge, L. Blake, K. Goulding, 1995. Modelling recent and historic soil data from the Rothamsted Experimental Station, UK using SAFE. *Agr., Ecosys. Environ.* 53: 161-177.

Tamm, C.O., 1991. *Nitrogen in terrestrial ecosystems. Questions of productivity, vegetational changes and ecosystem stability.* Springer Verlag, Berlin.

Ter Braak, C.J.F. and N.J.M. Gremmen, 1987. Ecological amplitudes of plant species and the internal consistency of Ellenberg's indicator values for moisture. *Vegetatio* 69: 79-87.

Thomas, R., W.G. van Arkel, H.P. Baars, E.C. van Ierland, K.F. de Boer, E. Buijsman, T.J.H.M. Hutten and R.J. Swart, 1988. *Emission of SO2, NOx, VOC and NH3 in the Netherlands and Europe in the period 1950-2030. The emission module in the Dutch Acidification Systems Model.* National Institute of Public Health and Environmental Protection, Report no. 758472002, Bilthoven, the Netherlands, 118 pp.

Thunnissen, H.A.M., R. Olthof, P. Getz and L. Vels, 1992. *Grondgebruiksdatabank van Nederland vervaardigd met behulp van Landsat Thematic Mapper opnamen.* SC-DLO rapport 168, Wageningen, the Netherlands, 225 pp.

Tietema, A., 1992. *Nitrogen cycling and soil acidification in forest ecosystems in the Netherlands.* PhD thesis, University of Amsterdam, the Netherlands, 139 pp

Tietema, A., 1999. *Nitraatuitspoeling in een intrekgebied bestudeerd met een dynamisch GIS.* Netherlands Centre for Geo-ecological Research rapport 99/2, University of Amsterdam, the Netherlands.

Tietema, A. and C. Beier, 1995. A correlative evaluation of nitrogen cycling in the forest ecosystems of the EC projects NITREX and EXMAN. *For. Ecol. Manage.* 71: 143-151.

Tiktak, A. and W. Bouten, 1990. *Soil hydrological system characterisation of the two ACIFORN stands using monitoring data and soil hydrological model 'SWIF'.* Dutch Priority Programme on Acidification report no. 102.2-01, RIVM, Bilthoven, Netherlands, pp. 62.

Tiktak, A. and W. Bouten, 1992. Modelling soil water dynamics in a forested ecosystem. III: Model description and evaluation of discretisation. *Hydrol. Proc.* 6: 455-465.

Tiktak, A. and W. Bouten, 1994. Soil water dynamics and long-term water balances of a Douglas fir stand in the Netherlands. *J. Hydrol. (Amst.)* 156: 265-283.

Tiktak, A. and J.J.M. van Grinsven, 1995. Review of sixteen forest-soil-atmosphere models. *Ecol. Model.* 83: 35-54.

Tiktak, A., C.J.M. Konsten, M.P. van der Maas and W. Bouten, 1988. *Soil chemistry and physics of two Douglas-fir stands affected by acid atmospheric deposition on the Veluwe, the Netherlands.* Dutch Priority Programme on Acidification, report no. 03-01, RIVM, Bilthoven, Netherlands, pp. 93.

274

Tiktak, A., F.A. Swartjes, R. Sanders and P.H.M. Janssen, 1994. Sensitivity analysis of model for pesticide leaching and accumulation. In: J. Grasman and G. van Straten (Eds.*), Predictability and nonlinear modeling in natural sciences and economics*, Kluwer, Dordrecht, pp. 471-484.

Tiktak, A., J.J.M. van Grinsven, J.E. Groenenberg, C. van Heerden, P.H.M. Janssen, J. Kros, G.J.M. Mohren, C. van der Salm, J.R. van der Veen and W. de Vries, 1995. *Application of three Forest-Soil-Atmosphere models to the Speuld experimental forest.* RIVM report 792310002, Bilthoven, the Netherlands.

Tiktak, A., J.R.M. Alkemade, J.J.M. van Grinsven, and G.B. Makaske, 1998, Modelling cadmium accumulation at a regional scale in the Netherlands. *Nutr. Cycl. Agroecosyst.* 50: 209-222.

Tinhout, A. and M.J.A. Werger, 1988. Fine roots in a dry Calluna heathland. *Acta. Bot. Neerl.* 37(2): 225-230.

Ulrich, B., 1983. Interaction of forest canopies with atmospheric constituents: SO_2, alkali and earth alkali cations and chloride. In: B. Ulrich and J. Pankrath (eds.). *Effects of accumulation of air pollutants in forest ecosystems.* Reidel, Dordrecht, Netherlands, pp. 33-45.

Ulrich, B. and E. Matzner, 1983. *Abiotische Folgewirkungen der weitraumigen Ausbreitung von Luftverunreinigung.* Umweltforschungsplan der Bundesministers der Innern. Forschungsbericht 1002615, BRD.

Van Amstel, A.R., L.C. Braat and A.C. Garritsen, 1989. *Verdroging van natuur en landschap in Nederland: beschrijving en analyse.* 's-Gravenhage, Ministerie van Verkeer & Waterstaat, the Netherlands.

Van Breemen, N., P.A. Burrough, E.J. Velthorst, H.F. van Dobben, T. de Wit, T.B. de Ridder and H.F.R. Reynders, 1982. Soil acidification from atmospheric ammonium sulfate in forest canopy throughfall. *Nature* 299: 548-550.

Van Breemen, N., C.T. Driscoll and J. Mulder, 1984. Acidic deposition and internal proton sources in acidification of soils and waters. *Nature* 307: 599-604.

Van Breemen, N., W.F.J. Visser and Th. Pape, (Eds.), 1988. *Biogeochemistry of an oak-woodland ecosystem in the Netherlands affected by acid atmospheric deposition.* PUDOC Scientific Publishers, Wageningen, the Netherlands, 197 pp.

Van Breemen, N., A. Jenkins, R.F. Wright, W.J. Arp, D.J. Beerling, F. Berendse, C. Beier, R. Collins, D. van Dam, L. Rasmussen, P.S.J. Verburg and M.A. Wills, 1998. Impacts of elevated carbon dioxide and temperature on a boreal forest ecosystem (CLIMEX project). *Ecosystems* 1: 345-351.

Van Dam, D., 1990. *Atmospheric deposition and nutrient cycling in chalk grassland.* PhD Thesis University of Utrecht, Utrecht, the Netherlands, 119 pp.

Van Dam, D. and N. van Breemen, 1995. NICCCE: a model for cycling of nitrogen and carbon isotopes inconiferous forest ecosystems. *Ecol. Model.* 79: 255-275.

Van den Burg, J. and H.P. Kiewiet, 1989. *Veebezetting en de naaldsamenstelling van grove den, Douglas en Corsicaanse den in het Peelgebied in de periode 1956 t/m 1988. Een onderzoek naar de betekenis van de veebezetting voor het optreden van bosschade,* Rapport 559, Instituut voor Bosbouw en Groenbeheer, 'De Dorschkamp', Wageningen, the Netherlands.

References

Van den Burg, J., P.W. Evers, G.F.P. Martakis, J.P.M. Relou, and D.C. van der Werf, 1988. *Miljø rapport 1988: 15*, Nordic Councel of Ministers, Copenhagen, pp. 295.

Van der Maas, M.P. and T. Pape, 1990. *Hydrochemistry of two Douglas fir ecosystems and a heather ecosystem in the Veluwe*. Dutch Priority Programme on Acidification 102.1.01, RIVM, Bilthoven, Netherlands, pp. 28 and appendixes.

Van der Salm, C., 1999. *Weathering of forest soils*. Ph.D. dissertation, University of Amsterdam.

Van der Salm, C., J. Kros, J.E. Groenenberg, W. de Vries and G.J. Reinds, 1995. Application of soil acidification models with different degrees of process aggregation on an intensively monitored spruce site, in S.T. Trudgill (Ed.): *Solute modelling in catchment systems*, John Wiley, Chichester, UK, pp. 327-346.

Van der Salm, C., E.J. Groenenberg, and A.W. Boxman, 1998. Modelling the response of soil and soil solution chemistry upon roofing a forest in an area with high nitrogen deposition. *Hydrol. Earth System Sci.* 2: 451-472.

Van der Salm, C., W. de Vries, M. Olsson and K. Raulund-Rasmussen, 1999. Modelling impacts of atmospheric deposition, nutrient cycling and soil weathering on the sustainability of nine forest ecosystems. *Water, Air, Soil Pollut.* 109: 101-135.

Van der Sluijs, P., 1990. 'Grondwatertrappen'. In: W.P. Locher and H. de Bakker (Eds.) *Bodemkunde van Nederland, deel 1, Algemene Bodemkunde*. Den Bosch, Malmberg, pp. 167-180.

Van der Zee, S.E.A.T.M., 1988. *Transport of reactive contaminants in heterogeneous soil systems*. Ph.D. Thesis, Wageningen University, Wageningen, Netherlands.

Van der Zee, S.E.A.T.M., 1999. *Grondgebonden residuen*. Inagural lecture, Wageningen University.

Van Dobben, H., J. Mulder, H. van Dam and H. Houweling, 1992. *Impact of atmospheric deposition on the biogeochemistry of Moorland pools and surrounding terrestial environment*. Agricultural Research Report 93, PUDOC Scientific Publishers, Wageningen, the Netherlands, 232 pp.

Van Dobben, H.F. , J.A. Klijn, F.J.E. van der Bolt, J. Kros, A.H. Prins, E.P.A.G. Schouwenberg en P. Verburg, 2001. *Geïntegreerd Ruimtelijk Evaluatie-Instrumentarium voor NatuurontwikkleingsScenario's (GREINS): koppeling van ecologische modellen aan de hand van een voorbeeldstudie in het stroomgebied van de Beerze-Reusel*, Alterra-rapport 407. Alterra, Wageningen.

Van Genuchten, M. Th., 1980. A closed form for predicting the hydraulic conductivity of unsaturated soils. *Soil Sci. Soc. Am. J.* 44: 892-898.

Van Grinsven, J.J.M., 1988. *Impact of acid atmospheric deposition on soils. Quantification of chemical and hydrological processes*. PhD Thesis, Wageningen University, Wageningen, Netherlands, pp. 215.

Van Grinsven, J.J.M., N. van Breemen and J. Mulder, 1987. Impacts of acid atmospheric deposition on woodland soils in the Netherlands. I.: Calculation of hydrological and chemical budgets. *Soil Sci. Soc. Am. J.* 51: 1629-1634.

Van Grinsven, J.J.M., C.T. Driscoll, and A. Tiktak, 1995. Workshop on comparison of forest-soil-atmosphere models: preface. *Ecol. Model.* 83: 1-6.

276

Van Veen, J.A., 1977. *The behaviour of nitrogen in soil: a computer simulation model.* PhD Thesis, Free University Amsterdam, Amsterdam, Netherlands.

Van Wirdum, G., 1986. Water-related impacts on nature protection sites. *Proc. and Inf.* 34. CHO-TNO, The Hague, 27-57.

Van Wirdum, G., 1991. *Vegetation and hydrology of floating rich-fens.* PhD Thesis, University of Amsterdam, Amsterdam, Netherlands, 310 pp.

Verburg, P.S.J., 1998. *Organic matter dynamics in a forest soil as affected by climate change.* PhD Thesis, Wageningen University, Wageningen, Netherlands.

Verburg, P.S.J., W.K.P. van Loon and A. Lükewille, 1999. The CLIMEX soil-heating experiment: soil response after 2 years of treatment. *Biol. Fertility Soils* 28: 271-276.

Vermeer, J.G. and F. Berendse, 1983. The relationship between nutrient availability, shoot biomass and species richness in grassland and wetland communities. *Vegetatio* 53: 121-126.

Wamelink, G.W.W., J.P. Mol-Dijkstra, H.F. van Dobben, J. Kros, F. Berendse, 2000. *Eerste fase van de ontwikkeling van het successie model SUMO 1.0. Verbetetering van de vegetatiemodellering in de natuurplanner.* Alterra rapport 045, Alterra, Wageningen.

Warfvinge, P. and P. Sandén, 1992. Sensitivity analysis, in Sandén, P. and Warfvinge, P. (eds.), *Modeling groundwater response to acidification*, SMHI, Norrköping, Sweden.

Wen, X.H. and J.J. Gómez-Hernández, 1996. Upscaling hydraulic conductivities in heterogeneous media: an overview. *J. Hydrol. (Amst.)* 183:ix-xxxii.

Wesselink, L.G. and J. Mulder, 1995. Aluminium solubility controls in acid forest soil (I): testing hypothesis on data from Solling, Germany. *Ecol. Model.* 83: 109-117.

Wesselink, L.G., J.J.M. van Grinsven and G. Grosskurth, 1994. Measuring and modelling mineral weathering in an acid forest soil. Solling, Germany. *Soil Sci. Soc. Am. J.* 39: 91-110.

Weterings, M., 1989. *Verzuring van radebrikgronden onder verschillend historisch gebruik.* Wageningen, Agricultural University, Internal report, 61 pp.

Wiertz, J., J. van Dijk and J.B. Latour, 1992. *De MOVE-vegetatie module: De kans op voorkomen van 700 plantesoorten als functie van vocht, pH, nutrienten en zout.*, Wageningen, IBN-DLO report no. IBN 92/24, RIVM report 711901006, Wageningen, Bilthoven, the Netherlands, 138 pp.

Wright, R.F., 1998. Effect of increased carbon dioxide and temperature on runoff chemistry at a forested catchment in Southern Norway (CLIMEX project). *Ecosystems* 1: 216-225.

Wright, R.F and A. Jenkins, 2001. Climate change as a confounding factor in reversibility of acidification: RAIN and CLIMEX projects. *Hydrol. Earth System Sci.* 5: 477-486.

Wright, R.F., E. Lotse and A. Semb, 1993. RAIN Project: Results after 8 years of experimentally reduced acid deposition to a whole catchment. *Can. J. Fish. Aquat. Sci.* 50: 258-268.

Wright, R.F., B.A. Emmet and A. Jenkins, 1998a. Acid deposition, land-use change and global change: MAGIC model applied to Aber, UK (NITREX project) and Risdalsheia, Norway (RAIN and CLIMEX projects). *Hydrol. Earth System Sci.* 2: 385-397.

References

Wright, R.F., C. Beier and B.J. Cosby, 1998b. Effects of nitrogen deposition and climate change on nitrogen runoff at Norwegian boreal forest catchments: the MERLIN model applied to Risdalsheia (RAIN and CLIMEX projects). *Hydrol. Earth System Sci.* 2: 399-414.

Annex 1 List of symbols used in the process descriptions in the SMART2 model

Symbol	Explanation	Unit
θ	volumetric moisture content of the soil	$m^3\ m^{-3}$
ϱ_{lt}	bulk density of the mineral soil	$kg\ m^{-3}$
ϱ_{rz}	bulk density of the soil in the root zone	$kg\ m^{-3}$
age_{lt}	age of the site	a
age_{tg}	age of the vegetation	a
Am_{lt}	amount of litter	$kg\ ha^{-1}$
Am_{lf}	actual amount of litterfall	$kg\ ha^{-1}\ a^{-1}$
$Am_{lf,mx}$	maximum amount of litterfall	$kg\ ha^{-1}\ a^{-1}$
AmN_{iz}	amount of nitrogen in the zone where N immobilisation occurs	$mol_c\ kg^{-1}$
Am_{st}	actual amount of stems and branches	$kg\ ha^{-1}$
$Am_{st,mx}$	maximum amount of stems and branches	$kg\ ha^{-1}$
CEC	cation exchange capacity	$mol_c\ kg^{-1}$
CN_{cr}	critical C/N ratio of the soil	$g\ g^{-1}$
CN_{mn}	minimum C/N ratio of the soil	$g\ g^{-1}$
CN_{om}	C/N ratio of the soil	$g\ g^{-1}$
$ctAl_{ox}$	content of Al in secondary Al compounds in the soil	$mol_c\ kg^{-1}$
$ctCa_{cb}$	amount of Ca in carbonates in the soil	$mol_c\ kg^{-1}$
ctC_{iz}	organic carbon content in the zone where N immobilisation occurs	$mol_c\ kg^{-1}$
$ctN_{lv,mx}$	maximum N content in leaves	$mol_c\ kg^{-1}$ or %
$ctN_{lv,mn}$	minimum N content in leaves	$mol_c\ kg^{-1}$ or %
ctX_{lv}	nutrient content in leaves of ion X (N, K, BC2)	$mol_c\ kg^{-1}$ or %
ctX_{sh}	nutrient content in shoot of ion X (N, K, BC2)	$mol_c\ kg^{-1}$ or %
$C_{\frac{1}{2}}$	half-saturation constant for sulphate sorption	$mol_c\ m^{-3}$
DA_{mo}	dissimilation to assimilation ratio of decomposing microbes	-
dt	time step	a
fdd	dry deposition factor	-
fr_{de}	actual denitrification fraction	-
$fr_{de,mx}$	maximum denitrification fraction	-
fr_{int}	interception fraction	-
fr_{mi}	actual mineralisation fraction fresh litter	-
$fr_{mi,mx}$	maximum mineralisation fraction fresh litter	-
fr_{ni}	actual nitrification fraction	-
$fr_{ni,mx}$	maximum nitrification fraction	-
frN_{re}	reallocation of N fraction before litterfall	-
$fr_{rt,lt}$	fraction roots in the litter layer	-
fr_{ru}	cumulative transpiration fraction	-
frX_{ac}	fraction of ion X (BC2, Al, H) on the adsorption complex	-
frX_{fe}	foliar exudation fraction	-
frX_{fu}	foliar uptake fraction	-
frX_{le}	leaching fraction from fresh litter of ion K and BC2	-
frX_{le}	leaching fraction from fresh litter of ion K and BC2	-
K_a	dissociation constant for organic acids	$mol_c\ m^{-3}$
KAl_{ex}	selectivity constant for Al/BC2 exchange	$mol_c^{-1}\ m^3$
KAl_{ox}	dissolution constant for Al-hydroxide	$mol_c^{-2}\ m^6$
KBC_{cb}	dissolution constant for calcium carbonate	$(mol_c\ m^{-3})^3\ hPa^{-1}$
KCO_2	dissociation constant for CO_2	$mol_c^2\ m^{-6}\ hPa^{-1}$
k_{gl}	growth rate constant for logistic growth	$kg\ ha^{-1}\ a^{-1}$

Annex 1

Symbol	Explanation	Unit
KH_{ex}	selectivity constant for H/BC2 exchange	$mol_c\ m^{-3}$
kr_{mi}	actual mineralisation rate constant old litter	a^{-1}
$kr_{mi,mx}$	maximum mineralisation rate constant old litter	a^{-1}
MHW	mean highest water-table	m
MLW	mean lowest water-table	m
ncf	nutrient cycling factor (ratio above ground N cycle/below ground N cycle)	-
N_{de}	denitrification flux	$mol_c\ m^{-2}\ a^{-1}$
N_{im}	N immobilisation flux	$mol_c\ m^{-2}\ a^{-1}$
$N_{le,mn}$	Minimum N leaching flux	$mol_c\ m^{-2}\ a^{-1}$
N_{ni}	nitrification flux	$mol_c\ m^{-2}\ a^{-1}$
$N_{td,mx}$	total N deposition above which $ctN_{lr} = ctN_{lr,mx}$	$mol_c\ m^{-2}\ a^{-1}$
$N_{td,mn}$	total N deposition below which $ctN_{lr} = ctN_{lr,mn}$	$mol_c\ m^{-2}\ a^{-1}$
OM	organic matter content	$g\ g^{-1}$
P	precipitation	$m\ a^{-1}$
pCO_2	partial CO_2 pressure in the soil	hPa
PE	precipitation excess	$m\ a^{-1}$
$rf_{,mi,MSW}$	reduction fraction of the mineralisation rate for the water-table	-
$rf_{,mi,CN}$	reduction fraction of the mineralisation rate for N content	-
$rf_{,ni,MSW}$	reduction fraction of the mineralisation rate for the water-table	-
$rf_{,de,MSW,mn}$	minimum denitrification reduction fraction for the water-table	-
$rf_{,de,pH}$	reduction fraction of the denitrification fraction for pH	-
$rf_{,de,MSW}$	reduction fraction of the denitrification fraction for the water-table	-
$rf_{,ni,pH}$	reduction fraction of the nitrification fraction for pH	-
$rf_{,ni,MSW,mn}$	minimum nitrification reduction fraction for the water-table	-
$rf_{,mi,pH}$	reduction fraction of the mineralisation rate for pH	-
ru_{exp}	root uptake exponent	-
Se	upward seepage flux	$m\ a^{-1}$
$ctSO_{4,ac}$	Sulphate content at the adsorption complex	$mmol_c\ kg^{-1}$
SSC	Sulphate adsorption capacity	$mmol_c\ kg^{-1}$
t	time	a
$t_{1/2}$	half-life time parameter of logistic growth function	a
T_{iz}	thickness of the zone where N mobilisation occurs	m
Tr	transpiration flux	$m\ a^{-1}$
T_{rz}	thickness of the root zone	m
X_{fe}	foliar exudation flux of ion X (K, BC2)	$mol_c\ m^{-2}\ a^{-1}$
X_{fu}	foliar uptake flux of ion X (NH$_4$, H)	$mol_c\ m^{-2}\ a^{-1}$
X_{gu}	growth uptake flux of element X (N, K, BC2)	$mol_c\ m^{-2}\ a^{-1}$
X_{in}	input flux of ion X (SO$_4$, NO$_3$, NH$_4$, Cl, RCOO, K, Na, BC2, HCO$_3$, Al)	$mol_c\ m^{-2}\ a^{-1}$
X_{int}	interaction flux of ion X (SO$_4$, NO$_3$, NH$_4$, Cl, RCOO, K, Na, BC2, HCO$_3$, Al)	$mol_c\ m^{-2}\ a^{-1}$
X_{la}	lateral output flux of ion X (SO$_4$, NO$_3$, NH$_4$, Cl, RCOO, K, Na, BC2, HCO$_3$, Al)	$mol_c\ m^{-2}\ a^{-1}$
X_{lf}	litterfall flux of ion X (NH$_4$, RCOO, K, BC2)	$mol_c\ m^{-2}\ a^{-1}$
X_{mi}	mineralisation flux fresh litter, old litter and the root decay in the litter layer of ion X (NH$_4$, RCOO, K, BC2)	$mol_c\ m^{-2}\ a^{-1}$
$X_{mi,lt}$	mineralisation flux old litter of ion X (NH$_4$, RCOO, K, BC2)	$mol_c\ m^{-2}\ a^{-1}$
$X_{mi,fl}$	mineralisation flux fresh litter of ion X (NH$_4$, RCOO, K, BC2)	$mol_c\ m^{-2}\ a^{-1}$
$X_{mi,tot}$	mineralisation flux fresh litter, old litter and the total root decay of ion X (NH$_4$, RCOO, K, BC2)	$mol_c\ m^{-2}\ a^{-1}$
$X_{rd,ms}$	root decay flux in the mineral soil of ion X (NH$_4$, RCOO, K, BC2)	$mol_c\ m^{-2}\ a^{-1}$

Symbol	Explanation	Unit
$X_{rd,lt}$	root decay flux in the litter layer of ion X (NH_4, RCOO, K, BC2)	mol_c m^{-2} a^{-1}
X_{se}	seepage flux of ion X (SO_4, NO_3, NH_4, Cl, K, Na, BC2, HCO_3, Al)	mol_c m^{-2} a^{-1}
X_{sen}	net seepage flux of ion X (SO_4, NO_3, NH_4, Cl, RCOO, K, Na, BC2, HCO_3, Al)	mol_c m^{-2} a^{-1}
X_{td}	total deposition of element X (SO_4, N, K, Na, BC2)	mol_c m^{-2} a^{-1}
X_{we}	weathering flux of base cation X (Na, K, BC2)	mol_c m^{-3} a^{-1}
$[X]$	concentration of ion X (SO_4, NO_3, K, Na, BC2, HCO_3, Al and H) in soil solution	mol_c m^{-3}
z	depth	m
z_{ni1}	soil dependent depth of MSW for determination of $rf_{ni\ MSW}$	m
z_{ni2}	soil dependent depth of MSW determination of $rf_{ni\ MSW}$	m
z_{de}	soil dependent depth of MSW for determination of $rf_{de\ MSW}$	m

Curriculum vitae

Johannes (Hans) Kros werd geboren op 30 oktober 1959 te De Bilt. Zijn lagere schooltijd bracht hij door in Nijmegen en zijn middelbare schooltijd in Eindhoven. Na eerst het Mavo en het Havo eindexamen te hebben behaald, behaalde hij in 1980 zijn VWO eindexamen aan het Eindhovens Protestants Lyceum. In datzelfde jaar begon hij met zijn studie Bodemkunde en Bemestingsleer aan de toenmalige Landbouwhogeschool te Wageningen. In 1984 behaalde hij zijn kandidaatsexamen. Zijn stage bracht hij door bij het adviesbureau Grontmij. In januari 1987 behaalde hij zijn doctoraalexamen Bodemkunde en Bemestingsleer aan de toenmalige Landbouwuniversiteit Wageningen. Zijn doctoraalvakken bestonden uit Bodemscheikunde, Kolloïdchemie, Informatica en Kennis van de Bodemverontreiniging. Tijdens zijn laatste doctoraalvak, op het gebied van bodemverzuringsmodellering onder begeleiding van Hans van Grinsven, kwam hij in contact met Wim de Vries. Dit resulteerde per 1 februari 1987 in een tijdelijke aanstelling voor 3 maanden bij de toenmalige Stichting voor Bodemkartering (STIBOKA). In deze periode heeft hij zich beziggehouden met de ontwikkeling van het nationale bodemverzuringsmodel RESAM. Op 1 mei 1987 kreeg hij een tijdelijke aanstelling voor 1 jaar bij het toenmalige Limnologisch Instituut te Nieuwersluis alwaar hij onderzoek heeft uitgevoerd naar de sediment-wateruitwisseling van fosfor om vervolgens met ingang van 15 februari 1988 weer terug te keren naar STIBOKA en het bodemverzuringsonderzoek. Bij STIBOKA, dat later opging in het DLO-Staring Centrum (SC-DLO) heeft hij zich op basis van diverse tijdelijke aanstellingen tot 1 februari 1991 beziggehouden met de verdere verfijning en toetsing van bodemverzuringsmodellen. Met ingang van 1 februari 1991 werd hij aangesteld als senior onderzoeker bij de afdeling Milieubescherming van SC-DLO en later bij de Afdeling Water en Milieu van Alterra. De afgelopen jaren heeft hij zich met name beziggehouden met het integreren van modellen op het gebied van hydrologie, bodemprocessen en vegetatieontwikkeling en ontwikkelen van beslissingsondersteunende systemen.

Hans is getrouwd met Yvonne Drissen. Samen hebben zij drie kinderen Mathijs, Koen en Eva.

Cover was designed by Martin Jansen
Satellite Image: processed by Henk Kramer, based on a Landsat 5 image in the year
          1995; © ESA/EURIMAGE
Photograph: Wieger Wamelink

286